The impact of submarine outfalls of treated wastewater on the microbial community structure and the resistome of the coastal marine environment

Kvesić Ivanković, Marija

University of Split

Faculty of Science

Postgraduate University Study in Biophysics

Doctoral thesis

THE IMPACT OF SUBMARINE OUTFALLS OF TREATED WASTEWATER ON THE MICROBIAL COMMUNITY STRUCTURE AND THE RESISTOME OF THE COASTAL MARINE ENVIRONMENT

Marija Kvesić Ivanković

Split, 2023

Sveučilište u Splitu

Prirodoslovno-matematički fakultet

Poslijediplomski sveučilišni studij Biofizika

Doktorski rad

UTJECAJ PODMORSKIH ISPUSTA PROČIŠĆENE OTPADNE VODE NA STRUKTURU MIKROBNE ZAJEDNICE I REZISTOM PRIOBALNOG MORA

Marija Kvesić Ivanković

Split, 2023

Odjel za fiziku, Poslijediplomski sveučilišni studij Biofizika

UTJECAJ PODMORSKIH ISPUSTA PROČIŠĆENE OTPADNE VODE NA STRUKTURU MIKROBNE ZAJEDNICE I REZISTOM PRIOBALNOG MORA

Doktorski rad autorice Marije Kvesić Ivanković kao dio obaveza potrebnih da se dobije doktorat znanosti, izrađen je pod vodstvom mentorice izv. prof. dr. sc. Ane Maravić i komentora prof. dr. sc. Roka Andričevića.
Dobiveni akademski naziv i stupanj: doktorica prirodnih znanosti iz polja biologija. Povjerenstvo za ocjenu i obranu doktorskog rada u sastavu:

1. doc. dr. sc. Ivica Šamanić _____
   (Prirodoslovno-matematički fakultet u Splitu, predsjednik)

2. doc. dr. sc. Marin Ordulj _____
   (Sveučilišni odjel za studije mora Sveučilišta u Splitu, član)

3. Dr. sc. Slaven Jozić _____
   (Institut za oceanografiju i ribarstvo u Splitu, član) potvrđuje da je disertacija

obranjena dana _____

Voditelj studija

_____

izv. prof. dr. sc. Damir Kovačić

Dekan

_____

prof. dr. sc. Mile Dželalija

BASIC DOCUMENTATION CARD

University of Split, Faculty of Science Ph.D. thesis

THE IMPACT OF SUBMARINE OUTFALLS OF TREATED WASTEWATER ON THE MICROBIAL COMMUNITY STRUCTURE AND THE RESISTOME OF THE COASTAL MARINE ENVIRONMENT

Marija Kvesić Ivanković

Thesis performed at:

Center of Excellence for Science and Technology-Integration of Mediterranean region (STIM), Faculty of Science, University of Split

Abstract:

The impact of submarine outfalls on the coastal marine microbiome and resistome remains insufficiently analysed, emphasizing the main objective of this dissertation. Modern technologies, including fast-profiling probes and next-generation sequencing, were employed to fill knowledge gaps and provide new insights into submarine outfalls as epidemiologically significant sources as well as hotspots of environmental contamination with antibiotic-resistant bacteria (ARB) and resistance genes (ARGs). Analysis of the water column stability and its influence on the effluent plume movement confirmed the role of stratification in submerging effluents beneath the pycnocline. Additionally, probes' utility in describing plume shape and its real-time detection was emphasized and subsequently used as a sampling methodology in the chapter Additional results. Metagenomic analyses furthermore demonstrated the negative influence of submarine outfalls on the marine microbial community, leading to the spread of nonindigenous and pathogenic bacteria potentially carrying ARGs. Furthermore, identification of carbapenemase-producing *Enterobacteriaceae* (CPE) in the vicinity of the submarine outfall associated with hospital wastewater was notable, evidencing the initial detection of environmental CP-*E. coli* containing both bla_{KPC-2} and bla_{OXA-48} carbapenemase genes. Additional findings highlighted differences in microbial community structure between outfall locations and areas unaffected by wastewater intrusion. Moreover, the integration of shotgun analysis across WWTPs and corresponding submarine outfalls provided insights into complex bacterial community and ARG variations, underlining AR's persistence and release into the marine environment. Emphasizing the need for holistic strategies, this work aligns with the One Health concept, recognizing the problem of antibiotic resistance in the environment.

(158 pages, 40 figures, 32 tables, 151 references, 2 supplements, original in English)

Thesis deposited in:

National and University Library in Zagreb, University Library in Split, and Library of the Faculty of Science, University of Split

Keywords: wastewater submarine outfalls impact, microbiome, resistome, carbapenemase-producing *Enterobacteriaceae*

Supervisor: izv. prof. dr. sc. Ana Maravić

Co-supervisor: prof. dr. sc. Roko Andričević

Reviewers:

1. Doc. dr. sc. Ivica Šamanić
2. Doc. dr. sc. Marin Ordulj
3. Dr. sc. Slaven Jozić

Thesis accepted:

TEMELJNA DOKUMENTACIJSKA KARTICA

Sveučilište u Splitu, Prirodoslovno-matematički fakultet Doktorska teza

UTJECAJ PODMORSKIH ISPUSTA PROČIŠĆENE OTPADNE VODE NA STRUKTURU MIKROBNE ZAJEDNICE I REZISTOM PRIOBALNOG MORA

Marija Kvesić Ivanković

Rad je izrađen na:

Centru izvrsnosti za znanost i tehnologiju-Integracija Mediteranske regije (STIM), Prirodoslovno-matematički fakultet, Sveučilište u Splitu

Sažetak:

U sklopu ove disertacije istražen je utjecaj podmorskih ispusta na mikrobiom i resistom priobalnog morskog okoliša. Suvremena tehnologija, uključujući višeparametarske sonde i sekvenciranje sljedeće generacije (NGS), korištena je kako bi se pružile nove spoznaje o podmorskim ispustima kao epidemiološki važnim izvorima ali i žarištima onečišćenja okoliša rezistentnim bakterijama i genima antibiotske rezistencije. Analizirana je stabilnost vodenog stupca i njegov utjecaj na širenje efluenta, potvrđujući ulogu stratifikacije u održavanju efluenta ispod piknokline. Nadalje, naglašena je i korisnost korištenja sondi za opis i praćenje oblaka efluenta u stvarnom vremenu, kao i kod uzorkovanja morske vode. Paralelno, analizom metagenomskih podataka utvrđen je negativan utjecaj rada podmorskih ispusta na sastav mikrobne zajednice, a koji je doveo do širenja alohtonih i patogenih bakterija. Nadalje, u blizini podmorskog ispusta povezanog s otpadnim vodama bolnica grada Splita, identificirane su karbapenemaza-producirajuće *Enterobacteriaceae*, a po prvi put je identificirana i okolišna KPC- i OXA-48-producirajuća *E. coli*. Dodatni rezultati istaknuli su razlike u strukturi mikrobne zajednice između točaka uzorkovanja u neposrednoj blizini podmorskih ispusta u odnosu na kontrolnu točku koja nije pod utjecajem otpadne vode. Nadalje, integracija analize mikrobioma i rezistoma na temelju nasumičnog sekvenciranja (engl. *Shotgun*) metagenomskih uzoraka prikupljenih unutar uređaja za pročišćavanje otpadnih voda i u blizini pripadajućih podmorskih ispusta, pružila je uvid u raznolikost bakterijske zajednice i gena antibiotske rezistencije, pri tome naglašavajući postojanost i ispuštanje gena antibiotske rezistencije u morski okoliš. Naglašavajući potrebu za holističkim strategijama, ovaj rad se uklapa i u 'One Health' koncept (Jedno zdravlje), prepoznajući i naglašavajući problem antibiotske rezistencije u okolišu.

(158 stranica, 40 slika, 32 tablice, 151 referencu, 2 priloga, jezik izvornika: engleski)

Rad je pohranjen u:

Nacionalnoj sveučilišnoj knjižnici u Zagrebu, Sveučilišnoj knjižnici u Splitu i Knjižnici Prirodoslovno-matematičkog fakulteta Sveučilišta u Splitu

Ključne riječi: podmorski ispusti otpadne vode, mikrobiom, rezistom, karbapenemaza-producirajuće *Enterobacteriaceae*

Mentorica: izv. prof. dr. sc. Ana Maravić

Komentor: prof. dr. sc. Roko Andričević

Ocjenjivači:

1. Doc. dr. sc. Ivica Šamanić
2. Doc. dr. sc. Marin Ordulj
3. Dr. sc. Slaven Jozić

Rad prihvaćen:

ACKNOWLEDGMENTS

I would like to express my appreciation and thanks to all people who supported and helped me while working on my thesis. It was a real rollercoaster, with all the ups and downs.

I am very grateful to my supervisor izv.prof.dr.sc. Ana Maravić. This research would not have been possible without your valuable insight, contribution and expertise. It has been a pleasure to work with you.

I extend my thanks to prof.dr.sc. Roko Andričević, my co-supervisor, for constructive suggestions and expertise. I also thank all the members of the review committee for your time and helpful suggestions.

This achievement would not have been possible without collaboration with many dear colleagues from the Department of Biology, University of Split. I am grateful to Mia Dželalija, Ivica Šamanić and Željana Fredotović for all the time they dedicated to me inside and outside the lab. Equally, a big thank you to my colleagues from Faculty of Civil Engineering, Architecture and Geodesy, University of Split - Morena Galešić Divić and Vladimir Divić - for every day of field campaigns and every minute spent explaining 'hard mathematics' to me.

I thank the Croatian Academy of Sciences and Arts for providing financial support through projects funding and Split Water and Sewerage Company employees for their assistance in collecting samples inside wastewater treatment plants. Furthermore, thanks to all colleagues from STIM-REI project. Thank you, Mateo Marco Pavičić, Marino Tešija and Vibor Grčić, for valuable help with field campaigns.

A special thanks goes to my colleagues who worked with me in the last (almost) five years. We had a really nice time of conversations and support. In the end, many of you (you know who you are) became real friends!

Last but not least, I am so grateful to my family and loving friends who supported me unconditionally throughout this journey. A special thank goes to Tomo for believing in me and being here for me all the time. You have been my reminder to take breaks, and without your belief and support, this achievement would not have been possible.

…Mama i tata: bez vaše potpore ne bi bilo ni truda ni rezultata. Ovu tezu posvećujem vama.

PUBLICATIONS

The following list of publications constitute the main part of the thesis:

1. Kvesić, M., Vojković, M., Kekez, T., Maravić, A., Andričević, R., 2021. Spatial and Temporal Vertical Distribution of Chlorophyll in Relation to Submarine Wastewater Effluent Discharges. Water 13, 2016.. https://doi.org/10.3390/w13152016

2. Kvesić, M., Kalinić, H., Dželalija, M., Šamanić, I., Andričević, R., Maravić, A., 2022. Microbiome and antibiotic resistance profiling in submarine effluent-receiving coastal waters in Croatia. Environmental Pollution 292, 118282. https://doi.org/10.1016/j.envpol.2021.118282

3. Kvesić M., Šamanić I., Novak A., Fredotović Ž., Dželalija M., Kamenjarin J., Goić Barišić I., Tonkić M. and Maravić A., 2022. Submarine Outfalls of Treated Wastewater Effluents are Sources of Extensively- and Multidrug-Resistant KPC- and OXA-48-Producing Enterobacteriaceae in Coastal Marine Environment. Frontiers in Microbiology 13:858821. doi: 10.3389/fmicb.2022.858821

ABBREVIATIONS:

AR	Antibiotic resistance
ARB	Antibiotic resistant bacteria
ARG	Antibiotic resistance genes
CDOM	Colored dissolved organic matter
CPE	Carbapenemase-producing *Enterobacteriaceae*
CRE	Carbapenem-resistant *Enterobacteriaceae*
DO	Dissolved oxygen
ESBL	Extended spectrum β-lactamases
FIB	Faecal indicator bacteria
HGT	Horizontal gene transfer
HWWs	Hospital wastewaters
KPC	*Klebsiella pneumoniae* carbapenemase
MBLs	Metallo-β-lactamases
MDR	Multidrug-resistant
MGE	Mobile genetic elements
NGS	Next-generation sequencing
OTUs	Operational taxonomic units
OXA	Oxacillin-hydrolyzing β-lactamases
PBPs	Penicillin-binding proteins
VREfm	Vancomycin-resistant *Enterococcus faecium*
WHO	World Health Organization
WWTPs	Wastewater treatment plants

CONTENTS

1.INTRODUCTION

1.1.SUBMARINE OUTFALLS – TRANSPORT AND DISPOSAL OF TREATED WASTEWATER IN COASTAL AREAS

Inherent complexities and dynamic nature render coastal areas among the most vulnerable ecosystems. Their importance goes beyond biodiversity and plays a crucial role in supporting the socio-economic aspects of human life and activities [1]. Unfortunately, these vital regions face escalating anthropogenic pressures, particularly due to tourism development and the growing coastal population, which now represents approximately one third of the world's population [2]. As a result, the quality of the coastal ecosystem is compromised, exerting substantial pressure on coastal water bodies. Moreover, as the expected human population will grow to 10 billion by 2050 [3], these environmental pressures are expected to increase. Therefore, effective protection of coastal ecosystems is now more important than ever.

The primary sources of pollution in coastal regions originate from untreated or inadequately treated wastewater, as well as runoff from agricultural areas and rivers [4]. These sources contribute to various forms of pollution that can directly or indirectly impact human health. Various physico-chemical (suspended matter, nutrients, heavy metals etc.) and biological stressors (pathogens, antibiotic resistance (AR) determinants etc.), being introduced into the ecosystem by sewage water, contribute to water quality degradation. Disturbances in the input and processing of organic matter and nutrients, both from natural sources and anthropogenic influence, disturb the fragile balance of this ecosystem. When the input of nutrients, particularly nitrogen and phosphorus compounds, exceeds the ecosystem's assimilation capacity, it leads to eutrophication [5,6]. However, among all mentioned pollution sources, wastewater treatment plants (WWTPs) are known routes through which most of the mentioned contaminants are processed and disseminated further into the environment. WWTP receives and processes large volumes of wastewater enriched in physico-chemical and biological pollutants originating from municipal, industrial and hospital sewage. Thus, coastal environments are under the combined pressure of a complex matrix of contaminants being introduced by WWTP effluents. Discharging wastewater effluent, furthermore, enables an import of non-native bacterial populations, including pathogenic and antibiotic resistant bacteria (ARB), into marine environments [7,8].

Particularly for coastal areas, transporting and disposing of treated wastewater effluent into the marine environment is maintained by wastewater submarine outfalls, the discharge components of WWTPs. Outfalls consist of a pipeline, with varying length and diameter, attached to the seabed which mostly terminates with a multiport diffuser section to obtain a rapid mix and dilution effect (Figure 1). Effluent hydrodynamics can be defined as a mixing process occurring in two different regions, near-field and far-field. During the initial dilution, known as near-field, buoyancy flux and outfall geometry influence the effluent trajectory and degree of mixing. As distance from the source increases, the waste plume's characteristics become progressively less governed by the source and more by ambient environmental factors. These include passive diffusion and advection driven by tides, waves, pressure, and density gradients (known as far-field). Vertical mixing depends on the water column stratification, precisely vertical density gradient and the pycnocline formation. During the formation of stable vertical stratification, the effluent plume is trapped below the pycnocline layer, while upwelling to the surface is characterized during the disruption of vertical stratification (e.g. significant wind disturbances) [9,10].

Geometrical shapes of sewage plume, although rarely observed in detail, are indicators of plume dispersion and its impact on the ecosystem [11]. Dilution of the effluent plume can be estimated from in-situ measurements of its major components (i.e. initial dilution, rise height and vertical dispersion) performed in the near-field and far-field mixing zones. As the dilution effect often obscures the impact of effluent discharge into the sea, the difference between recipient and wastewater is minor and difficult to discern [12,13], even in cases involving substantial flows of inadequately treated wastewater [14]. Notably, the most pronounced effect of effluent discharge is visible in the near-field mixing zone, which weakens as it moves away toward the far-field mixing zone. While submarine outfalls are generally considered environmentally acceptable, they still pose a significant source of pollutants in the marine environment. Thus, precise measurements of variations of different parameters, which reflect the sewage impact, are crucial.

Water column density is one of the most crucial parameters for understanding the physical processes of wastewater effluent plume behaviour. It depends on temperature, salinity and pressure which all together describe vertical water column stability [15]. In addition to the physical properties of the water column, chlorophyll *a*, turbidity, organic matter and dissolved oxygen are also important parameters to obtain information about the water quality status [16]. Since primary producers are most sensitive to an increase in nutrient concentration,

phytoplankton biomass is considered a good indicator of the trophic state of coastal water [17], and due to the challenges in the direct measuring of phytoplankton, chlorophyll *a* is mainly used as a proxy for phytoplankton biomass [18–21]. Changes in chlorophyll *a* response will be followed by dissolved oxygen variation, as it primarily depends on respiration rate, but also the bacterial decomposition of elevated organic matter introduced by effluent.

The most traditional technique to determine the plume effect in the intrusion area is based on continuous monitoring of effluent and physicochemical parameters within the water body. This approach is based on conventional sampling and laboratory analysis, and it is crucial to obtain long-term ecosystem health. Although such analysis provides key information about the plume effect, it lacks high spatial and temporal resolution and does not permit real-time plume detection. Nowadays, different fast-profiling probes equipped with various physico-chemical sensors are used to obtain high-quality real-time data to map and describe effluent plume shapes.

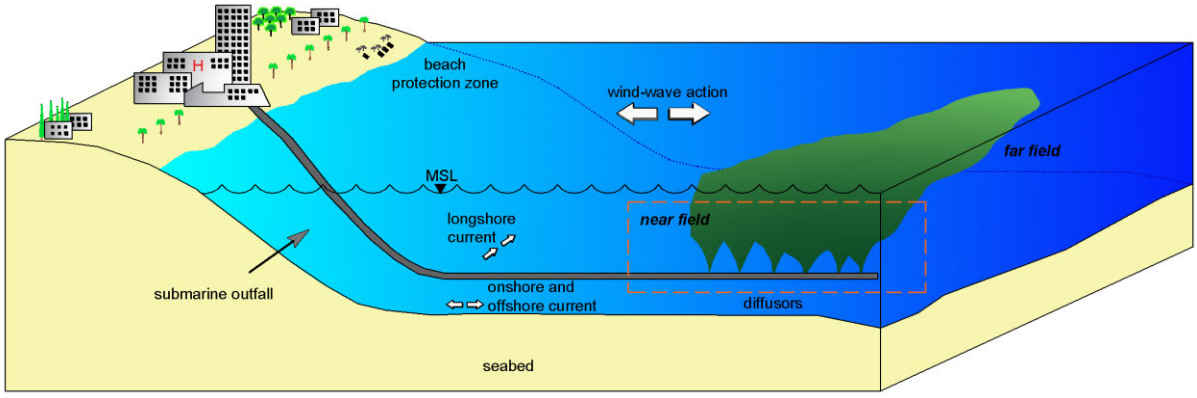

Figure 1. Schematic representation of submarine outfalls design (Credits: Morena Galešić Divić and Vladimir Divić)

1.2. MICROBIOME AND RESISTOME OF THE AQUATIC ENVIRONMENT – ROLE OF WWTPs AND SUBMARINE OUTFALLS

1.2.1. MICROBIAL COMMUNITY – IMPORTANT ASPECT OF AQUATIC HEALTH

Coastal ecosystems as a natural habitat have a high diversity of bacterial species, but at the same time are receptors of microorganisms originating from land (animal and human waste, runoffs etc.). Due to their pivotal role in water purification and biogeochemical cycling, microbial communities play a crucial role in these ecosystems [22]. Therefore, understanding their composition, abundance, and driving forces holds paramount importance for the effective management of coastal areas.

Along with all physico-chemical agents that WWTPs receive, treat and discharge further into the environment, diverse microbial communities from different sources make up the vast majority of sewage composition, as bacteria are the most abundant and diverse group of organisms living in wastewater. While WWTPs are designed to remove a considerable portion of pollutants, residues still expose environment to so-called "second-hand" pollution [23]. As a result, the release of insufficiently treated or untreated wastewater leads to significant changes in the microbial communities of lakes [24], rivers [25,26], and seas [27], and can impact the long-term biodiversity of the coastal marine microbiome as well [28,29].

The link between marine microbial communities and different physico-chemical and biological stressors in WWTPs and the environment is well known, and all of them affect microbial communities in terms of structure [30] and function [31]. Generally, marine microorganisms are highly sensitive with prompt responses to most of the environmental variations. Thus, microbiome composition depends on nutrient concentration changes, promoting the shift in the composition which could lead to reduced biodiversity [32]. Additionally, other physicochemical parameters such as pH [33], temperature [34], salinity [35], and organic matter [36] are also closely linked to the composition and abundance of the microbial community. Hence, microorganisms are considered *in situ* biosensors, detecting environmental changes [37], and therefore, retrieving quantitative data and understanding the mechanisms that influence microbial community is essential to predict the microbial response to the changes on local and global scale [38]. However, among allochthonous microbial

community discharged into the coastal area by submarine outfalls, the presence of different opportunistic pathogens (e.g., *Enterococcus faecalis*, *Escherichia coli*, *Klebsiella pneumoniae*, *Pseudomonas aeruginosa* etc.) is of additional concern. If mentioned bacteria are resistant to different antimicrobials by harbouring AR genes (ARG), such a concern increases even more.

1.2.2. ANTIBIOTIC DETERMINANTS IN COASTAL AREA

Whether produced naturally (from different microorganisms) or synthetically, all antibiotics have the same role: to inhibit bacterial growth or reproduction (bacteriostatic) or to kill the bacteria (bactericidal) [39]. The historical lineage of antibiotics extends into the ancient past, with evidence of their presence dating as far back as 2 billion to 30 million years ago [40]. Anyhow, the human discovery of antibiotics dates back to Fleming's discovery of penicillin in 1929 [41], and there is no doubt, that antibiotics are one of the most important discoveries of modern medicine. These 'miracle drugs,' once referred to as such, transformed life-threatening bacterial infections into easily treatable conditions. [42]. However, a miracle has its own price, an AR, a phenomenon present all around the world. What has happened that switched 'miracle drugs' into the 'problem of a modern century'?

Antibiotics have shown high potential in the treatment of different diseases in humans, plants and animals, but their excessive and inappropriate use [43] became the main driving force of the AR spread, which has led to this phenomenon being widely recognized by international entities as a growing public health. It stands as one of the foremost challenges in modern medicine [44], giving rise to increased healthcare costs and elevated patient mortality. While earlier projections estimated approximately 10 million deaths attributable to AR by 2050 [45], recent analyses have shown that only in 2019 almost 5 million deaths were caused by multidrug-resistant (MDR) bacteria [46], which implies that the development of novel antimicrobials will not meet the future needs of human medicine [47].

While the AR phenomenon was initially regarded as a concern mainly within hospital settings, the widespread and excessive use of antibiotics has hastened the emergence and dispersion of acquired AR. Notably, WWTPs are recognized as primary sources of AR determinants into the environment, including ARB, ARGs, and mobile genetic elements (MGE) [48–51]. They are important for successful horizontal gene transfer (HGT) even among unrelated bacterial species [52,53]. HGT can occur between two bacterial cells (donor-acceptor) through four different ways: 1) transformation – the pathway in which bacteria uptake

DNA from their environment, 2) transduction – genetic elements are transferred by bacteriophages, 3) conjugation – pathway in which bacteria accepts new genes by physical contact between two cells (formation of conjugation bridge), and 4) vesiduction – recently discovered fourth way of DNA transfer by extracellular vesicles [54]. ARB and ARGs experience heightened levels within patients and hospital environments. These elements are subsequently propagated into the broader community as a component of the biome or transported into WWTPs through hospital effluents. Additionally, sub-therapeutic antibiotic concentrations, along with their residues, are introduced into wastewater, intensifying the issue of AR by promoting selective pressures during prolonged microorganism-pollutant interactions (Figure 2). Consequently, hospital wastewaters deserves special attention as it directly introduces human opportunistic pathogens into the natural ecosystem [48,55,56], providing a platform for genetic material exchange with indigenous bacterial populations. However, from everything mentioned above, it is clear that WWTPs promote the persistence and spread of better adapted microorganisms [57], which makes the WWTPs considered reservoirs and hot spot sources of dissemination of AR determinants further into the environment. Although there are opposite findings about the removal of ARGs during different treatment processes in WWTPs, as some of the studies showed a reduction in their abundancy [58,59], while others found elevated levels in treated effluent [60,61], most of the scientific literature agrees in one: most of the WWTPs are not capable to remove ARGs from the system and more studies together with new removal technologies are needed [62]. Given that AR poses a public health challenge on a global scale, in order to manage the risk of AR spread it becomes imperative to underscore the significance of researching this phenomenon in the environment too, as highlighted by the World Health Organization (WHO) under the One Health concept.

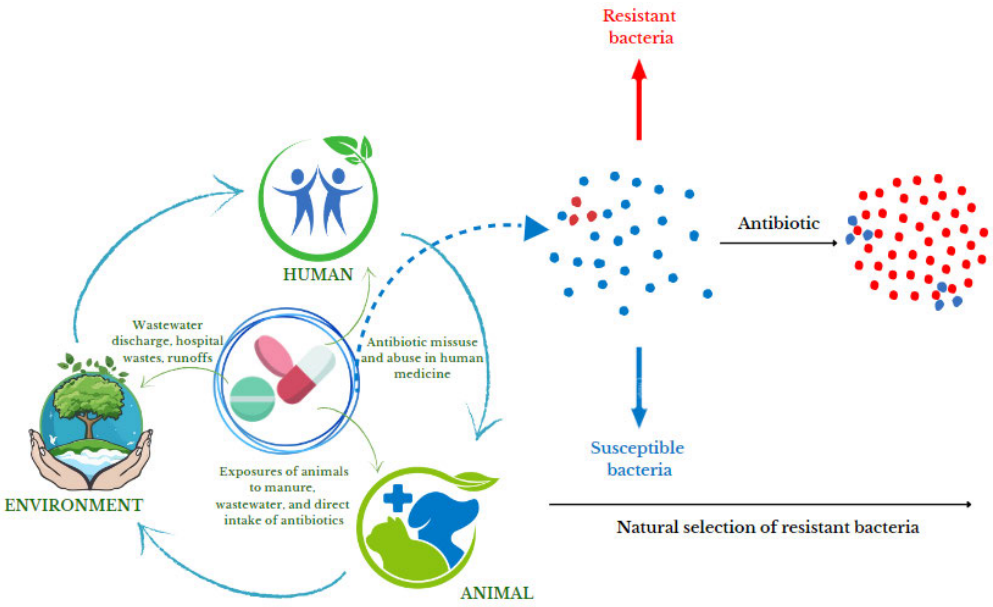

Figure 2. Distribution of ARGs through human, animal and environmental habitats providing an excellent opportunity for promoting AR

1.2.3. ENVIRONMENTAL METAGENOMICS

The determination of limits for microbiological parameters in bathing water is governed by the EU Directive on bathing water [63] which is incorporated in Croatian legislation through Regulation on Sea bathing water quality [64]. While this screening method is considered as 'the golden' standard, it relies on conventional approaches that assess seawater quality by quantifying indicator bacteria (*Escherichia coli* and intestinal enterococci). However, this method offers only a limited comprehension of environmental health. These traditional methods are time-consuming and yield information for less than 1% of cultivable bacteria [65]. To address these limitations, recent years have witnessed the growing adoption of advanced molecular biology and computer analysis techniques in environmental microbiology [66,67].

Slow growth with specific requirements, microbial competition and environmental stressors affect the bacterial culturing processes, remaining 80% of human gut bacteria and 99% of environmental bacteria being uncultured [68,69]. However, Next-generation sequencing (NGS), a powerful tool based on DNA sequencing directly from environmental samples [67], has found diverse applications, while enhancing our current understanding and generating novel insights across various environmental microbiology domains. Specifically, 16s rRNA amplicon sequencing can elucidate bacterial and archaeal community structures, while shotgun sequencing is able to assess information about viral communities, ARGs and MGE as well [70,71]. Metagenomics ensures non-targeted approaches to describe complex

microbial communities and associations between such microorganisms in the environment. It enables the study of both, culturable and non-culturable bacteria, overcoming the limitations of laboratory isolation and cultivation. In this way, new insights about the current understanding of microbial community structure, richness and distribution are and will be more provided [72]. Moreover, such a non-targeted approach has the potential for a wider application in public health surveillance as an early warning system [73].

After NGS became commercially available in 2005, it evolved into a standard technique driven by the quest to compare different domains (especially the environment associated with the human gut) [74,75]. Consequently, various statistical analyses have been developed and used [76–78], and additionally, the comprehensive reference genome catalogue of the human microbiome has been compiled [79]. However, as the cost of NGS methods decreased, their application was no longer limited to the human gut, but was also used in other habitats (aquatic environment, WWTPs, animal microbiome, etc.). This led to several studies that provided insights on species or operational taxonomic units (OTUs), a species-like concept, conceived to explain the clusters obtained by NGS. These methods provided valuable new insights into species diversity around the world and how these communities change in response to environmental changes, as mentioned in earlier chapters.

1.3.CARBAPENEM RESISTANCE REMAINS IN HOSPITALS?

Over the past decade, the alarming and widespread dissemination of gram-negative bacteria resistant to Beta-lactam (β-lactam) antibiotics, notably carbapenems, has emerged as an imposing public health concern, transcending national boundaries and triggering a global alarm. Carbapenems, regarded as the last line of defence against infections caused by MDR bacteria [80], now face a dire threat from carbapenem-resistant bacteria, particularly those from the *Enterobacteriaceae* family (CRE). This has established itself as one of the most critical threats to public health [81,82]. Of particular distress is the limited progress in the development of antimicrobial drugs, especially for gram-negative pathogens [47].

Enterobacteria, commensals of the digestive systems of humans and animals and integral members of the normal intestinal flora, exhibit a dual nature, as particular species can also manifest as opportunistic human pathogens causing an array of diseases. These pathogenic species make up 70% of all infections caused by Gram-negative bacteria, and it includes infection of different human body systems (urinary, respiratory, gastrointestinal, etc.) with various organisms responsible for those diseases (*E. coli*, *Acinetobacter baumannii*, *Pseudomonas aeruginosa* and different *Klebsiella*, *Proteus* and *Enterobacter* species) [83]. The majority of these Gram-negative bacteria are resistant to multiple classes of antibiotics and are increasingly becoming resistant to almost all available antibiotics worldwide [84].

β-lactams are frequently used antibiotics worldwide, and several antibiotics, including penicillins, cephalosporins, monobactams and carbapenems, belong to this class. They all share the common beta-lactam ring and act mostly by binding and inactivating the penicillin-binding proteins (PBPs), responsible for bacterial cell wall formation. Among all β-lactams, carbapenems (ertapenem, imipenem, meropenem, and doripenem) are the most potent members against Gram-negative and Gram-positive bacteria. Their structure ensures stability and effectiveness against most β-lactamases, enzymes which inactivate β-lactams, including AmpC beta-lactamases (AmpC), and the extended spectrum β-lactamases (ESBLs) [85]. Due to their wide and safe use, it is clear why the problem of carbapenem resistance is a globally disseminated problem. Therefore, in 2017, the WHO classified CRE in the highest-critical category among priority groups for multi-resistant pathogens requiring urgent drug discovery [44].

Resistance to carbapenems may be caused by different mechanisms (augmented drug efflux, a mutation in or loss of outer membrane porins, and production of carbapenemases), however, it primarily arises from the production of bacterial carbapenemases, enzymes that hydrolyse carbapenems, rendering them ineffective [86,87]. As mentioned earlier, the problem of AR is ancient and naturally founded in some species, and thus, carbapenem resistance is found intrinsically in some species like *Stenotrophomonas maltophilia, Aeromonas* spp., *Chryseobacterium* spp., and *Bacillus* spp. They possess intrinsic chromosomal β-lactamases, and therefore the use of carbapenems in a treatment for infections caused by those bacteria is not an option. Intrinsic carbapenem resistance is less common among clinically significant gram-negative bacterial species, yet it is often a result of mutational events or horizontal gene transfer. These acquired carbapenemases are classified into three molecularly distinct classes: A, B, and D (Figure 3). The respective genes are capable of dissemination among bacterial populations through mobile genetic elements such as plasmids, transposons, and integrons [88,89]. In class A, a plasmid-mediated *K. pneumoniae* carbapenemase (KPC) is the most important, as it is the most prevalent and widely distributed carbapenemases [90]. Metallo-β-lactamases (MBLs) are part of Class B carbapenemases, not inhibited by avibactam, normally used for carbapenemase-producing *Enterobacteriaceae* (CPE) infections. Finally, in class D are counted plasmid-mediated oxacillin-hydrolyzing β-lactamases (OXA) i.e. OXA-48, OXA-23 and other derivatives, of which some are frequently found in Europe countries [91]. The first report about CPE was back in the early 1990s [92], and from that, CPE has spread all across the world [93].

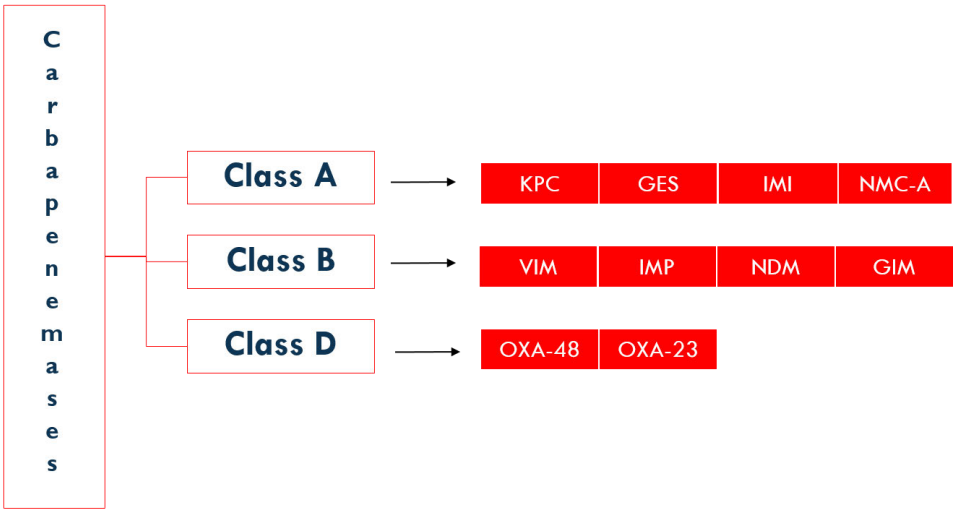

Figure 3. Molecular classification of acquired carbapenemases

While CRE presents a therapy challenge for patients, CPE poses a more significant issue for infection prevention and treatment. This is due to carbapenemase production in CPE, often facilitated by plasmids, enabling bacteria to transfer carbapenem resistance genes to other clinically pertinent species. Consequently, this hampers treatment options for various organisms, such as other *Enterobacteriaceae*, *Pseudomonas,* or *Acinetobacter*.

Information on ARGs in coastal areas is still scarce and mostly without mechanisms to explain certain significant relationships between environmental factors and ARGs. Moreover, it is difficult to make predictions about the impact of AR on environmental and health risks due to a lack of data [51]. However, it is clear that AR determinants occur in different environments, especially those under anthropogenic pressure, and WWTP effluents are considered to be important pathways for their spread. Besides WWTPs generally, hospital wastewaters (HWWs) play an important role in the spread of AR determinants as they are enriched with various ARBs and ARGs. However, only a few countries have recommended additional treatments for HWWs, although the enrichment of ARB are found through WWTPs [94–96]. Several studies have shown the spread of various CRE from WWTPs to the environment: CR *K. pneumonia*, [48,97,98], *E. coli* [97,98], *Citrobacter freundii* [99], etc. However, most of them have been found in freshwater rather than marine ecosystems. So far, carbapenemases have been identified in various pathogens worldwide, both in hospitals and outside hospitals [100].

In Croatia, *Enterobacteriaceae* producing KPC carbapenemase were first detected in hospitals in the northern part of the country [101], followed by observations in the southern region [102]. Notably, within Croatian hospitals situated in Zagreb and Split, the carbapenemases VIM and KPC exhibit the highest prevalence. Specifically, VIM-1 predominates in clinical *Enterobacteriaceae,* while KPC-2 is identified in *K. pneumoniae* [103,104]. In the natural environment of Croatia, the only case of KPC-producing *K. pneumoniae* was discovered in the Krapina River, downstream from the wastewater outlet of the Zabok General Hospital, indicating the hospital environment as its source [105].

A comprehensive review of the scientific literature shows that the focus is rather on CPE in hospitals, WWTPs, and freshwater ecosystems, while their occurrence in the marine environment has been insufficiently studied. Certainly, the effects of submarine discharges, especially in the near-field zone, have been insufficiently studied in the context of metagenomic analysis and the global problem of AR. Moreover, no research has been

conducted in Croatia on this critical issue. Considering the fact that AR is an urgent public health challenge on a global scale, it is essential to emphasise the importance of environmental research as highlighted by WHO under the One Health concept. Furthermore, the escalating trend of KPC-producing *Enterobacteriaceae* in hospitals in the Republic of Croatia points to their possible presence in the environment. This dynamic adds further motivation for this dissertation, which seeks to address the aforementioned global predicament and its growing impact within Croatia.

2. AIM AND SCOPES OF THE THESIS

Coastal areas under intense anthropogenic influence have emerged as significant reservoirs of bacterial resistance to antibiotics, where microbial community structure serves as an indicator of adverse influences. Framed within the One Health concept and considering the continuous increase of global AR, this research aims to provide new insights into the influence of submarine discharges on the spread of ARGs and resistant opportunistic pathogens in the coastal marine environment. Simultaneous analysis of the water column under the influence of the submarine outfall, by using fast-profiling probes and various molecular methods will provide solid insights into the extent to which WWTPs contribute to the spread of AR in the coastal marine environment.

Aims of this study:

1. Determination of the stability and quality of the water column by vertical profiling with multiparameter probes. Description of the effluent shape and behaviour by analysing physico-chemical parameters (temperature, salinity, density, buoyancy frequency (Brunt - Väisälä frequency), chlorophyll *a*, turbidity, colored dissolved organic matter and dissolved oxygen)
2. Assessment of the biodiversity of the coastal marine bacterial community under the pressure of wastewater discharge through submarine outfalls using modern Next Generation Sequencing (NGS) methods
3. Analysis of the repertoire of ARGs available to the bacterial community using bioinformatics tools and shotgun sequencing
4. Analysis of the CRE genome with particular emphasis on resistance genes, virulence factors and types of resistant plasmids using the Whole Genome Sequencing (WGS) and appropriate bioinformatics tools

Main hypothesis from which this study proceeds:

H1: Vertical profiling of physico-chemical parameters using in-situ profiling probes will provide information on the effluent upwelling to the surface of the water column and provide better insight into the behaviour of the effluent plume

H2: Unstratified conditions allow effluent to upwell to the surface, leading to microbiological contamination of the surface layer of the water column

H3: Both the surface and bottom layers of the water column are under the influence of wastewater, as indicated by the composition of the microbial community, which is dominated by taxonomic groups characteristic of the human digestive tract and whose commensals also dominate the composition of the microbiome in WWTPs around the world

H4: There is a difference in the composition of the microbiome at the locations of the two different outfalls, suggesting that the composition of the effluent shapes the recipient microbial community

H5: The dissemination of carbapenem-resistant and carbapenemase-producing *Enterobacteriaceae* is facilitated by hospital wastewater, as indicated by the elevated prevalence of antibiotic-resistant opportunistic pathogens detected at the outfall which WWTP treats hospital effluents

H6: The most abundant antibiotic classes and ARGs in WWTPs reflect the most used antibiotics in Croatian community and hospitals

H7: WWTPs have limited removal efficiency, with the purification properties of seawater emerging as the predominant factor in the dilution of the effluent plume.

Specific scientific questions:

- What bacterial populations are prevalent at the bottom and surface of the water column at submarine outfall locations?
- Are clinically significant human pathogens such as *E. coli*, *K. pneumoniae*, *C. freundii*, and *A. baumannii* present at selected localities? If found, do they have lower susceptibility to antimicrobial drugs?
- Are there similarities between the carbapenem-resistant strains isolated in this study and clinical isolates at KBC Split or other hospitals in Croatia?
- Which classes of antibiotics and ARGs are the most abundant in both WWTPs and marine ecosystems? How much the concentration of pollutants (*E. coli*, intestinal enterococci, ARGs etc.) decreases during the treatments?

Scientific contribution:

The analysis of the environment, particularly those influenced by wastewater exposure, is extremely important for biodiversity preservation, environmental quality, and human well-being. Current public health challenges include monitoring of AR pathogens and the ubiquitous presence of ARGs, which exhibit robust survival within WWTPs. However, critical knowledge gap persists concerning the impact of submarine outfalls on the water column quality, with the specific focus on metagenomic analyses and the global distribution of ARGs.

This PhD thesis endeavours to make a scientific contribution, expanding existing knowledge and opening new perspectives on submarine outfalls as important epidemiological sources as well as potential hotspots of environmental pollution by ARB and ARGs. Furthermore, analyses such as these fit seamlessly into the One Health concept initiated by WHO revealing the intricate interdependencies between human, animal, and environmental health. Understanding the impact of submarine discharges on water column stability, microbial diversity and the spread of ARGs as well as AR human pathogens is important worldwide to assess the consequences for human health and to effectively control the problem of further resistance development. The results of this research can serve as a basis for a comprehensive risk assessment and the formulation of holistic strategies. These strategies in turn serve a dual purpose: reducing pollution and improving the protection of human health, both locally and globally.

3. SCIENTIFIC PAPERS

3.1. Spatial and temporal vertical distribution of chlorophyll in relation to submarine wastewater effluent discharges

Reproduced from:

Kvesić, M., Vojković, M., Kekez, T., Maravić, A., Andričević, R., 2021. Spatial and Temporal Vertical Distribution of Chlorophyll in Relation to Submarine Wastewater Effluent Discharges. Water 2021, 13, 2016. https://doi.org/10.3390/ w13152016

The distribution of chlorophyll *a* in coastal waters is influenced by various factors, including hydrodynamics, biotic and abiotic processes. Spatial and temporal variations in chlorophyll *a* profiles provide valuable insights into changes occurring in the marine environment. Therefore, this study aims to characterise the vertical distribution of chlorophyll *a* and describe its variability as a function of factors such as stratification conditions and the presence of wastewater effluent. By obtaining high resolution data, these modern fast-profiling probes have been able to successfully describe the stability of the water column and the different vertical chlorophyll *a* profiles.

In addition to the successful use of fast-profiling probes in describing the characteristics of the effluent plume and the consequences left behind after intrusion (in terms of changes in physico-chemical parameters), these techniques can also be used to obtain real-time data and identify possible locations where wastewater has been discharged and could cause microbiological pollution and pose a health risk to humans. Such an application is used as a method to locate the effluent plume and perform sampling at that location. The results are discussed in the chapter ‘Additional results’.

water

MDPI

Article

Spatial and Temporal Vertical Distribution of Chlorophyll in Relation to Submarine Wastewater Effluent Discharges

Marija Kvesić [1,2,*], Marin Vojković [1], Toni Kekez [3], Ana Maravić [4] and Roko Andričević [1,3]

[1] Center of Excellence for Science and Technology-Integration of Mediterranean Region, University of Split, 21000 Split, Croatia; mvojkovic@gradst.hr (M.V.); rokoand@gradst.hr (R.A.)
[2] Doctoral Study of Biophysics, Faculty of Science, University of Split, 21000 Split, Croatia
[3] Faculty of Civil Engineering, Architecture and Geodesy, University of Split, M. Hrvatske 15, 21000 Split, Croatia; tkekez@gradst.hr
[4] Department of Biology, Faculty of Science, University of Split, R. Boškovića 33, 21000 Split, Croatia; amaravic@pmfst.hr
* Correspondence: mkvesic@unist.hr

Abstract: The vertical distribution of chlorophyll in coastal waters is influenced by a combination of the hydrodynamic environment and different biotic and abiotic processes. The spatial and temporal occurrences of chlorophyll profiles provide a good representation of the changes in the marine environment. The majority of studies in the Adriatic Sea have so far been conducted in areas unaffected by anthropogenic pressure. Our study site is located near two marine outfalls, which are part of the public sewage system. This study aims to characterize the chlorophyll vertical distribution and describe its variability based on the stratification conditions and the presence of a wastewater effluent plume. Based on these conditions, we identified three characteristic scenarios/types of chlorophyll profiles. The first one occurs when the vertical mixing of the water column creates the upwelling of chlorophyll and nutrients to the upper part of the water column. The second and third scenarios occur during stratified conditions and differ by the extent of the effluent plume intrusion. Using modern fluorescence techniques, we identified and described three different vertical chlorophyll profiles, characterizing them according to their physical and biological parameters and processes. For cases with a visible effluent intrusion, we confirmed the importance of the pycnocline formation in keeping the effluent below and maintaining the higher water quality status at the top of the water column.

Keywords: chlorophyll vertical profiles; stratification; wastewater effluent plume intrusion

Citation: Kvesić, M.; Vojković, M.; Kekez, T.; Maravić, A.; Andričević, R. Spatial and Temporal Vertical Distribution of Chlorophyll in Relation to Submarine Wastewater Effluent Discharges. *Water* **2021**, *13*, 2016. https://doi.org/10.3390/w13152016

Academic Editors: Sabina Susmel, Elisa Baldrighi, Maja Krzelj, Josipa Bilic, Viviana Scognamiglio and Mauro Celussi

Received: 15 June 2021
Accepted: 21 July 2021
Published: 23 July 2021

1. Introduction

Phytoplankton has a major influence on marine ecosystems because of its role in oxygen production and overall significance in supporting and maintaining marine life. Due to the challenges in the direct measuring of phytoplankton, chlorophyll *a* is mainly used as a proxy for phytoplankton biomass [1–5]. Traditional techniques for chlorophyll analysis are based on bottle sampling, which is limited in terms of obtaining a high spatial and temporal resolution. This was corrected by modern in situ fluorescence techniques and remote sensing observations, which allow for measurements of chlorophyll in a high resolution. The research on chlorophyll temporal and spatial variability in the Mediterranean Sea is mostly restricted to the surface, as most of the collected data come from satellite observations and ex-situ laboratory measurements [5]. The oligotrophic status of the Mediterranean basin [6], with a decreasing trend from west to east [7,8], and seasonal and interannual variability [4,9,10] were observed based on surface chlorophyll analysis.

The vertical distribution of chlorophyll is under the influence of many biotic and abiotic processes, whose interplay affects the depth of the upper mixed layer and controls

the vertical chlorophyll distribution [4,11]. So far, information about vertical chlorophyll profiles has been derived from different kinds of measurements [12–23].

A similar chlorophyll seasonality was noticed in the Adriatic Sea by remote sensing observations [24–26] and laboratory measurements [27,28]. The Adriatic Sea is a semi-enclosed basin of the Mediterranean Sea, where the biogeochemical parameters are influenced mainly by the circulation of the water masses. The chlorophyll trends in the Adriatic Sea have been investigated by remote sensing [29–31] and laboratory-based measurements [27,32] to find deep chlorophyll maxima [28,33] and to investigate the anthropogenic impact on the phytoplankton community structure and abundancy [34–36].

Coastal waters are highly sensitive ecosystems and may become even more vulnerable when exposed to the negative impact of human activities. Wastewater effluents contain high concentrations of pollutants, which can cause a large amount of deterioration to marine environments [37]. Bacteria are the most abundant and diverse group of organisms living in wastewater [38,39], and bathing water status is mainly determined using fecal indicator bacteria (FIB) as indicators of water quality and related human health issues [40,41]. Besides fecal pollution, eutrophication is another important aspect of coastal water quality. Since primary producers are the first components of an ecosystem to react to an increase in nutrient concentration, phytoplankton biomass is considered a good indicator of the trophic state of coastal water [42]. Changes in phytoplankton biomass abundance occur following nutrient enrichment, which can happen naturally (through riverine influence or the upwelling of nutrients from the bottom) or under anthropogenic influence (urban and industrial wastewater discharges and surface runoff). Anthropogenically introduced nutrients are the major problem of coastal ecosystems [43,44], and their mixing with seawater contributes to the eutrophication of coastal zone waters [45], thus increasing the biomass of macroalgae and seston algae [46].

This paper aims to characterize chlorophyll vertical profiles and describe their spatial and temporal variability based on the stratification status of a water column and the presence of a marine wastewater effluent plume. Due to the nature of fluorescence measurements, which change with the taxonomic species or environmental conditions [47] and can be affected by dissolved materials [48] or by different light irradiation statuses [49–51], the present study is focused on the relative distribution of vertical chlorophyll fluorescence in a water column by comparing different segments of the water column for each considered profile. To our knowledge, this is the first classification of chlorophyll vertical profiles in the presence of a wastewater effluent plume. The spatiotemporal variability of the different vertical profiles concerning stratification was also investigated.

2. Materials and Methods

2.1. Study Site

The study area is the eastern central Adriatic Sea, near the city of Split in Croatia (Figure 1). Two main marine wastewater outfalls are located within the study area, about 5 km away from each other, as a part of the Split–Solin public sewage system.

The submarine outfall at Location 1 discharges treated wastewater from the Kaplinića brig wastewater treatment plant (WWTP) via a Ø 800 mm pipeline, ending with two diffuser sections 1.3 km away from the shore at a 43 m depth. The Kaplinića brig WWTP is designed for the mechanical treatment of both municipal and rainfall-runoff wastewater, with a capacity of 122.000 population equivalents (PE) and an average flow rate equal to 35.000 m^3/day approximately.

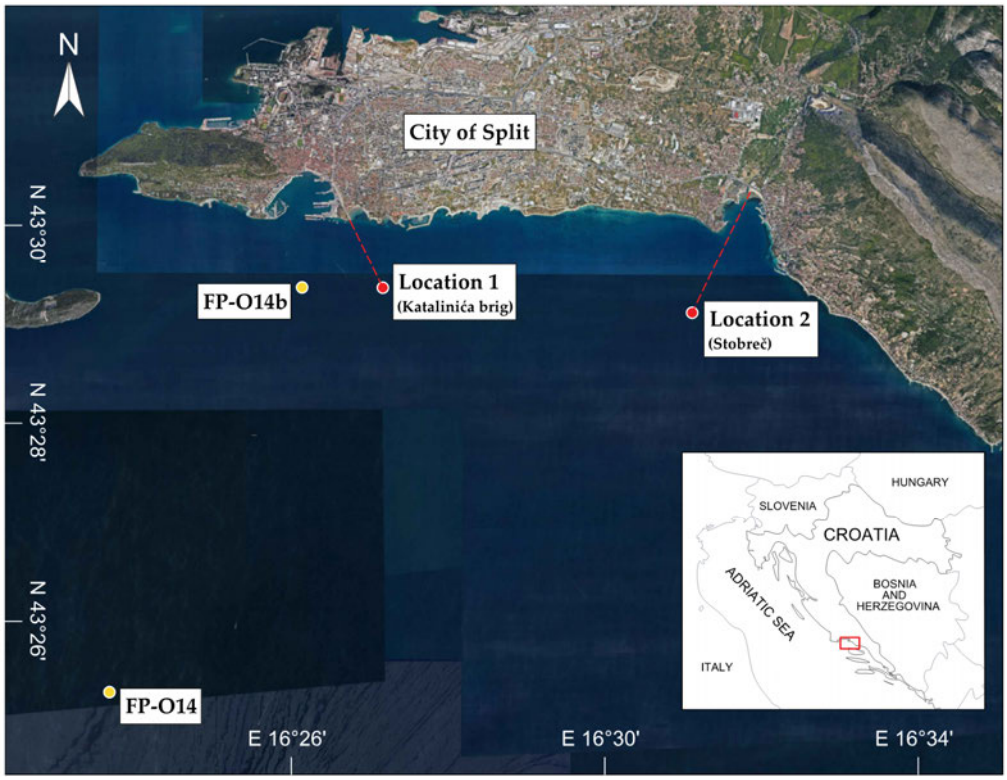

Figure 1. Locations of marine wastewater outfalls and national monitoring program stations.

The marine outfall at Location 2 (Stobreč) discharges the wastewater coming from the Stupe WWTP, where the wastewater is mechanically treated, along with grit and grease removal. The Stupe WWTP facility is designed for municipal wastewater only, with a capacity of 138.000 PE and an average flow rate equal to 30.000 m^3/day. The length of the submarine outfall Ø 900 mm pipeline is 2.76 km, with a 200 m long diffuser section ending at a 37 m depth.

Additionally, the monitoring of different physical and chemical parameters is performed several times a year, at stations FP-O14 and FP-O14b, as shown in Figure 1, as a part of the national monitoring program.

To understand the background of the wastewater being discharged into the seawater, we provide data (Table 1) about the seasonal flowrate and available water effluent parameters for two WWTPs.

Table 1. Available data for two WWTP locations, considering the average discharge (m^3/day) and different wastewater effluent parameter concentrations (mg/L), presented as the mean ± standard deviation.

Location/ Parameter	Q_{SUMMER} (m^3/Day)	Q_{WINTER} (m^3/Day)	COD (mg/L)	BOD (mg/L)	TSS (mg/L)	TN (mg/L)	TP (mg/L)
Stupe	30.000	26.000	372 ± 235	199 ± 113	89 ± 59	52 ± 15	6 ± 1.5
Katalinića brig	38.000	34.000	246 ± 107	135 ± 58	69 ± 38	32 ± 5	4 ± 2

2.2. Sampling Methodology

This study was performed during the implementation of the Interreg Italy–Croatia project AdSWiM (Managed use of treated urban wastewater for the quality of the Adriatic Sea). The measurements were performed with the CTD fast profiling probe (The Sea & Sun Technology) and C3 fluorometer during sampling sessions conducted with a boat (Nautica 600) every month from February to September 2020 (with the exception of March and August due to the COVID restrictions).

CTD fast profiling probe, with an additional sensor for dissolved oxygen (model: 48M), was used for temperature, salinity, density anomaly, and dissolved oxygen measurements. The temperature is measured by a classical resistance thermometer using a platinum resistor, while the salinity is calculated from the seawater conductivity using a 7-poll cell sensor. The density anomalies were calculated automatically by the CTD/DO probe internal software using the international thermodynamic equation of seawater-2010 [52]. The dissolved oxygen sensor works on the principle of a Clark electrode. The depth is calculated from the pressure, measured by a strain gauge, and is converted to depth as 1dbar = 1 m. The turbidity, chlorophyll, and colored dissolved organic matter (CDOM) were measured using a C3 Submersible fluorometer (Turner Design). The chlorophyll measurements were performed with a blue mercury lamp, with a peak emission at 460 nm, and the fluorescence was collected at 680 nm. The CDOM was measured using a UV LED (CWL: 365 nm), with a peak emission at 350 nm and fluorescence collection at 450 nm. The turbidity was measured with the IR lamp, with a peak emission at 850 nm, and the collection of scattered light at 90°. Since the relationship between phytoplankton biomass and chlorophyll fluorescence is highly variable and depends on the physiological state and community composition [53–55], in this study, we focused on the general distribution of chlorophyll profiles in the water column concerning the stratification and effluent discharge.

The fecal pollution was estimated by the level of FIB. The FIB concentration was assessed by the membrane filtration method and the enumeration of fecal coliforms (*E. coli*) [56,57] and intestinal enterococci (ENT) [58], as indicated in the Croatian legislation (Regulation on the Quality of Marine Bathing Waters; OG 73/08). The number of viable heterotrophic bacteria was determined using the spread plate method. An automated Protos3 colony counting system (Synbiosis, UK) was used to determine the bacteriological concentration. Sampling was conducted from the boat using a Niskin sampler. The samples were collected in sterile bottles, protected from light in cool boxes, and transported to the microbiology laboratory of the Faculty of Science in Split to be processed within 4 h.

The chlorophyll concentration data at locations FP-O14 and FP-O14b were collected during the regular monitoring performed by the water management agency (Croatia Waters). The chlorophyll *a* concentrations were determined by the laboratory fluorometric method, with filtration through Whatman GF/C glass filters, at 0, 5, 10, 20, and 50 m depths at the FP-O14 location and at 0, 5, 10, and 43 m depths at FP-O14b.

2.3. Data Analysis

The data collection was performed by the vertical profiling of the water column down to 40 m and 35 m depths at location 1 and location 2, respectively. A moving average filter was applied to raw data sampled at a maximum spatial resolution of 3 cm to achieve spatial uniformity. The data were smoothed by a moving average filter, with a 20 cm window.

The vertical distributions of the different layers were examined by calculating the vertical gradients of the density anomalies and derived buoyancy frequency. The buoyancy frequency or Brunt-Väisälä frequency (N) represents the strength of the density stratification and, consequently, the stability of the water column. It is defined as:

$$N = \sqrt{\frac{g}{\rho_0}\frac{d\rho}{dz}} \quad (1)$$

where g is the gravitational acceleration, ρ_0 is the averaged density of the whole water profile, and $d\rho/dz$ is the water density gradient at each sampling step. To identify events when stratification occurred, data points are selected where N^2 exceeds 0.001 s^{-2} as possible pycnocline candidates [59]. The data points are then aggregated if the distance between them was less than 0.8 m, forming a possible pycnocline layer. Layers thinner than 0.8 m are neglected to exclude the impact of anomalous extremes. Aggregated layers are classified as a pycnocline and their profiles as stratified, which potentially aids in the creation of chlorophyll layers. To support the analysis of forming chlorophyll layers under

the influence of marine wastewater discharge, the vertical profiles of dissolved oxygen, turbidity, CDOM, temperature, and salinity are also examined.

3. Results

The main results from six sampling cruises are presented in Figures 2 and 3 for location 1 and location 2, respectively. Each Figure contains six vertical profiles, corresponding to the sampling month with the set of parameters measured. Analysis of the buoyancy frequency showed that stratification occurred in May, June, July, and September for both locations. In February and April, the winter and early spring, lower temperatures induced vertical mixing in the water column. As a result of the strong sea surface warming, the shallowest stratification occurred in July, while the deepest occurred in September. At both locations 1 and 2, the temperature and salinity followed their seasonal pattern, with low gradients in winter and steeper gradients during stratified periods.

3.1. Location 1

3.1.1. February 2020

During the February sampling cruise, the winter mixing of the water column, induced by wind and low temperatures, allowed the upwelling of the bottom seawater rich with nutrients, causing the rise of chlorophyll concentrations from the bottom to the upper layers of the water column (Figure 2, February). The February vertical profiles shown in Figure 2 also depict a slight increase in the turbidity and CDOM around a 25 m depth, probably due to the phytoplankton activity, which can contribute to the organic matter by excreting photosynthetic products or by lysing [60]. The homogeneous vertical dissolved oxygen profile indicates a high oxygen enrichment throughout the water column, mostly as a consequence of the higher oxygen production and water column aeration during the winter weather conditions.

3.1.2. April 2020

The April vertical profiles shown in Figure 2 show a higher concentration of chlorophyll at the bottom, along with higher values of CDOM and turbidity. The observed dip in the dissolved oxygen levels near the bottom indicates the presence of a wastewater plume. To support this hypothesis, the observed high level of fecal pollution is presented in Figure 4. The high levels of *E. coli* and ENT support the dissolved oxygen dip, as bacteria consume oxygen from seawater during the process of decomposition of organic matter from the wastewater plume. The homogeneous vertical profile of dissolved oxygen in the upper part of the water column indicates that the oxygen production exceeds the consumption in that part of the water column.

3.1.3. May 2020

The stratification of the water column started in May. The chlorophyll vertical profile, shown in Figure 2, has no gradients in the upper layer, with a steady increase below the forming stratification point. The increase in the chlorophyll concentration is followed by an increase in CDOM and turbidity. Since the dissolved oxygen profile was homogeneous, we presume that the phytoplankton production of oxygen dominated over the consumption, without any observed effluent effect.

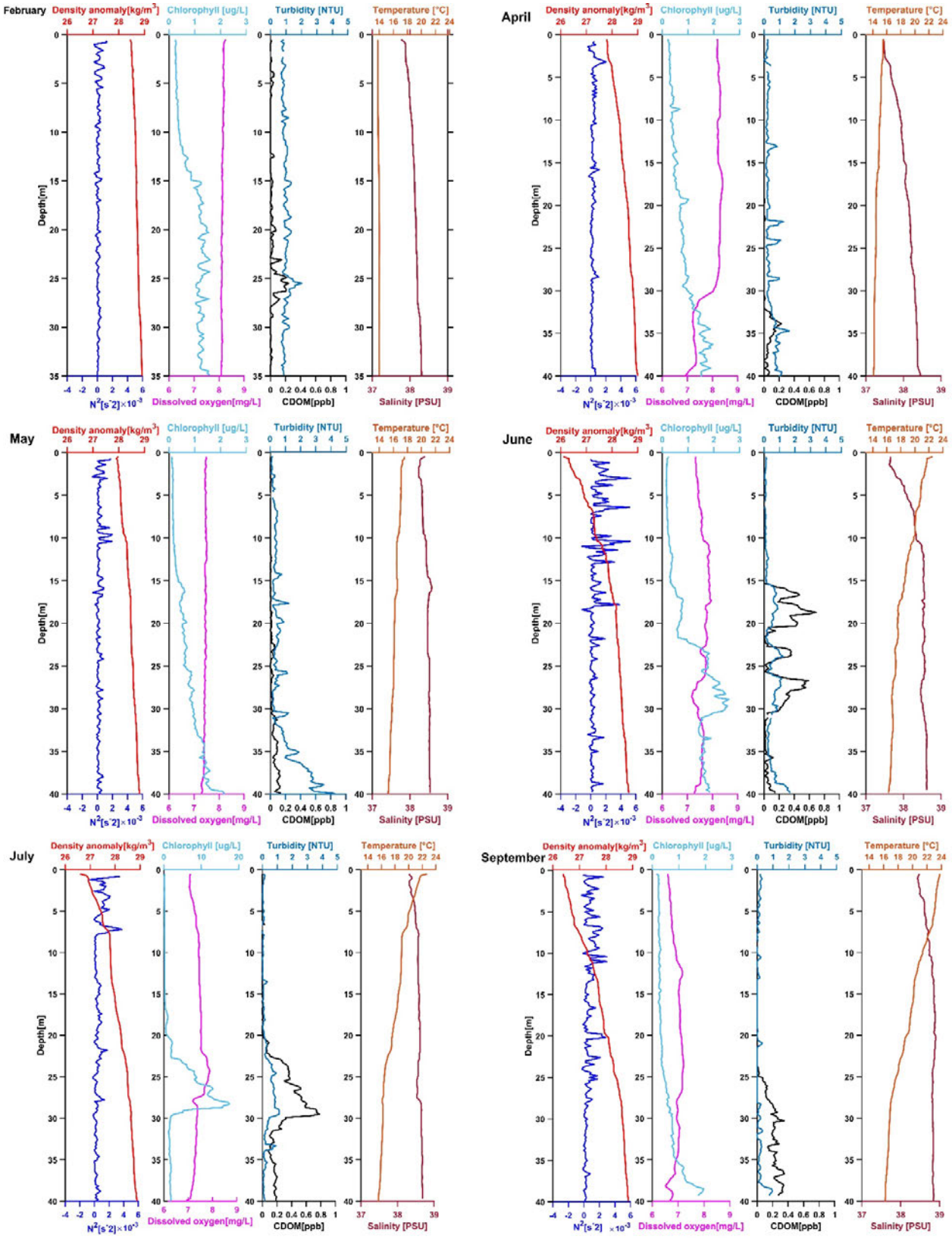

Figure 2. Vertical profiles sampled during 2020 at location 1. The measured parameters are density anomaly (red line), buoyancy frequency (blue line), chlorophyll (light blue line), dissolved oxygen (magenta line), turbidity (green line), CDOM (black line), temperature (orange line), and salinity (brown line).

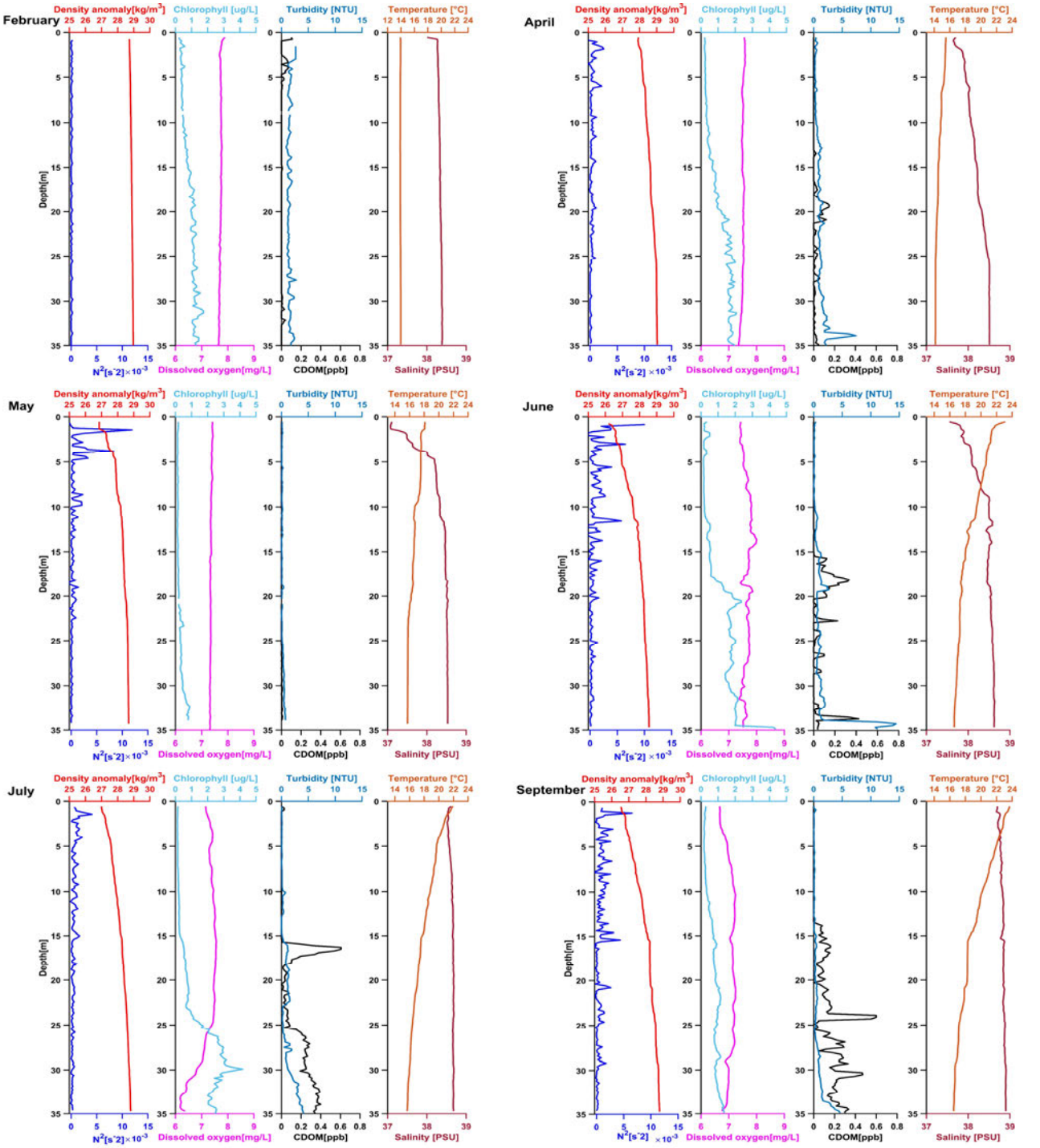

Figure 3. Vertical profiles sampled during 2020 at location 2. The measured parameters are density anomaly (red line), buoyancy frequency (blue line), chlorophyll (light blue line), dissolved oxygen (magenta line), turbidity (green line), CDOM (black line), temperature (orange line), and salinity (brown line).

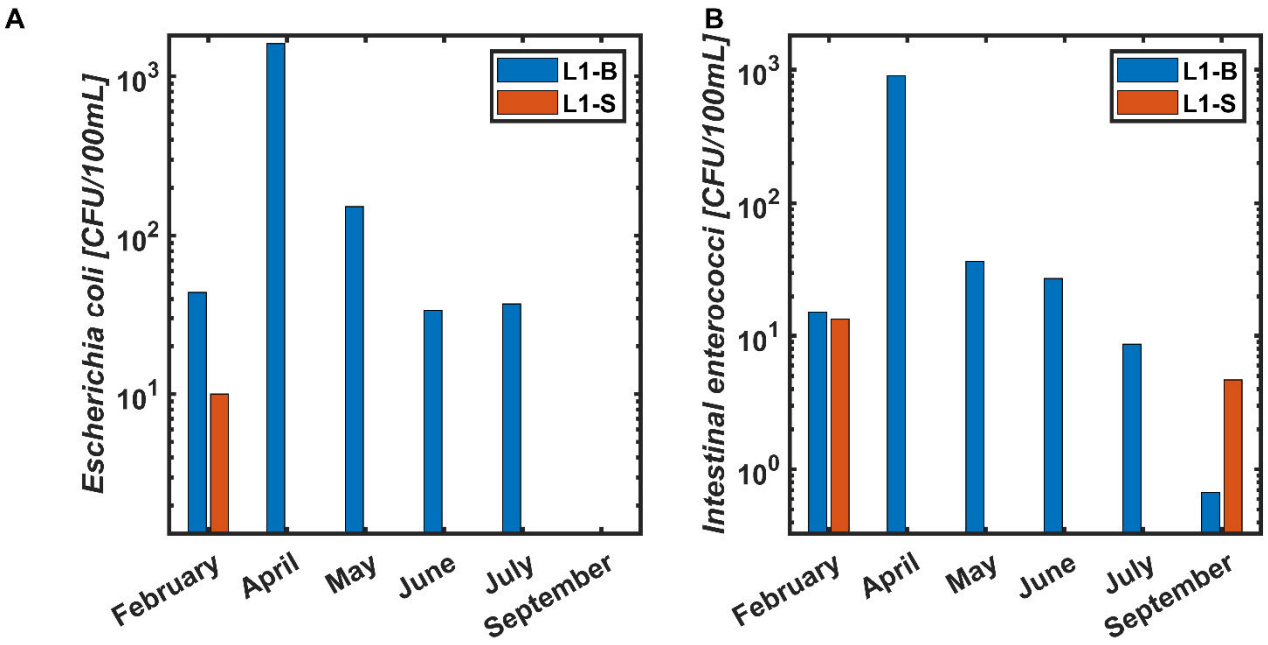

Figure 4. Microbial water quality ((**A**) *Escherichia coli*, (**B**) Intestinal enterococci) at location 1. L1-B refers to location 1 bottom (blue), while L1-S refers to location 1 surface location (orange).

3.1.4. June 2020

During the June sampling cruise (Figure 2), we observe a broad chlorophyll peak with three plateaus, starting below a depth of 15 m. The chlorophyll peaks coincide with the CDOM and turbidity peaks, indicating an effluent plume layer. Consequently, the phytoplankton biomass increases, further contributing to the organic matter concentration and turbidity rise. This increase is matched by a decrease in salinity and dissolved oxygen. The oxygen decrease is a consequence of the bacterial oxidation of organic matter, which is flushed into the seawater by the marine outfall discharge. In the June sampling cruise, the stratification is much steeper, compared to May, and it occurs at a depth of around 18 m.

3.1.5. July 2020

The July vertical profiles shown in Figure 2 show that the chlorophyll vertical profile is not comprised of several plateaus, like the one in June, but has a steep slope on the deeper side and two shoulders on the shallow side. Furthermore, it is present much deeper than the stratification layer, which occurs at a depth of 7 m. The increase in chlorophyll is matched by an increase in CDOM and turbidity values and a decrease in dissolved oxygen and salinity. The observed peaks of different parameters during the July cruise indicate the presence of an effluent plume below the pycnocline. The dissolved oxygen increases down to the 24 m depth and then begins to decline near the chlorophyll peak.

3.1.6. September 2020

The September vertical profiles shown in Figure 2 show the pycnocline presence down to the 22–23 m depth, which was the deepest pycnocline observed during our cruises. Below the pycnocline, at a 25 m depth, an increase in chlorophyll, CDOM, and turbidity is observed, together with a small decrease in dissolved oxygen at the same depth. Near the bottom of the water column, the oxidation of organic matter reduced the dissolved oxygen concentration, indicating that more oxygen was being used than produced. In this case, the deep pycnocline probably submerged the effluent plume, keeping it near the bottom of the water column.

3.2. Location 2

3.2.1. February 2020

During the February sampling cruise, a similar vertical chlorophyll profile occurred at location 2 as that at location 1. The February chlorophyll profile shown in Figure 3 shows a rise in the chlorophyll concentrations from the bottom to the top of the water column. The homogeneous vertical turbidity, CDOM, salinity, and dissolved oxygen profiles indicate the water column mixing. Furthermore, the elevated levels of FIB (Figure 5) at the surface of the water column indicate the effluent rising to the surface of the water column due to the mixing process under the unstratified water column conditions.

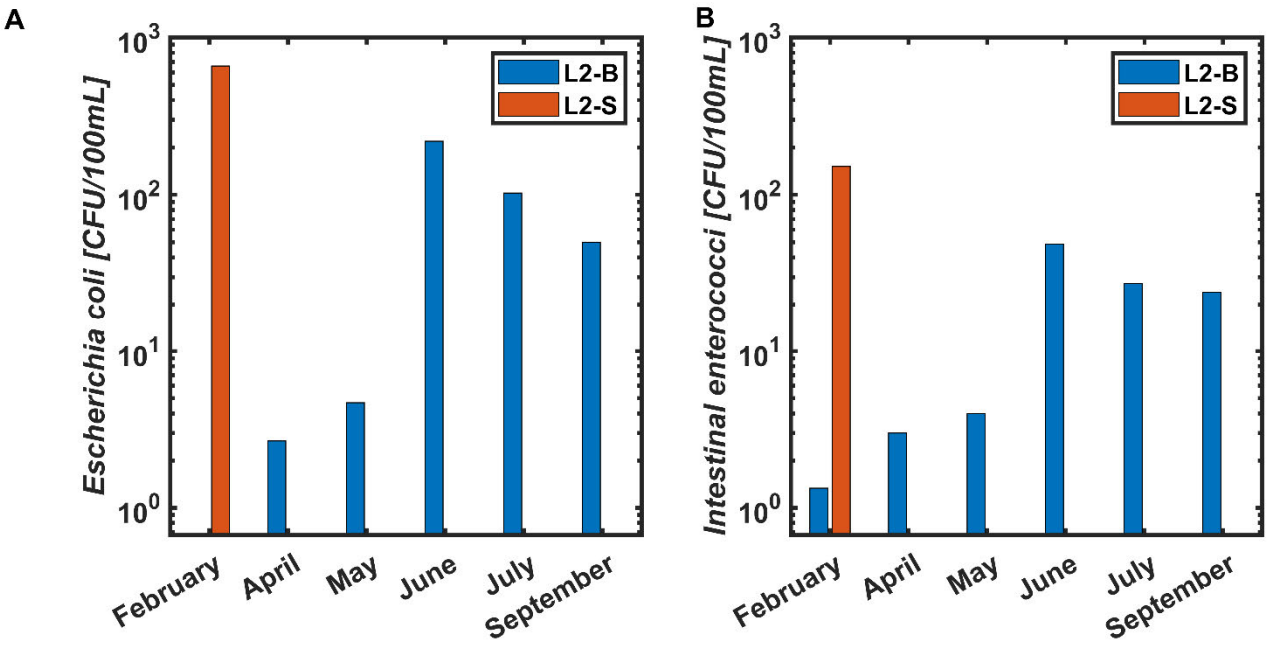

Figure 5. Microbial water quality ((**A**) *Escherichia coli*, (**B**) Intestinal enterococci) at location 2. L2-B refers to location 2 bottom (blue), while L2-S refers to location 2 surface location (orange).

3.2.2. April 2020

The April vertical profiles shown in Figure 3 indicate that the mixing of the water column creates the upwelling of the bottom water, causing a similar vertical chlorophyll profile to the one observed in February. The observed peaks in CDOM and turbidity, within the mixing process, are due to the available nutrients for primary production, resulting in the phytoplankton activity. The homogeneous dissolved oxygen vertical profile indicates a high oxygen enrichment throughout the water column, reflecting surplus phytoplankton production and an aerated water column due to the lack of stratification.

3.2.3. May 2020

Stratification of the water column at location 2 was first observed in May 2020. The observed chlorophyll, CDOM, and turbidity profiles in May 2020 (Figure 3) reveals no significant concentration and/or gradients. Such situations are mostly a consequence of the complex physical, biological, and chemical interactions, together with hydrodynamic processes, particularly due to the fact that the wastewater effluent is only periodically discharged into the sea. However, the May chlorophyll profile, shown in Figure 3, shows an increase in values near the bottom of the water column. The increase in the chlorophyll concentration is matched by a small increase in CDOM and turbidity near the bottom, without a decline in the dissolved oxygen vertical profile. Since the dissolved oxygen profile was homogeneous, we presume that the phytoplankton production of oxygen exceeded the consumption by bacteria.

3.2.4. June 2020

The June vertical profiles presented in Figure 3 show the pycnocline at a 14 m depth, after which an increase in chlorophyll, CDOM, and turbidity is observed. Higher chlorophyll concentrations below a 15 m depth, in conjunction with the CDOM and turbidity increase, indicate the presence of an effluent plume layer accumulated below the pycnocline. The presence of organic matter, together with a higher phytoplankton biomass, leads to an increase in turbidity. Furthermore, the input of organic material contributes to the reduction of available oxygen through bacteria oxidation processes, which is supported by the shape of the vertical dissolved oxygen profile. The reduced salinity at 15 to 20 m depths supports the conclusion that these changes are a direct consequence of the wastewater plume. In comparison to the other months, in June 2020 the highest chlorophyll, CDOM, and turbidity values are measured at the bottom of the water column. The concentration of 220 CFU/100 mL of *E. coli* indicates the presence of an effluent, in agreement with other observed parameters.

3.2.5. July 2020

During the July sampling cruise (Figure 3, July), pycnocline occurred at a very shallow depth of 4 m. Increased values of chlorophyll, CDOM, and turbidity are observed from 15 m to 35 m depths. The observed peaks of chlorophyll, turbidity, and CDOM, with a homogeneously dissolved oxygen profile, down to the 25 m depth, indicate the presence of phytoplankton biomass, producing dissolved oxygen, which prevailed over the consumption. A sharp CDOM peak at the 15 m depth was due to the phytoplankton activity, as no dissolved oxygen decrease was observed at that depth. The decrease in the dissolved oxygen below the 25 m depth indicates that the plume effluent had a more significant effect in this layer. The oxygen consumption during the organic matter decomposition at this depth prevailed over the production, causing an increase of CDOM and turbidity in the bottom layer. The observed concentration of 103 CFU/100 mL for *E. coli* indicates an intrusion of fecal material by the marine outfall. Thus, the July profile showed the characteristics of two competing processes. One is a higher oxygen production from the phytoplankton activity and the other is a higher oxygen consumption from the oxidation of organic material entering the marine system by the wastewater discharge.

3.2.6. September 2020

September vertical profiles in Figure 3 show a homogeneous chlorophyll profile within the upper layer up to the pycnocline at a 15 m depth. Below the stratification, the chlorophyll concentration is increasing towards the bottom of the water column. The organic matter peaks were observed below the pycnocline, while the turbidity increases only near the bottom. As the vertical dissolved oxygen profile shows little variability, we presume that the organic matter reflects phytoplankton activity, indicating that the production dominated over the consumption.

4. Discussion

The majority of the vertical chlorophyll profile studies conducted in coastal region and estuaries are based on laboratory measurements or satellite techniques, lacking direct in situ measurements, especially the influence of marine outfalls. Therefore, this study aimed to identify the chlorophyll vertical profiles under the influence of the water column stratification status and the presence of an effluent plume. Based on the measurement results, we classify the chlorophyll profiles into three types (Table 2). The profiles observed in February and April 2020, with the observed rise of the chlorophyll concentrations from the bottom to the top of the water column, are classified as the Upper Chlorophyll Profile (UCP). The other two profile types are divided between the sampling sessions when stratification of the water column was observed, and they differ by the presence of an effluent plume. In May at both locations and in September at location 2, the vertical chlorophyll profile was characterized by a higher concentration near the bottom, without

a decrease in dissolved oxygen. These profiles are classified as the Bottom Chlorophyll Profile (BCP). The third profile type is characterized by peaks of chlorophyll coinciding with CDOM and turbidity peaks and a matching decrease in salinity and dissolved oxygen, which is a consequence of an effluent plume intrusion. These profiles are classified as the Effluent Chlorophyll Profile (ECP). A summary of this classification is given in Table 2.

Table 2. Vertical profile classification summary.

	Location 1			Location 2		
Month	**Stratification**	**Effluent**	**Type**	**Stratification**	**Effluent**	**Type**
February	X	X	UCP	X	X	UCP
April	X	√	UCP-ECP	X	X	UCP
May	√	X	BCP	√	X	BCP
June	√	√	ECP	√	√	ECP
July	√	√	ECP	√	√	ECP
September	√	√	ECP	√	X	BCP

In unstratified conditions, observed in February and April 2020, at both locations, the upwelling of the bottom, nutrient-rich waters induced a rise in the chlorophyll concentrations from the bottom to the top of the water column, which we classified as UCP. This rise is supported by the CDOM and turbidity vertical profiles, which show only small variations along the vertical column. The bottom water upwelling also resulted in a higher FIB level at the surface, indicating a rise in fecal pollution due to marine outfalls. In unstratified conditions, the dissolved oxygen vertical profiles were homogeneous. This is due to vertical mixing, which allows air–sea gas exchange with the bottom waters and the influence of external forces, such as wind [61]. An exception occurred in April 2020 at location 1 due to an effluent plume intrusion, which decreased the dissolved oxygen values. These conditions induce the characteristics of the chlorophyll profile of both the ECP and UCP (Figure 2). The oxygenation of the water column down to a 30 m depth was due to the primary production of phytoplankton, but it was also due to the unstratified water column, which caused vertical mixing and aeration of the entire water column. At the bottom of the water column, the dissolved oxygen concentration and chlorophyll are inversely correlated, suggesting that the consumption of oxygen dominates over its production. Similar observations have been made in many estuaries with nutrient inputs from rivers [62–67]. Marine outfalls discharge nutrients into the sea, resulting in similar biological processes occurring as those when rivers discharge nutrients into the estuary.

From May to September, stratification occurred at both locations, and the observed profiles are classified as BCP (May 2020, September 2020) and ECP (June 2020, July 2020, September 2020) (Table 2). BCPs are characterized by a higher chlorophyll concentration near the bottom of the water column. This increase is likely due to the phytoplankton activity and resuspension of the bottom sediment, where dead plankton and other sources of organic matter fertilizer, unconsumed food, and fecal matter settle. In May 2020, despite the water column stratification, the vertical distribution of dissolved oxygen was homogeneous, similar to a phenomenon observed in some estuaries, where, under stratified conditions and higher temperatures, hypoxia occurred [68–70]. In our case, hypoxia was never observed, even in summer, but a higher dissolved oxygen variability was present.

To confirm the occurrence of UCP and BCP types in the absence of an effluent plume, we used data from measurements conducted by the Croatian water management agency in the period from 2012–2019, sampled at two locations (FP-O14 and FP-O14b). Both stations are used to represent coastal seawater unaffected by marine outfalls. At both of these locations, during months when no stratification is present, the vertical chlorophyll profile shows upwelling, indicating the existence of UCP (Figures 6 and 7). Under stratified conditions, narrower ranges of the chlorophyll concentrations are observed in the upper part, with the highest values measured at the bottom, which are classified as

BCP (Figures 6 and 7). These data show the existence of UCP and BCP profiles in coastal, unpolluted waters, which follow a seasonal cycle of sea warming and the formation of stratified conditions, and differentiate the naturally occurring chlorophyll profiles from the ones induced by anthropogenic influence.

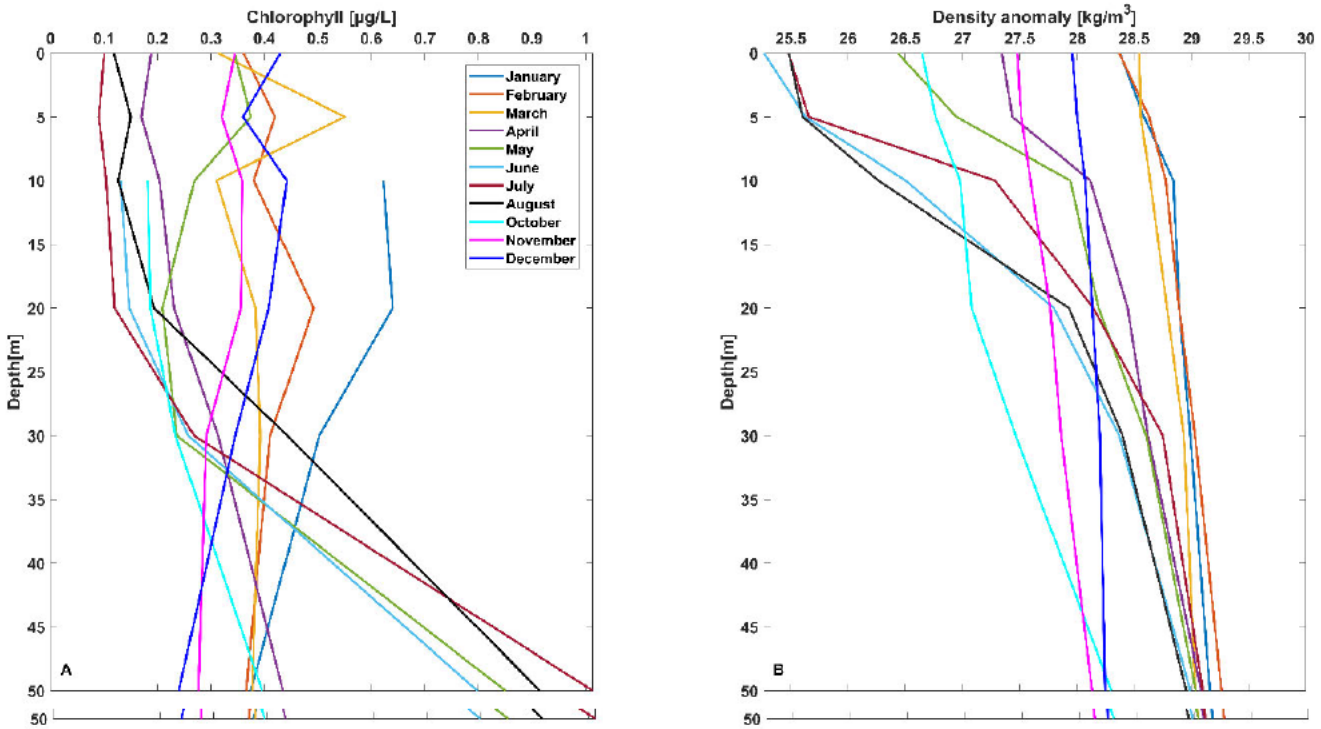

Figure 6. Geometric mean vertical chlorophyll (**A**) and density anomaly (**B**) concentrations observed during the 2012–2019 period at the measuring station, FP-O14.

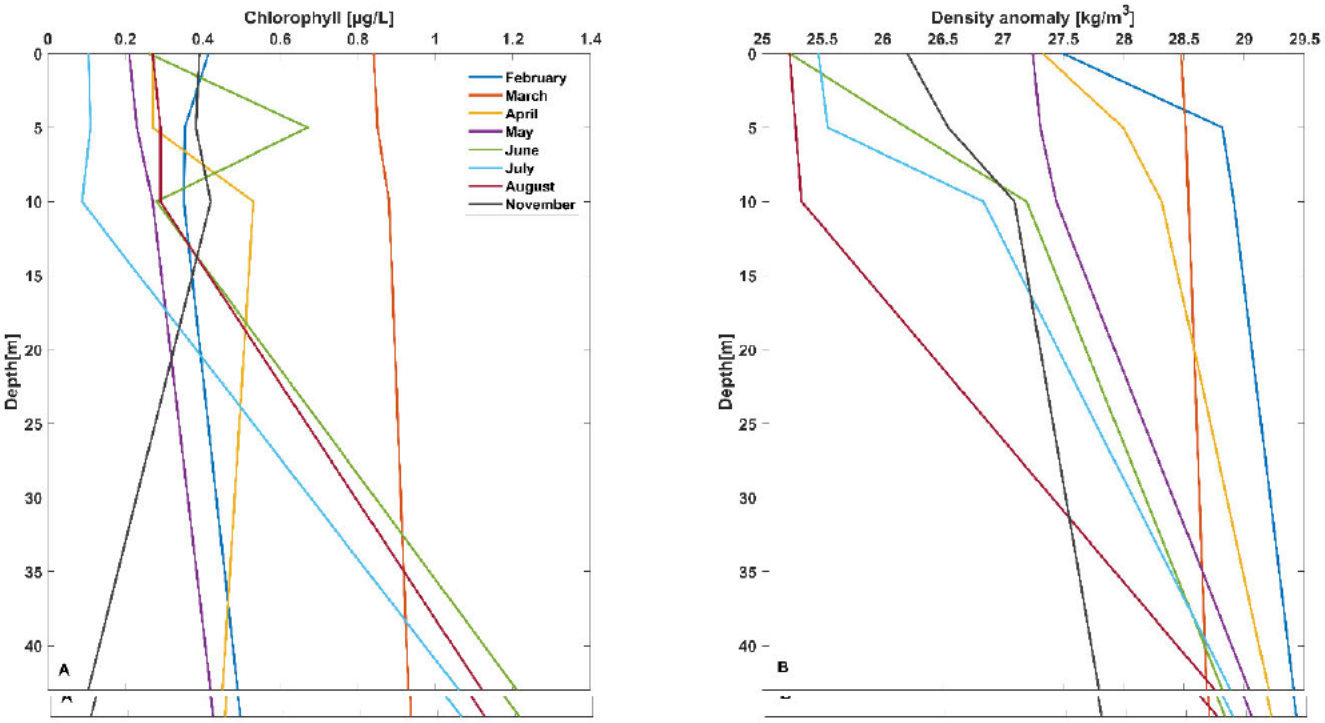

Figure 7. Geometric mean vertical chlorophyll (**A**) and density anomaly (**B**) concentrations observed during the 2012–2019 period at the measuring station, FP-O14b.

The vertical profiles of CDOM, turbidity, dissolved oxygen, and salinity further highlight the difference between ECP and BCP. The nutrient enrichment by marine outfalls induces phytoplankton biomass growth and increases the chlorophyll concentration. The highest chlorophyll concentration observed was at location 1 in July 2020. Such a surge in the chlorophyll concentration could be due to the accumulation of living algae, supported by raw sewage, containing higher amounts of nutrients, especially nitrogen and phosphorus. Besides nutrients, the marine outfalls also discharge organic matter into the coastal waters, resulting in increased organic matter concentrations and turbidity. The increased turbidity levels are the result of the input of organic matter from the wastewater discharge, creating a good condition for the presence of fecal bacteria. The effluent intrusion creates conditions where the oxygen consumption, during the bacterial oxidation of organic matter and decomposition of dead algae and plants, exceeds the production of dissolved oxygen by photosynthesis. The observed decrease in the dissolved oxygen profiles furthermore separates the BCP and ECP types. The gradient of dissolved oxygen with depth (higher concentration above the pycnocline) indicates that stratification may play a role in lowering the oxygen concentration by reducing the gas exchange between the air and sea surface layer [61]. While stratification can influence the dissolved oxygen profile, the homogeneously dissolved oxygen profiles observed in May suggest that the highest variability of dissolved oxygen concentration is due to the influence of a wastewater effluent plume and not stratification. The variations in salinity also supported our hypothesis about the nature of ECP. Similar changes in salinity were previously observed for other submarine outfall sites and provide further evidence of a freshwater input through the outfall system [71–74].

Due to the fact that both WWTPs are discharging a municipal wastewater effluent, the seasonal variations are due to the variations in the residential population of the Split municipal area, which increases during the summer months. Consequently, such changes can influence the wastewater volume. Thus, the summer discharges are approximately 12% higher than those during the winter period, as presented in Table 1. This is also shown in Figures 2 and 3 in terms of an increased concentration and/or gradients of measured parameters. While the discharged wastewater and the seawater start mixing quickly and reaching equilibrium with the surrounding seawater, the salinity profiles may serve as additional information, aiding in distinguishing the chlorophyll profiles. During the observed stratification, the effluent plume was held below the pycnocline, which is generally ecologically favorable, as it maintains a higher quality of the surface waters.

In addition, the circulation in the wider area surrounding the two studied outfalls has a typical barocline current pattern, with relatively larger surface layer velocities due to the regular wind intensities. Furthermore, during the unstratified conditions, the bottom upwelling is intensified, creating the potential for effluent plume surfacing. In such cases, it is expected that surface currents will further contribute to the mixing and spreading of chlorophyl.

5. Conclusions

To study the wastewater impact on the chlorophyll vertical distribution, measurements were performed in the eastern central Adriatic Sea at two locations of marine outfalls, near the city of Split in Croatia. We describe the three vertical chlorophyll profile types, based on the stratification conditions and the effluent plume presence. The water column mixing induced the upwelling of the bottom water, generating UCP and enabling the rise of the effluent towards the surface. In the stratified conditions, categorized as the ECP type, the pycnocline prevents the plume from rising, keeping it in the lower part of the water column, while the BCP type of the profile represents a case when the water column is stratified, but no effluent plume is present. Our categorization of the different vertical chlorophyll profiles is supported by data collected by the Croatian water agency at the locations unaffected by the marine outfalls. All three observed chlorophyll profile types are the consequence of the interplay between the physical, biological, and chemical processes. To distinguish these processes and confidently identify the presence of the effluent plume

we use the FIB measurements, along with dissolved oxygen gradients, to examine the conditions when the oxygen consumption exceeds the production, indicating organic matter oxidation. This, together with the salinity, CDOM, and turbidity measurements, allows us to separate the wastewater influence from the natural processes. We confirm the importance of the stratification in submerging the effluent below the pycnocline, which is highlighted in February 2020, when column mixing allowed the FIB to rise to the surface of the water column. To our knowledge, this is a first study involving in situ vertical measurements coupled with the submarine outfall, analyzing its influence on the vertical chlorophyll distribution.

Author Contributions: Conceptualization, M.K.; Methodology, M.K., M.V., T.K., A.M. and R.A.; Investigations: M.K., M.V., T.K. and R.A.; Writing—Original Draft Preparation, M.K.; Writing—Review and Editing, M.V., T.K., A.M. and R.A.; Visualization, M.K. and T.K.; Project Administration, R.A.; Funding Acquisition, R.A. All authors have read and agreed to the published version of the manuscript.

Funding: The contributions of M.K., M.V. and R.A. were supported by the project, STIM-REI, Contract Number: KK.01.1.1.01.0003, funded by the European Union through the European Regional Development Fund—the Operational Programme Competitiveness and Cohesion 2014–2020 (KK.01.1.1.01). T.K. and R.A. acknowledge the support from the project, CAAT (Coastal Autopurification Assessment Technology), also funded by European Union from European Structural and Investment Funds 2014–2020, Contract Number: KK.01.1.1.04.0064. The contribution of R.A. was supported by the project, COMON (COastal zone MONitoring using multi-scaling methods), funded by European Union from European Structural and Investment Funds 2014–2020, Contract Number: KK.01.1.07.0033. This research is partially supported through project KK.01.1.1.02.0027, a project co-financed by the Croatian Government and the European Union through the European Regional Development Fund—the Competitiveness and Cohesion Operational Programme.

Institutional Review Board Statement: Not applicable.

Informed Consent Statement: Not applicable.

Data Availability Statement: The data are available from the corresponding author, upon a request.

Acknowledgments: The cruise monitoring was completed through the implementation of the Interreg CBC Italy–Croatia project, "Managed use of treated urban wastewater for the quality of the Adriatic Sea" (AdSWiM), by the Faculty of Civil Engineering, Architecture and Geodesy, University of Split. Microbiological data from April 2020 are obtained by the Institute of Public Health Zadar. Seawater data gathered at stations FP-O14 and FP-O14b was provided by the Croatian water management administration (Croatia Waters). We thank Nika Ugrin for her valuable help during the measurement campaigns.

Conflicts of Interest: The authors declare no conflict of interest.

References

1. Lorenzen, C.J. A method for the continuous measurement of in vivo chlorophyll concentration. *Deep Sea Res. Oceanogr. Abstr.* **1966**, *13*, 223–227. [CrossRef]
2. Cullen, J.J. The Deep Chlorophyll Maximum: Comparing Vertical Profiles of Chlorophyll a. *Can. J. Fish. Aquat. Sci.* **1982**, *39*, 791–803. [CrossRef]
3. Palter, J.; Coto, S.L.; Ballestero, D. The distribution of nutrients, dissolved oxygen and chlorophyll a in the upper Gulf of Nicoya, Costa Rica, a tropical estuary. *Rev. Biol. Trop.* **2007**, *55*, 427–436. [CrossRef]
4. Lavigne, H.; D'Ortenzio, F.; Migon, C.; Claustre, H.; Testor, P.; D'Alcalà, M.R.; Lavezza, R.; Houpert, L.; Prieur, L. Enhancing the comprehension of mixed layer depth control on the Mediterranean phytoplankton phenology. *J. Geophys. Res. Ocean.* **2013**, *118*, 3416–3430. [CrossRef]
5. Lavigne, H.; D'Ortenzio, F.; Ribera D'Alcalà, M.; Claustre, H.; Sauzède, R.; Gacic, M. On the vertical distribution of the chlorophyll a concentration in the Mediterranean Sea: A basin-scale and seasonal approach. *Biogeosciences* **2015**, *12*, 5021–5039. [CrossRef]
6. Dugdale, R.C.; Wilkerson, F.P. Nutrient sources and primary production in the Eastern Mediterranean. Oceanologica Acta. In Proceedings of the Oceanographie Pelagique Mediterraneene, Villefranche-sur-Mer, France, 16–20 September 1988; pp. 179–184.
7. Bosc, E.; Bricaud, A.; Antoine, D. Seasonal and interannual variability in algal biomass and primary production in the Mediterranean Sea, as derived from 4 years of SeaWiFS observations. *Glob. Biogeochem. Cycles* **2004**, *18*. [CrossRef]

8. Barale, V.; Jaquet, J.M.; Ndiaye, M. Algal blooming patterns and anomalies in the Mediterranean Sea as derived from the SeaWiFS data set (1998–2003). *Remote Sens. Environ.* **2008**, *112*, 3300–3313. [CrossRef]
9. D'Ortenzio, F.; Ribera d'Alcalà, M. On the trophic regimes of the Mediterranean Sea: A satellite analysis. *Biogeosciences* **2009**, *6*, 139–148. [CrossRef]
10. Volpe, G.; Nardelli, B.B.; Cipollini, P.; Santoleri, R.; Robinson, I.S. Seasonal to interannual phytoplankton response to physical processes in the Mediterranean Sea from satellite observations. *Remote Sens. Environ.* **2012**, *117*, 223–235. [CrossRef]
11. Falkowski, P.; Woodhead, A. *Primary Productivity and Biogeochemical Cycles in the Sea*; Springer: Heidelberg, Germany, 1992; Volume 43, ISBN 0306441926.
12. Macías, D.; Stips, A.; Garcia-Gorriz, E. The relevance of deep chlorophyll maximum in the open Mediterranean Sea evaluated through 3D hydrodynamic-biogeochemical coupled simulations. *Ecol. Modell.* **2014**, *281*, 26–37. [CrossRef]
13. Crise, A.; Allen, J.I.; Baretta, J.; Crispi, G.; Mosetti, R.; Solidoro, C. The Mediterranean pelagic ecosystem response to physical forcing. *Prog. Oceanogr.* **1999**, *44*, 219–243. [CrossRef]
14. Moutin, T.; Raimbault, P. Primary production, carbon export and nutrients availability in western and eastern Mediterranean Sea in early summer 1996 (MINOS cruise). *J. Mar. Syst.* **2002**, *33–34*, 273–288. [CrossRef]
15. Crombet, Y.; Leblanc, K.; Quéuiner, B.; Moutin, T.; Rimmelin, P.; Ras, J.; Claustre, H.; Leblond, N.; Oriol, L.; Pujo-Pay, M. Deep silicon maxima in the stratified oligotrophic Mediterranean Sea. *Biogeosciences* **2011**, *8*, 459–475. [CrossRef]
16. Dolan, J.R.; Claustre, H.; Carlotti, F.; Plounevez, S.; Moutin, T. Microzooplankton diversity: Relationships of tintinnid ciliates with resources, competitors and predators from the Atlantic Coast of Morocco to the Eastern Mediterranean. *Deep. Res. Part I Oceanogr. Res. Pap.* **2002**, *49*, 1217–1232. [CrossRef]
17. Christaki, U.; Giannakourou, A.; Van Wambeke, F.; Grégori, G. Nanoflagellate predation on auto- and heterotrophic picoplankton in the oligotrophic Mediterranean Sea. *J. Plankton Res.* **2001**, *23*, 1297–1310. [CrossRef]
18. Estrada, M.; Marrase, C.; Latasa, M.; Berdalet, E.; Delgado, M.; Riera, T. Variability of deep chlorophyll maximum characteristics in the northwestern Mediterranean. *Mar. Ecol. Prog. Ser.* **1993**, *92*, 289–300. [CrossRef]
19. Casotti, R.; Landolfi, A.; Brunet, C.; D'Ortenzio, F.; Mangoni, O.; Ribera d'Alcalà, M.; Denis, M. Composition and dynamics of the phytoplankton of the Ionian Sea (eastern Mediterranean). *J. Geophys. Res. Ocean.* **2003**, *108*. [CrossRef]
20. Marty, J.C.; Chiavérini, J.; Pizay, M.D.; Avril, B. Seasonal and interannual dynamics of nutrients and phytoplankton pigments in the western Mediterranean Sea at the DYFAMED time-series station (1991–1999). *Deep. Res. Part II Top. Stud. Oceanogr.* **2002**, *49*, 1965–1985. [CrossRef]
21. Psarra, S.; Tselepides, A.; Ignatiades, L. Primary productivity in the oligotrophic Cretan Sea (NE Mediterranean): Seasonal and interannual variability. *Prog. Oceanogr.* **2000**, *46*, 187–204. [CrossRef]
22. Krom, M.D.; Brenner, S.; Kress, N.; Neori, A.; Gordon, L.I. Nutrient dynamics and new production in a warm-core eddy from the Eastern Mediterranean Sea. *Deep Sea Res. Part A Oceanogr. Res. Pap.* **1992**, *39*, 467–480. [CrossRef]
23. Siokou-Frangou, I.; Christaki, U.; Mazzocchi, M.G.; Montresor, M.; Ribera D'Alcala, M.; Vaque, D.; Zingone, A. Plankton in the open mediterranean Sea: A review. *Biogeosciences* **2010**, *7*, 1543–1586. [CrossRef]
24. Barale, V.; Rizzoli, P.M.; Hendershott, M.C. Remotely sensing the surface dynamics of the Adriatic Sea. *Deep Sea Res. Part A Oceanogr. Res. Pap.* **1984**, *31*, 1433–1459. [CrossRef]
25. Barale, V.; McClain, C.R.; Malanotte-Rizzoli, P. Space and time variability of the surface color field in the northern Adriatic Sea. *J. Geophys. Res.* **1986**, *91*, 12957. [CrossRef]
26. Böhm, E.; Banzon, V.; D'Acunzo, E.; D'Ortenzio, F.; Santoleri, R. Adriatic Sea surface temperature and ocean colour variability during the MFSPP. *Ann. Geophys.* **2003**, *21*, 137–149. [CrossRef]
27. Krivokapić, S.; Stanković, Ž.; Vuksanović, N. Seasonal variations of phytoplankton biomass and environmental conditions in the inner Boka Kotorska Bay (Eastern Adriatic sea). *Acta Bot. Croat.* **2009**, *68*, 45–55.
28. Ninčević, Ž.; Marasović, I.; Kuspilić, G. Deep chlorophyll-a maximum at one station in the middle Adriatic Sea. *J. Mar. Biol. Assoc. UK* **2002**, *82*, 9–19. [CrossRef]
29. Mauri, E.; Poulain, P.M.; Južnič-Zonta, Ž. MODIS chlorophyll variability in the northern Adriatic Sea and relationship with forcing parameters. *J. Geophys. Res. Ocean.* **2007**, *112*. [CrossRef]
30. Kišević, M.; Morović, M.; Smailbegović, A.; Andričević, R. Above and in-water measurements of reflectance and chlorophyll algorithms in the Kaštela Bay in the Adriatic Sea. In Proceedings of the 2nd Workshop on Hyperspectral Image and Signal Processing: Evolution in Remote Sensing, WHISPERS 2010—Workshop Program, Reykjavik, Iceland, 14–16 June 2010; pp. 1–4. [CrossRef]
31. Mozetič, P.; Solidoro, C.; Cossarini, G.; Socal, G.; Precali, R.; Francé, J.; Bianchi, F.; De Vittor, C.; Smodlaka, N.; Fonda Umani, S. Recent trends towards oligotrophication of the northern adriatic: Evidence from chlorophyll a time series. *Estuaries Coasts* **2010**, *33*, 362–375. [CrossRef]
32. Cozzi, S.; Cabrini, M.; Kralj, M.; De Vittor, C.; Celio, M.; Giani, M. Climatic and anthropogenic impacts on environmental conditions and phytoplankton community in the gulf of trieste (Northern adriatic sea). *Water* **2020**, *12*, 2652. [CrossRef]
33. Viličić, D.; Orlić, M.; Jasprica, N. The deep chlorophyll maximum in the coastal north eastern Adriatic Sea, July 2007. *Acta Bot. Croat.* **2008**, *67*, 33–43.
34. Mozetič, P.; Malačič, V.; Turk, V. A case study of sewage discharge in the shallow coastal area of the Northern Adriatic Sea (Gulf of Trieste). *Mar. Ecol.* **2008**, *29*, 483–494. [CrossRef]

35. Ninčević-Gladan, Ž.; Bužančić, M.; Kušpilić, G.; Grbec, B.; Matijević, S.; Skejić, S.; Marasović, I.; Morović, M. The response of phytoplankton community to anthropogenic pressure gradient in the coastal waters of the eastern Adriatic Sea. *Ecol. Indic.* **2015**, *56*, 106–115. [CrossRef]
36. Bužančić, M.; Ninčević Gladan, Ž.; Marasović, I.; Kušpilić, G.; Grbec, B. Eutrophication influence on phytoplankton community composition in three bays on the eastern Adriatic coast. *Oceanologia* **2016**, *58*, 302–316. [CrossRef]
37. Teodoro, A.C.; Duleba, W.; Gubitoso, S.; Prada, S.M.; Lamparelli, C.C.; Bevilacqua, J.E. Analysis of foraminifera assemblages and sediment geochemical properties to characterise the environment near Araçá and Saco da Capela domestic sewage submarine outfalls of São Sebastião Channel, São Paulo State, Brazil. *Mar. Pollut. Bull.* **2010**, *60*, 536–553. [CrossRef] [PubMed]
38. Despland, L.M.; Vancov, T.; Aragno, M.; Clark, M.W. Diversity of microbial communities in an attached-growth system using Bauxsol^{TM} pellets for wastewater treatment. *Sci. Total Environ.* **2012**, *433*, 383–389. [CrossRef] [PubMed]
39. Yu, J.; Seon, J.; Park, Y.; Cho, S.; Lee, T. Electricity generation and microbial community in a submerged-exchangeable microbial fuel cell system for low-strength domestic wastewater treatment. *Bioresour. Technol.* **2012**, *117*, 172–179. [CrossRef]
40. Decision, C. Directive 2006/7/EC of the European Parliament and of the Council of 15 February 2006 concerning the management of bathing water quality and repealing Directive 76/160/EEC. *Off. J. Eur. Union* **2006**, *L064*, 37–51.
41. Di Dato, M.; Galešić, M.; Šimundić, P.; Andričević, R. A novel screening tool for the health risk in recreational waters near estuary: The Carrying Capacity indicator. *Sci. Total Environ.* **2019**, *694*. [CrossRef] [PubMed]
42. Brettum, P.; Andersen, T. The use of phytoplankton as indicators of water quality. In *Norwegian Institute for Water Research SNO Report*; NIVA: Oslo, Norway, 2004; p. 33.
43. Howarth, R.W.; Sharpley, A.; Walker, D. Sources of nutrient pollution to coastal waters in the United States: Implications for achieving coastal water quality goals. *Estuaries* **2002**, *25*, 656–676. [CrossRef]
44. Halpern, B.S.; Walbridge, S.; Selkoe, K.A.; Kappel, C.V.; Micheli, F.; D'Agrosa, C.; Bruno, J.F.; Casey, K.S.; Ebert, C.; Fox, H.E.; et al. A global map of human impact on marine ecosystems. *Science* **2008**, *319*, 948–952. [CrossRef]
45. Windom, H.L. Contamination of the marine environment from land-based sources. *Mar. Pollut. Bull.* **1992**, *25*, 32–36. [CrossRef]
46. Lapointe, B.E.; Thacker, K.; Hanson, C.; Getten, L. Sewage pollution in Negril, Jamaica: Effects on nutrition and ecology of coral reef macroalgae. *Chin. J. Oceanol. Limnol.* **2011**, *29*, 775–789. [CrossRef]
47. Kiefer, D.A. Fluorescence properties of natural phytoplankton populations. *Mar. Biol.* **1973**, *22*, 263–269. [CrossRef]
48. Röttgers, R.; Koch, B.P. Spectroscopic detection of a ubiquitous dissolved pigment degradation product in subsurface waters of the global ocean. *Biogeosciences* **2012**, *9*, 2585–2596. [CrossRef]
49. Sosik, H.M.; Chisholm, S.W.; Olson, R.J. Chlorophyll fluorescence from single cells: Interpretation of flow cytometric signals. *Limnol. Oceanogr.* **1989**, *34*, 1749–1761. [CrossRef]
50. Kolber, Z.; Falkowski, P.G. Use of active fluorescence to estimate phytoplankton photosynthesis in situ. *Limnol. Oceanogr.* **1993**, *38*, 1646–1665. [CrossRef]
51. Müller, P.; Li, X.P.; Niyogi, K.K. Update on Photosynthesis Non-Photochemical Quenching. A Response to Excess Light Energy. *Plant Physiol.* **2001**, *125*, 1558–1566. [CrossRef]
52. Intergovernmental Oceanographic Commission; Scientific Committee on Oceanic Research; International Association for the Physical Sciences of the Ocean. The international thermodynamic equation of seawater—2010: Calculation and use of thermodynamic properties. In *Intergovernmental Oceanographic Commission, Manuals and Guides No. 56*; UNESCO: Paris, France, 2010; p. 196.
53. Petersen, W.; Schroeder, F.; Bockelmann, F.-D. FerryBox—Application of continuous water quality observations along transects in the North Sea. *Ocean Dyn.* **2011**, *61*, 1541–1554. [CrossRef]
54. Cunningham, A. Variability of In-Vivo Chlorophyll Fluorescence and Its Implication for Instrument Development in Bio-Optical Oceanography. *Sci. Mar.* **1996**, *60*, 309–315.
55. Falkowski, P.; Kiefer, D.A. Chlorophyll a fluorescence in phytoplankton: Relationship to photosynthesis and biomass. *J. Plankton Res.* **1985**, *7*, 715–731. [CrossRef]
56. Croatian Standards Institute (HRN EN ISO 9308-1:2014/A1:2017). *Water Quality—Enumeration of Escherichia Coli and Coliform Bacteria—Part 1: Membrane Filtration Method for Waters with Low Bacterial Background Flora*; Croatian Standards Institute: Zagreb, Croatia, 2017.
57. Jozić, S.; Vukić Lušić, D.; Ordulj, M.; Frlan, E.; Cenov, A.; Diković, S.; Kauzlarić, V.; Fiorido Đurković, L.; Stilinović Totić, J.; Ivšinović, D.; et al. Performance characteristics of the temperature-modified ISO 9308-1 method for the enumeration of Escherichia coli in marine and inland bathing waters. *Mar. Pollut. Bull.* **2018**, *135*, 150–158. [CrossRef] [PubMed]
58. Croatian Standards Institute (HR EN ISO 7899-2:2000). *Water Quality—Detection and Enumeration of Intestinal Enterococci—Part 2: Membrane Filtration Method*; Croatian Standards Institute: Zagreb, Croatia, 2000.
59. Zhao, C.; Maerz, J.; Hofmeister, R.; Röttgers, R.; Wirtz, K.; Riethmüller, R.; Schrum, C. Characterizing the vertical distribution of chlorophyll a in the German Bight. *Cont. Shelf Res.* **2019**, *175*, 127–146. [CrossRef]
60. Goosen, N.K.; Kromkamp, J.; Peene, J.; Van Rijswijk, P.; Van Breugel, P. Bacterial and phytoplankton production in the maximum turbidity zone of three European estuaries: The Elbe, Westerschelde and Gironde. *J. Mar. Syst.* **1999**, *22*, 151–171. [CrossRef]
61. Ni, X.; Huang, D.; Zeng, D.; Zhang, T.; Li, H.; Chen, J. The impact of wind mixing on the variation of bottom dissolved oxygen off the Changjiang Estuary during summer. *J. Mar. Syst.* **2016**, *154*, 122–130. [CrossRef]
62. Epifanio, C.E.; Maurer, D.; Dittel, A.I. Seasonal changes in nutrients and dissolved oxygen in the Gulf of Nicoya, a tropical estuary on the Pacific coast of Central America. *Hydrobiologia* **1983**, *101*, 231–238. [CrossRef]

63. Frankignoulle, M.; Abril, G.; Borges, A.; Bourge, I.; Canon, C.; Delille, B.; Libert, E.; Théate, J.M. Carbon dioxide emission from European estuaries. *Science* **1998**, *282*, 434–436. [CrossRef] [PubMed]
64. Kress, N.; Coto, S.L.; Brenes, C.L.; Brenner, S.; Arroyo, G. Horizontal transport and seasonal distribution of nutrients, dissolved oxygen and chlorophyll-a in the Gulf of Nicoya, Costa Rica: A tropical estuary. *Cont. Shelf Res.* **2002**, *22*, 51–66. [CrossRef]
65. Gazeau, F.; Smith, S.V.; Gentili, B.; Frankignoulle, M.; Gattuso, J.P. The European coastal zone: Characterization and first assessment of ecosystem metabolism. *Estuar. Coast. Shelf Sci.* **2004**, *60*, 673–694. [CrossRef]
66. Gazeau, F.; Gattuso, J.P.; Middelburg, J.J.; Brion, N.; Schiettecatte, L.S.; Frankignoulle, M.; Borges, A.V. Planktonic and whole system metabolism in a nutrient-rich estuary (the Scheldt estuary). *Estuaries* **2005**, *28*, 868–883. [CrossRef]
67. Yuan, X.; Yin, K.; Harrison, P.J.; Cai, W.J.; He, L.; Xu, J. Bacterial production and respiration in subtropical Hong Kong waters: Influence of the Pearl River discharge and sewage effluent. *Aquat. Microb. Ecol.* **2010**, *58*, 167–179. [CrossRef]
68. Stanley, D.W.; Nixon, S.W. Stratification and bottom-water hypoxia in the Pamlico River estuary. *Estuaries* **1992**, *15*, 270–281. [CrossRef]
69. Breitburg, D.L.; Adamack, A.; Rose, K.A.; Kolesar, S.E.; Decker, M.B.; Purcell, J.E.; Keister, J.E.; Cowan, J.H. The pattern and influence of low dissolved oxygen in the Patuxent River, a seasonally hypoxic estuary. *Estuaries* **2003**, *26*, 280–297. [CrossRef]
70. Bergondo, D.L.; Kester, D.R.; Stoffel, H.E.; Woods, W.L. Time-series observations during the low sub-surface oxygen events in Narragansett Bay during summer 2001. *Mar. Chem.* **2005**, *97*, 90–103. [CrossRef]
71. Roth, F.; Lessa, G.C.; Wild, C.; Kikuchi, R.K.P.; Naumann, M.S. Impacts of a high-discharge submarine sewage outfall on water quality in the coastal zone of Salvador (Bahia, Brazil). *Mar. Pollut. Bull.* **2016**, *106*, 43–48. [CrossRef]
72. Ramos, P.A.; Neves, M.V.; Pereira, F.L. Mapping and initial dilution estimation of an ocean outfall plume using an autonomous underwater vehicle. *Cont. Shelf Res.* **2007**, *27*, 583–593. [CrossRef]
73. Petrenko, A.A. Effects of a sewage plume on the biology, optical characteristics, and particle size distributions of coastal waters. *J. Geophys. Res. C Ocean.* **1997**, *102*, 25061–25071. [CrossRef]
74. Washburn, B.L.; Jones, B.H.; Bratkovich, A.; Dickey, D.; Chen, M. Mixing, Dispersion, and resuspension in vicinity of ocean wastewater plume. *J. Hydraul. Eng.* **1992**, *118*, 38–58. [CrossRef]

3.2. Microbiome and antibiotic resistance profiling in submarine effluent-receiving coastal waters in Croatia

Reproduced from:

Kvesić, M., Kalinić, H., Dželalija, M., Šamanić, I., Andričević, R., Maravić, A., 2022. Microbiome and antibiotic resistance profiling in submarine effluent-receiving coastal waters in Croatia. Environmental Pollution 292, 118282.. https://doi.org/10.1016/j.envpol.2021.11828

Wastewater treatment plant (WWTP) effluents are an important source of both commensal and pathogenic bacteria and their antibiotic resistance genes (ARGs) into water bodies. This research, for the first time, analyse the impact of partially treated submarine effluents on the water quality of two distinct water columns. Its aim is to comprehensively investigate and understand the water column microbiome and resistome using 16S rRNA amplicon sequencing. This study highlights the adverse effects of submarine effluent discharge, which enriches bacterial communities with non-native taxa carrying various ARGs, potentially increasing the spread of antibiotic resistance in nature.

Analysis of the coastal marine microbiome and resistome contributes to a better understanding of the impact of submarine outfalls on water column quality, in terms of the presence of different allochthonous bacterial species and human pathogens as potential carriers of a variety of ARGs.

Environmental Pollution 292 (2022) 118282

Contents lists available at ScienceDirect

Environmental Pollution

journal homepage: www.elsevier.com/locate/envpol

Microbiome and antibiotic resistance profiling in submarine effluent-receiving coastal waters in Croatia☆

Marija Kvesić [a,b], Hrvoje Kalinić [c], Mia Dželalija [d], Ivica Šamanić [d], Roko Andričević [a,e], Ana Maravić [d,*]

[a] Center of Excellence for Science and Technology-Integration of Mediterranean Region, University of Split, Ruđera Boškovića 31, 21000, Split, Croatia
[b] Faculty of Science, University of Split, Ruđera Boškovića 33, Split, Croatia
[c] Department of Informatics, Faculty of Science, University of Split, Ruđera Boškovića 33, 21000, Split, Croatia
[d] Department of Biology, Faculty of Science, University of Split, Ruđera Boškovića 33, 21000, Split, Croatia
[e] Faculty of Civil Engineering, Architecture and Geodesy, University of Split, Matice Hrvatske 15, Split, Croatia

ARTICLE INFO

Keywords:
Marine microbiome
Wastewater effluent plume impact
Resistome prediction
Anthropogenic impact
Coastal marine environment

ABSTRACT

Wastewater treatment plant (WWTP) effluents are pointed as hotspots for the introduction of both commensal and pathogenic bacteria as well as their antibiotic resistance genes (ARGs) in receiving water bodies. For the first time, the effect of partially treated submarine effluents was explored at the bottom and surface of the water column to provide a comprehensive overview of the structure of the microbiome and associated AR, and to assess environmental factors leading to their alteration. Seawater samples were collected over a 5-month period from submarine outfalls in central Adriatic Sea, Croatia. 16S rRNA amplicon sequencing was used to establish taxonomic and resistome profiles of the bacterial communities. The community differences observed between the two discharge areas, especially in the abundance of *Proteobacteria* and *Firmicutes*, could be due to the origin of wastewaters treated in WWTPs and the limiting environmental conditions such as temperature and nutrients. PICRUSt2 analysis inferred the total content of ARGs in the studied microbiomes and showed the highest abundance of resistance genes encoding multidrug efflux pumps, such as MexAB-OprM, AcrEF-TolC and MdtEF-TolC, followed by the modified peptidoglycan precursors, transporter genes encoding tetracycline, macrolide and phenicol resistance, and the *bla* operon conferring β-lactam resistance. A number of pathogenic genera introduced by effluents, including *Acinetobacter, Arcobacter, Bacteroides, Escherichia-Shigella, Klebsiella, Pseudomonas,* and *Salmonella*, were predicted to account for the majority of efflux pump-driven multidrug resistance, while *Acinetobacter, Salmonella, Bacteroides* and *Pseudomonas* were also shown to be the predominant carriers of non-efflux ARGs conferring resistance to most of nine antibiotic classes. Taken together, we evidenced the negative impact of submarine discharges of treated effluents via alteration of physico-chemical characteristics of the water column and enrichment of bacterial community with nonindigenous taxa carrying an arsenal of ARGs, which could contribute to the further propagation of the AR in the natural environment.

1. Introduction

In many coastal areas, submarine sewage outfalls are used to dispose of partially or fully treated wastewater. Although such disposal is environmentally acceptable, it can also be a significant factor of pollutants' influent and further spread to the pristine marine environment. Namely, the effluents commonly contain microbiological and chemical pollutants (Lapointe et al., 2011; Roth et al., 2016; Vidal-Dorsch et al., 2012; Wang et al., 2014; Yang, 2000) which can impact the biodiversity of coastal marine microbiota (Mittal et al., 2019; Zheng

Abbreviations: Wastewater treatment plant, (WWTP); antibiotic resistance gene, (ARG); antibiotic resistance, (AR); antibiotic-resistant bacteria, (ARB); fecal indicator bacteria, (FIB); temperature, (T); salinity, (SAL); density anomaly, (SIGMA); dissolved oxygen, (DO); chlorophyll *a*, (CHL); turbidity, (TUR); nitrite nitrogen, (NO2–N); nitrate nitrogen, (NO3–N); ammonia nitrogen, (NH3–N); total nitrogen, (TN); total phosphate, (TP); silicate ions, (SiO_4^{3-}); colored dissolved organic matter, (CDOM); imipenem, (IMP); colistin, (CL); operational taxonomic units, (OTUs); oxacillinase, (OXA); (CAMP), cationic antimicrobial peptide.

☆ This paper has been recommended for acceptance by Dr. Sarah Harmon.

* Corresponding author. Associate professor Department of Biology Faculty of Science, University of Split A, Ruđera Boškovića 33, 21000, Split, Croatia.
E-mail address: ana.maravic@pmfst.hr (A. Maravić).

https://doi.org/10.1016/j.envpol.2021.118282
Received 1 July 2021; Received in revised form 10 September 2021; Accepted 3 October 2021
Available online 4 October 2021

et al., 2021; Zheng et al., 2019) and alter environmental parameters, including pH (Shen et al., 2013; Yannarell and Triplett, 2005), salinity (Hou et al., 2017), temperature (Zheng et al., 2019) and level of nutrients (Lu et al., 2020; Wang et al., 2018).

In addition to microbial diversity, significant changes in gene abundances, especially virulence and antibiotic resistance genes (ARGs) have been identified in anthropogenically impacted marine and freshwater environments (Bondarczuk and Piotrowska-Seget, 2019; Fresia et al., 2018). Antibiotic resistance (AR) is a particularly challenging problem in these ecosystems, being the final recipient of a municipal, hospital, industrial, agricultural, and aquaculture wastewaters (Rizzo et al., 2013). In this regard, wastewater treatment plants (WWTPs) are considered as major sources of ARGs and antibiotic-resistant bacteria (ARB) with sewage effluents acting as hot spots for their further dissemination to the environment (Griffin et al., 2020; Kotlarska et al., 2015; Proia et al., 2018; Su et al., 2020). WWTP effluents in coastal waters in China were found to be enriched with genes encoding for resistance to multiple classes of antibiotics (Chen et al., 2020; Su et al., 2020) that positively correlated with nitrate, active phosphorus and pH (Chen et al., 2020).

Molecular biology and computational biology tools are now being widely used for investigating microbial communities (Dinsdale et al., 2008; Fresia et al., 2018), while PICRUSt2 (Douglas et al., 2020) annotates the functional features, among which the ARGs (Šamanić et al., 2021), expanding the possibility for a comprehensive study of the vast environmental resistance reservoirs associated to wastewaters (Cai et al., 2014; García-Aljaro et al., 2019; Narciso-da-Rocha et al., 2018; Port et al., 2012).

Importantly, a better understanding of the microbial wastewater communities can provide an important framework for the more effective design and operation of novel and robust wastewater treatment systems. Based on the available literature, this study is the first to provide a comprehensive analysis of the bottom and the surface of the water body receiving the effluents from the submarine outfalls with respect to the microbiome diversity and AR prediction, in combination with the vertical profiling of the water column.

The objectives of this study were to (i) determine the microbial communities at the bottom and at the surface of the water column adjacent to the effluent plume discharge; (ii) determine if there is a difference in microbial composition between the two submarine outfall discharges, particularly in regards to human pathogenic bacteria (iii) functionally predict the repertoire of ARGs in bacterial communities based on taxonomic outlining of effluent and surface water samples (iv) assess the potential of pathogenic bacterial genera as reservoirs of AR in analyzed marine microbiomes.

2. Materials and methods

2.1. Description of the study sites

This study focused on the highly urbanized central part of the eastern Adriatic coast in Croatia (Fig. S1.), covering the municipalities of Split, Solin and Stobreč with a population of >200,000. Two WWTPs, Katalinića brig and Stupe-Stobreč, are processing wastewaters from the wider Split area and discharging it through submarine outlets into the Brač and Split Channels. While Stobreč WWTP processes only municipal wastewater, Katalinića brig WWTP combines municipal and rainfall-runoff wastewater. Both WWTPs have only mechanical treatments, including coarse and fine screens, while Stobreč WWTP also provides oil and sand removal. The Stobreč WWTP is designed for municipal wastewater only, with capacity of 138.000 population equivalent (PE) and an average flow rate equal to 30,000 m^3/day, while Katalinića brig WWTP is designed for 122,000 PE with an averaged flow rate of 35,000 m^3/day. Another important feature of the Katalinića Brig WWTP is that it also collects the wastewater from University Hospital Centre Split, a leading medical center in southern Croatia with 1400 beds. After treatment, the Stobreč WWTP is discharging the effluent by gravity through the submarine outfall of 2.76 km in length with a 200 m diffuser section at depth of 37 m (43°28′53.6 ″N 16°31′04.3 ″E). The Katalinića Brig WWTP is discharging the treated wastewater by pumping through the submarine outfall of 1.3 km in length at depth of 42 m (43°29′22.7 ″N 16°27′11.2 ″E), respectively.

2.2. Sampling

Samplings were conducted once a month during campaigns in February, May, June, July, and September 2020. At each site, three 500-mL water samples were taken consecutively as a representative grab sample set for further analysis. At Katalinića Brig, seawater was collected at the surface (abbreviated as KS) and at the sea bottom adjacent to the submarine outfall (abbreviated as KB). Same approach was carried out at the Stupe submarine outfall, abbreviated as SS (Stobreč surface) and SB (Stobreč bottom). Sampling was done with the boat (Nautica 600, Croatia) using a Niskin sampler. Grab samples were collected in sterile bottles, protected from light in cool boxes, transported to the laboratory within 4h at 4 °C and processed immediately. Seawater samples for chemical analyses were transported within 8h at 4 °C to the laboratory of Public Health Institute in Zadar, Croatia, and then stored at 80 °C for further analyses.

2.3. Physico-chemical analysis

Physical parameters were measured during field samplings. Sea & Sun Technology CTD fast profiling probe with an additional sensor for dissolved oxygen (DO) (model: 48M) was used for temperature (T), salinity (SAL), and density anomaly (SIGMA). Data collection was performed by downward profiling of water column up to 40m depth at Katalinića Brig station and up to 35m depth at Stupe station. SIGMA was calculated automatically by CTD/DO probe software using an international thermodynamic equation of seawater-2010 (IOC et al., 2010). Chlorophyll *a* (CHL) was determined by a standard method for *in vivo* determination of CHL in marine waters (Arar and Collins, 1997). Turbidity (TUR) (ISO 7027–1), nitrite nitrogen (NO2–N) and nitrate nitrogen (NO3–N) (Baird and Bridgewater, 2017), ammonia nitrogen (NH3–N) (Ivancic and Degobbis, 1984), total nitrogen (TN) (ISO 12260), total phosphate (TP) (ISO 6878), and silicate ions (SiO_4^{3-}) (Grasshoff et al., 1998) were analyzed by laboratory standard methods, listed for each parameter in brackets. Colored dissolved organic matter (CDOM) was measured by a C3 Submersible fluorometer (Turner Design), using a UV LED, with peak emission at 350 nm and fluorescence collection at 450 nm.

2.4. Bacterial enumeration

The level of fecal pollution was assessed by the membrane filtration method and enumeration of FIB, including the fecal coliforms (*E. coli*) (ISO 9308–1; Jozić et al., 2018) and intestinal enterococci (ISO 7899–2), as indicated in the Croatian legislation (Regulation on the Quality of Marine Bathing Waters; OG 73/08). The number of viable heterotrophic bacteria was determined using the spread plate method. Aliquots of 0.1 mL were plated on Marine agar (MA; BD Difco, USA) and the plates were incubated at room temperature for up to one week to ensure the growth of the slow-growing bacteria. To determine the proportion (in %) of imipenem (IMP)- and colistin (CL)-resistant bacteria, aliquots from 1 to 50 mL of each water sample were filtered through a 0.22 μm pore-size MCE membranes and the filters were placed on MA (BD Difco) supplemented with IMP (4 μg/mL) or CL (8 μg/mL) and without antibiotics. The two antibiotics were chosen regarding their global relevance in treatment of infections caused by emerging multidrug- and carbapenem-resistant pathogens (WHO, 2017). The concentration of IMP was selected according to international guidelines (CLSI, 2020). On the other hand, a two-fold higher concentration of CL than the MIC

breakpoint was used due to poor diffusion of this drug in solid media (Turlej-Rogacka et al., 2018). An automated Protos3 colony counting system (Synbiosis, UK) was used in all experiments. All plate counts were performed in triplicate and the number of bacteria was expressed as mean count (CFU/100 mL) ± standard deviation (SD).

2.5. DNA extraction and illumina-based 16S rRNA amplification

One liter of each water sample was filtered through 0.22 μm pore-size MCE membrane filters and DNeasy PowerWater Kit (Qiagen, Germany) was used to extract genomic DNA. The concentration and quality of DNA were analyzed using a NanoDrop® Spectrophotometer 1000 (Thermo Scientific, USA). DNA samples were sent to a Novogene Europe (Cambridge, UK) for 16S amplicon metagenome sequencing. A 470 bp hypervariable region V3–V4 of the 16S rRNA gene was amplified using standard primers 341F and 806R and Phusion® High-Fidelity PCR Master Mix (New England Biolabs, UK). PCR products were purified, libraries generated using NEBNext® UltraTM DNA Library Prep Kit (Illumina, UK) and analyzed on a NovaSeq platform (Illumina). 250 bp paired-end raw reads were merged using FLASH (V1.2.7) and high-quality clean tags were obtained after quality filtering (Caporaso et al., 2010) using QIIME (V1.7.0). Sequences were analyzed using Uparse (v7.0.1001) and those with ≥97% similarity were assigned to the same Operational Taxonomic Units (OTUs). Representative sequences were compared with SILVA Database (Quast et al., 2013) for species annotation at each taxonomic rank (threshold: 0.8–1) using MUSCLE (White et al., 2009).

2.6. PICRUSt functional prediction

The PICRUSt2 (Douglas et al., 2020) was used for functional gene annotation of the 16S rRNA amplicon sequences to assess the molecular AR mechanisms, including the β-lactam, aminoglycoside, tetracycline, macrolide, phenicol, fosfomycin, sulfonamide, trimethoprim, rifamycin, quinolone and vancomycin resistance genes, as well as vancomycin, multidrug and cationic antimicrobial peptide (CAMP) resistance modules. Appropriate gene sets and gene variants were analyzed using the KEGG Brite Antimicrobial Resistance Genes database (KO01504) (Šamanić et al., 2021). Heatmap was generated to depict the relationship of the most common pathogenic genera in microbiomes (relative abundance expressed as square roots of the percentage values; threshold: 0.73) with resistance gene sets and variants by using reads from trimmed OTUs table and custom Python 3.9 scripts. Graphical design was done with Inkscape 1.0.1.

2.7. Data analysis

Relative abundance of bacterial taxa was calculated by dividing an absolute abundance with a total abundance of species at each taxonomic rank. Alpha diversity indices (Chao1, Shannon, Simpson, ACE, Good's coverage) were calculated using QIIME (v1.7.0) and plotted using MATLAB R2021a. Beta diversity was calculated on both weighted and unweighted Unifrac using QIIME software (v1.7.0). The PCoA analysis was displayed using the WGCNA, stat and ggplot2 packages in R software (v15.3). Analysis of similarities (ANOSIM) and multi-response permutation procedure (MRPP) analysis were performed by R software (Vegan package) to evaluate the significance of variations between and within the structure of bacterial communities from two WWTP submarine effluents. To determine the significantly different OTUs, the linear discriminant analysis (LDA) effect size (LEfSe) algorithm was conducted (Segata et al., 2011) using a threshold greater than 2.0 for the logarithmic LDA scores. Metastat was calculated by R software and p-value using a permutation test ($p < 0.05$ was statistically significant). Pearson correlations analysis and figures were done in MATLAB R2021a.

3. Results

3.1. Environmental parameters and bacterial counts at the two effluent-receiving area

The physical and chemical characteristics of the bottom and surface water layers were analyzed at both submarine outfalls (Fig. 1, Table S1). The T and SAL values showed an opposite pattern as colder and saltier water sinks. Unstratified water column prevailed during February, while formation of stratification started in May and followed seasonal cycle, with shallowest pycnocline detected in July and the deepest in September (Fig. S2.). The water column was well oxygenated at both sites based on dissolved oxygen levels. Higher levels of CHL, TUR, and CDOM were found at the bottom, at both stations, while an opposite pattern was observed for TN. The highest NO2–N and NO3–N concentrations were found at SB. The highest abundance of *E. coli* (660 CFU/100 mL) and fecal enterococci (151 CFU/100 mL) was observed at SS during sampling in February (Table 1). Overall, the median values of *E. coli* (50 CFU/100 mL) and enterococci (24 CFU/100 mL) counts were highest in SB and were followed by KB.

3.2. 16S rRNA sequencing analysis

The total number of filtered reads generated on the Illumina platform was 1,472,326. After quality filtering, a total of 967,900 effective tags, with a mean length of 411 bp, were clustered into 15,200 OTUs. On average, 760 OTUs were identified per sample, with 767, 451, 666 and 1156 OTUs detected in SB, SS, KB and KS samples, respectively. A total of 332 OTUs were common to samples from the two sites (Fig. S3). As expected, the highest overlap was found between the two bottom locations, which included 516 OTUs in common. On contrary, two surface locations shared the least OTUs (n = 452) (Fig. S3).

3.3. Composition of bacterial community at two WWTP submarine effluents

A total of 37 bacterial phyla were identified at two effluent sites. The highest number of phyla was observed in SB (n = 29), followed by KS, KB, and SS with 26, 25, and 24 identified phyla, respectively.

Differences between the two submarine discharge areas were noticeable at the phylum and class level (Fig. 2). The most abundant phylum at Stobreč effluent site was *Firmicutes* with the relative abundance of 45.64% in the bottom (SB) and 50.51% in surface (SS) samples and was followed by *Proteobacteria* (30.33% and 23.40%). *Cyanobacteria, Bacteroidetes* and *Actinobacteria* were present in a range from 3.53% to 10.97% in SB samples and from 5.24% to 6.45% in SS samples, respectively. On the other hand, *Proteobacteria* was the predominant phylum at the Katalinića brig effluent site with the relative abundance of 44.04% and 59.30% in KB and KS samples. These were followed by *Firmicutes* (32.90% and 15.54%), *Cyanobacteria* (6.33% and 14.30%), *Bacteroidetes* (<5%) and *Actinobacteria* (<3%).

The comparison of the community diversity at the class level was more informative, evidencing a distinctive pattern of each sample. A total of 71 bacterial classes were identified in this study, with *Clostridia*, *Alphaproteobacteria* and *Gammaproteobacteria* being the most abundant ones (Fig. 2). These were differently distributed between the samples. *Clostridia* was found to be the most abundant class in SB, SS and KB, while it was the fourth most prevalent in KS. *Gammaproteobacteria* was the second most abundant class in KS, KB and SS, and, depending on the sample, were followed by *Oxyphotobacteria, Alphaproteobacteria* and *Bacilli* (Fig. 2).

The relative abundance of bacterial taxa at the order, family, and genus levels is shown in Fig. S4. *Clostridiales* was the most abundant order except in KS, where SAR 11 clade of marine autochthonous bacteria occupied this position. Consequently, the human gut-related bacteria of the *Lachnospiraceae* of the order *Clostridiales* were the most

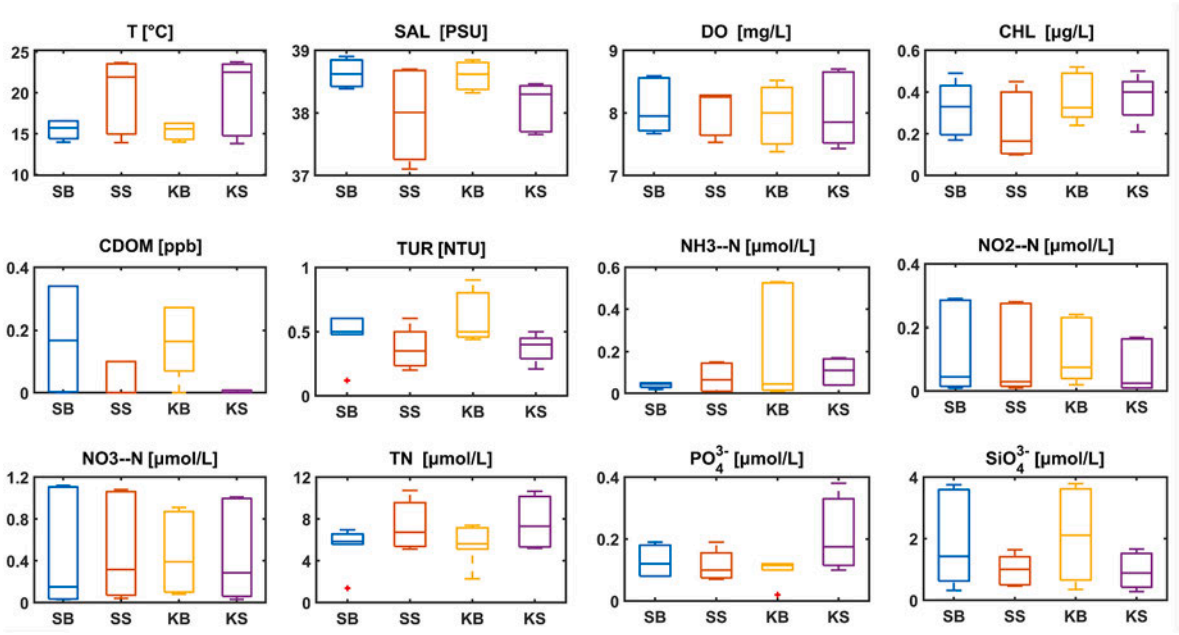

Fig. 1. Boxplots of environmental parameters at effluent discharge of Stobreč (bottom and surface, SB and SS) and Katalinića Brig (bottom and surface, KB and KS) WWTPs. Central line indicates the median value, and the bottom and top edges of the box indicate the 25th and 75th percentiles. The outliers are plotted individually using the '+' symbol.

Table 1
Total counts of FIB (CFU±SD/100 mL), total heterotrophic bacteria (CFU± SD/1 mL) and estimated percentage of the viable heterotrophic bacteria resistant (%R) to IMP and CL.

Bacteria	Site	February	May	June	July	September
E. coli	SB	0.7 ± 0.6	4.67 ± 2.5	219 ± 6.7	102.7 ± 10.7	50 ± 7
	SS	660 ± 14.7	0	0	0	0
	KB	44 ± 4.4	152 ± 10.8	34 ± 4.6	37.3 ± 8.9	1.3 ± 0.6
	KS	10 ± 4.6	0	0	0	0
Intestinal enterococci	SB	1.3 ± 0.6	4 ± 1	48.7 ± 4.2	27.3 ± 3.2	24 ± 4.6
	SS	151.6 ± 3.2	0	0	0.7 ± 0.6	0
	KB	15.3 ± 2.5	36.6 ± 3.2	27.3 ± 4.0	8.7 ± 0.6	0.7 ± 0.6
	KS	13.3 ± 2.3	6 ± 1	0	0	4.7 ± 3.2
Total viable heterotrophic bacteria	SB	163.3 ± 1.2	776.67 ± 16.2	3017 ± 47.5	2577 ± 12.7	1071 ± 59.8
	SS	630 ± 17.5	1300 ± 30.3	1450 ± 5.57	2140 ± 63.3	1227 ± 37.5
	KB	2090 ± 47.5	2993 ± 27.3	1407 ± 48.5	1607 ± 68.1	1016 ± 12.0
	KS	456.6 ± 8.4	966.7 ± 5.8	2950 ± 21.9	2940 ± 16.1	1596 ± 17.6
% R-IMP	SB	0.43	0.86	1.50	0.47	15.69
	SS	0.39	2.55	2.21	0.23	29.34
	KB	0.10	1.34	2.84	0.26	35.43
	KS	0.45	2.75	7.81	0.37	22.56
% R-CL	SB	14.76	22.66	9.41	1.67	15.97
	SS	5.65	6.09	15.86	4.86	24.45
	KB	7.52	46.78	15.78	4.79	42.81
	KS	7.07	20.69	11.28	6.94	38.85

abundant family, accounting for between 26.1% and 18.6% of the bacterial community in SB, SS and KB. *Agathobacter* (7.1%), *Lactobacillus* (8.1%) and *Salmonella* (6.5%) were the most abundant genera in SB, SS and KB. On the other hand, *Cyanobiaceae* (10.7%) of the order *Synechococcales* (Oxyphotobacteria) were the most frequently presented family in KS, with *Synechococcus* CC9902 being the most abundant bacterial genus (8%). It is noteworthy that genera with a relative abundance of less than 2% accounted for more than 55% of the bacterial community in the samples from Katalinića brig (KS and KB). On the other hand, this percentage was about 45% in the samples from the Stobreč effluent site.

Furthermore, Fig. S5 shows a heatmap of the 35 most abundant genera in each sample, providing information on abundance and clustering them by origin. The most abundant genera found in samples from the seafloor near both submarine outfalls (KB and SB) are rarely present in surface samples (KS and SS) and *vice versa*.

The microbial communities from the Katalinića brig site (KB and KS) showed higher richness and microbial diversity compared to the Stobreč outfall samples (Table 2, Fig. S6), as indicated by a higher number of genera with a relative abundance of <2%, as well as other less abundant genera (Fig. S4). Community diversity estimated by the Shannon's and Simpson's indices was highest in the surface samples (KS > SS > KB > SB). KS also had the highest community richness among surface and bottom samples and was significantly different ($p < 0.05$; Wilcox test) from SS.

According to the ANOSIM and MRPP analyses (Table S2), the

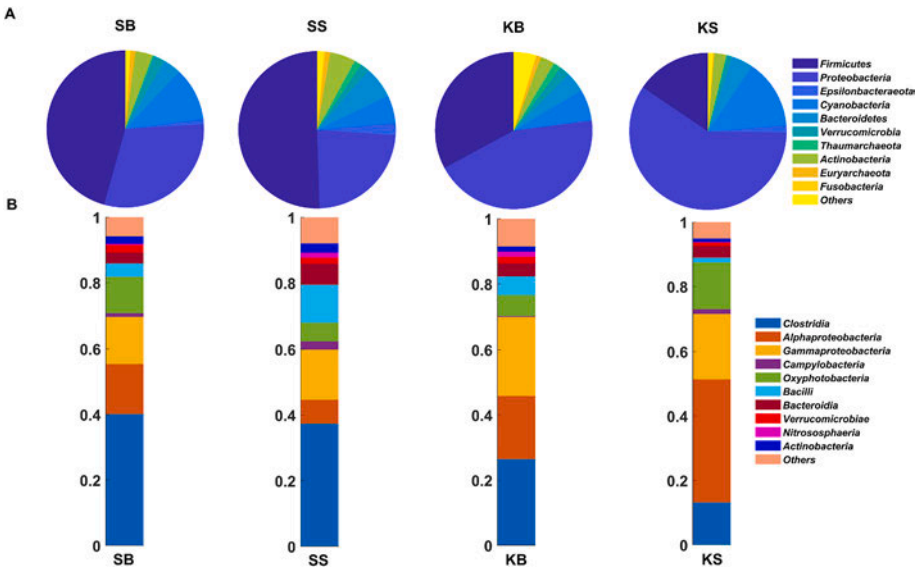

Fig. 2. Relative abundance of the ten most abundant taxa at phylum (A) and class (B) levels comprising the bacterial communities from the Stobreč (bottom and surface, SB and SS) and Kaliniića Brig (bottom and surface, KB and KS) WWTPs effluent sites.

Table 2
Alpha diversity indices showing the richness (observed species, Chao1 indices), diversity (Shannon and Simpson indices) and evenness of bacterial communities at two effluent-receiving sites over five-month period.

Indices	SB	SS	KB	KS
Observed species	307	285[a]	308	374[b]
Chao1	474.77	387.65[a]	483.32	687.73[b]
Shannon	5.95	6.15	5.89	6.29
Simpson	0.96	0.96	0.95	0.97
Evenness	0.94	0.98	0.93	0.94
Pathogenic genera[c]	17.78	32.45	22.65	9.50

[a] Significantly different (p-value <0.05) by Wilcox-test.
[b] Significantly different (p-value <0.05) by Wilcox-test.
[c] Abundance (%) was defined as the ratio of the read count of the genus per total number of read counts in the sample.

variations in bacterial community structure between KS and the other 3 groups were greater than within these groups, being statistically significant in the case of KS and SS ($p < 0.05$). Of note, the bacterial community at KS differed from the other samples already at the class level (*Alphaproteobacteria* > *Gammaproteobacteria* > *Oxyphotobacteria* > *Clostridia*).

3.4. Spatial variations of microbial community composition

Beta diversity was presented by the weighted UniFrac PCoA biplot based on Bray-Curtis distance (Fig. 3). SS and SB microbiomes plotted more closely, while differences were more evident between KS and KB. As expected, KS was the most distant from SS, as supported by Venn diagrams (Fig. S3). The monthly surface samples clustered very tightly except for those obtained in February (KS.2 and SS.2) that were plotted separately from the rest of the pool. For SS, this discrepancy is mainly due to the reduction of *Clostridia* and the higher abundance of *Alphaproteobacteria, Gammaproteobacteria, Campylobacteria* and *Oxyphotobacteria*, while for KS this is related to the increase of *Clostridia* and the lower abundance of *Alphaproteobacteria* and *Gammaproteobacteria*.

Significant differences in the composition of bacterial community between KS and SS were further confirmed by ANOSIM (R = 0.412, p = 0.032) and MRPP (p = 0.013) tests (Table S2). According to LEfSE analysis, the classes with statistically significant difference ($p < 0.05$) were *Bacilli* in SS and *Alphaproteobacteria* in KS (Fig. 4., Fig. S7). In this regard, the histogram of LDA scores showed that KS was much more enriched in *Rhodospirillales, Rhodobacterales* and *Puniceispirillales* of the *Alphaproteobacteria* class and these were followed by *Oceanospirillales* and *Alteromonadales* of the *Gammaproteobacteria* class, when compared to SS. On the other hand, SS was characterized by a higher abundance of *Lactobacillales* from the class of *Bacilli,* following by *Enterobacteriales* and *Bacteroidales* (Fig. 4).

The weighted UniFrac distance boxplot of beta diversity indices (Fig. S8) showed the differences in microbial community structure from bottom and surface samples collected at both effluent sites, and these were statistically significant ($p < 0.05$, Wilcox test) in the case of KS and KB. In support of the UniFrac analysis, LEfSE analysis showed that KS was more enriched in *Alphaproteobacteria* (o_*Puniceispirillales*; f_SAR116_clade), *Gammaproteobacteria* (f_*Alteromonadaceae*; g_*Glaciecola*) and *Oxyproteobacteria* (g_*Synechococcus*_CC9902), when compared to KB (Fig. S9a). The bacterial taxon with the highest differential abundance in KS was *Synechococcus*_CC9902 (LDA score [log10]>4). Between SS and SB (Fig. S9b), significantly different abundances occurred only for members of the order *Lactobacillales*, which were more abundant in SS (LDA score [log10]>4).

3.5. Influence of environmental factors on structure of the bacterial community

The dependence of the bacterial classes in studied samples and environmental conditions were investigated using CCA analysis (Fig. S10). The abundance of *Clostridia* was mainly influenced by CDOM. Furthermore, *Alphaproteobacteria* were positively correlated with PO_4^3 and negatively correlated with CHL. The abundance of *Bacilli, Bacteroidia, Nitrososphaeria,* and *Termoplasmata* was influenced by nitrogen nutrients (NO3–N, NO2–N and NH3–N). This was confirmed by Pearson correlation analysis in which *Bacilli* (r = 0.50; $p < 0.05$) and *Nitrososphaeria* (r = 0.55; $p < 0.05$) were positively correlated with NO2–N. *Bacilli, Nitrososphaeria* and *Termoplasmata* correlated positively and significantly correlated with NO3–N (r = 0.55; r = 0.48; r = 0.44). *Bacteroidia* (r = 0.58; $p < 0.05$) and *Termoplasmata* (r = 0.44; $p < 0.05$) correlated significantly with NH3–N. CDOM had influence on abundance of *Clostridia* (r = 0.60; $p < 0.05$), while *Alphaproteobacteria* correlated positively with PO_4^3 (r = 0.51; $p < 0.05$) and negatively with CHL (r = 0.46; $p < 0.05$).

Pearson correlation analysis (Fig. 4) showed that *Lactobacillales* of the class *Bacilli* correlated negatively with temperature, while a positive

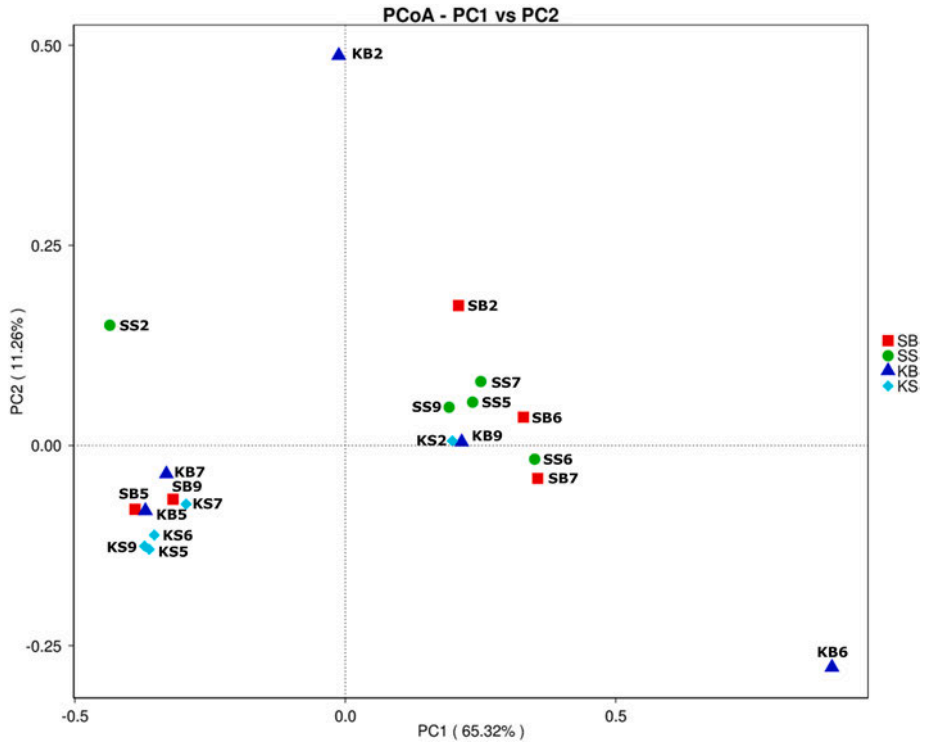

Fig. 3. Beta diversity of the bacterial communities at studied WWTPs effluent sites. Principal coordinates analysis (PcoA) plots were constructed applying the weighted Unifrac distance matrix on the CSS normalized OTU table data.

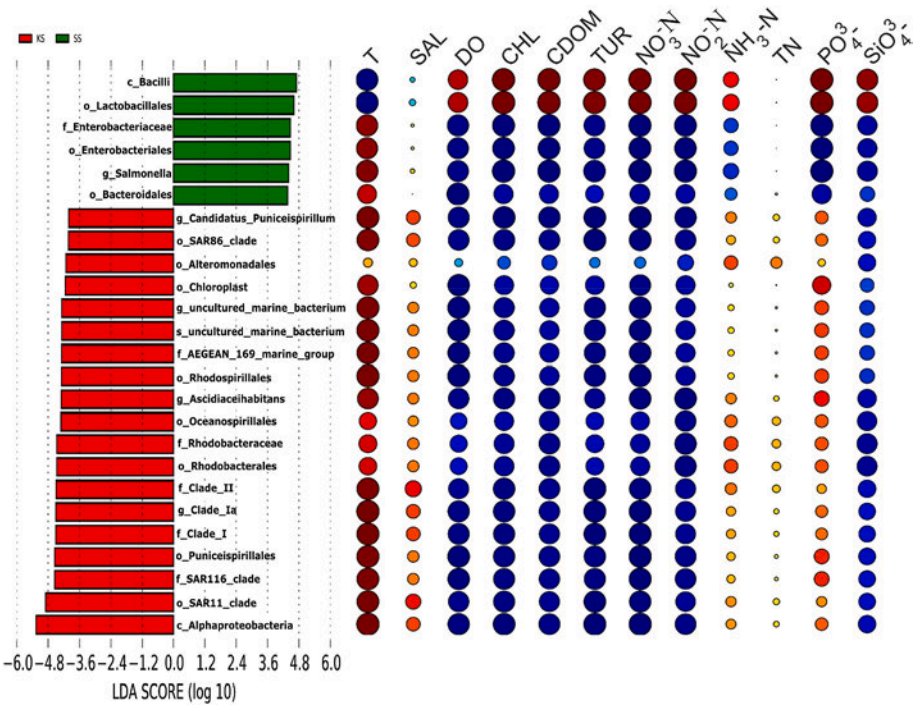

Fig. 4. Pearson correlation matrix of microbial taxa in KS and SS of LDA values higher than 2.0 with environmental factors. The circles indicate positive (red) and negative (blue) correlation, while circle size indicates the size of the correlation. T, temperature; SAL, salinity; DO, dissolved oxygen; CDOM, colored dissolved organic matter; NO_3^-, nitrate anion; NO_2^-, nitrite anion; NH_4^+, ammonium cation; TN, total nitrogen; PO_4^{3-}, phosphate anion. (For interpretation of the references to color in this figure legend, the reader is referred to the Web version of this article.)

correlation was found with most parameters, including CDOM, TUR, CHL, nitrites and nitrates. The opposite pattern of *Lactobacillales* was observed for the order *Enterobacteriales* of the class *Gammaproteobacteria* and the rest of the microbes persisting at both surface sites with environmental parameters. Only the orders *Enterobacteriales* and *Bacteroidales* showed a negative correlation with NH3–N and PO_4^3 , while the rest of the microbes from both stations correlated positively.

3.6. Bacterial genera associated with human pathogenesis

Of the total of 628 identified genera, 74 include species associated with disease in humans. The relative abundance of these taxa per microbiome is shown in Table 2 and was the highest in SS and KB (32.45 and 22.65%). Of these, *Acinetobacter, Salmonella, Escherichia-Shigella, Paenibacillus*, *Bacteroides*, *Lactobacillus, Bifidobacterium* and *Arcobacter,*

were among the most prevalent pathogenic genera, and were abundant by >2% in at least one of the analyzed bacterial communities (Fig. 5).

3.7. Resistome prediction

PICRUSt2 inferred ARGs content in studied microbiomes (Fig. 6, Table S3). We detected the highest abundance of genes encoding for multidrug resistance efflux pumps, particularly the MexAB-OprM (max 20.9% in KS, avg 15.3%), AcrEF-TolC (max 10.4% in KS, avg 8%) and MdtEF-TolC (max 10.4% in KS, avg 6.8%). This was followed by the genes encoding for modified peptidoglycan precursors in Gram-positive bacteria, D-alanyl-D-lactate (*vanA*, *vanB*, *vanD* and *vanM*) and D-alanyl-D-serine (*vanC*, *vanE*, *vanG*, and *vanL*) ligase responsible for resistance to vancomycin and teicoplanin. These were primarily associated with microbiome from Strobreč WWTP, with 16% and 8.3% of relative abundances in SB (avgs 12.6% and 6.2%). This was followed by transporter genes encoding for tetracycline (including *tet*-like genes), macrolide and phenicol resistance (avg 6.8%), genes of *bla* operon (including regulator genes *blaR1* and *blaI,* and β-lactamase genes *blaZ* and *penP*) conferring β-lactam resistance (avg 5.9%), acetyltransferases (avg 3.2%) mediating phenicol resistance and the genes related to the repression of OprD porin (avg 3%) leading to imipenem resistance.

When comparing the ARGs content, SS was significantly enriched with genes related to cationic antimicrobial peptide (CAMP) resistance, such as *dltABCD* operon (abundance 5.6%, avg 3.1%, $p < 0.05$). In addition, genes encoding for OXA-type of class D β-lactamases were enriched in SS in comparison to SB and KS (0.25%, avg 0.18%). In addition, SS microbiome displayed a significant increase of genes encoding for multidrug resistance efflux pumps AcrEF-TolC, MdtEF-TolC and MexEF-OprN when compared to KS. Fig. 7 and Table S4. show more specifically in which extent the most abundant pathogenic genera contribute to the resistance to nine classes of antimicrobial drugs as well as to multiple classes. For instance, genus *Klebsiella* greatly contributed to aminoglycoside, CAMP, macrolide, phenicol, quinolone, β-lactam and multidrug resistance in the KB microbiome. On the other hand, a number of genera, among which *Acinetobacter, Arcobacter, Bacteroides, Escherichia-Shigella, Pseudomonas* and *Salmonella,* account for the most of multidrug resistance genotypes in analyzed microbiomes regardless of their origin. Overall, *Acinetobacter, Bacteroides* and *Pseudomonas* are the genera that contributed to the resistance to the most of antibiotic classes in analyzed bacterial communities (Fig. 7.).

4. Discussion

The main objective of this study was to provide a comprehensive overview of the microbiome structure and associated AR in treated effluent from submarine outfalls in the central Adriatic Sea in Croatia, as well as to assess environmental factors leading to microbiome variation at the bottom and the surface of the effluent-receiving water column.

4.1. Microbial counts

Higher counts of FIB in most of the samples collected from the bottom compared to those from the surface indicate that bottom sites are influenced by fecal pollution from the submarine outfalls. In addition, due to a lockdown caused by the COVID-19 pandemic, sampling was mainly conducted in the warmer months (May, June, July and September) characterized by a stratified water column. A significant decrease and complete absence of FIB in most surface samples suggest that the stratification of the water column was strong enough to maintain discharge below the pycnocline. On the other hand, the lack of stratification could explain the higher level of FIB as well as organic matter, TN, and PO_4^3 detected in surface samples in February at both stations, especially in SS. Nevertheless, gulls as sources of point pollution could have also contributed to the higher FIB counts in these samples (Araujo et al., 2014).

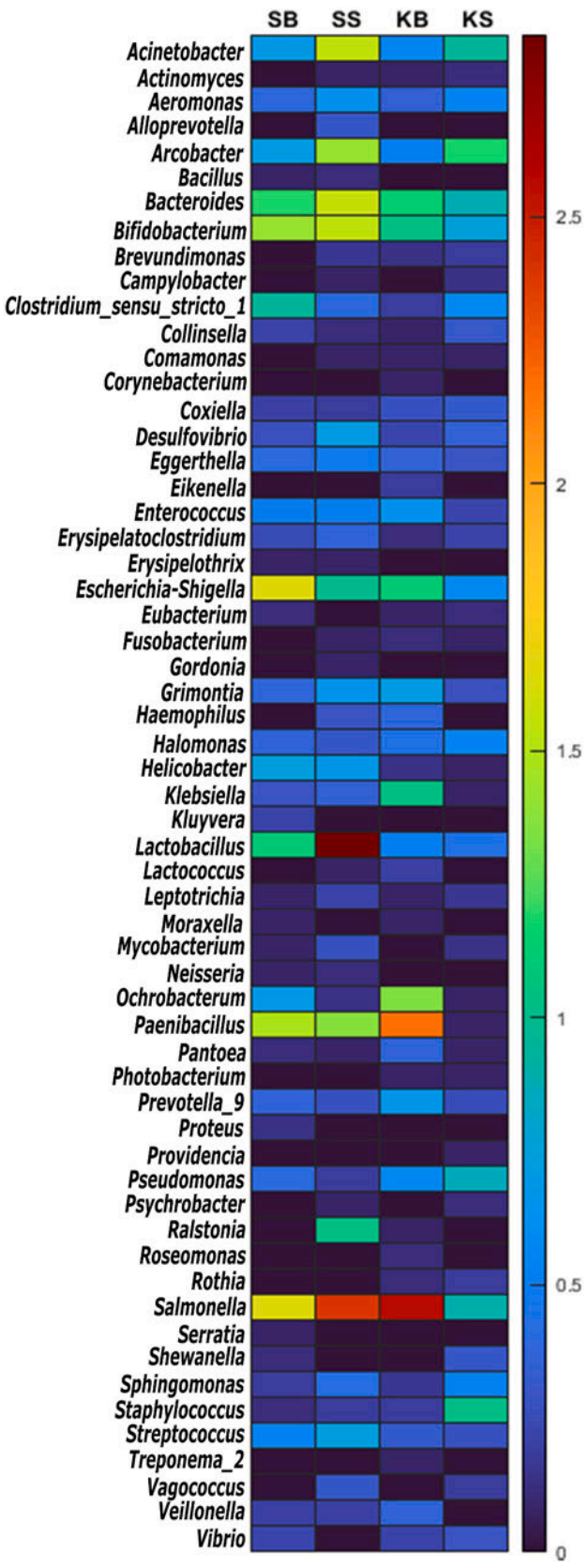

Fig. 5. Heatmap of the 74 pathogenic genera in water samples from Stobreč bottom (SB), Stobreč surface (SS), Katalinića Brig bottom (KB), and Katalinića Brig surface (KS), showing variations in relative abundance (expressed as square roots of the percentage values).

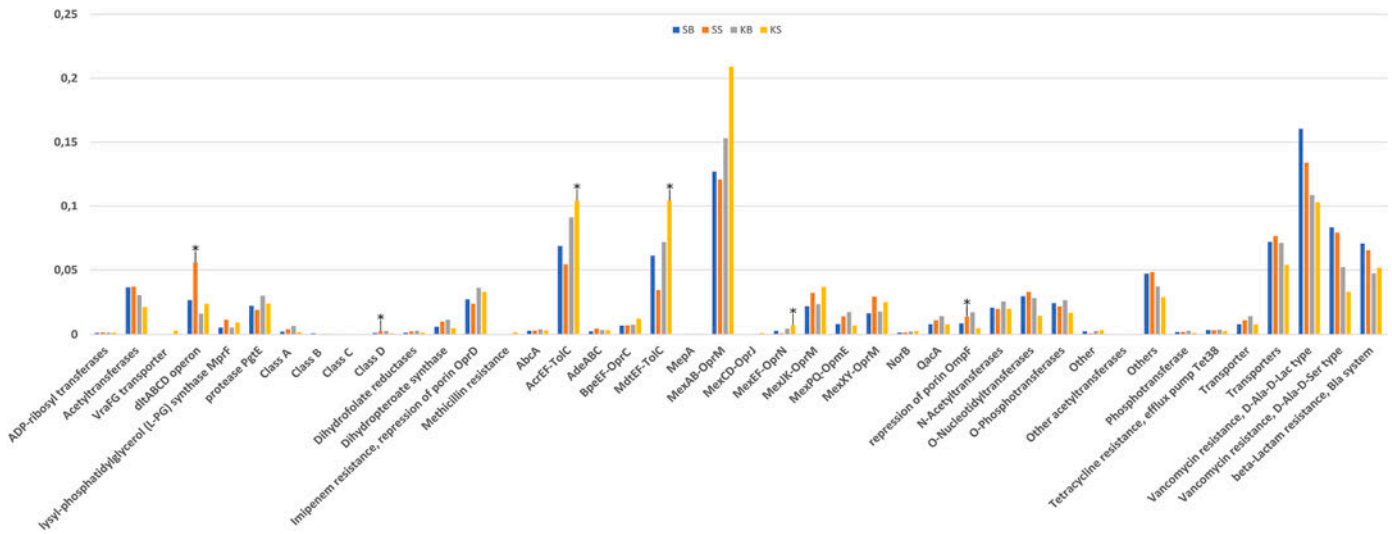

Fig. 6. Repertoire of antibiotic resistance mechanisms associated with the effluent-impacted microbiomes as predicted by PICRUSt tool, representing the average of the relative abundances of each gene set and gene variant available in the KEGG Brite Antimicrobial Resistance Genes database. Significant difference (in term of increase) in abundance between the studied microbiomes is denoted by * for $p < 0.05$ and **$p < 0.01$. Supporting information is available in Table S1. Sampling sites: Stobreč (bottom and surface, SB and SS) and Katalinića Brig (bottom and surface, KB and KS) WWTPs discharge sites.

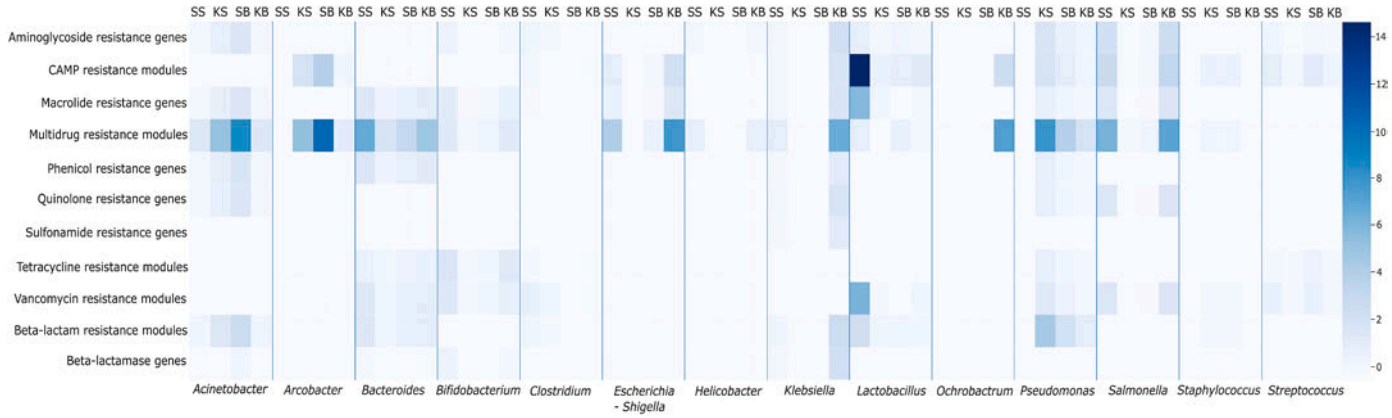

Fig. 7. Heatmap depicting the relative abundance of 14 most common pathogenic genera (expressed as square roots of the percentage values) in studied microbiomes with regards to their reference to KEGG Brite Antimicrobial Resistance Genes database.

Higher bacterial community diversity detected at the surface than at the bottom of the water column at both locations provides additional evidence that the microbiome in the bottom layer is under more anthropogenic pressure, particularly regarding human commensal bacteria and nutrients, resulting in a less divergent microbial profile. In this regard, KS was found to be under the least anthropogenic influence (as for human commensals, environmental parameters, and nutrients) and had the highest community diversity, which also corresponded to the highest richness as observed by alpha indices.

4.2. Most prevalent bacterial taxa at two effluent-receiving marine areas

Two WWTPs in the central Adriatic Sea process diverse types of wastewaters. Notably, Katalinića Brig WWTP treats municipal, hospital and rainfall-runoff wastewater, while Stobreč WWTP processes only the municipal wastewater. This could be one of the factors leading to a difference in microbial community structure between those two locations, with *Firmicutes* being the most abundant phyla near Stobreč wastewater submarine outfall (SB and SS) and *Proteobacteria* near Katalinića Brig submarine outfall (KB and KS). At both locations, bottom and surface microbiomes consist of typical phyla found in WWTPs effluents worldwide (Cai et al., 2014; García-Aljaro et al., 2019; Narciso-da-Rocha et al., 2018; Port et al., 2012) and in adjacent freshwater (Bondarczuk and Piotrowska-Seget, 2019) or seawater (Zheng et al., 2019). Notably, the commonly detected phyla in treated wastewater include *Firmicutes, Proteobacteria, Actinobacteria* and *Bacteroidetes* with classes such as *Clostridia, Bacilli, Bacteroidia, Alpha-* and *Gammaproteobacteria,* reflecting the profile of the human gut microbiome. As expected, *Clostridia*, whose members are commonly found in human and animal feces (Cook et al., 2010; Liu et al., 2008), were the most abundant class in SB, SS, and KB. Besides *Firmicutes*, the most dominant phyla in this study were *Proteobacteria* and the class *Bacteroidia,* which prevail in the human and animal gastrointestinal tract and are thus highly abundant in sewage (Su et al., 2017). On the other hand, the presence of *Actinobacteria,* which were among the four most abundant phyla in this study, in coastal marine areas suggests an influence of terrestrial or freshwater runoff (Kelly and Chistoserdov, 2001; Port et al., 2012). The predominant phylum in such sewer systems is mostly *Proteobacteria* (Hu et al., 2017; Newton et al., 2013), Moreover, a handful of environmental studies point to *Firmicutes* as the dominant phyla in various WWTPs discharges (McLellan et al., 2010; Port et al., 2012). In accordance, *Firmicutes* were among the two most abundant phyla at surveyed sites, and were mainly represented by the families *Lachnospiraceae, Ruminococcaceae, Lactobacillaceae* and *Paenibacillaceae.* Both *Lachnospiraceae*

and *Ruminococcaceae* are commonly associated with the human and animal gastrointestinal tracts and have been previously proposed as microbial source detection markers (Newton et al., 2013, 2011).

Proteobacteria were in this study mainly represented by *Enterobacteriaceae, Rhodobacteraceae, Saccharospirillaceae,* SAR116_clade and Clade_I. *Enterobacteriaceae* constitute an important part of the human gut (Pitout, 2008) and were found to be the most prevalent in KB, which could be related to the fact that hospital wastewater is processed in this particular WWTP, although University Hospital Split had a samewhat decrease in a number of hospitalized patients in 2020 when compared to a pre-pandemic 2019 (Croatian Institute of Public Health, 2020, 2021). It is noteworthy that hospital wastewater is a significant source of multidrug-resistant *Enterobacteriaceae* (Chagas et al., 2011; Galvin et al., 2010; Kotlarska et al., 2015; Picão et al., 2013). On the other hand, autochthonous marine *Rhodobacteraceae* and SAR116_clade which represent ubiquitous lineages of marine bacterioplankton (Giovannoni and Rappé, 2000; Garrity et al., 2005) contributed significantly to the higher diversity of KS microbiome. Regarding the less abundant bacterial taxa (Fig. 2), most of them were human gut commensals, whereas *Deltaproteobacteria* were found to be related with antibiotic polluted sites (Guan et al., 2018; Xiong et al., 2015).

4.3. Environmental influences on bacterial community structure

T, CDOM and nitrogen nutrients were shown to be the most determining factors related to the changes in the microbial community. The positive correlation of *Alphaproteobacteria, Gammaproteobacteria* and *Bacilli* with nutrients and CHL is a consequence of enrichment of water column with nutrient sources from the wastewater, which is in accordance with previous studies (Fierer et al., 2007; Wang et al., 2018; Zoppini et al., 2010). Clostridia indicate sewage pollution (Hill et al., 1993) and correlate with CDOM which is used for wastewater mapping in coastal waters (Nezlin et al., 2020; Rogowski et al., 2012). T and SAL were limiting factors for microbial growth (Miller et al., 2009; Wang et al., 2016). In our study, SAL was not the predominant factor, as chemical, rather than physical parameters, influenced the structure of microbial community, probably due to the loads of nutrients. Zheng et al. (2019) found that nutrient concentration was not significantly related to microbial community, which is contrary to our study but in agreement with some other studies (Lu et al., 2020; Wang et al., 2018). The observed differences could be related to the composition of influent, wastewater treatment stages used in different WWTPs, as well as the proximity of the marine outfalls and surveyed sites.

4.4. Spatial and vertical variations of microbiome composition

PCoA did not identify a clear pattern of grouping the microbiomes according to the site. Clustering of the surface microbiomes, at both marine outfall locations, was tighter when compared to the bottom microbiomes. This could be because the bottom of the water column is under intrusion of the wastewater plume as the wastewater discharge is discrete rather than continuous. The WWTP operates by pumping the effluent approximately every 45 min when the compensation basin is filled. In addition, the difference in the composition of the wastewater and the time lag between the plume intrusion and field sampling could also contribute to a higher heterogeneity of the monthly sampled bottom microbiomes. Surface microbiomes, besides KS.2 and SS.2, clustered tightly at the monthly level, but separately regarding the effluent site which proves our presumption about the lower effluent impact on surface microbial communities. During February, the vertical mixing of the water column may have attributed to such variations in microbial structure at surface locations. Additionally, FIB enumeration and the values of some environmental parameters support our presumptions about effluent rising to the surface due to unstratified conditions, which further induced changes in surface microbiome structure.

LEfSE analysis of surface microbiomes revealed a higher anthropogenic impact in case of SS than KS. Members of classes *Bacilli* and *Gammaproteobacteria* were found to be significant taxonomic biomarkers in SS and *Alphaproteobacteria* in KS. *Alphaproteobacteria* members are morphologically, physiologically and metabolically diverse and adapted to different habitats (Rathsack et al., 2011; Williams et al., 2007), participating in several important metabolic processes such as photosynthesis, nitrogen fixation and ammonia oxidation (Campagne et al., 2012). Thus, the significance of *Alphaproteobacteria* in KS points to this site as the most diverse and under the lowest anthropogenic impact. On contrary, SS was more abundant with members of clinically important bacteria, such as *Gammaproteobacteria* and *Bacilli*, which are more associated with the anthropogenic impact. It is also important to note that KS bacterial community correlated positively with SAL, unlike SS, probably due to a larger abundance of autochthonous marine bacteria in KS.

LEfSE analysis revealed more differences in microbial composition between the bottom and surface microbiomes at the Katalinića Brig than at the Stobreč submarine outfall. These results provide additional evidence of a higher anthropogenic impact (as for nutrients, environmental parameters and human commensal bacteria) in SS than in KS. Moreover, KS biomarkers in comparison to KB were bacterial genera which commonly persist in surface coastal waters, such as SAR_116 clade (Treusch et al., 2009) and *Synechococcus* sp. (Agawin et al., 2003; Kim et al., 2018), evidencing higher variability of KS microbiome and lower impact of human gut-associated bacteria.

4.5. PICRUSt prediction of AR determinants

Annotation of microbiome-specific AR profiles based on 16S rRNA data revealed differences among the studied sites. KB was found to have the highest average incidence of CL and IMP resistance over a 5-month sampling period compared to other sites (Table 1). This may be related to the overabundance of multidrug efflux-related genes indicated by PICRUSt as predominant AR markers (Fig. 6). Notably, KB was found to have the highest relative abundance of chromosomally encoded tripartite RND efflux systems such as AcrAB-TolC, which contributes to the resilience of *E. coli* to nine classes of antibiotics, including carbapenems (Kobylka et al., 2020), as well as the MexAB-OprM, whose upregulation in *Pseudomonas aeruginosa* is generally associated with IMP resistance (Moubareck et al., 2019) and also tolerance to CL (Pamp et al., 2008). Moreover, genes encoding oxacillinases (OXA) of the class D β-lactamases were enriched in SS compared to SB, which was supported by the increased levels of IMP resistance (Table 1) as well as the highest detected abundance of *Acinetobacter* (Suppl Fig. S3) in this bacterial community. Various *Acinetobacter* spp. intrinsically possess class D enzymes (Evans and Amyes, 2014) with some, such as OXA-23 and OXA-58, being detected in *Enterobacteriaceae* and *P. aeruginosa* are spread globally (Munita and Arias, 2016).

Moreover, various emerging pathogenic genera were introduced by effluents and found at the bottom and surface of the water column, indicating anthropogenic effluent impact on the indigenous bacterial community. Introduced bacteria were found to carry characteristic AR signature (Fig. 7) and enrich the marine resistome, pointing to the potential risk for further inter- and intra-species transmission of AR determinants (Maravić et al., 2013, 2014; Rizzo et al., 2013; Zhuang et al., 2021).

5. Conclusions

Our study evidenced the impact of submarine discharges of inadequately treated wastewater on seawater quality at the bottom and surface of effluent-receiving waters of the central Adriatic. Despite stratified conditions during most sampling, the water column surface was affected by the effluent plume, resulting in alteration of physicochemical properties and enrichment of the marine bacterial community with nonindigenous and pathogenic bacteria carrying an arsenal of AR

determinants. An integrated approach annotating the ARGs repertoire based on the taxonomic profile of the whole bacterial community enables a powerful basis for a comprehensive investigation of the extent of ARGs and bacterial pollution in the environment without using time-consuming and often limiting culture-based techniques, providing an important framework for the design and operation of more effective wastewater management.

Credit author statement

MK: Investigation, Formal analysis, writing of original draft, Visualization, Data curation; HK, MDŽ; , IŠ; : Validation, Methodology, Formal analysis; RA: Conceptualization; Funding acquisition; AM: Conceptualization, Formal analysis, writing of original draft, Visualization, Supervision, Data curation, Funding acquisition. All authors read and approved the final manuscript.

Funding

This research was partially supported by project STIM-REI (KK.01.1.1.01.0003) through the European Regional Development Fund – the Operational Programme Competitiveness and Cohesion 2014–2020 (KK.01.1.1.01), Croatian Science Foundation (UIP-2019-04-9778), Interreg CBC Italy-Croatia project "Managed use of treated urban wastewater for the quality of the Adriatic Sea" (AdSWiM), the project CAAT "Coastal Auto-purification Assessment Technology" funded by European Union from European Structural and Investment Funds (2014).–2020., Contract Number: KK.01.1.1.04.0064, and the annual funds for institutional financing of scientific activity from Ministry of Science and Education of Republic of Croatia.

Declaration of competing interest

The authors declare that they have no known competing financial interests or personal relationships that could have appeared to influence the work reported in this paper.

Acknowledgments

The authors acknowledge the Public Health Institute in Zadar, Croatia, for sample collection and chemical analysis.

Appendix A. Supplementary data

Supplementary data to this article can be found online at https://doi.org/10.1016/j.envpol.2021.118282.

Availability of data

The raw data obtained by Illumina-based amplicon sequencing of 16S rRNA gene have been deposited in the European Nucleotide Archive (ENA) at EMBL-EBI under accession number PRJEB45742.

References

Agawin, N.S.R., Duarte, C.M., Agustí, S., McManus, L., 2003. Abundance, biomass and growth rates of Synechococcus sp. in a tropical coastal ecosystem (Philippines, South China Sea). Estuar. Coast Shelf Sci. 56, 493–502. https://doi.org/10.1016/S0272-7714(02)00200-7.

Arar, E.J., Collins, G.B., 1997. Method 445.0: Chlorophyll A. U.S. Environ. Prot. Agency.

Araujo, S., Henriques, I.S., Leandro, S.M., Alves, A., Pereira, A., Correia, A., 2014. Gulls identified as major source of fecal pollution in coastal waters: a microbial source tracking study. Sci. Total Environ. 470, 84–91. https://doi.org/10.1016/j.scitotenv.2013.09.075.

Baird, R., Bridgewater, L., 2017. Standard Methods for the Examination of Water and Wastewater. American Public Health Association, Washington, D.C.

Bondarczuk, K., Piotrowska-Seget, Z., 2019. Microbial diversity and antibiotic resistance in a final effluent-receiving lake. Sci. Total Environ. 650, 2951–2961. https://doi.org/10.1016/j.scitotenv.2018.10.050.

Cai, L., Ju, F., Zhang, T., 2014. Tracking human sewage microbiome in a municipal wastewater treatment plant. Appl. Microbiol. Biotechnol. 98, 3317–3326. https://doi.org/10.1007/s00253-013-5402-z.

Campagne, S., Damberger, F.F., Kaczmarczyk, A., Francez-Charlot, A., Allain, F.H.T., Vorholt, J.A., 2012. Structural basis for sigma factor mimicry in the general stress response of Alphaproteobacteria. Proc. Natl. Acad. Sci. U.S.A. 109 https://doi.org/10.1073/pnas.1117003109.

Caporaso, J.G., Kuczynski, J., Stombaugh, J., Bittinger, K., Bushman, F.D., Costello, E.K., Fierer, N., Peña, A.G., Goodrich, J.K., Gordon, J.I., Huttley, G.A., Kelley, S.T., Knights, D., Koenig, J.E., Ley, R.E., Lozupone, C.A., McDonald, D., Muegge, B.D., Pirrung, M., Reeder, J., Sevinsky, J.R., Turnbaugh, P.J., Walters, W.A., Widmann, J., Yatsunenko, T., Zaneveld, J., Knight, R., 2010. QIIME allows analysis of high-throughput community sequencing data. Nat. Methods 7, 335–336. https://doi.org/10.1038/nmeth.f.303.

Chagas, T.P.G., Seki, L.M., da Silva, D.M., Asensi, M.D., 2011. Occurrence of KPC-2-producing Klebsiella pneumoniae strains in hospital wastewater. J. Hosp. Infect. 77, 281. https://doi.org/10.1016/j.jhin.2010.10.008.

Chen, J., Zhang, Z., Lei, Z., Shimizu, K., Yao, P., Su, Z., Wen, D., 2020. Occurrence and distribution of antibiotic resistance genes in the coastal sediments of effluent-receiving areas of WWTPs, China. Bioresour. Technol. Reports 11, 100511. https://doi.org/10.1016/j.biteb.2020.100511.

CLSI, 2020. M100Ed30 | Performance Standards for Antimicrobial Susceptibility Testing, 30th Edition. Performance Standards for Antimicrobial Susceptibility Testing.

Cook, K.L., Rothrock, M.J., Lovanh, N., Sorrell, J.K., Loughrin, J.H., 2010. Spatial and temporal changes in the microbial community in an anaerobic swine waste treatment lagoon. Anaerobe 16, 74–82. https://doi.org/10.1016/j.anaerobe.2009.06.003.

Croatian Institute of Public Health, 2020. Work of Hospitals in Croatia in 2019 [in Croatian]. https://www.hzjz.hr/wp-content/uploads/2020/09/Rad-bolnica-u-Hrvatskoj-2019.pdf. (Accessed 3 September 2021).

Croatian Institute of Public Health, 2021. Work of Hospitals in Croatia in 2020 [in Croatian]. https://www.hzjz.hr/wp-content/uploads/2021/07/Rad-bolnica-u-2020.pdf. (Accessed 3 September 2021).

Dinsdale, E.A., Edwards, R.A., Hall, D., Angly, F., Breitbart, M., Brulc, J.M., Furlan, M., Desnues, C., Haynes, M., Li, L., McDaniel, L., Moran, M.A., Nelson, K.E., Nilsson, C., Olson, R., Paul, J., Brito, B.R., Ruan, Y., Swan, B.K., Stevens, R., Valentine, D.L., Thurber, R.V., Wegley, L., White, B.A., Rohwer, F., 2008. Functional metagenomic profiling of nine biomes. Nature 452, 629–632. https://doi.org/10.1038/nature06810.

Douglas, G.M., Maffei, V.J., Zaneveld, J.R., Yurgel, S.N., Brown, J.R., Taylor, C.M., Huttenhower, C., Langille, M.G.I., 2020. PICRUSt2 for prediction of metagenome functions. Nat. Biotechnol. 38, 685–688. https://doi.org/10.1038/s41587-020-0548-6.

Evans, B.A., Amyes, S.G.B., 2014. OXA β-lactamases. Clin. Microbiol. Rev. 27, 241. https://doi.org/10.1128/CMR.00117-13.

Fierer, N., Bradford, M.A., Jackson, R.B., 2007. Toward an ecological classification of soil bacteria. Ecology 88, 1354–1364. https://doi.org/10.1890/05-1839.

Fresia, P., Antelo, V., Salazar, C., Giménez, M., D'Alessandro, B., Afshinnekoo, E., Mason, C., Gonnet, G.H., Iraola, G., 2018. City-wide metagenomics uncover antibiotic resistance reservoirs in urban beach and sewage waters. bioRxiv 1–10. https://doi.org/10.1101/456517.

Galvin, S., Boyle, F., Hickey, P., Vellinga, A., Morris, D., Cormican, M., 2010. Enumeration and characterization of antimicrobial-resistant escherichia coli bacteria in effluent from municipal, hospital, and secondary treatment facility sources. Appl. Environ. Microbiol. 76, 4772–4779. https://doi.org/10.1128/AEM.02898-09.

García-Aljaro, C., Blanch, A.R., Campos, C., Jofre, J., Lucena, F., 2019. Pathogens, faecal indicators and human-specific microbial source-tracking markers in sewage. J. Appl. Microbiol. 126, 701–717. https://doi.org/10.1111/jam.14112.

Garrity, G.M., Bell, J.A., Lilburn, T., Class, I., 2005. Alphaproteobacteria class. nov. In: Brenner, D.J., Krieg, N.R., Stanley, J.T., Garrity, G.M. (Eds.), The Proteobacteria), Part C the Alpha -, Beta -, Delta -, and Epsilonproteobacteria, Bergey's Manual of Sytematic Bacteriology, second ed., vol. 2. Springer, New York, USA, p. 1.

Giovannoni, S.J., Rappé, M.S., 2000. Evolution, diversity and molecular ecology of marine prokaryotes. In: Kirchman, D.L. (Ed.), Microbial Ecology of the Oceans. Wiley, New York, USA, pp. 47–84.

Grasshoff, K., Kremling, K., Ehrhardt, M., 1998. Methods of Seawater Analysis: Third, Completely Revised and Extended Edition, Methods of Seawater Analysis: Third, Completely Revised and Extended Edition. https://doi.org/10.1002/9783527613984.

Griffin, D.W., Banks, K., Gregg, K., Shedler, S., Walker, B.K., 2020. Antibiotic resistance in marine microbial communities proximal to a Florida sewage outfall system. Antibiotics 9. https://doi.org/10.3390/antibiotics9030118.

Guan, Y., Jia, J., Wu, L., Xue, X., Zhang, G., Wang, Z., 2018. Analysis of bacterial community characteristics, abundance of antibiotics and antibiotic resistance genes along a pollution gradient of Ba river in Xi'an, China. Front. Microbiol. 9, 3191. https://doi.org/10.3389/fmicb.2018.03191.

Hill, R.T., Knight, I.T., Anikis, M.S., Colwell, R.R., 1993. Benthic distribution of sewage sludge indicated by Clostridium perfringens at a deep-ocean dump site. Appl. Environ. Microbiol. 59, 47–51. https://doi.org/10.1128/aem.59.1.47-51.1993.

Hou, D., Huang, Z., Zeng, S., Liu, J., Wei, D., Deng, X., Weng, S., He, Z., He, J., 2017. Environmental factors shape water microbial community structure and function in shrimp cultural enclosure ecosystems. Front. Microbiol. 8, 1–12. https://doi.org/10.3389/fmicb.2017.02359.

Hu, W., Murata, K., Horikawa, Y., Naganuma, A., Zhang, D., 2017. Bacterial community composition in rainwater associated with synoptic weather in an area downwind of

the Asian continent. Sci. Total Environ. 601–602, 1775–1784. https://doi.org/10.1016/j.scitotenv.2017.06.052.
IOC, SCOR, IAPSO, 2010. The international thermodynamic equation of seawater -2010. Oceaographci com. Manuals Guid 26, 220.
Ivancic, I., Degobbis, D., 1984. An optimal manual procedure for ammonia analysis in natural waters by the indophenol blue method. Water Res. 18, 1143–1147. https://doi.org/10.1016/0043-1354(84)90230-6.
Jozić, S., Vukić Lušić, D., Ordulj, M., Frlan, E., Cenov, A., Diković, S., Kauzlarić, V., Fiorido Đurković, L., Stilinović Totić, J., Ivšinović, D., Eleršek, N., Vučić, A., Peroš-Pucar, D., Unić Klarin, B., Bujas, L., Puljak, T., Mamić, M., Grilec, D., Jadrušić, M., Šolić, M., 2018. Performance characteristics of the temperature-modified ISO 9308-1 method for the enumeration of Escherichia coli in marine and inland bathing waters. Mar. Pollut. Bull. 135, 150–158. https://doi.org/10.1016/j.marpolbul.2018.07.002.
Kelly, K.M., Chistoserdov, A.Y., 2001. Phylogenetic analysis of the succession of bacterial communities in the great South Bay (Long Island). FEMS Microbiol. Ecol. 35, 85–95. https://doi.org/10.1016/S0168-6496(00)00115-X.
Kim, Y., Jeon, J., Kwak, M.S., Kim, G.H., Koh, I.S., Rho, M., 2018. Photosynthetic functions of Synechococcus in the ocean microbiomes of diverse salinity and seasons. PLoS One 13, 4–8. https://doi.org/10.1371/journal.pone.0190266.
Kobylka, J., Kuth, M.S., Müller, R.T., Geertsma, E.R., Pos, K.M., 2020. AcrB: a mean, keen, drug efflux machine. Ann. N. Y. Acad. Sci. 1459, 38–68. https://doi.org/10.1111/nyas.14239.
Kotlarska, E., Łuczkiewicz, A., Pisowacka, M., Burzyński, A., 2015. Antibiotic resistance and prevalence of class 1 and 2 integrons in Escherichia coli isolated from two wastewater treatment plants, and their receiving waters (Gulf of Gdansk, Baltic Sea, Poland). Environ. Sci. Pollut. Res. 22 https://doi.org/10.1007/s11356-014-3474-7, 2018–2030.
Lapointe, B.E., Thacker, K., Hanson, C., Getten, L., 2011. Sewage pollution in Negril, Jamaica: effects on nutrition and ecology of coral reef macroalgae. Chin. J. Oceanol. Limnol. 29, 775–789. https://doi.org/10.1007/s00343-011-0506-8.
Liu, C., Finegold, S.M., Song, Y., Lawson, P.A., 2008. Reclassification of Clostridium coccoides, Ruminococcus hansenii, Ruminococcus hydrogenotrophicus, Ruminococcus luti, Ruminococcus productus and Ruminococcus schinkii as Blautia coccoides gen. nov., comb. nov., Blautia hansenii comb. nov., Blautia hydroge. Int. J. Syst. Evol. Microbiol. 58 https://doi.org/10.1099/ijs.0.65208-0, 1896–1902.
Lu, Q., Song, Y., Mao, G., Lin, B., Wang, Y., Gao, G., 2020. Spatial variation in bacterial biomass, community composition and driving factors across a eutrophic river. Ecotoxicol. Environ. Saf. 205, 111113. https://doi.org/10.1016/j.ecoenv.2020.111113.
Maravić, A., Skočibušić, M., Šamanić, I., Fredotović, Ž., Cvjetan, S., Jutronić, M., Puizina, J., 2013. Aeromonas spp. simultaneously harbouring blaCTX-M-15, blaSHV-12, blaPER-1 and blaFOX-2, in wild-growing Mediterranean mussel (Mytilus galloprovincialis) from Adriatic Sea, Croatia. Int. J. Food Microbiol. 166 (2), 301–308. https://doi.org/10.1016/j.ijfoodmicro.2013.07.010.
Maravić, A., Skočibušić, M., Cvjetan, S., Šamanić, I., Fredotović, Ž., Puizina, J., 2014. Prevalence and diversity of extended-spectrum-β-lactamase-producing Enterobacteriaceae from marine beach waters. Mar. Pollut. Bull. 90 (1–2), 60–67. https://doi.org/10.1016/j.marpolbul.2014.11.021.
McLellan, S.L., Huse, S.M., Mueller-Spitz, S.R., Andreishcheva, E.N., Sogin, M.L., 2010. Diversity and population structure of sewage-derived microorganisms in wastewater treatment plant influent. Environ. Microbiol. 12, 378–392. https://doi.org/10.1111/j.1462-2920.2009.02075.x.
Miller, S.R., Strong, A.L., Jones, K.L., Ungerer, M.C., 2009. Bar-coded pyrosequencing reveals shared bacterial community properties along the temperature gradients of two alkaline hot springs in Yellowstone National Park. Appl. Environ. Microbiol. 75, 4565–4572. https://doi.org/10.1128/AEM.02792-08.
Mittal, P., Prasoodanan Pk, V., Dhakan, D.B., Kumar, S., Sharma, V.K., 2019. Metagenome of a polluted river reveals a reservoir of metabolic and antibiotic resistance genes. Environ. Microbiomes 14, 1–12. https://doi.org/10.1186/s40793-019-0345-3.
Moubareck, C.A., Halat, D.H., Akkawi, C., Nabi, A., AlSharhan, M.A., AlDeesi, Z.O., Peters, C.C., Celiloglu, H., Karam Sarkis, D., 2019. Role of outer membrane permeability, efflux mechanism, and carbapenemases in carbapenem-nonsusceptible Pseudomonas aeruginosa from Dubai hospitals: results of the first cross-sectional survey. Int. J. Infect. Dis. 84, 143–150. https://doi.org/10.1016/j.ijid.2019.04.027.
Munita, J.M., Arias, C.A., 2016. Mechanisms of antibiotic resistance. Virulence Mechanisms of Bacterial Pathogens. ASM Press, Washington, DC, USA, pp. 481–511. https://doi.org/10.1128/9781555819286.ch17.
Narciso-da-Rocha, C., Rocha, J., Vaz-Moreira, I., Lira, F., Tamames, J., Henriques, I., Martinez, J.L., Manaia, C.M., 2018. Bacterial lineages putatively associated with the dissemination of antibiotic resistance genes in a full-scale urban wastewater treatment plant. Environ. Int. 118, 179–188. https://doi.org/10.1016/j.envint.2018.05.040.
Newton, R.J., Bootsma, M.J., Morrison, H.G., Sogin, M.L., McLellan, S.L., 2013. A microbial signature approach to identify fecal pollution in the waters off an urbanized coast of lake Michigan. Microb. Ecol. 65, 1011–1023. https://doi.org/10.1007/s00248-013-0200-9.
Newton, R.J., VandeWalle, J.L., Borchardt, M.A., Gorelick, M.H., McLellan, S.L., 2011. Lachnospiraceae and bacteroidales alternative fecal indicators reveal chronic human sewage contamination in an Urban harbor. Appl. Environ. Microbiol. 77, 6972–6981. https://doi.org/10.1128/AEM.05480-11.
Nezlin, N.P., Beegan, C., Feit, A., Gully, J.R., Latker, A., McLaughlin, K., Mengel, M.J., Robertson, G.L., Steele, A., Weisberg, S.B., 2020. Colored Dissolved Organic Matter (CDOM) as a tracer of effluent plumes in the coastal ocean. Reg. Stud. Mar. Sci. 35, 101163. https://doi.org/10.1016/j.rsma.2020.101163.
Pamp, S.J., Gjermansen, M., Johansen, H.K., Tolker-Nielsen, T., 2008. Tolerance to the antimicrobial peptide colistin in Pseudomonas aeruginosa biofilms is linked to metabolically active cells, and depends on the pmr and mexAB-oprM genes. Mol. Microbiol. 68 (1), 223–240.
Picão, R.C., Cardoso, J.P., Campana, E.H., Nicoletti, A.G., Petrolini, F.V.B., Assis, D.M., Juliano, L., Gales, A.C., 2013. The route of antimicrobial resistance from the hospital effluent to the environment: focus on the occurrence of KPC-producing Aeromonas spp. and Enterobacteriaceae in sewage. Diagn. Microbiol. Infect. Dis. 76, 80–85. https://doi.org/10.1016/j.diagmicrobio.2013.02.001.
Pitout, J.D.D., 2008. Multiresistant Enterobacteriaceae: new threat of an old problem. Expert Rev. Anti Infect. Ther. 6, 657–669. https://doi.org/10.1586/14787210.6.5.657.
Port, J.A., Wallace, J.C., Griffith, W.C., Faustman, E.M., 2012. Metagenomic profiling of microbial composition and antibiotic resistance determinants in puget Sound. PLoS One 7. https://doi.org/10.1371/journal.pone.0048000.
Proia, L., Anzil, A., Subirats, J., Borrego, C., Farrè, M., Llorca, M., Balcázar, J.L., Servais, P., 2018. Antibiotic resistance along an urban river impacted by treated wastewaters. Sci. Total Environ. 628–629, 453–466. https://doi.org/10.1016/j.scitotenv.2018.02.083.
Quast, C., Pruesse, E., Yilmaz, P., Gerken, J., Schweer, T., Yarza, P., Peplies, J., Glöckner, F.O., 2013. The SILVA ribosomal RNA gene database project: Improved data processing and web-based tools. Nucleic Acids Res. 41, 590–596. https://doi.org/10.1093/nar/gks1219.
Rathsack, K., Reitner, J., Stackebrandt, E., Tindall, B.J., 2011. Reclassification of Aurantimonas altamirensis (Jurado et al. 2006), Aurantimonas ureilytica (Weon et al. 2007) and Aurantimonas frigidaquae (Kim et al. 2008) as members of a new genus, Aureimonas gen. nov., as Aureimonas altamirensis gen. nov., comb. nov. Int. J. Syst. Evol. Microbiol. 61, 2722–2728. https://doi.org/10.1099/ijs.0.027029-0.
Rizzo, L., Manaia, C., Merlin, C., Schwartz, T., Dagot, C., Ploy, M.C., Michael, I., Fatta-Kassinos, D., 2013. Urban wastewater treatment plants as hotspots for antibiotic resistant bacteria and genes spread into the environment: a review. Sci. Total Environ. 447, 345–360. https://doi.org/10.1016/j.scitotenv.2013.01.032.
Rogowski, P., Terrill, E., Otero, M., Hazard, L., Middleton, W., 2012. Mapping ocean outfall plumes and their mixing using autonomous underwater vehicles. J. Geophys. Res. Ocean. 117, 1–12. https://doi.org/10.1029/2011JC007804.
Roth, F., Lessa, G.C., Wild, C., Kikuchi, R.K.P., Naumann, M.S., 2016. Impacts of a high-discharge submarine sewage outfall on water quality in the coastal zone of Salvador (Bahia, Brazil). Mar. Pollut. Bull. 106, 43–48. https://doi.org/10.1016/j.marpolbul.2016.03.048.
Šamanić, I., Kalinić, H., Fredotović, Ž., Dželalija, M., Bungur, A.M., Maravić, A., 2021. Bacteria Tolerant to Colistin in Coastal Marine Environment: Detection, Microbiome Diversity and Antibiotic Resistance Genes' Repertoire.
Segata, N., Izard, J., Waldron, L., Gevers, D., Miropolsky, L., Garrett, W.S., Huttenhower, C., 2011. Metagenomic biomarker discovery and explanation. Genome Biol. 12 (6), R60. https://doi.org/10.1186/gb-2011-12-6-r60.
Shen, C., Xiong, J., Zhang, H., Feng, Y., Lin, X., Li, X., Liang, W., Chu, H., 2013. Soil pH drives the spatial distribution of bacterial communities along elevation on Changbai Mountain. Soil Biol. Biochem. 57, 204–211. https://doi.org/10.1016/j.soilbio.2012.07.013.
Su, J.Q., An, X.L., Li, B., Chen, Q.L., Gillings, M.R., Chen, H., Zhang, T., Zhu, Y.G., 2017. Metagenomics of urban sewage identifies an extensively shared antibiotic resistome in China. Microbiome 5, 1–15. https://doi.org/10.1186/s40168-017-0298-y.
Su, Z., Li, A., Chen, J., Huang, B., Mu, Q., Chen, L., Wen, D., 2020. Wastewater discharge drives ARGs spread in the coastal area: a case study in Hangzhou Bay, China. Mar. Pollut. Bull. 151, 110856. https://doi.org/10.1016/j.marpolbul.2019.110856.
Treusch, A.H., Vergin, K.L., Finlay, L.A., Donatz, M.G., Burton, R.M., Carlson, C.A., Giovannoni, S.J., 2009. Seasonality and vertical structure of microbial communities in an ocean gyre. ISME J. 3, 1148–1163. https://doi.org/10.1038/ismej.2009.60.
Turlej-Rogacka, A., Xavier, B.B., Janssens, L., Lammens, C., Zarkotou, O., Pournaras, S., Goossens, H., Malhotra-Kumar, S., 2018. Evaluation of colistin stability in agar and comparison of four methods for MIC testing of colistin. Eur. J. Clin. Microbiol. Infect. Dis. 37, 345–353. https://doi.org/10.1007/s10096-017-3140-3.
Vidal-Dorsch, D.E., Bay, S.M., Maruya, K., Snyder, S.A., Trenholm, R.A., Vanderford, B.J., 2012. Contaminants of emerging concern in municipal wastewater effluents and marine receiving water. Environ. Toxicol. Chem. 31, 2674–2682. https://doi.org/10.1002/etc.2004.
Wang, L., Zhang, J., Li, H., Yang, H., Peng, C., Peng, Z., Lu, L., 2018. Shift in the microbial community composition of surface water and sediment along an urban river. Sci. Total Environ. 627, 600–612. https://doi.org/10.1016/j.scitotenv.2018.01.203.
Wang, N.F., Zhang, T., Yang, X., Wang, S., Yu, Y., Dong, L.L., Guo, Y.D., Ma, Y.X., Ye Zang, J., 2016. Diversity and composition of bacterial community in soils and lake sediments from an arctic lake area. Front. Microbiol. 7, 1–9. https://doi.org/10.3389/fmicb.2016.01170.
Wang, Z.H., Yang, J.Q., Zhang, D.J., Zhou, J., Zhang, C.D., Su, X.R., Li, T.W., 2014. Composition and structure of microbial communities associated with different domestic sewage outfalls. Genet. Mol. Res. 13, 7542–7552. https://doi.org/10.4238/2014.
White, J.R., Nagarajan, N., Pop, M., 2009. Statistical methods for detecting differentially abundant features in clinical metagenomic samples. PLoS Comput. Biol. 5 https://doi.org/10.1371/journal.pcbi.1000352.
WHO, 2017. Essential Medicines and Health Products: Global Priority List of Antibiotic-Resistant Bacteria to Guide Research, Discovery, and Development of New Antibiotics. Available online at: (Last accessed 7th July 2021). http://www.who.int/medicines/publications/globalpriority-list-antibiotic-resistant-bacteria.

Williams, K.P., Sobral, B.W., Dickerman, A.W., 2007. A robust species tree for the Alphaproteobacteria. J. Bacteriol. 189, 4578–4586. https://doi.org/10.1128/JB.00269-07.

Xiong, W., Sun, Y., Ding, X., Wang, M., Zeng, Z., 2015. Selective pressure of antibiotics on ARGs and bacterial communities in manure-polluted freshwater-sediment microcosms. Front. Microbiol. 6, 194. https://doi.org/10.3389/fmicb.2015.00194.

Yang, L., 2000. Natural disinfection of wastewater in marine outfall fields. Water Res. 34, 743–750. https://doi.org/10.1016/S0043-1354(99)00209-2.

Yannarell, A.C., Triplett, E.W., 2005. Geographic and environmental sources of variation in lake bacterial community composition. Appl. Environ. Microbiol. 71 (227) https://doi.org/10.1128/AEM.71.1.227-239.2005. LP – 239.

Zheng, B., Liu, W., Xu, H., Li, J., Jiang, X., 2021. Occurrence and distribution of antimicrobial resistance genes in the soil of an industrial park in China: a metagenomics survey. Environ. Pollut. 273, 116467. https://doi.org/10.1016/j.envpol.2021.116467.

Zheng, Y., Su, Z., Dai, T., Li, F., Huang, B., Mu, Q., Feng, C., Wen, D., 2019. Identifying human-induced influence on microbial community: a comparative study in the effluent-receiving areas in Hangzhou Bay. Front. Environ. Sci. Eng. 13 https://doi.org/10.1007/s11783-019-1174-8.

Zhuang, M., Achmon, Y., Cao, Y., Liang, X., Chen, L., Wang, H., Siame, B.A., Leung, K.Y., 2021. Distribution of antibiotic resistance genes in the environment. Environ. Pollut. 285, 117402. https://doi.org/10.1016/j.envpol.2021.117402.

Zoppini, A., Amalfitano, S., Fazi, S., Puddu, A., 2010. Dynamics of a benthic microbial community in a riverine environment subject to hydrological fluctuations (Mulargia River, Italy). Hydrobiologia 657, 37–51. https://doi.org/10.1007/s10750-010-0199-6.

3.3. Submarine outfalls of treated wastewater effluents are sources of extensively- and multidrug-resistant KPC- and OXA-48-producing *Enterobacteriaceae* in coastal marine environment

Reproduced from:

Kvesić M., Šamanić I., Novak A., Fredotović Ž., Dželalija M., Kamenjarin J., Goić Barišić I., Tonkić M. and Maravić A., 2022. Submarine Outfalls of Treated Wastewater Effluents are Sources of Extensively- and Multidrug-Resistant KPC- and OXA-48-Producing *Enterobacteriaceae* in Coastal Marine Environment. Frontiers in Microbiology 13:858821. doi: 10.3389/fmicb.2022.85882

This study addresses the global health threat posed by carbapenemase-producing Enterobacteriaceae (CPE) present in the environment and introduced through submarine outfalls. Of fifteen KPC-producing *Enterobacteriaceae*, eight isolates were analysed by whole genome sequencing (WGS) and showed resistance to 19 antimicrobial classes, virulence genes and plasmid replicons. Several isolates carried 43-90 antibiotic resistance genes, while four carried the carbapenemase genes $bla_{\text{KPC-2}}$ and $bla_{\text{OXA-48}}$. Remarkably, $bla_{\text{KPC-2}}$ was identified on ~40kb IncP6 plasmids, which is a first European report.

This study highlights the occurrence of XDR and potentially virulent KPC -producing *E. coli* in coastal waters and highlights the risk of an infectious threat from submarine outfalls. Furthermore, all these strains were found only in submarine outfalls receiving hospital effluent from associated WWTP. This underlines the influence of hospital effluents on the further spread of AR determinants in the environment.

frontiers | Frontiers in Microbiology

ORIGINAL RESEARCH
published: 06 May 2022
doi: 10.3389/fmicb.2022.858821

Submarine Outfalls of Treated Wastewater Effluents are Sources of Extensively- and Multidrug-Resistant KPC- and OXA-48-Producing *Enterobacteriaceae* in Coastal Marine Environment

*Marija Kvesić[1,2], Ivica Šamanić[3], Anita Novak[4,5], Željana Fredotović[3], Mia Dželalija[3], Juraj Kamenjarin[3], Ivana Goić Barišić[4,5], Marija Tonkić[4,5] and Ana Maravić[3]**

[1]Center of Excellence for Science and Technology, Integration of Mediterranean Region, University of Split, Split, Croatia, [2]Doctoral Study of Biophysics, Faculty of Science, University of Split, Split, Croatia, [3]Department of Biology, Faculty of Science, University of Split, Split, Croatia, [4]School of Medicine, University of Split, Split, Croatia, [5]University Hospital Split, Split, Croatia

OPEN ACCESS

Edited by:
Satoru Suzuki,
Ehime University, Japan

Reviewed by:
Milena Dropa,
University of São Paulo, Brazil
Cristian Ruiz Rueda,
California State University, Northridge, United States

***Correspondence:**
Ana Maravić
ana.maravic@pmfst.hr

Specialty section:
This article was submitted to Antimicrobials, Resistance and Chemotherapy, a section of the journal Frontiers in Microbiology

Received: 20 January 2022
Accepted: 06 April 2022
Published: 06 May 2022

Citation:
Kvesić M, Šamanić I, Novak A, Fredotović Ž, Dželalija M, Kamenjarin J, Goić Barišić I, Tonkić M and Maravić A (2022) Submarine Outfalls of Treated Wastewater Effluents are Sources of Extensively- and Multidrug-Resistant KPC- and OXA-48-Producing Enterobacteriaceae in Coastal Marine Environment. Front. Microbiol. 13:858821. doi: 10.3389/fmicb.2022.858821

The rapid and ongoing spread of carbapenemase-producing *Enterobacteriaceae* has led to a global health threat. However, a limited number of studies have addressed this problem in the marine environment. We investigated their emergence in the coastal waters of the central Adriatic Sea (Croatia), which are recipients of submarine effluents from two wastewater treatment plants. Fifteen KPC-producing *Enterobacteriaceae* (nine *Escherichia coli*, four *Klebsiella pneumoniae* and two *Citrobacter freundii*) were recovered, and susceptibility testing to 14 antimicrobials from 10 classes showed that four isolates were extensively drug resistant (XDR) and two were resistant to colistin. After ERIC and BOX-PCR typing, eight isolates were selected for whole genome sequencing. The *E. coli* isolates belonged to serotype O21:H27 and sequence type (ST) 2795, while *K. pneumoniae* isolates were assigned to STs 37 and 534. Large-scale genome analysis revealed an arsenal of 137 genes conferring resistance to 19 antimicrobial drug classes, 35 genes associated with virulence, and 20 plasmid replicons. The isolates simultaneously carried 43–90 genes encoding for antibiotic resistance, while four isolates co-harbored carbapenemase genes bla_{KPC-2} and bla_{OXA-48}. The bla_{OXA-48} was associated with IncL-type plasmids in *E. coli* and *K. pneumoniae*. Importantly, the bla_{KPC-2} in four *E. coli* isolates was located on ~40 kb IncP6 broad-host-range plasmids which recently emerged as bla_{KPC-2} vesicles, providing first report of these bla_{KPC-2}-bearing resistance plasmids circulating in *E. coli* in Europe. This study also represents the first evidence of XDR and potentially virulent strains of KPC-producing *E. coli* in coastal waters and the co-occurrence of bla_{KPC-2} and bla_{OXA-48} carbapenemase genes in this species. The leakage of these strains through submarine effluents into coastal waters is of concern, indicating a reservoir of this infectious threat in the marine environment.

Keywords: carbapenemase-producing *Enterobacteriaceae*, marine environment, coastal waters, Croatia, KPC, OXA-48

INTRODUCTION

Antibiotic resistance is one of the greatest threats to global health nowadays, leading to the higher mortality rates and increased economic costs (Pulingam et al., 2021). The natural environment has been recognized as one of its major reservoirs (Amarasiri et al., 2020), as antibiotic-resistant human pathogens have been detected in coastal marine areas (Šamanić et al., 2021), rivers (Ekwanzala et al., 2020), lakes (Su et al., 2020) and shellfish (Maravić et al., 2013). Effluents from the wastewater treatment plants (WWTPs) have been evidenced as particularly significant routes for dissemination of antibiotic resistance in the natural environment (Ekwanzala et al., 2020), especially the hospital effluents through which the emerging opportunistic pathogens directly enter from the hospital to the aquatic environment (Ekwanzala et al., 2019).

In recent decades, the rapid spread of Gram-negative bacteria resistant to the most potent β-lactam antibiotics, the carbapenems, and the continuous emergence of new resistant strains have raised the global alarm. In 2017, the World Health Organization defined priority categories for emerging multidrug-resistant pathogens for which new antimicrobials are urgently needed, with carbapenem-resistant *Enterobacteriaceae* (CRE) identified as critical (WHO, 2017). Carbapenem resistance in these bacteria arises mainly from the production of carbapenemases, of which KPC, SME, IMI and NMC belonging to Ambler class A, IMP, VIM and NDM metallo-β-lactamases (MBLs) belonging to class B, and OXA-48 and its derivatives belonging to class D have been detected worldwide (Bonomo et al., 2018; Brolund et al., 2019). In Croatia, CRE isolates are being increasingly reported in hospitals, mainly due to the rapid spread of KPC-producing *Enterobacteriaceae* first in the northwest (Jelić et al., 2016) and later in the southern coastal regions (Bedenić et al., 2021).

Considering the importance of CRE for public health and the One Health approach, we aimed to study for the first time their occurrence in the coastal waters of the eastern Adriatic, focusing on the area influenced by the submarine sewage outlets of two WWTPs, which could serve as potential routes for the introduction of these bacteria into the coastal marine environment. The isolated CRE were analyzed by PCR for the presence of carbapenemase-encoding genes, after which eight KPC-2-producing *Enterobacteriaceae* isolates were subjected to high-throughput DNA sequencing. We then performed a detailed search of the obtained genome sequences, focusing on the antibiotic resistance genes (ARGs), virulence factors and plasmid replicons. The isolates were also assigned to sequence types (STs) using the multi-locus sequence typing (MLST) scheme and their serotype was determined. This study led to the first identification of potentially virulent CRE in the marine environment in Croatia, evidencing a transmission route through submarine outfalls and a new reservoir of these opportunistic pathogens in Croatia outside hospital settings.

MATERIALS AND METHODS

Sampling

Fifteen *Enterobacteriaceae* isolates were recovered in June, July, and September 2020 as part of the project aimed to study the impact of treated submarine effluents in the coastal waters of the central Adriatic Sea in Croatia. Details of the sampling procedure and locations have been described previously (Kvesić et al., 2021). Briefly, the study focused on submarine effluents from the two WWTPs, the Kaplinića brig and the Stupe-Stobreč, which mechanically treat wastewater from the wider Split area at an average flow rate of 35,000 and 30,000 m^3/day, respectively, and discharge it through submarine outfalls into the coastal waters of the Brač and Split channels (**Figure 1**). While the Stobreč WWTP processes only municipal wastewater, the Kaplinića brig WWTP treats municipal wastewater and stormwater runoff. The Kaplinića brig WWTP also collects wastewater from the University Hospital Centre Split, the largest medical center in southern Croatia with 1,400 beds serving a population of approximately 500,000, which increases sharply in the summer months during the tourist season. The submarine outfalls of the Kaplinića brig (43°29′22.7 ″N, 16°27′11.2 ″E) and the Stobreč WWTP (43°28′53.6 ″N 16°31′04.3 ″E) are located at a depth of 42 and 37 m, respectively.

Water samples were collected from the boat using a Niskin sampler, transferred to sterile 1 L bottles, protected from light, and transported to the laboratory for further analysis within 4 h at 4°C.

Bacterial Identification and Antibiotic Susceptibility Testing

One hundred milliliters of the water samples were filtered through 0.2 μm pore size MCE membrane filters (GE Healthcare, United Kingdom), which were then placed on CHROMID® Carba agar (bioMérieux, France) and incubated for 48 h. This chromogenic medium selects for the growth of CRE and allows the typical pink to the burgundy appearance of *Escherichia coli* colonies and blue-green to blue-grey of *Klebsiella*, *Enterobacter*, *Serratia* and *Citrobacter* spp. Incubation was carried out at 42°C to suppress the growth of autochthonous environmental species that are unable to grow under mesophilic conditions. Based on colony morphology, all putative Enterobacteriaceae isolates were cultivated in pure culture on MacConkey agar (Biolife, Italy) at 37°C for 18 h and identified to species level using MALDI-TOF MS (Microflex LT mass spectrometer and MALDI Biotyper 4.1.80, Bruker Daltonics, Germany).

The isolates were tested for susceptibility to 14 antibiotics using Etest strips (AB Biodisk, Sweden) except for colistin (CL) whose susceptibility was tested using the broth microdilution method. The tests were performed, and the minimum inhibitory concentrations (MICs) were interpreted based on the European Committee on Antimicrobial Susceptibility Testing (EUCAST) guidelines (EUCAST, 2020). The MIC value of CL was recorded as the lowest concentration showing no visually detectable bacterial growth in the 96-well microtiter plates and was the

FIGURE 1 | Sampling sites (represented by squares) at the submarine outfalls of the two WWTPs, central Adriatic Sea, Croatia.

consensus value of the experiment performed in triplicate. The antibiotics tested (except CL) and their maximum concentrations were as follows: piperacillin/tazobactam (TZP, 256 μg), piperacillin (PIP, 256 μg), ceftazidime (CAZ, 256 μg), cefotaxime (CTX, 32 μg), cefepime (FEP, 256 μg), aztreonam (ATM, 256 μg), imipenem (IMP, 32 μg), meropenem (MER, 32 μg), ertapenem (ETP, 32 μg), ciprofloxacin (CIP, 32 μg), gentamicin (GEN, 256 μg), tetracycline (TET, 256 μg), and trimethoprim-sulfamethoxazole (SXT, 1/19 μg). *E. coli* ATCC 25922 was used as a control. According to Magiorakos et al. (2012), multidrug-resistant (MDR) phenotype was defined as acquired non-susceptibility to at least one antibiotic from three or more classes, while the extensively drug-resistant (XDR) phenotype was designated as non-susceptibility to at least one agent from all but two or fewer antibiotic classes (i.e., remaining susceptible to only one or two categories).

Isolates were further tested for the presence of class C AmpC β-lactamases with AmpC Etest (AB Biodisk) and carbapenemases with MBL Etest (AB Biodisk) and Rapidec Carba NP test (bioMérieux) according to the manufacturer's instructions. The production of extended-spectrum β-lactamases (ESBLs) was tested using clavulanic acid (CLA) combination discs. The phenotype consistent with the production of ESBLs was defined by an increase in zone diameter of ≥5 mm for CAZ and/or CTX in combination with CLA compared to its zone when tested alone (EUCAST, 2013).

PCR Screening for Carbapenemase Encoding Genes and *mcr-1* Gene

Genomic DNA was extracted using the NucleoSpin Microbial DNA kit (Macherey-Nagel, United Kingdom) and the concentration and quality of DNA were analyzed using the NanoDrop® Spectrophotometer 1000 (Thermo Scientific, United States). Multiplex PCR assays were performed to screen for the presence of carbapenemase genes encoding class A KPC and class B IMP, VIM and NDM using the primers and PCR conditions described previously (Poirel et al., 2011). Isolates were screened by standard PCR for the presence of the *mcr-1* gene, which encodes plasmid-mediated colistin resistance (Liu et al., 2016). The amplified fragments were separated on a 1% (w/v) agarose gel, purified using the ReliaPrep™ DNA Clean-Up and Concentration System (Promega, United States) and subjected to Sanger sequencing of both strands in Macrogen Europe

service (Netherlands). The obtained nucleotide sequences were compared with the homologous sequences from the GenBank database using the BLASTn algorithm.[1]

Molecular Typing of Bacterial DNA

To exclude the possibility of clonal relatedness between the isolates of the same species, enterobacterial repetitive intergenic consensus (ERIC) and BOX PCR analyses were performed using the primers and conditions previously described (Araújo et al., 2014).

High-Throughput DNA Sequencing and Computational Data Analysis

Genomic DNA was sent to Novogene (Cambridge, United Kingdom) for whole genome sequencing (WGS) and bioinformatics analysis of the raw sequencing data. DNA libraries were prepared using the NEBNext® DNA Library Prep Kit (Illumina, United States) and, after a quality check, were subjected to pair-end sequencing on the Illumina NovaSeq 6000 platform with a read length of 150 bp at each end. The obtained reads were subjected to further quality control. Then, the clean reads were mapped to the reference genomes to detect and annotate single nucleotide polymorphism (SNP), structural variants (SV) and copy number variation (CNV) according to the mapping results. FASTQ files containing clean sequences were further analyzed using tools available at the Center for Genomic Epidemiology,[2] including multi-locus sequence typing (MLST) with MLST 2.0, sequence type (ST) with SerotypeFinder 2.0, presence of virulence genes (VirulenceFinder 2.0), resistance genes (ResFinder 4.1), and plasmid replicons (PlasmidFinder 2.1). In addition, antibiotic resistance and virulence profiling was performed using the ARESdb cloud platform introduced by Ferreira et al. (2020).[3] This involved searching for marker sequences with coverage of ≥60% and identity of ≥90% to those cataloged in ARESdb (Ferreira et al., 2021).

To link carbapenemase KPC-2 and OXA-48 encoding genes to specific Inc. plasmid groups, plasmids were reconstructed with SPAdes v3.13.1 from trimmed (trimmomatic v0.39) sequencing reads, after which the replicon types and resistance markers were cross referenced to the *de novo* assemblies (Kudirkiene et al., 2018). Plasmid Finder v2.1 determined replicon types from the WGS assemblies generated by SPAdes. Because plasmid reconstruction from short-read sequencing is challenging and assembly typically results in many fragmented contigs per genome of unclear origin, plasmidSPAdes tool was used to identify as much as plasmid contigs. The algorithm in plasmidSPAdes predicted which contigs belong to plasmid DNA and assigned those contigs into components. Components containing specific plasmid replicons and their combinations from a selected strain were further used to search against NCBI nr database using BlastN for the most similar plasmids. *De novo* assembled plasmids were aligned against ARESdb with thresholds set at >60% query coverage and > 90% alignment identity to detect resistance markers. Further analysis of the generated assemblies was conducted using the Proksee server to create circular alignments of the reads to the reference plasmids available in the NCBI database.[4]

RESULTS

This study investigated the emergence and antibiotic resistance of CRE in submarine effluent-receiving coastal waters of central Adriatic to contribute to the global surveillance of these opportunistic pathogens outside of hospital settings.

Strain Isolation and Antibiotic Susceptibility Pattern

Twenty-two isolates that exhibited characteristic pink or blue-green colony morphology were recovered on selective CHROMID® Carba agar (bioMérieux). By MALDI-TOF MS, seven isolates were identified as *Enterococcus faecium* and excluded from further investigation. The remaining 15 isolates belonged to the *Enterobacteriaceae* family (nine *E. coli*, four *Klebsiella pneumoniae* and two *Citrobacter freundii*) and were obtained from water samples collected in June, July, and September 2020 near the submarine outfall of the Kataliniće Brig WWTP. All but one isolate showed resistance to at least one carbapenem antibiotic. Among them, four isolates (one *E. coli* and three *K. pneumoniae*) were designated extensively drug resistant (XDR), while nine isolates (seven *E. coli*, one *K. pneumoniae* and one *C. freundii*) were multidrug resistant (MDR). Although two *K. pneumoniae* isolates (C1 and C2) were resistant to colistin, the *mcr-1* gene was not detected by PCR. The detailed antibiotic resistance profiles of the *Enterobacteriaceae* isolates are shown in **Table 1**.

The Rapidec Carba NP test indicated carbapenemase production in all 15 isolates. PCR screening and Sanger sequencing further confirmed the presence of the carbapenemase gene bla_{KPC-2} in all but one *C. freundii* isolate (CF2), which carried bla_{KPC-29}. This carbapenemase gene is derived from the ancestral allele bla_{KPC-3}, and its expression does not affect the activity of carbapenems (Hobson et al., 2020). However, the CF2 isolate remained sensitive to all beta-lactam antibiotics tested, including cephalosporins (**Table 1**), casting doubt on the full expression of this gene in this isolate.

Based on the ERIC and BOX profiles (**Supplemental Figure S1**), eight isolates (four *E. coli*, three *K. pneumoniae*, and one *C. freundii*) that exhibited the most diverse profiles were subjected to WGS.

The draft genome sizes of the isolates ranged from 5.1 to 5.8 Mb, with diverse sizes of N50, and numbers of coding sequences and contigs (**Table 2**). A total of 137 genes were identified mediating intrinsic or acquired resistance to 19 antimicrobial drug classes, including penicillins, cephamycins,

[1]www.ncbi.nlm.nih.gov
[2]http://www.genomicepidemiology.org
[3]https://ares-genetics.cloud
[4]https://beta.proksee.ca/

TABLE 1 | Antibiotic resistance profiles of 15 KPC-producing *Enterobacteriaceae* isolates recovered in this study[a].

Isolate no.	M18	M12	M13	M14	M15	M16	M17	M19	M20	5a	M11	C2	C1	CF1	CF2
Species	*Escherichia coli*	*Escherichia coli*	*Escherichia coli*	*Escherichia coli*	*Escherichia coli*	*Escherichia coli*	*Escherichia coli*	*Escherichia coli*	*Escherichia coli*	*Klebsiella pneumoniae*	*Klebsiella pneumoniae*	*Klebsiella pneumoniae*	*Klebsiella pneumoniae*	*Citrobacter freundii*	*Citrobacter freundii*
Isolation date[b]	06/2020	06/2020	06/2020	06/2020	06/2020	06/2020	06/2020	06/2020	06/2020	06/2020	06/2020	07/2020	07/2020	09/2020	09/2020
KPC type	KPC-2	KPC-2	KPC-2	KPC-2	KPC-2	KPC-2	KPC-2	KPC-2	KPC-2	KPC-2	KPC-2	KPC-2	KPC-2	KPC-2	KPC-29
PIP	1.5	>256	>256	>256	>256	>256	>256	>256	>256	>256	>256	>256	>256	64	2
PIP/TZB	0.75	32	>256	>256	256	192	>256	>256	256	32	32	192	>256	8	1
CTX	0.047	16	16	>32	>32	>32	12	24	16	>32	>32	24	>32	32	0.5
CAZ	0.19	8	8	8	8	3	8	4	12	12	8	8	64	32	0.38
FEP	0.032	1.5	32	48	256	4	32	8	8	32	16	32	256	1.5	0.094
ATM	0.094	1.5	96	>256	>256	64	256	6	128	8	12	1,5	>256	6	0.125
IPM	0.19	>32	32	>32	24	8	32	8	8	8	8	>32	>32	0.19	0.19
MER	8	>32	>32	>32	>32	12	8	16	>32	32	6	>32	32	1	0.5
ETP	0.004	32	32	>32	8	8	32	24	32	>32	32	>32	>32	0.006	0.004
CIP	0.012	6	4	4	0.75	12	6	4	12	6	6	4	6	0.75	0.012
GEN	0.5	16	1	1	0.5	2	1	2	3	8	8	8	1	0.5	0.5
TET	4	16	2	3	32	3	3	2	12	12	>256	16	4	4	4
SXT	0.064	0.5	32	>32	0.75	0.19	>32	0.38	32	0.25	0.25	0.5	0.038	0.064	0.038
CL	0.125	2	0.125	0.25	0.125	0.5	0.125	0.0625	1	0.125	0.0625	32	16	0.125	0.0625
Resistance phenotype		MDR	MDR	MDR	MDR	MDR	MDR	MDR	XDR	XDR	XDR	XDR	MDR	MDR	
AmpC Etest	neg	pos	neg	neg	neg	neg	neg	neg	neg	neg	neg	neg	neg	pos	neg
Rapidec Carba NP test	pos	pos	pos	pos	pos	pos	pos	pos	pos	pos	pos	pos	pos	pos	pos
ESBL test	neg	pos	neg	pos	pos	neg	neg	neg	pos	pos	pos	pos	pos	neg	neg

TZP, piperacillin/tazobactam; PIP, piperacillin; CAZ, ceftazidime; CTX, cefotaxime; FEP, cefepime; ATM, aztreonam; IMP, imipenem; MER, meropenem; ETP, ertapenem; CIP, ciprofloxacin; GEN, gentamicin; TET, tetracycline; SXT, trimethoprim-sulfamethoxazole; CL, colistin; MDR, multidrug-resistant; XDR, extensively drug-resistant; neg, negative; and pos, positive.

[a]*Resistance phenotype is indicated by shading according to EUCAST (2020) except for TET that was evaluated based on CLSI (2020) breakpoints.*

[b]*Isolation date is given as month/year.*

TABLE 2 | Metadata of the whole-genome sequenced CRE isolates from Croatia.

	M12	M14	M17	M20	5a	M11	C2	CF1
Species	*Escherichia coli*	*Escherichia coli*	*Escherichia coli*	*Escherichia coli*	*Klebsiella pneumoniae*	*Klebsiella pneumoniae*	*Klebsiella pneumoniae*	*Citrobacter freundii*
Genome size (bp)	5,207,851	5,243,436	5,173,484	5,186,809	5,667,286	5,659,465	5,826,947	5,103,429
No. of CDS[a]	5,028	5,082	4,969	5,023	5,339	5,345	5,554	4,865
No. of contings	240	231	207	224	342	289	195	74
No. of contings >1,000 bp	159	164	135	164	204	199	132	45
Average depth (x)	223	185	205	199	224	248	229	264
GC content (%)	50.54	50.55	50.59	50.6	56.92	56.92	57.04	51.84
N_{50} (bp)	89,262	87,097	90,500	78,173	70,753	74,345	116,900	372,763
No. of tRNAs	78	81	79	82	77	77	81	78
SRA accession no.	SAMN22028927	SAMN22028930	SAMN22028929	SAMN22028928	SAMN22028932	SAMN22028933	SAMN22028931	SAMN22028934

[a]*CDS, coding DNA sequences.*

cephalosporins, carbapenems, penems, monobactams, fluoroquinolones, aminoglycosides, macrolides, phenicols, quinolones, sulfonamides, trimethoprim, rifampicin, tetracyclines, fosfomycin, nitroimidazoles, peptides, and aminocoumarin (**Supplemental Table S1**). The isolates were found to harbor between 43 and 90 gene markers associated with resistance phenotypes, with the highest number detected in *E. coli* genomes (**Table 3**). Most of these genes were associated with intrinsic resistance mechanisms such as regulation and transport by resistance-nodulation-cell division (RND) and major facilitator superfamily (MFS) antibiotic efflux pumps or porin uptake (**Supplemental Table S1**). Moreover, the isolates harbored three to nine *bla* genes, out of which four isolates (*E. coli* M12, M14, and M20 and *K. pneumoniae* C2) simultaneously possessed two carbapenemase-encoding genes, $bla_{\text{KPC-2}}$ and $bla_{\text{OXA-48}}$. In addition, eight sequenced genomes possessed a total of 20 resistance-associated plasmid replicons and 35 genes involved in bacterial virulence (**Table 3**; **Supplemental Table S1**).

Escherichia coli M12, M14, M17, and M20 Isolates

The four bla_{KPC}-carrying *E. coli* isolates subjected to WGS were all of serotype O21:H27 and ST2795. Furthermore, the isolates shared a set of 26–30 virulence-related genes (**Table 3**), including those encoding the outer membrane usher protein (FimD), flagellar biosynthesis protein (FlhA), and the locus of enterocyte effacement (LEE) encoding the type III secretion system effector protein (EspX1). A number of other genes involved in pathogenicity were discovered as well, including glutamate decarboxylase (*gad*), long polar fimbriae (*lpfA*), tellurium resistance protein (*terC*), toxin-antitoxin systems (*yafQ*, *pemK*, *pemI*), type 1 fimbriae (S - fimbrial adhesion minor subunit; genes *sfaH* and *sfaG*), small toxic polypeptide (*ldrD*), polyamine transport protein D (*potD*), flagellar *fli* genes, laminin-binding fimbriae (*elfG*) and carbon starvation protein A (*cstA*), pointing to the virulence potential of these isolates.

The further similarity between these strains was observed in their plasmid replicon content, with *Inc* replicons of plasmids FIB(K) and P6 detected in all four strains. Nevertheless, each strain exhibited a unique plasmid replicon pattern, comprising 6–10 replicon types per genome (**Table 3**). More diversity was observed among the ARGs, of which strains M12, M14, M17, and M20 possessed a total of 90, 79, 82, and 79 genes associated with the regulation or acquisition of antibiotic resistance (**Table 3**; **Supplemental Table S1**). Nine *bla* genes were identified, including the carbapenemase encoding genes $bla_{\text{KPC-2}}$ and $bla_{\text{OXA-48}}$, and ESBL genes $bla_{\text{GES-1}}$, $bla_{\text{GES-2}}$, $bla_{\text{OXA-2}}$, $bla_{\text{OXA-10}}$, and $bla_{\text{CTX-M-3}}$. Three strains (M12, M14 and M20) co-harbored $bla_{\text{KPC-2}}$ and $bla_{\text{OXA-48}}$. Among others, ARGs mediating resistance to trimethoprim (*dfrA14*), quinolones (*qnrVC4*, *qnrS1*, *qnrB6*), aminoglycosides (*ant(3″)-Ii-aac(6′)-IId*, *ant(3″)-Ia*, *aph(3″)-Ib*) and sulphonamide (*sul1*, *sul2*) were continuously detected.

Moreover, further analysis of the genomes identified the $bla_{\text{KPC-2}}$ gene in IncP6 plasmid contigs of 38,767, 14,644, 25,016, and 14,644 bp in *E. coli* M12, M14, M17, and M20, respectively.

BlastN search against NCBI nr database revealed that a 38,767-bp contig from *E. coli* M12 had query coverage of 91% and nucleotide identity of 99.75%, 99.75%, and 99.68% with IncP6 plasmids deposited in GenBank: p121SC21-KPC2 from Spanish wastewater *C. freundii* (Genbank accession no. LT992437; Yao et al., 2017), pKOX3-P5- KPC from a clinical *Klebsiella oxytoca* in China (GenBank accession no. KY913901; Wang et al., 2017), and pWW14A-KPC2 from wastewater *Klebsiella quasipneumoniae* in Argentina (Ghiglione et al., 2021). Hybrid plasmids pM12-KPC2, pM14-KPC2, pM17-KPC2, and pM20-KPC2 were reconstructed to a size of ~40 kb and compared to plasmids of both environmental and clinical origin previously reported in the literature (Dai et al., 2016; Wang et al., 2017;

TABLE 3 | Molecular characteristics of eight whole-genome sequenced CRE isolates.

	M12	M14	M17	M20	5a	M11	C2	CF1
Species	*Escherichia coli*	*Escherichia coli*	*Escherichia coli*	*Escherichia coli*	*Klebsiella pneumoniae*	*Klebsiella pneumoniae*	*Klebsiella pneumoniae*	*Citrobacter freundii*
Serotype	O21:H27	O21:H27	O21:H27	O21:H27				
ST	2795	2795	2795	2795	37	37	534	128
Selected antibiotic resistance genes (total no.)[a]	*dfrA14*, *qnrVC4*, *cmlA5*, *mdf(A)*, *mph(B)*, bla_{KPC-2}, bla_{GES-2}, bla_{OXA-2}, bla_{OXA-48}, bla_{OXA-10}, *ant(3″)-Ia*, *ant(3″)-Ii-aac(6′)-Iid* (90)	*dfrA14*, *qnrS1*, *sul2*, *mdf(A)*, *mph(B)*, bla_{KPC-2}, bla_{OXA-48}, bla_{GES-1}, bla_{OXA-10}, *aac(6′)-Ib-cr*, *aph(3″)-Ib*, (79)	*aac(6′)-Ib-cr*, *aadA16*, bla_{KPC-2}, *sul1*, *qnrB6*, *mdf(A)*, *mph(B)*, *arr-3*, *dfrA27* (82)	*dfrA14*, *sul2*, bla_{OXA-10}, bla_{GES-1}, bla_{KPC-2}, bla_{OXA-48}, *aph(3″)-Ib*, *mdf(A)*, *qnrS1*, (79)	*sul1*, *tet(A)*, *oqxA*, *oqxB*, *aac(6′)-Ib-cr* $bla_{CTX-M-3}$, bla_{OXA-2}, bla_{GES-5}, bla_{KPC-2}, *fosA*, *aph(3″)-Ib*, *aph(6)-Id*, (62)	*fosA*, *oqxA* *oqxB*, bla_{GES-5}, bla_{KPC-2}, bla_{OXA-2}, $bla_{CTX-M-3}$, *aph(3″)-Ib*, *aph(6)-Id*, *tet(A)*, *sul1* (62)	*oqxB*, *oqxA* *aac(6′)-Ib-cr*, *sul1*, *fosA*, bla_{KPC-2}, bla_{GES-5}, bla_{SHV-11}, bla_{OXA-48} (58)	bla_{KPC-2}, $bla_{CMY-157}$ (43)
Selected genes linked to virulence (total no.)[a]	*gad*, *lpfA*, *terC*, *yafQ*, *sfaH*, *ldrD*, *potD*, *pemK*, *pemI*, *fliY*, *fliZ*, *fliQ*, *fliA*, *fliG*, *fliI*, *nagA*, *flhA*, *fimD*, *fdeC*, *EspX1*, *epsJ*, *elfG*, *cstA* (30)	*gad*, *lpfA*, *terC*, *sfaH*, *ldrD*, *potD*, *pemK*, *pemI*, *nagA*, *fliY*, *fliZ*, *fliQ*, *fliA*, *fliG*, *fliI*, *flhA*, *fimD*, *EspX1*, *epsJ*, *elfG*, *cstA* (26)	*gad*, *lpfA*, *terC*, *ldrD*, *potD*, *pemK*, *pemI*, *nagA*, *flhA*, *fliY*, *fliZ*, *fliQ*, *fliA*, *fliG*, *fliI*, *fimD*, *EspX1*, *epsJ*, *elfG*, *cstA* (26)	*gad*, *lpfA*, *terC*, *sfaH*, *ldrD*, *potD*, *pemK*, *pemI*, *nagA*, *flhA*, *fliY*, *fliZ*, *fliQ*, *fliA*, *fliG*, *fliI*, *fimD*, *EspX1*, *epsJ*, *elfG*, *cstA* (26)	*sinR*, *sfaG*, *potD*, *fliY*, *fimD*, *feoB* *eutB* (9)	*sinR*, *sfaG*, *potD*, *fliY*, *fimD*, *feoB*, *eutB* (9)	*sinR*, *sfaG*, *potD*, *pemK*, *pemI*, *fliY*, *fimD*, *feoB*, *eutB*, *cstA* (12)	*potD*, *fliY*, *fliQ*, *fliP*, *fliI*, *fliG*, *fliA*, *flhA*, *eutB*, *cstA* (10)
Plasmids (Inc)	FIB(K), L, P6, C, Col440I, Col(pHAD28)	FIB(K), FII, FII(Yp), L, N, P6, X5, Y, Col440I, Col440II	FIB(K), FII, P6, R, Col440I, Col(pHAD28)	FIB(K), FII, FII(Yp), L, N, P6, Y, Col(IRGK), Col440I, Col440II	FIA(HI1), FII(K), FII(Yp), X5, Y, Col440I, Col440II, Col(pHAD28)	FIA(HI1), FII(K), FII(Yp), X5, Y, Col440I, Col440II, Col(pHAD28)	FIB(K), L, R, Q1, FII(pMET), FII(pKP91), Col440I, Col(pHAD28)	FIB(pHCM2)

[a]*List of total genes associated with the antibiotic resistance and virulence is available in the* **Supplementary Material**.

Yao et al., 2017; Pérez-Vazquez et al., 2019; Ghiglione et al., 2021; **Figure 2**). Analysis of the genetic environment of bla_{KPC-2} revealed that this gene is located within a Δ*ISKpn6*/bla_{KPC-2}-Δbla_{TEM-1}-*ISKpn27* sequence within a Tn3-based transposon interrupted by an ISApu-flanked element (**Figure 2**), consistent with previous reports (Dai et al., 2016; Ghiglione et al., 2021).

The bla_{OXA-48} was associated with IncL-like plasmids in *E. coli*, but the hybrid bla_{OXA-48}-bearing plasmids could not be reconstituted (the contigs containing this carbapenemase gene were 2,231-bp long in all four OXA-48-positive *E. coli* and *K. pneumoniae* isolates). However, the IS1R element flanking the OXA-48-encoding gene was detected in *E. coli* M12 isolate.

Klebsiella pneumoniae 5a, M11 and C2 Isolates

Three KPC-2-producing *K. pneumoniae* isolates concurrently carried a total of 62, 58, and 62 genes mediating resistance to multiple antibiotics, respectively (**Table 3**; **Supplemental Table S1**). Isolates 5a and M11 were affiliated to ST37, while C2 belonged to ST534. Moreover, isolates 5a and M11 exhibited the same antibiogram and XDR phenotype (**Table 1**), and a similar ARGs content (**Table 3**; **Supplemental Table S1**). However, ERIC and BOX-PCR typing excluded their clonality, and WGS data analysis revealed that these differed by the *aac(6′)-Ib-cr* gene, conferring fluoroquinolone and aminoglycoside resistance, which was found in the genome of strain 5a and not M11. On the other hand, *K. pneumoniae* C2 harbored less ARGs than the former two strains but was resistant to 13 out of 14 tested antimicrobial drugs, remaining susceptible only to trimethoprim-sulfamethoxazole. Nevertheless, identification of *sul1* gene in its genome could eventually result in nonsusceptibility even to this antibiotic. Unfortunately, we were not able to reconstruct bla_{KPC-2}-and bla_{OXA-48}-bearing plasmids in *K. pneumoniae* isolates due to the short-read genome sequences.

Moreover, some virulence-related genes have been concurrently detected in all three *K. pneumoniae* genomes (**Table 3**), codifying for type 1 fimbriae (*fimD*, *sfaG*), ferrous ion transport (*feoB*), ethanolamine-ammonia lyase (*eutB*), extracellular matrix production (*sinR*), flagellae (*fliY*), polyamine transport (*potD*), and nickel and cobalt resistance (*cnrA*), respectively. The C2 strain harbored additional three virulence genes encoding the toxin-antitoxin system (*pemK*, *pemI*) and carbon starvation protein A (*cstA*; **Table 3**).

Citrobacter freundii CF1

KPC-2-producing *C. freundii* CF1 belonged to ST128 (**Table 3**). Compared to *E. coli* and *K. pneumoniae* isolates, this strain showed the least diversity of virulence markers, mainly harboring the genes encoding the flagellar apparatus (*fli*), polyamine transport protein D (*potD*), ethanolamine ammonia lyase (*eutB*) and carbon starvation protein A (*cstA*; **Table 3**). Furthermore, this strain contained the fewest ARGs, 43 in total (**Table 3**; **Supplemental Table S1**), and was sensitive to all tested antimicrobial agents (**Table 1**).

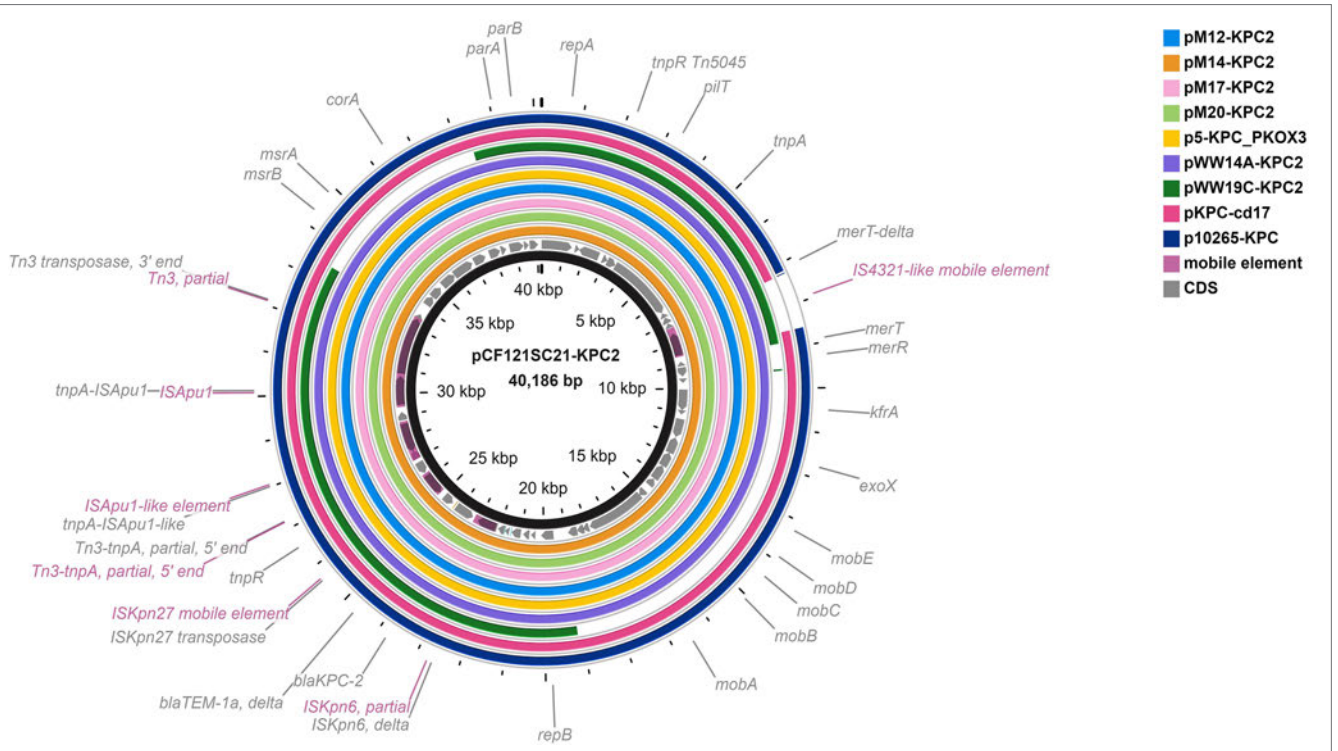

FIGURE 2 | Comparison of plasmids pM12-KPC2, pM14-KPC2, pM17-KPC2, and pM20-KPC2 with IncP6 bla_{KPC-2}-bearing plasmids of environmental and clinical origin described in the literature: pCF121SC21-KPC2 from Spanish wastewater *Citrobacter freundii* (Genbank accession no. LT992437; Yao et al., 2017), pKOX3-P5-KPC from clinical *Klebsiella oxytoca* in China (GenBank accession no. KY913901; Wang et al., 2017), pWW14A-KPC2 from wastewater *Klebsiella quasipneumoniae* in Argentina (GenBank accession no. CP080103; Ghiglione et al., 2021), pWW19C-KPC2 from wastewater *Enterobacter asburiae* in Argentina (GenBank accession no. CP080110; Ghiglione et al., 2021), p10265-KPC from clinical *Pseudomonas aeruginosa* in China (GenBank accession no. KU578314; Dai et al., 2016), and pKPC-cd17 from *Aeromonas* sp. from hospital environment in United States (GenBank accession no. CP026224) which is 100% identical to the bla_{KPC-2}-carrying plasmid in *Klebsiella oxytoca* from Spanish hospitals (Pérez-Vazquez et al., 2019). The plasmid pCF121SC21-KPC2 was taken as a reference plasmid (black circle).

DISCUSSION

Carbapenemase-Producing *Escherichia coli* Isolates

All four bla_{KPC}-carrying *E. coli* isolates that were subjected to WGS belonged to the serotype O21:H27 and ST2795, which was previously identified in the United Kingdom.[5] The strains carried several genes involved in pathogenicity or other function. For instance, we identified genes encoding the outer membrane usher protein FimD and flagellar biosynthesis protein FlhA associated with the urinary pathogenic *E. coli* (UPEC), and the effector protein EspX1 of the type III secretion system common to enterohemorrhagic *E. coli* (EHEC), all of which were previously detected in wastewater from WWTPs (Zhi et al., 2019). Furthermore, *gad* gene, also detected in all four *E. coli* genomes, is commonly involved in resistance to gastric acid, allowing *E. coli* to survive in the acidic host environment (Mates et al., 2007). The *lpfA* gene, encoding for the long polar fimbriae, was found to be associated with the gut colonization and the attachment to Peyer's patches in mice (Cordonnier et al., 2017), and was identified in adherent-invasive *E. coli* enrolled in the pathogenesis of Crohn's disease (Chassaing et al., 2011). Both genes were also identified in the KPC-producing *E. coli* from the riverine environments (Bleichenbacher et al., 2020). Moreover, *terC* gene, encoding the heavy metal resistance, is found to be significantly correlated with the presence of other virulence factors in the pathogenic strains of *E. coli* isolated from humans, animals, and food (Orth et al., 2006).

The PemK/pemI type II toxin-antitoxin system was also detected in the genomes of bla_{KPC}-positive *E. coli* isolates from this study. This module is consisted of a stable toxin and an unstable antitoxin that degrades under stress conditions, enabling the toxin to inhibit the basic cellular processes. Notably, it has been associated with the bacterial persistence in inhospitable conditions, phage inhibition and biofilm formation (Ramage et al., 2009; Hernandez-Ramirez et al., 2017), as well as the IncF plasmid maintenance, conjugation, and spreading (Walling and Butler, 2016; Diaz-Orejas et al., 2017). This system was previously identified in hypermucoviscous carbapenem-resistant *E. coli* within and outside the hospital environment (Woodford et al., 2009; Mathers et al., 2015; Zurfluh et al., 2018).

Moreover, total of nine carbapenem-resistant *E. coli* isolates from this study were found to harbor bla_{KPC-2} gene. It is

[5]https://enterobase.warwick.ac.uk/

important to note that the environmental *E. coli* carrying this carbapenemase gene have rarely been reported, and they have all been recovered from the river water (Poirel et al., 2012; Xu et al., 2015; Yang et al., 2017). To the best of our knowledge, this is the first identification of KPC-producing *E. coli* in coastal marine waters. More importantly, the co-occurrence of $bla_{\text{KPC-2}}$ and $bla_{\text{OXA-48}}$ in *E. coli* has not been previously reported in the literature. So far, the bla_{KPC} gene in *E. coli* has been mainly reported in countries with a high prevalence of KPC-producing *K. pneumoniae*, indicating the possibility of interspecies gene transfer with *K. pneumoniae* serving as a bla_{KPC} reservoir (Grundmann et al., 2017). In this regard, we should take into consideration a high prevalence of KPC-producing *K. pneumoniae* in University Hospital Split (Bedenić et al., 2021) and the fact that the isolates were recovered from the water samples collected near the submarine outfall of the WWTP that treats the hospital wastewater. Nevertheless, this presumption should be carefully addressed in future research, focusing on the genetic environment of the hospital KPC-producing strains. To the best of our knowledge, there are no available data on KPC-producing *E. coli* or *K. pneumoniae* from the University Hospital Split analyzed by WGS. The molecular characterization of plasmids harbouring $bla_{\text{KPC-2}}$ gene in Croatia was performed for clinical *K. pneumoniae*, including those from University Hospital Split that were found to carry this gene on IncFII plasmids (Jelić et al., 2016; Bedenić et al., 2021), or those untyped by PCR-based replicon typing (PBRT; D'Onofrio et al., 2020), as well as in case of river *K. pneumoniae* that harboured $bla_{\text{KPC-2}}$ gene on IncFII plasmids (Jelić et al., 2019). Notably, $bla_{\text{KPC-2}}$ _bearing IncP6 plasmids were not previously reported in Croatia.

Moreover, all four $bla_{\text{KPC-2}}$ _bearing plasmids from *E. coli* isolates in this study were of ~40 kb and highly similar to the IncP6 $bla_{\text{KPC-2}}$-containing plasmids from wastewater *C. freundii* in Spain (Yao et al., 2017), clinical *K. oxytoca* in China (Wang et al., 2017) and wastewater *K. quasipneumoniae* in Argentina (Ghiglione et al., 2021), pointing to their global circulation. In comparison to plasmids from other incompatibility (Inc) groups, the KPC-2-encoding gene has been rarely detected in IncP6 resistance plasmids (Yao et al., 2017). However, recent studies confirmed that emergence of $bla_{\text{KPC-2}}$ gene on mobilizable IncP6 broad-host-range plasmids enhanced its dissemination among different members of *Enterobacteriaceae* in clinical settings and the environment (Pérez-Vazquez et al., 2019; Ghiglione et al., 2021). This study provides further evidence to this speculation, documenting for the first time the $bla_{\text{KPC-2}}$ association with IncP6 plasmids in *E. coli* in Europe.

Furthermore, 6–10 plasmid replicons were detected in *E. coli* genomes. Among them, IncN and Col-type replicons have been previously associated with the occurrence of bla_{KPC} in human *E. coli* from the global surveillance studies (Stoesser et al., 2017). In addition, three out of four analysed *E. coli* genomes contained the $bla_{\text{OXA-48}}$ carbapenemase gene associated with IncL plasmids. Notably, OXA-48-producing *Enterobacteriaceae* have widely disseminated in Croatian hospitals over the past years (Bedenić et al., 2018), with OXA-48-positive *K. pneumoniae* reported at different wards in University Hospital Split. Since IncL-like plasmids were found to enable the transferability of $bla_{\text{OXA-48}}$ in *E. coli* strains from northern Croatia (Bedenić et al., 2018; Drenjančević et al., 2019), findings from this study further enhance their relevance as reservoirs of $bla_{\text{OXA-48}}$ in Croatia.

Moreover, Ambler class A GES-type ESBLs which were identified in KPC-2-producing *E. coli*, including GES-1 (isolates M14 and M20) and GES-2 (isolate M12) may have additionally enhanced their nonsusceptibility to beta-lactams as these enzymes effectively hydrolyse penicillins and expanded-spectrum cephalosporins (Castanheira et al., 2021). GES-2, in comparison to GES-1, also displayes hydrolytic activity against imipenem (Poirel et al., 2001).

In addition, other resistance determinants identified in the genome of our *E. coli* isolates, including the aminoglycoside resistance gene *aph(3″)-Ib*, trimethoprim resistance gene *drfA17* and sulfonamide resistance gene *sul2*, were previously identified in clinical *E. coli* from Croatia (Bedenić et al., 2018).

Carbapenemase-Producing *Klebsiella pneumoniae* Isolates

In this study, we found that two $bla_{\text{KPC-2}}$-positive isolates (5a and M11) belong to ST37. Notably, MDR *K. pneumoniae* strains of the same lineage, bearing the $bla_{\text{KPC-2}}$ (Bedenić et al., 2012) and $bla_{\text{OXA-48}}$ (Jelić et al., 2018) carbapenemase genes were previously reported in Croatian hospitals, but not in the natural environment. KPC-producing *K. pneumoniae* of other STs were previously isolated from aquatic environments (Ekwanzala et al., 2019), including ST258 in river water in Croatia (Jelić et al., 2019). Therefore, this study reports the first identification of KPC-producing *K. pneumoniae* in the marine environment in Croatia. Both of *K. pneumoniae* ST37 isolates in this study harbored replicons of plasmids known to enable the spread of ARGs in *Enterobacteriaceae*. Namely, multiple IncF replicons (FIIK, FIB, FIA, and/or FII) were previously identified in *K. pneumoniae* and other *Enterobacteriaceae* (Carattoli, 2009; Huang et al., 2012). On the other hand, *K. pneumoniae* strain C2 was affiliated to ST534, which was previously detected in the hospital environment in Israel (Adler et al., 2015). Our strain additionally harbored IncL and IncR-type plasmid replicons which have been previously described as vehicles of $bla_{\text{KPC-2}}$ (Garbari et al., 2015) as well as $bla_{\text{OXA-48}}$ in Croatia (Bedenić et al., 2018; Drenjančević et al., 2019).

K. pneumoniae 51, M11, and C2 isolates produced the Ambler class A GES-5 variant, which confers low carbapenemase activity in addition to penicillins and cephalosporins (Gomi et al., 2018; Castanheira et al., 2021), although GES-5-positive isolates with elevated MICs for imipenem, meropenem, and ertapenem have also been reported (Literacka et al., 2020). In this regard, production of GES-5 may have increased the resistance to carbapenems and other beta-lactams in our isolates. It should be noted that the epidemiology of GES producers is poorly understood, as GES carbapenemase-producing *Enterobacteriaceae* often stay unreported by resulting falsely negative in the Carba NP test due to the relatively weak activity toward carbapenems (Gomi et al., 2018; Literacka et al., 2020). Nevertheless, hospital outbreaks due to carbapenem-resistant GES-5-positive *K. pneumoniae* have recently been reported in Portugal (Mendes et al., 2022) and Poland (Literacka et al.,

2020), highlighting their clinical relevance. Apart from the carbapenemases, changes in membrane permeability and activity of membrane efflux pumps may have also contributed to carbapenem resistance in *K. pneumoniae* isolates from this study. Namely, it was observed that a mutant *ompK36* porin gene, like the one detected in these three carbapenemase-producing *K. pneumoniae* isolates, increases nonsusceptibility to this group of antibiotics (Wong et al., 2019). In addition, 7 mutations (P161R, G164A, F172S, R173G, L195V, F197I, and K201M) detected in transcriptional regulator gene *acrR* in C2 isolate were previously shown to highly increase the expression of a major multidrug efflux pump AcrAB-TolC (Sato et al., 2020) that effectively extrude multiple antimicrobials among which carbapenems (Chetri et al., 2019).

Moreover, the environmental *K. pneumoniae* isolates from our study shared similar determinants of resistance to other classes of antibiotics, which were previously described in *K. pneumoniae* clinical isolates from Croatia (Bedenić et al., 2018), such as the aminoglycoside and fluoroquinolone resistance gene *aac(6')Ib-cr*, disinfectant resistance genes *oqxA* and *oqxB*, sulfonamide resistance gene *sul1*, *fosA* encoding fosfomycin resistance and ESBL gene $bla_{\text{CTX-M}}$. Moreover, an amino acid substitution R256G was detected in PmrB protein sequence in 5a and M11 strains, which has been previously associated with colistin resistance in *Enterobacteriaceae* (Cheng et al., 2015), as well as in case of CL-resistant and carbapenemase-producing hospital *K. pneumoniae* in Croatia (D'Onofrio et al., 2020). Namely, variations in the PmrB protein, which is a part of the two-component regulatory system PmrA/PmrB enrolled in modification of lipopolysaccharide (LPS) structure, lead to the neutralization of its negative charge and consequently, the reduced susceptibility to cationic peptide antibiotics such as CL. However, as no increased MIC for CL was observed in these isolates, we speculate that the combined action of multiple mechanisms is likely needed to induce resistance to this antibiotic (Cheng et al., 2015). On the other hand, *K. pneumoniae* C2 was resistant to CL (MIC 32 μg/ml), yet no variations in PmrB were found. Limited number of studies have pointed to the underestimated role of the energy-driven efflux pump of peptide antibiotics in *K. pneumoniae*, involving two pumps, AcrAB-TolC and KpnEF (Binsker et al., 2021). It was observed that AcrR deficient mutant strains can successfully extrude polymyxin B, another peptide antibiotic, out of the cell using AcrAB-TolC pump (Padilla et al., 2010). More recent study of Naha et al. (2020) revealed that nonmutated and increasingly expressed RamA, a positive regulator of AcrAB-TolC pump, mediates alterations of LPS which along with the upregulation of the pump have contributed to the CL-resistant phenotype in clinical *K. pneumoniae*. RamA-mediated changes of lipid A moiety have been previously shown to decrease susceptibility to CL in this pathogen (De Majumdar et al., 2015). Therefore, it is likely that a functional AcrAB-TolC system and RamA could also be involved in nonsuceptibility to CL in *K. pneumoniae* C2, but this should be addressed more carefully in the future research.

Moreover, several common virulence-related genes were simultaneously detected in all three *K. pneumoniae* genomes, among which those coding the type 1 fimbriae (*fimD*, *sfaG*) and ferrous ion transport (*feoB*). According to Struve et al. (2008) type 1 fimbriae are significantly enrolled in *K. pneumoniae* infections of urinary tract. The FeoB is the component of the major prokaryotic ferrous ion transport (Feo) system, and the main protein enabling the iron uptake through the lipid bilayer in almost all bacteria (Cartron et al., 2006; Lau et al., 2007). Nevertheless, in this study it was only detected in *K. pneumoniae*, which could be explained by the fact that a single species can adjust its iron import depending on the type of infection (acute or chronic) and the availability of iron in its environment (Cornelis and Dingemans, 2013). On the other hand, the C2 isolate, like *E. coli*, additionally harbored two virulence genes (*pemK*, and *pemI*) encoding the PemK/PemI type II toxin-antitoxin system that has been previously described in hypermucoviscous carbapenem-resistant *K. pneumoniae* (Fu et al., 2018; Bleriot et al., 2020).

Citrobacter freundii CF1 Isolate

C. freundii CF1 isolate was affiliated to ST128, which was first described by Bonnin et al. (2020) in an isolate from the rectal swab of a French patient. To date, KPC-producing *Citrobacter* spp. have been isolated from hospital effluents (Zhang et al., 2012), river sediments (Xu et al., 2018), and the recreational areas (Montezzi et al., 2015), but none of them belonged to ST128. To the best of our knowledge, KPC-2-producing *C. freundii* of the ST128 lineage has not been previously reported. It was unexpected that this carbapenem-sensitive isolate resulted positive by CarbaNP test. However, although rare, there are previous reports of KPC-producing Enterobacterales showing unusual carbapenems susceptibility profile while testing positive by CarbaNP (Shinde et al., 2017; Cury et al., 2020), suggesting low gene expression.

Furthermore, we found that the strain CF1 also carried the $bla_{\text{CMY-159}}$, a variant gene identified only recently (Piotrowska et al., 2019) that encodes for the eponymous AmpC beta-lactamase of the CMY family intrinsic to *Citrobacter* spp. In a later study, this *bla* gene was detected in a *Citrobacter* sp. isolate resistant to cefotaxime, ceftazidime, cefepime and aztreonam, which is similar to the CF1 susceptibility profile. Overall, the majority of the 43 gene markers involved in the antibiotic resistance in this strain was associated with the activity of intrinsic antibiotic efflux including ATP-binding cassette (ABC), RND or MFS pumps. Notably, missense mutations of the AcrAB-TolC efflux pump regulators marR (Y137H) and soxR (T38S) which were detected in this strain were previously found to increase pump expression, leading to the multidrug resistance, among which to beta-lactams and ciprofloxacin (Al-Farsi et al., 2020). Giving the beta-lactam resistance profile of the CF1 isolate (sensitive to carbapenems and cefepime, but resistant to aztreonam and third generation cephalosporins) we can speculate that the mutation-driven expression of the AcrAB-TolC pump did not influence the activity against carbapenems. This would be a case when coincided with the membrane permeability defects resulted from porin loss or porin structural changes (Pages et al., 2008; Vardakas et al., 2012; Sadeghi, 2019), which have not been detected in CF1 isolate.

Moreover, among the 10 virulence-related genes detected in CF1 genome, the major virulence factors of this pathogen such as Shiga-like and heat-stable toxins, or the cholera toxin B subunit homolog (Bai et al., 2012) were not identified, thus we can speculate about the low virulence potential of this isolate (Pepperell et al., 2002).

CONCLUSION

This study reports the introduction of XDR and carbapenemase-producing potentially virulent strains of *Enterobacteriaceae* into the Croatian marine environment through the submarine outfall of the treated wastewater located at a depth of 42 m. Among other antibiotic resistance and virulence determinants previously assigned exclusively to clinical strains, we report for the first time KPC-producing *E. coli* in coastal waters and the co-occurrence of $bla_{\text{KPC-2}}$ and $bla_{\text{OXA-48}}$ carbapenemase genes in this species. While $bla_{\text{OXA-48}}$ was located on an IncL-type plasmids in this species, $bla_{\text{KPC-2}}$ was harbored by recently described broad-host-range IncP6 resistance plasmids, providing first record of their circulation in *E. coli* and highlighting their importance in the epidemiology of this globally disseminated carbapenemase encoding gene. Leakage of these highly resistant strains into coastal waters through the submarine outlet is of serious concern as it provides a route for their continuous introduction into the marine environment and a reservoir for their further spread.

DATA AVAILABILITY STATEMENT

The genomic sequences are deposited in the NCBI Sequence Read Archive (BioProject number PRJNA768347) under accession numbers listed in **Table 2**. The sequence of plasmid pM12-KPC2 from *E. coli* was deposited in GenBank under accession number CP093216.

AUTHOR CONTRIBUTIONS

MK and AM: conceptualization and writing—original draft preparation. MDŽ and IŠ: formal analysis. AN, AM, IGB, and MT: validation. MK and AN: investigation. IŠ, JK and AM: resources and funding acquisition. AM: data curation, visualization, and supervision. All authors writing--review and editing and contributed to the article and approved the submitted version.

FUNDING

This research was funded by the Croatian Science Foundation (grant number UIP-2019-04-9778), project STIM-REI (KK.01.1.1.01.0003) through the European Regional Development Fund—the Operational Programme Competitiveness and Cohesion 2014–2020 (KK.01.1.1.01), Croatian Academy of Sciences and Arts, and the annual funds for institutional financing of scientific activity from Ministry of Science and Education of Republic of Croatia. The project CAAT "Coastal Auto-purification Assessment Technology" funded by European Union from European Structural and Investment Funds 2014–2020 (KK.01.1.1.04.0064).

ACKNOWLEDGMENTS

The authors acknowledge the Public Health Institute in Zadar, Croatia, for sample collection.

SUPPLEMENTARY MATERIAL

The Supplementary Material for this article can be found online at: https://www.frontiersin.org/articles/10.3389/fmicb.2022.858821/full#supplementary-material

Supplementary Table S1 | 480 Molecular characteristics of eight whole-genome sequenced KPC-producing isolates.

REFERENCES

Adler, A., Hussein, O., Ben-David, D., Masarwa, S., Navon-Venezia, S., Schwaber, M. J., et al. (2015). Persistence of *Klebsiella pneumoniae* ST258 as the predominant clone of carbapenemase-producing *Enterobacteriaceae* in post-acute-care hospitals in Israel, 2008-13. *J. Antimicrob. Chemother.* 70, 89–92. doi: 10.1093/jac/dku333

Al-Farsi, H. M., Camporeale, A., Ininbergs, K., Al-Azri, S., Al-Muharrmi, Z., Al-Jardani, A., et al. (2020). Clinical and molecular characteristics of carbapenem non-susceptible *Escherichia coli*: a nationwide survey from Oman. *PLoS One* 15:e0239924. doi: 10.1371/journal.pone.0239924

Amarasiri, M., Sano, D., and Suzuki, S. (2020). Understanding human health risks caused by antibiotic resistant bacteria (ARB) and antibiotic resistance genes (ARG) in water environments: current knowledge and questions to be answered. *Crit. Rev. Environ. Sci. Technol.* 50, 2016–2059. doi: 10.1080/10643389.2019.1692611

Araújo, S., Henriques, I. S., Leandro, S. M., Alves, A., Pereira, A., and Correia, A. (2014). Gulls identified as major source of fecal pollution in coastal waters: A microbial source tracking study. *Sci. Total Environ.* 470-471, 84–91. doi: 10.1016/j.scitotenv.2013.09.075

Bai, L., Xia, S., Lan, R., Liu, L., Ye, C., Wang, Y., et al. (2012). Isolation and characterization of cytotoxic, aggregative *Citrobacter freundii*. *PLoS One* 7:e33054. doi: 10.1371/journal.pone.0033054

Bedenić, B., Mazzariol, A., Plečko, V., Bošnjak, Z., Barl, P., Vraneš, J., et al. (2012). First report of KPC-producing *Klebsiella pneumoniae* in Croatia. *J. Chemother.* 24, 237–239. doi: 10.1179/1973947812Y.0000000017

Bedenić, B., Sardelić, S., Bogdanić, M., Zarfel, G., Beader, N., Šuto, S., et al. (2021). *Klebsiella pneumoniae* carbapenemase (KPC) in urinary infection isolates. *Arch. Microbiol.* 203, 1825–1831. doi: 10.1007/s00203-020-02161-x

Bedenić, B., Slade, M., Starčević, L. Ž., Sardelić, S., Vranić-Ladavac, M., Benčić, A., et al. (2018). Epidemic spread of OXA-48 beta-lactamase in Croatia. *J. Med. Microbiol.* 67, 1031–1041. doi: 10.1099/jmm.0.000777

Binsker, U., Käsbohrer, A., and Hammerl, J. A. (2021). Global colistin use: a review of the emergence of resistant Enterobacterales and the impact on their genetic basis. *FEMS Microbiol. Rev.* 46:fuab049. doi: 10.1093/femsre/fuab049

Bleichenbacher, S., Stevens, M. J. A., Zurfluh, K., Perreten, V., Endimiani, A., Stephan, R., et al. (2020). Environmental dissemination of carbapenemase-producing *Enterobacteriaceae* in rivers in Switzerland. *Environ. Pollut.* 265:115081. doi: 10.1016/j.envpol.2020.115081

Bleriot, I., Blasco, L., Delgado-Valverde, M., Gual-de-Torrella, A., Ambroa, A., Fernandez-Garcia, L., et al. (2020). Mechanisms of tolerance and resistance to chlorhexidine in clinical strains of *Klebsiella pneumoniae* producers of carbapenemase: role of new type II toxin-antitoxin system, PemIK. *Toxins* 12:566. doi: 10.3390/toxins12090566

Bonnin, R. A., Jousset, A. B., Gauthie, R. L., Emeraud, C., Girlich, D., Sauvadet, A., et al. (2020). First occurrence of the OXA-198 carbapenemase in enterobacterales. *Antimicrob. Agents Chemother.* 64, e01471–e01419. doi: 10.1128/AAC.01471-19

Bonomo, R. A., Burd, E. M., Conly, J., Limbago, B. M., Poirel, L., Segre, J. A., et al. (2018). Carbapenemase-producing organisms: a global scourge. *Clin. Infect. Dis.* 66, 1290–1297. doi: 10.1093/cid/cix893

Brolund, A., Lagerqvist, N., Byfors, S., Struelens, M. J., Monnet, D. L., Albiger, B., et al. (2019). Worsening epidemiological situation of carbapenemase-producing *Enterobacteriaceae* in Europe; assessment by national experts from 37 countries. *Euro Surveill.* 24:1900123. doi: 10.2807/1560-7917.ES.2019.24.9.1900123

Carattoli, A. (2009). Resistance plasmid families in *Enterobacteriaceae*. *Antimicrob. Agents Chemother.* 53, 2227–2238. doi: 10.1128/aac.01707-08

Cartron, M. L., Maddocks, S., Gillingham, P., Craven, C. J., and Andrews, S. C. (2006). Feo – transport of ferrous iron into bacteria. *Biometals* 19, 143–157. doi: 10.1007/s10534-006-0003-2

Castanheira, M., Simner, P. J., and Bradford, P. A. (2021). Extended-spectrum β-lactamases: An update on their characteristics, epidemiology and detection. *JAC Antimicrob. Resist.* 3:dlab092. doi: 10.1093/jacamr/dlab092

Chassaing, B., Rolhion, N., de Vallée, A., Salim, S. Y., Prorok-Hamon, M., Neut, C., et al. (2011). Crohn disease-associated adherent-invasive *E. coli* bacteria target mouse and human Peyer's patches via long polar fimbriae. *J. Clin. Investig.* 121, 966–975. doi: 10.1172/JCI44632

Cheng, Y. H., Lin, T. L., Pan, Y. J., Wang, Y. P., Lin, Y. T., and Wang, J. T. (2015). Colistin resistance mechanisms in *Klebsiella pneumoniae* strains from Taiwan. *Antimicrob. Agents Chemother.* 59, 2909–2913. doi: 10.1128/aac.04763-14

Chetri, S., Bhowmik, D., Paul, D., Pandey, P., Chanda, D. D., Chakravarty, A., et al. (2019). AcrAB-TolC efflux pump system plays a role in carbapenem non-susceptibility in *Escherichia coli*. *BMC Microbiol.* 19, 210–217. doi: 10.1186/s12866-019-1589-1

Cordonnier, C., Etienne-Mesmin, L., Thévenot, J., Rougeron, A., Renier, S., Chassaing, B., et al. (2017). Enterohemorrhagic *Escherichia coli* pathogenesis: role of long polar fimbriae in Peyer's patches interactions. *Sci. Rep.* 7:44655. doi: 10.1038/srep44655

Cornelis, P., and Dingemans, J. (2013). Pseudomonas aeruginosa adapts its iron uptake strategies in function of the type of infections. *Front. Cell. Infect. Microbiol.* 3:75. doi: 10.3389/fcimb.2013.00075

Cury, A. P., Girardello, R., da Silva Duarte, A. J., and Rossi, F. (2020). KPC-producing Enterobacterales with uncommon carbapenem susceptibility profile in Vitek 2 system. *Int. J. Infect. Dis.* 93, 118–120. doi: 10.1016/j.ijid.2020.01.016

D'Onofrio, V., Conzemius, R., Varda-Brkić, D., Bogdan, M., Grisold, A., Gyssens, I. C., et al. (2020). Epidemiology of colistin-resistant, carbapenemase-producing *Enterobacteriaceae* and *Acinetobacter baumannii* in Croatia. *Infect. Genet. Evol.* 81:104263. doi: 10.1016/j.meegid.2020.104263

Dai, X., Zhou, D., Xiong, W., Feng, J., Luo, W., Luo, G., et al. (2016). The IncP-6 plasmid p10265-KPC from *Pseudomonas aeruginosa* carries a novel DISEc33-associated blaKPC-2 gene cluster. *Front. Microbiol.* 7:310. doi: 10.3389/fmicb.2016.00310

De Majumdar, S., Yu, J., Fookes, M., McAteer, S. P., Llobet, E., Finn, S., et al. (2015). Elucidation of the RamA regulon in *Klebsiella pneumoniae* reveals a role in LPS regulation. *PLoS Pathog.* 11:e1004627. doi: 10.1371/journal.ppat.1004627

Diaz-Orejas, R., Espinosa, M., and Yeo, C. C. (2017). The importance of the expendable: toxin-antitoxin genes in plasmids and chromosomes. *Front. Microbiol.* 8:1479. doi: 10.3389/fmicb.2017.01479

Drenjančević, D., Presečki-Stanko, A., Kopić, J., Talapko, J., Zarfel, G., and Bedenić, B. (2019). Hidden carbapenem resistance in OXA-48 and extended-spectrum β-lactamase-positive *Escherichia coli*. *Microb. Drug Resist.* 25, 696–702. doi: 10.1089/mdr.2018.0309

Ekwanzala, M. D., Dewar, J. B., Kamika, I., and Momba, M. N. B. (2019). Tracking the environmental dissemination of carbapenem-resistant *Klebsiella pneumoniae* using whole genome sequencing. *Sci. Total Environ.* 691, 80–92. doi: 10.1016/j.scitotenv.2019.06.533

Ekwanzala, M. D., Dewar, J. B., Kamika, I., and Momba, M. N. B. (2020). Comparative genomics of vancomycin-resistant *Enterococcus* spp. revealed common resistome determinants from hospital wastewater to aquatic environments. *Sci. Total Environ.* 719:137275. doi: 10.1016/j.scitotenv.2020.137275

EUCAST (2013). EUCAST guidelines for detection of resistance mechanisms and specific resistances of clinical and/or epidemiological importance. Version 1.0. EUCAST, 2013. Available at: https://www.eucast.org (Accessed 24 June 2020).

EUCAST (2020). Breakpoint Tables for Interpretation of MICs and Zone Diameters. Version 10.0. EUCAST, 2020. Available at: https://www.eucast.org (Accessed 24 June 2020).

Ferreira, I., Beisken, S., Lueftinger, L., Weinmaier, T., Klein, M., Bacher, J., et al. (2020). Species identification and antibiotic resistance prediction by analysis of whole-genome sequence data by use of ARESdb: an analysis of isolates from the Unyvero lower respiratory tract infection trial. *J. Clin. Microbiol.* 58, e00273–e00220. doi: 10.1128/JCM.00273-20

Ferreira, I., Lepuschitz, S., Beisken, S., Fiume, G., Mrazek, K., Frank, B. J. H., et al. (2021). Culture-free detection of antibiotic resistance markers from native patient samples by hybridization capture sequencing. *Microorganisms* 9:1672. doi: 10.3390/microorganisms9081672

Fu, L., Tang, L., Wang, S., Liu, Q., Liu, Y., Zhang, Z., et al. (2018). Co-location of the bla_{KPC-2}, $bla_{CTX-M-65}$, rmtB and virulence relevant factors in an IncFII plasmid from a hypermucoviscous *Klebsiella pneumoniae* isolate. *Microb. Pathog.* 124, 301–304. doi: 10.1016/j.micpath.2018.08.055

Garbari, L., Busetti, M., Dolzani, L., Petix, V., Knezevich, A., Bressan, , et al. (2015). pKBuS13, a KPC-2-encoding plasmid from *Klebsiella pneumoniae* sequence type 833, carrying Tn4401b inserted into an Xer site-specific recombination locus. *Antimicrob. Agents Chemother.* 59, 5226–5231. doi: 10.1128/AAC.04543-14

Ghiglione, B., Haim, M. S., Penzotti, P., Brunetti, F., Di Conza, J., Figueroa-Espinosa, R., et al. (2021). Characterization of emerging pathogens carrying blaKPC-2 gene in IncP-6 plasmids isolated from urban sewage in Argentina. *Front. Cell. Infect. Microbiol.* 11:722536. doi: 10.3389/fcimb.2021.722536

Gomi, R., Matsuda, T., Yamamoto, M., Chou, P. H., Tanaka, M., Ichiyama, S., et al. (2018). Characteristics of carbapenemase-producing *Enterobacteriaceae* in wastewater revealed by genomic analysis. *Antimicrob. Agents Chemother.* 62, e02501–e02517. doi: 10.1128/AAC.02501-17

Grundmann, H., Glasner, C., Albiger, B., Aanensen, D. M., Tomlinson, C. T., Tambić Andrašević, A., et al. (2017). Occurrence of carbapenemase-producing *Klebsiella pneumoniae* and *Escherichia coli* in the European survey of carbapenemase-producing Enterobacteriaceae (EuSCAPE): a prospective, multinational study. *Lancet Infect. Dis.* 17, 153–163. doi: 10.1016/S1473-3099(16)30257-2

Hernandez-Ramirez, K. C., Chavez-Jacobo, V. M., Valle-Maldonado, M. I., Patino-Medina, J. A., Diaz-Perez, S. P., Jacome-Galarza, I. E., et al. (2017). Plasmid pUM505 encodes a toxin-antitoxin system conferring plasmid stability and increased *Pseudomonas aeruginosa* virulence. *Microb. Pathog.* 112, 259–268. doi: 10.1016/j.micpath.2017.09.060

Hobson, C. A., Bonacorsi, S., Jacquier, H., Choudhury, A., Magnan, M., Cointe, A., et al. (2020). KPC beta-lactamases are permissive to insertions and deletions conferring substrate spectrum modifications and resistance to ceftazidime-avibactam. *Antimicrob. Agents Chemother.* 64, e01175–e01120. doi: 10.1128/AAC.01175-20

Huang, X. Z., Frye, J. G., Chahine, M. A., Glenn, L. M., Ake, J. A., Su, W., et al. (2012). Characteristics of plasmids in multi-drug-resistant *Enterobacteriaceae* isolated during prospective surveillance of a newly opened hospital in Iraq. *PLoS One* 7:e40360. doi: 10.1371/journal.pone.0040360

Jelić, M., Butić, I., Plecko, V., Cipris, I., Jajić, I., Bejuk, D., et al. (2016). KPC-producing *Klebsiella pneumoniae* isolates in Croatia: a nationwide survey. *Microb. Drug Resist.* 22, 662–667. doi: 10.1089/mdr.2015.0150

Jelić, M., Hrenović, J., Dekić, S., Goić-Barišić, I., and Tambić Andrašević, A. (2019). First evidence of KPC-producing ST258 Klebsiella pneumoniae in river water. *J. Hosp. Infect.* 103, 147–150. doi: 10.1016/j.jhin.2019.04.001

Jelić, M., Škrlin, J., Bejuk, D., Košćak, I., Butić, I., Gužvinec, M., et al. (2018). Characterization of isolates associated with emergence of OXA-48-producing *Klebsiella pneumoniae* in Croatia. *Microb. Drug Resist.* 24, 973–979. doi: 10.1089/mdr.2017.0168

Kudirkiene, E., Andoh, L. A., Ahmed, S., Herrero-Fresno, A., Dalsgaard, A., Obiri-Danso, K., et al. (2018). The use of a combined bioinformatics approach to locate antibiotic resistance genes on plasmids from whole genome sequences of Salmonella enterica serovars from humans in Ghana. *Front. Microbiol.* 9:1010. doi: 10.3389/fmicb.2018.01010

Kvesić, M., Kalinić, H., Dželalija, M., Šamanić, I., Andričević, R., and Maravić, A. (2021). Microbiome and antibiotic resistance profiling in submarine effluent-receiving coastal waters in Croatia. *Environ. Pollut.* 292:118282. doi: 10.1016/j.envpol.2021.118282

Lau, H. Y., Clegg, S., and Moore, T. A. (2007). Identification of Klebsiella pneumoniae genes uniquely expressed in a strain virulent using a murine model of bacterial pneumonia. *Microb. Pathog.* 42, 148–155. doi: 10.1016/j.micpath.2007.01.001

Literacka, E., Izdebski, R., Urbanowicz, P., Żabicka, D., Klepacka, J., Sowa-Sierant, , et al. (2020). Spread of *Klebsiella pneumoniae* ST45 producing GES-5 carbapenemase or GES-1 extended-spectrum β-lactamase in newborns and infants. *Antimicrob. Agents Chemother.* 64, e00595–e00520. doi: 10.1128/AAC.00595-20

Liu, Y. Y., Wang, Y., Walsh, T. R., Yi, L. X., Zhang, R., Spencer, J., et al. (2016). Emergence of plasmid-mediated colistin resistance mechanism MCR-1 in animals and human beings in China: a microbiological and molecular biological study. *Lancet Infect. Dis.* 16, 161–168. doi: 10.1016/S1473-3099(15)00424-7

Magiorakos, A. P., Srinivasan, A., Carey, R. B., Carmeli, Y., Falagas, M. E., Giske, C. G., et al. (2012). Multidrug-resistant, extensively drug-resistant and pandrug-resistant bacteria: an international expert proposal for interim standard definitions for acquired resistance. *Clin. Microbiol. Infect.* 18, 268–281. doi: 10.1111/j.1469-0691.2011.03570.x

Maravić, A., Skočibušić, M., Šamanić, I., Fredotović, Ž., Cvjetan, S., Jutronić, M., et al. (2013). *Aeromonas* spp. simultaneously harbouring blaCTX-M-15, blaSHV-12, blaPER-1 and blaFOX-2 in wild-growing Mediterranean mussel (*Mytilus galloprovincialis*) from Adriatic Sea; Croatia. *Int. J. Food Microbiol.* 166, 301–308. doi: 10.1016/j.ijfoodmicro.2013.07.010

Mates, A. K., Sayed, A. K., and Foster, J. W. (2007). Products of the *Escherichia coli* acid fitness island attenuate metabolite stress at extremely low pH and mediate a cell density-dependent acid resistance. *J. Bacteriol.* 189, 2759–2768. doi: 10.1128/JB.01490-06

Mathers, A. J., Peirano, G., and Pitout, J. D. D. (2015). *Escherichia coli* ST131: the quintessential example of an international multiresistant high-risk clone. *Adv. Appl. Microbiol.* 90, 109–154. doi: 10.1016/bs.aambs.2014.09.002

Mendes, G., Ramalho, J. F., Bruschy-Fonseca, A., Lito, L., Duarte, A., Melo-Cristino, J., et al. (2022). Whole-genome sequencing enables molecular characterization of non-clonal group 258 high-risk clones (ST13, ST17, ST147 and ST307) among Carbapenem-resistant *Klebsiella pneumoniae* from a tertiary University Hospital Centre in Portugal. *Microorganisms* 10, 416. doi: 10.3390/microorganisms10020416

Montezzi, L. F., Campana, E. H., Corrêa, L. L., Justo, L. H., Paschoal, R. P., da Silva, I. L., et al. (2015). Occurrence of carbapenemase-producing bacteria in coastal recreational waters. *Int. J. Antimicrob. Agents* 45, 174–177. doi: 10.1016/j.ijantimicag.2014.10.016

Naha, S., Sands, K., Mukherjee, S., Roy, C., Rameez, M. J., Saha, B., et al. (2020). KPC-2-producing *Klebsiella pneumoniae* ST147 in a neonatal unit: clonal isolates with differences in colistin susceptibility attributed to AcrAB-TolC pump. *Int. J. Antimicrob. Agents* 55:105903. doi: 10.1016/j.ijantimicag.2020.105903

Orth, D., Grif, K., Dierich, M. P., and Würzner, R. (2006). Variability in tellurite resistance and the ter gene cluster among Shiga toxin-producing *Escherichia coli* isolated from humans, animals and food. *Res. Microbiol.* 158, 105–111. doi: 10.1016/j.resmic.2006.10.007

Padilla, E., Llobet, E., Doménech-Sánchez, A., Martínez-Martínez, L., Bengoechea, J. A., and Albertí, S. (2010). Klebsiella pneumoniae AcrAB efflux pump contributes to antimicrobial resistance and virulence. *Antimicrob. Agents Chemother.* 54, 177–183. doi: 10.1128/AAC.00715-09

Pages, J. M., James, C. E., and Winterhalter, M. (2008). The porin and the permeating antibiotic: a selective diffusion barrier in Gram-negative bacteria. *Nat. Rev. Microbiol.* 6, 893–903. doi: 10.1038/nrmicro1994

Pepperell, C., Kus, J. V., Gardam, M. A., Humar, A., and Burrows, L. L. (2002). Low-virulence Citrobacter species encode resistance to multiple antimicrobials. *Antimicrob. Agents Chemother.* 46, 3555–3560. doi: 10.1128/AAC.46.11.3555-3560.2002

Pérez-Vazquez, M., Oteo-Iglesias, J., Sola-Campoy, P. J., Carrizo-Manzoni, H., Bautista, V., Lara, N., et al. (2019). Characterization of carbapenemase-producing *Klebsiella oxytoca* in Spain, 2016–2017. *Antimicrob. Agents Chemother.* 63, e02529–e02518. doi: 10.1128/AAC.02529-18

Piotrowska, M., Kowalska, S., and Popowska, M. (2019). Diversity of β-lactam resistance genes in Gram-negative rods isolated from a municipal wastewater treatment plant. *Ann. Microbiol.* 69, 591–601. doi: 10.1007/s13213-019-01450-1

Poirel, L., Barbosa-Vasconcelos, A., Simoes, R. R., Da Costa, P. M., Liu, W., and Nordmann, P. (2012). Environmental KPC-producing *Escherichia coli* isolates in Portugal. *Antimicrob. Agents Chemother.* 56, 1662–1663. doi: 10.1128/AAC.05850-11

Poirel, L., Walsh, T. R., Cuvillier, V., and Nordmann, P. (2011). Multiplex PCR for detection of acquired carbapenemase genes. *Diagn. Microbiol. Infect. Dis.* 70, 119–123. doi: 10.1016/j.diagmicrobio.2010.12.002

Poirel, L., Weldhagen, G. F., Naas, T., De Champs, C., Dove, M. G., and Nordmann, P. (2001). GES-2, a class A β-lactamase from *Pseudomonas aeruginosa* with increased hydrolysis of imipenem. *Antimicrob. Agents Chemother.* 45, 2598–2603. doi: 10.1128/AAC.45.9.2598-2603.2001

Pulingam, T., Parumasivam, T., Gazzali, A. M., Sulaiman, A. M., Chee, J. Y., Lakshmanan, M., et al. (2021). Antimicrobial resistance: prevalence, economic burden, mechanisms of resistance and strategies to overcome. *Eur. J. Pharm. Sci.* 170:106103. doi: 10.1016/j.ejps.2021.106103

Ramage, H. R., Connolly, L. E., and Cox, J. S. (2009). Comprehensive functional analysis of *mycobacterium tuberculosis* toxin-antitoxin systems: implications for pathogenesis, stress responses, and evolution. *PLoS Genet.* 5:e1000767. doi: 10.1371/journal.pgen.1000767

Sadeghi, M. (2019). Molecular characterization of multidrug-resistant *Escherichia coli* isolates in Azerbaijan hospitals. *Microb. Drug Resist.* 25, 1287–1296. doi: 10.1089/mdr.2019.0006

Šamanić, I., Kalinić, H., Fredotović, Ž., Dželalija, M., Bungur, A.-M., and Maravić, A. (2021). Bacteria tolerant to colistin in coastal marine environment: detection; microbiome diversity and antibiotic resistance genes' repertoire. *Chemosphere* 281:130945. doi: 10.1016/j.chemosphere.2021.130945

Sato, T., Wada, T., Nishijima, S., Fukushima, Y., Nakajima, C., Suzuki, Y., et al. (2020). Emergence of the novel aminoglycoside Acetyltransferase variant aac (6′)-Ib-D179Y and Acquisition of Colistin Heteroresistance in Carbapenem-resistant *Klebsiella pneumoniae* due to a disrupting mutation in the DNA repair enzyme MutS. *MBio* 11, e01954–e01920. doi: 10.1128/mBio.01954-20

Shinde, S., Gupta, R., Raut, S. S., Nataraj, G., and Mehta, P. R. (2017). Carba NP as a simpler, rapid, cost-effective, and a more sensitive alternative to other phenotypic tests for detection of carbapenem resistance in routine diagnostic laboratories. *J. Lab. Physicians* 9, 100–103. doi: 10.4103/0974-2727.199628

Stoesser, N., Sheppard, A. E., Peirano, G., Anson, L. W., Pankhurst, L., Sebra, R., et al. (2017). Genomic epidemiology of global *Klebsiella pneumoniae* carbapenemase (KPC)-producing *Escherichia coli*. *Sci. Rep.* 7:5917. doi: 10.1038/s41598-017-06256-2

Struve, C., Bojer, M., and Krogfelt, K. A. (2008). Characterization of *Klebsiella pneumoniae* type 1 fimbriae by detection of phase variation during colonization and infection and impact on virulence. *Infect. Immun.* 76, 4055–4065. doi: 10.1128/IAI.00494-08

Su, S., Li, C., Yang, J., Xu, Q., Qiu, Z., Xue, B., et al. (2020). Distribution of antibiotic resistance genes in three different natural water bodies-A Lake; river and sea. *Int. J. Environ. Res. Publ. Health.* 17, 552. doi: 10.3390/ijerph17020552

Vardakas, K. Z., Tansarli, G. S., Rafailidis, P. I., and Falagas, M. E. (2012). Carbapenems versus alternative antibiotics for the treatment of bacteraemia due to Enterobacteriaceae producing extended-spectrum beta-lactamases: a systematic review and meta-analysis. *J. Antimicrob. Chemother.* 67, 2793–2803. doi: 10.1093/jac/dks301

Walling, L. R., and Butler, J. S. (2016). Structural determinants for antitoxin identity and insulation of cross talk between homologous toxin-antitoxin systems. *J. Bacteriol.* 198, 3287–3295. doi: 10.1128/JB.00529-16

Wang, J., Yuan, M., Chen, H., Chen, X., Jia, Y., Zhu, X., et al. (2017). First report of *Klebsiella oxytoca* strain simultaneously producing NDM-1, IMP-4, and KPC-2 Carbapenemases. *Antimicrob. Agents Chemother.* 61, e00877–e00817. doi: 10.1128/AAC.00877-17

WHO, (2017). Essential medicines and health products: Global priority list of antibiotic-resistant bacteria to guide research, discovery, and development of new antibiotics. Available at: http://www.who.int/medicines/publications/globalpriority-list-antibiotic-resistant-bacteria (Accessed 7 July 2021).

Wong, J. L., Romano, M., Kerry, L. E., Kwong, H. S., Low, W. W., Brett, S. J., et al. (2019). OmpK36-mediated carbapenem resistance attenuates ST258

Klebsiella pneumoniae in vivo. *Nat. Commun.* 10:3957. doi: 10.1038/s41467-019-11756-y

Woodford, N., Carattoli, A., Karisik, E., Underwood, A., Ellington, M. J., and Livermore, D. M. (2009). Complete nucleotide sequences of plasmids pEK204, pEK499, and pEK516, encoding CTX-M enzymes in three major *Escherichia coli* lineages from the United Kingdom, all belonging to the international O25:H4-ST131 clone. *Antimicrob. Agents Chemother.* 53, 4472–4482. doi: 10.1128/AAC.00688-09

Xu, G., Jiang, Y., An, W., Wang, H., and Zhang, X. (2015). Emergence of KPC-2-producing Escherichia coli isolates in an urban river in Harbin, China. *World J. Microbiol. Biotechnol.* 31, 1443–1450. doi: 10.1007/s11274-015-1897-z

Xu, H., Wang, X., Yu, X., Zhang, J., Guo, L., Huang, C., et al. (2018). First detection and genomics analysis of KPC-2-producing *Citrobacter* isolates from river sediments. *Environ. Pollut.* 235, 931–937. doi: 10.1016/j.envpol.2017.12.084

Yang, F., Huang, L., Li, L., Yang, Y., Mao, D., and Luo, Y. (2017). Discharge of KPC-2 genes from the WWTPs contributed to their enriched abundance in the receiving river. *Sci. Total Environ.* 581-582(581–582), 136–143. doi: 10.1016/j.scitotenv.2016.12.063

Yao, Y., Lazaro-Perona, F., Falgenhauer, L., Valverde, A., Imirzalioglu, C., Dominguez, L., et al. (2017). Insights Into a novel blaKPC-2-encoding IncP-6 plasmid reveal Carbapenem-resistance circulation in several Enterobacteriaceae species From wastewater and a hospital source in Spain. *Front. Microbiol.* 8:1143. doi: 10.3389/fmicb.2017.01143

Zhang, X., Lu, X., and Zong, Z. (2012). *Enterobacteriaceae* producing the KPC-2 carbapenemase from hospital sewage. *Diagn. Microbiol. Infect. Dis.* 73, 204–206. doi: 10.1016/j.diagmicrobio.2012.02.007

Zhi, S., Banting, G., Stothard, P., Ashbolt, N. J., Checkley, S., Meyer, K., et al. (2019). Evidence for the evolution, clonal expansion and global dissemination of water treatment-resistant naturalized strains of *Escherichia coli* in wastewater. *Water Res.* 156, 208–222. doi: 10.1016/j.watres.2019.03.024

Zurfluh, K., Stevens, M. J. A., Stephan, R., and Nüesch-Inderbinen, M. (2018). Complete and assembled genome sequence of an NDM-5- and CTX-M-15-producing *Escherichia coli* sequence type 617 isolated from wastewater in Switzerland. *J. Glob. Antimicrob. Resist.* 15, 105–106. doi: 10.1016/j.jgar.2018.08.015

Conflict of Interest: The authors declare that the research was conducted in the absence of any commercial or financial relationships that could be construed as a potential conflict of interest.

Publisher's Note: All claims expressed in this article are solely those of the authors and do not necessarily represent those of their affiliated organizations, or those of the publisher, the editors and the reviewers. Any product that may be evaluated in this article, or claim that may be made by its manufacturer, is not guaranteed or endorsed by the publisher.

4. ADDITIONAL RESULTS AND DISCUSSION

To gain a deeper insight into our findings, we have carried out an additional analysis. This allowed us to better understand how submarine discharges affect the water quality of the entire water column. For this purpose, we compared our data with information collected at a reference site Split Channel (SC), which is considered a location free of anthropogenic pressures (Figure 4) [106]. These results are discussed in the next subsection 'Comparison of microbial community structure in coastal waters not affected by wastewater'. Moreover, to fortify the validity of our results, to gain new insights and to extend the current knowledge, additional analyses were carried out. This encompasses the simultaneous collection of samples from both influent and effluent of two distinct WWTPs, as well as from the locations of the corresponding submarine outfalls. We have provided detailed explanations of the used methods and the obtained results in the subsection ‘Microbiome and resistome of WWTPs and submarine outfalls'. These analyses contribute to a more comprehensive and insightful perspective on our research.

Figure 4. The location of sampling sites near the submarine outfalls (Katalinića Brig and Stupe) and a reference location (Split Channel).

4.1. Comparison of microbial community structure in coastal waters not affected by wastewater

4.1.1. Methodology

As part of a comprehensive investigation, the present chapter compares two geographically distinct locations: one that is affected by wastewater discharges (Katalinića Brig and Stupe submarine outfalls) and one that is unaffected (SC) which served as a control. Selected locations belong to the same water body [107]. For this comparative analysis, a dataset from another study was used [106] and compared with the partial datasets of the study presented in Paper II. This analytical endeavour not only enriches our understanding of the dynamics behind the impacts of wastewater discharge but also extends the scientific dissertation concerning the intricate reactions of coastal ecosystems to various factors. We utilized datasets from the winter (March 2021) and summer (August 2021) seasons, collected from both the bottom (SCB) and surface (SCS) locations. To ensure comparability with our analysis, we selected a pair of field samples (from the study in Paper II), opting for those field campaigns that closely aligned with the study conducted by Dželalija et al. in 2023 [106]. Specifically, we included datasets from February 2020 (winter season) and July 2020 (summer season) collected from the bottom (Katalinića Brig (KB) and Stupe (SB)) and surface (Katalinića Brig (KS) and Stupe (SS)) locations. The datasets selected for analysis were collected in different years, which may account for the observed variations in subsequent analyses. However, despite this temporal discrepancy, the comparability of these datasets is acceptable, as supported by the findings from a study conducted in a nearby area [108]. Across a 12-month sampling period covering winter seasons in two distinct years, this study highlighted the influence of environmental conditions on the microbial community structure, surpassing the impact of time or geographical factors.

Consistent with our prior analysis approach (as outlined in Paper II), Dželalija et al., 2023 employed the same metagenomic DNA extraction kit (DNeasy PowerWater Kit) and conducted 16S rRNA amplicon sequencing on the extracted DNA [106]. This strict adherence to methodology ensures the analogy of these datasets. For a comprehensive understanding of the methodology employed and the results obtained in the context of the mentioned study, refer to [106]. Analyses and data visualization in this study were done by Matlab R2021a.

4.1.1. Result and discussion

Differences in microbial community structure between the three selected locations are visible at the phylum level (Figure 5), although they are even more pronounced at the lower taxonomic levels (Figure 6). In winter (Figure 5a), *Proteobacteria* dominated at the SS and SCS locations (41.66% and 54.77%, respectively), while *Firmicutes* were most abundant at the KS location, with a frequency of 61.66%. *Proteobacteria* dominated at the SCB location too (39.37%), while at both bottom locations near the submarine outfalls dominated *Firmicutes* (62.20% at SB and 40.15% at KB). Both phyla, *Proteobacteria* and *Firmicutes*, together with *Bacteroides* are common human-gut members but are also found in coastal waters [106,109]. However, shift in its abundancies are noticed at the locations with different trophic status [106]. In this study, a decrease in *Firmicutes*, and an increase in *Proteobacteria* abundancy at the SCS and SCB locations support such findings. Furthermore, *Verrucomicrobia* together with *Fusobacteria*, are commonly found in WWTPs [110,111] and are noticed in our study during the winter only in locations near the submarine outfalls. However, its low abundancy (<2%) suggest possible marine origin as noticed in another studies [108,112]. *Actinobacteria* was more abundant at SCS (10.47%) compared with SS and KS locations (<6%), and compared with bottom locations, which supported the observed shift in microbial community toward the SCS and SCB locations, similar to the observations in another study [106]. In summer (Figure 5b), locations near Katalinića Brig submarine outfall and locations at Split channel shared the top two phyla. *Proteobacteria* dominated at KS and KB locations (77.28% and 73.48%, respectively), as at SCS and SCB (57.85% and 66.75%, respectively), followed by *Cyanobacteria* with abundancy >20% at SCS and SCB locations, and <20% at KS and KB locations. SS and SB locations showed different microbiome communities. At both locations, *Firmicutes* were the most abundant phyla (59.58% and 79.87%, respectively), followed by *Proteobacteria*. Contrarily with previous findings, *Actinobacteria* shared similar abundancies (>5%) at SS, SB, SCS, and SCB, while at KS and KB were less abundant (<1%). Compared with winter observations, fewer *Firmicutes* and much more *Proteobacteria* was observed in KS, KB, SCS, and SCB locations, while at SS and SB location, the opposite finding was observed.

Finally, as submarine outfalls do not discharge effluent continuously, but after the pool has been full, variation in microbiome analysis could be thus dependent on the overlapping of

sampling time and effluent discharge. However, along with observed results, opposite findings among some phyla and the fact that some phyla contain both, environmental and human-related bacteria, suggest that lower taxonomic levels encompass much more information and are necessary to analyse in order to obtain relevant conclusions.

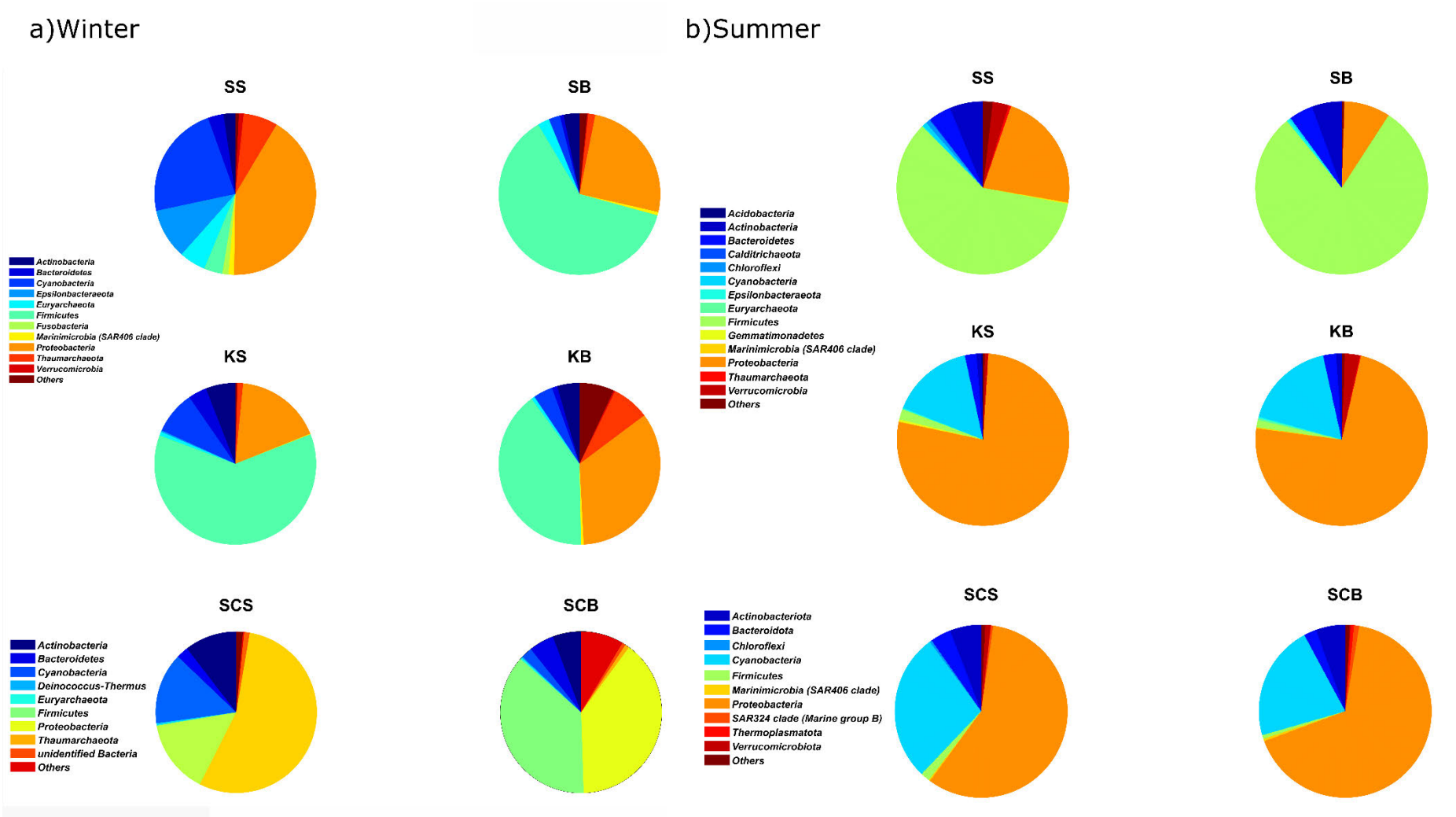

Figure 5. Relative abundance of the ten most abundant taxa at phylum level comprising the bacterial communities from the Stobreč (surface and bottom, SS and SB), Katalinića Brig (surface and bottom, KS and KB) WWTPs effluent sites, and Split channel (surface and bottom, SCS and SCB) reference location.

At the lower taxonomic levels (Figure 6), the differences in microbial community composition are even more visible. During the winter season (Figure 6a), there were no common genera among the selected locations, while in summer only two common genera were found at all selected stations (*Synechococcus*_CC9902 and Clade_Ia) (Figure 6b). In winter, *Faecalibacterium* and *Escherichia-Shigella* were the most abundant on SB (10%), *Paenibacillus* on KB (23.86%), while *Synechococcus*_CC9902 and *Blautia* were predominant on SS (17.67%) and KS (7%), respectively. *Acinetobacter* was second most abundant in SS (11.78%), with lower abundancies at other locations near submarine outfalls and not among the top 10 in SC locations. Moreover, locations near the submarine outfalls were enriched with human-related genera such as *Acinetobacter*, *Aeromonas*, *Bacteroides*, *Blautia*, *Escherichia-Shigella*, *Faecalibacterium, Salmonella* and *Staphylococcus*, while at SCS and SCB were not among the top 10 observed. At the SCS and SCB locations, among the top 10 bacterial genera, the most abundant (unidentified_*Alphaproteobacteria*) comprised abundancy about 8%, which highlights the higher diversity and lower richness of these locations compared with locations near the submarine outfalls. In summer, at SCS and SCB locations, the most abundant genus was *Synechococcus_CC9902* (22.55% and 14.38%, respectively). Such increase in richness, along with other autochthonous marine bacteria (AEGEAN-169, Clade and SAR11 lineages) is seasonally driven as previously observed for this region [106,113]. Observation of such native marine bacteria was characteristic for summer at the locations near the submarine outfalls too, although with some differences. Lower abundancies of *Synechococcus_CC9902* were observed at all four locations near the submarine outfalls compared with SC locations, while opposite findings were observed for Clade_Ia. Although at the locations near the submarine outfalls, only Clade_Ia was found, its abundance was higher at KS and KB locations (10.74% and 12.62%, respectively), compared with the SC locations (<6%). However, at the SS and SB locations, its abundancy was below 0.2%. In the summer, there were still observed human-related genera, as *Bacteroides*, *Blautia*, *Dorea*, *Faecalibacterium*, and *Salmonella* only at the locations near the submarine outfalls. At the SC locations, an increase in abundancy of *Acinetobacter* and *Pseudomonas* occurred.

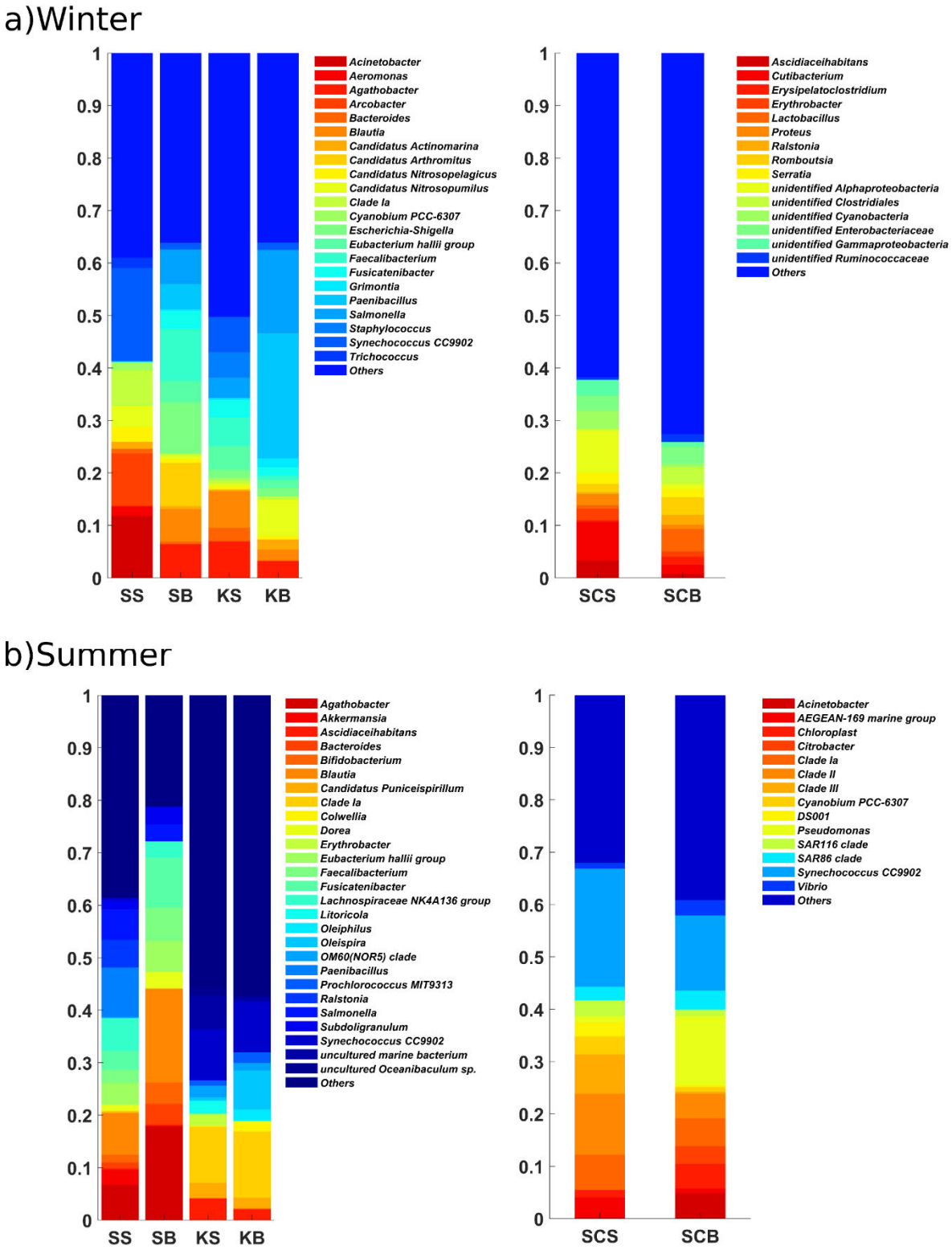

Figure 6. Relative abundance of the ten most abundant taxa at genus level comprising the bacterial communities from the Stobreč (surface and bottom, SS and SB), Kaliniića Brig (surface and bottom, KS and KB) WWTPs effluent sites, and Split channel (surface and bottom, SCS and SCB) reference location.

In order to better understand the abundancy of the top 10 genera across sampling locations, a clustergram was obtained (Figure 7). Supporting the above discussed results, in the winter season (Figure 7a) dendrogram clustered submarine locations together, while SC locations clustered separately. However, in summer (Figure 7b), KS and KB locations were clustered together with SCS and SCB, while SS and SB locations clustered separately. This analysis supported the obtained results at both taxonomic levels addressing the complex dynamics of microbial communities in response to locations and seasons. Segregation of SS and SB locations in summer, compared with other locations which showed similar microbial community composition (Katalinića Brig and Split Channel), could be due to the more concentrated wastewater load in the Stupe WWTP. This could be because Stupe WWTP doesn't receive rainfall-runoff wastewater like Katalinića Brig WWTP. This is supported by higher concentrations of different wastewater effluent parameters (BOD, COD, TSS and nutrients) presented in Paper I. Moreover, a higher FIB concentrations at SB compared with KB in summer support such observations(Paper II). Furthermore, in the same sampling month, a higher CDOM, turbidity, and Chl *a* concentration with lower dissolved oxygen values are noticed as well at SB compared with KB (Paper I).

In conclusion, this analysis revealed differences in the structure of microbial communities among the selected locations, particularly evident at both the phylum and lower taxonomic levels. Winter and summer seasons exhibit distinct patterns, revealing the influence of submarine outfalls and seasonal changes on microbial populations. Seasonal shifts were observed in both, allochthonous and autochthonous bacteria. However, human-related genera are enriched near the outfalls, underscoring the potential impact of anthropogenic activities on coastal microbial ecosystems. However, future sampling including NGS sequencing together with physico-chemical parameters during the whole year at least are necessary to better understand complex dynamics of microbial communities in response to submarine outfall and seasonal changes. These findings suggest intricate ecological interactions influenced by seasonal and location-specific factors, offering a comprehensive view of the microbial communities' responses to different conditions and impacts.

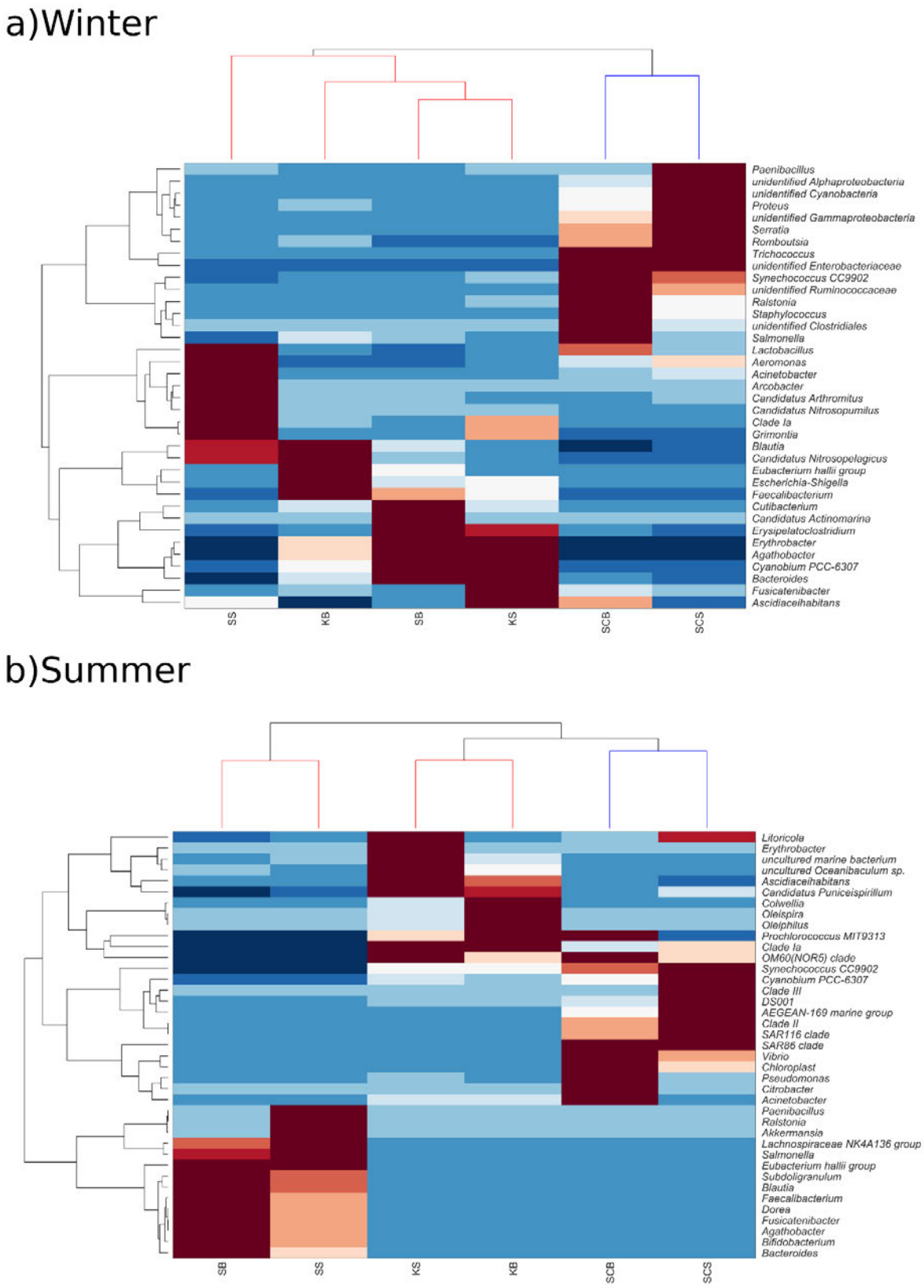

Figure 7. Clustergram (heatmap of relative abundancy at the genus level with dendogram) for winter (a) and summer (b) seasons over the sampling locations. Clustergram standardizes the values along the columns of data. The data has been standardized across all samples, so that the mean is 0 and the standard deviation is 1.

CONFIDENTIAL

CONFIDENTIAL

CONFIDENTIAL

CONFIDENTIAL

CONFIDENTIAL

CONFIDENTIAL

CONFIDENTIAL

CONFIDENTIAL

CONFIDENTIAL

CONFIDENTIAL

CONFIDENTIAL

CONFIDENTIAL

CONFIDENTIAL

CONFIDENTIAL

5. CONCLUSION AND FUTURE REMARKS

Within this doctoral dissertation, a comprehensive analysis was undertaken to examine the impact of submarine outfalls on the coastal marine environment's microbiome and resistome. Employing cutting-edge methods, including fast-profiling probes and advanced NGS techniques encompassing 16S rRNA and shotgun sequencing, this study aimed to address knowledge gaps and provide novel insights about the globally disseminated problem of antibiotic resistance. The initial phase (Paper I) focused on elucidating water column stability, a crucial determinant which influence the vertical movement of effluent plume, in tandem with physico-chemical parameters reflecting plume shape. Stratification's essential role in keeping effluents below the pycnocline was confirmed, underscoring the utility of fast-profiling probes. Simultaneously, samples were collected from submarine outfalls' water column bottom and surface locations for metagenomic analysis, as presented in Paper II, which clearly demonstrated the influence of submarine outfalls on the water column's microbial community. This resulted in the spread of nonindigenous and pathogenic bacteria, potentially harbouring AR determinants. Further investigations (Paper III) utilized plate-based methods to identify carbapenemase-producing *Enterobacteriaceae* strains, revealing their presence near the submarine outfall linked to hospital wastewater discharge. Strikingly, environmental carbapenemase-producing *E. coli* co-occurring bla_{KPC-2} and bla_{OXA-48} carbapenemase genes was detected for the first time, along with genes harbouring on IncP6 resistance plasmids. As this was the first record of IncP6 circulation in *E. coli*, this study moreover highlighted the importance of environmental monitoring in the epidemiology of this globally disseminated carbapenemase encoding gene. To support and expand our finding, additional results were made and presented in this thesis. Focusing on microbial community structure, we compared locations near the submarine outfalls with one location considered as free of wastewater impact. It reveals differences at both phylum and lower taxonomic levels, revealing the complex ecological dynamics influenced by seasonal and location-specific factors. Finally, an extensive shotgun analysis across both WWTPs (influent and effluent) and corresponding submarine outfalls provided insights into the intricate interplay between bacterial communities and ARGs, emphasizing the persistence and dissemination of AR within WWTPs and its subsequent release into the marine environment. This culmination of knowledge serves as a base for decision-makers, enabling a comprehensive strategies and maintenance of the delicate balance of marine ecosystems and public health. This thesis, underscores the imperative of

holistic approaches in unravelling the complex interactions between human activities and marine ecosystems.

However, it is imperative to acknowledge that the present findings represent a initial step, rather than a conclusive endpoint. This study underscores potential paths for future research endeavours, specifically emphasizing the importance of interdisciplinary collaborations. Future field campaigns should integrate advanced methodologies, including fast-profiling probes and remotely operated vehicles (ROVs), alongside with established microbiological and molecular techniques. These prospective investigations should encompass both within-WWTP and submarine outfall contexts. The deployment of sophisticated equipment such as probes and ROVs holds the promise of real-time insight into the precise localization, shape, and dynamics of effluent plumes. This, in tandem with assessments of vertical water column stability and seawater currents, promises an enhanced understanding of both vertical and horizontal dispersion patterns of effluent plumes. The integration of diverse seasonal observations could unveil disruptions to water column stability during the delicate human health risk periods of summer. Emerging tools such as NGS coupled in tandem with a spectrum of physiochemical measurements offer a platform for unravelling main stressors and driving forces that shape microbial community dynamics, as well as the distribution and diversity of ARGs. Expanding this investigation with sediment sampling could amplify our understanding and provides a more comprehensive knowledge about the complex interactions between aquatic environments and anthropogenic impacts. The consolidation of findings from diverse chapters seamlessly aligns with the One Health concept, revealing the intricate interdependencies between human, animal, and environmental health. This comprehensive investigation underscores the need for collaborative efforts across disciplines to mitigate the escalating challenges posed by antibiotic resistance and environmental impact.

6. ADDITIONAL REFERENCES

1. Basset, A.; Barbone, E.; Elliott, M.; Li, B.-L.; Jorgensen, S.E.; Lucena-Moya, P.; Pardo, I.; Mouillot, D. A Unifying Approach to Understanding Transitional Waters: Fundamental Properties Emerging from Ecotone Ecosystems. Estuarine, Coastal and Shelf Science 2013, 132, 5–16, doi:10.1016/j.ecss.2012.04.012.

2. Kummu, M.; Guillaume, J.H.A.; De Moel, H.; Eisner, S.; Flörke, M.; Porkka, M.; Siebert, S.; Veldkamp, T.I.E.; Ward, P.J. The World's Road to Water Scarcity: Shortage and Stress in the 20th Century and Pathways towards Sustainability. Sci Rep 2016, 6, 38495, doi:10.1038/srep38495.

3. United Nations Department of Economic and Social Affairs, Population Division World Population Prospects 2022: Summary of Results; 2022;

4. Kennish, M.J. Pollution in Estuaries and Coastal Marine Waters. Journal of Coastal Research 1994, 27–49.

5. Rabalais, N.N. Nitrogen in Aquatic Ecosystems. AMBIO: A Journal of the Human Environment 2002, 31, 102–112, doi:10.1579/0044-7447-31.2.102.

6. Silva, M.A.M.; Eça, G.F.; Santos, D.F.; Guimarães, A.G.; Lima, M.C.; De Souza, M.F.L. Dissolved Inorganic Nutrients and Chlorophyll a in an Estuary Receiving Sewage Treatment Plant Effluents: Cachoeira River Estuary (NE Brazil). Environ Monit Assess 2013, 185, 5387–5399, doi:10.1007/s10661-012-2953-x.

7. Kotlarska, E.; Łuczkiewicz, A.; Pisowacka, M.; Burzyński, A. Antibiotic Resistance and Prevalence of Class 1 and 2 Integrons in Escherichia Coli Isolated from Two Wastewater Treatment Plants, and Their Receiving Waters (Gulf of Gdansk, Baltic Sea, Poland). Environ Sci Pollut Res 2015, 22, 2018–2030, doi:10.1007/s11356-014-3474-7.

8. O'Mullan, G.D.; Elias Dueker, M.; Juhl, A.R. Challenges to Managing Microbial Fecal Pollution in Coastal Environments: Extra-Enteric Ecology and Microbial Exchange Among Water, Sediment, and Air. Curr Pollution Rep 2017, 3, 1–16, doi:10.1007/s40726-016-0047-z.

9. Bleninger, T.; Jirka, G. Near and Far-Field Model Coupling Methodology for Wastewater Discharges. 2004, doi:10.1201/b16814-73.

10. Hunt, C.D.; Mansfield, A.D.; Mickelson, M.J.; Albro, C.S.; Geyer, W.R.; Roberts, P.J.W. Plume Tracking and Dilution of Effluent from the Boston Sewage Outfall. Mar Environ Res 2010, 70, 150–161, doi:10.1016/j.marenvres.2010.04.005.

11. Petrenko, A.; Jones, B.; Dickey, T. Shape and Initial Dilution of Sand Island, Hawaii Sewage Plume. Journal of Hydraulic Engineering-asce - J HYDRAUL ENG-ASCE 1998, 124, doi:10.1061/(ASCE)0733-9429(1998)124:6(565).

12. Faganeli, J. Nutrient Dynamics in Seawater Column in the Vicinity of Piran Submarine Sewage Ouffall (North Adriatic). Marine Pollution Bulletin 1982, 13.

13. Mozetič, P.; Malačič, V.; Turk, V. Ecological Characteristics of Seawater Influenced by Sewage Outfall. Annales. Ser. hist. nat. 1999, 9, 177–190.

14. Figueiredo Da Silva, J.; Duck, R.W.; Hopkins, T.S.; Anderson, J.M. Nearshore Circulation Revealed by Wastewater Discharge from a Submarine Outfall, Aveiro Coast, Portugal. Hydrol. Earth Syst. Sci. 2002, 6, 983–988, doi:10.5194/hess-6-983-2002.

15. Stamates, S.J.; Craynock, J.; Proni, J.R.; Fox-Norse, V.; Tomey, D.A. Acoustic Reflector of Opportunity Distribution as a Surrogate for Inferring Effluent Distribution in a Survey of Massachusetts Bay. In Proceedings of the OCEANS 96 MTS/IEEE Conference Proceedings. The Coastal Ocean - Prospects for the 21st Century; IEEE: Fort Lauderdale, FL, USA, 1996; Vol. 1, pp. 313–320.

16. IOCCG Earth Observations in Support of Global Water Quality Monitoring. (Eds. Greb, S., Dekker, A. and Binding, C.) Dartmouth, NS, Canada, International Ocean-Colour Coordinating Group (IOCCG), 125pp. (Reports of the International Ocean-Colour Coordinating Group, No. 17). DOI: Http://Dx.Doi.Org/10.25607/OBP-113 (accessed on 7 November 2023).

17. Brettum, P.; Andersen, T. The Use of Phytoplankton as Indicators of Water Quality; In Norwegian Institute for Water Research SNO Report; NIVA: Oslo, Norway, 2004; p. 33;.

18. Lorenzen, C.J. A Method for the Continuous Measurement of in Vivo Chlorophyll Concentration. Deep Sea Research and Oceanographic Abstracts 1966, 13, 223–227, doi:10.1016/0011-7471(66)91102-8.

19. Cullen, J. The Deep Chlorophyll Maximum: Comparing Vertical Profiles of Chlorophyll a. Can. J. Fish. Aquat. Sci. 1982, 39, 791–803, doi:10.1139/f82-108.

20. Palter, J.; Coto, S.L.; Ballestero, D. The Distribution of Nutrients, Dissolved Oxygen and Chlorophyll a in the Upper Gulf of Nicoya, Costa Rica, a Tropical Estuary. Rev. Biol. Trop. 2007, 55, 427–436.

21. Lavigne, H.; D'Ortenzio, F.; Migon, C.; Claustre, H.; Testor, P.; d'Alcalà, M.R.; Lavezza, R.; Houpert, L.; Prieur, L. Enhancing the Comprehension of Mixed Layer Depth Control on the Mediterranean Phytoplankton Phenology. Journal of Geophysical Research: Oceans 2013, 118, 3416–3430, doi:10.1002/jgrc.20251.

22. Madsen, E.L. Microorganisms and Their Roles in Fundamental Biogeochemical Cycles. Current Opinion in Biotechnology 2011, 22, 456–464, doi:10.1016/j.copbio.2011.01.008.

23. Zhang, Y.; Chen, L.; Sun, R.; Dai, T.; Tian, J.; Liu, R.; Wen, D. Effect of Wastewater Disposal on the Bacterial and Archaeal Community of Sea Sediment in an Industrial Area in China. FEMS Microbiol Ecol 2014, 88, 320–332, doi:10.1111/1574-6941.12298.

24. Bondarczuk, K.; Piotrowska-Seget, Z. Microbial Diversity and Antibiotic Resistance in a Final Effluent-Receiving Lake. Science of The Total Environment 2019, 650, 2951–2961, doi:10.1016/j.scitotenv.2018.10.050.

25. Godoy, R.G.; Marcondes, M.A.; Pessôa, R.; Nascimento, A.; Victor, J.R.; Duarte, A.J.D.S.; Clissa, P.B.; Sanabani, S.S. Bacterial Community Composition and Potential Pathogens along the Pinheiros River in the Southeast of Brazil. Sci Rep 2020, 10, 9331, doi:10.1038/s41598-020-66386-y.

26. Wang, L.; Zhang, J.; Li, H.; Yang, H.; Peng, C.; Peng, Z.; Lu, L. Shift in the Microbial Community Composition of Surface Water and Sediment along an Urban River. Science of The Total Environment 2018, 627, 600–612, doi:10.1016/j.scitotenv.2018.01.203.

27. Narciso-da-Rocha, C.; Manaia, C.M. Multidrug Resistance Phenotypes Are Widespread over Different Bacterial Taxonomic Groups Thriving in Surface Water. Science of The Total Environment 2016, 563–564, 1–9, doi:10.1016/j.scitotenv.2016.04.062.

28. Wang, Z.H.; Yang, J.Q.; Zhang, D.J.; Zhou, J.; Zhang, C.D.; Su, X.R.; Li, T.W. Composition and Structure of Microbial Communities Associated with Different Domestic Sewage Outfalls. Genet. Mol. Res. 2014, 13, 7542–7552, doi:10.4238/2014.September.12.21.

29. Zheng, Y.; Su, Z.; Dai, T.; Li, F.; Huang, B.; Mu, Q.; Feng, C.; Wen, D. Identifying Human-Induced Influence on Microbial Community: A Comparative Study in the Effluent-Receiving Areas in Hangzhou Bay. Front. Environ. Sci. Eng. 2019, 13, 90, doi:10.1007/s11783-019-1174-8.

30. Allison, S.D.; Martiny, J.B.H. Resistance, Resilience, and Redundancy in Microbial Communities. Proceedings of the National Academy of Sciences 2008, 105, 11512–11519, doi:10.1073/pnas.0801925105.

31. Shade, A.; Peter, H.; Allison, S.; Baho, D.; Berga, M.; Buergmann, H.; Huber, D.; Langenheder, S.; Lennon, J.; Martiny, J.; et al. Fundamentals of Microbial Community Resistance and Resilience. Frontiers in Microbiology 2012, 3.

32. Yang, W.; Zheng, C.; Zheng, Z.; Wei, Y.; Lu, K.; Zhu, J. Nutrient Enrichment during Shrimp Cultivation Alters Bacterioplankton Assemblies and Destroys Community Stability. Ecotoxicology and Environmental Safety 2018, 156, 366–374, doi:10.1016/j.ecoenv.2018.03.043.

33. Shen, C.; Xiong, J.; Zhang, H.; Feng, Y.; Lin, X.; Li, X.; Liang, W.; Chu, H. Soil pH Drives the Spatial Distribution of Bacterial Communities along Elevation on Changbai Mountain. Soil Biology and Biochemistry 2013, 57, 204–211, doi:10.1016/j.soilbio.2012.07.013.

34. Miller, S.R.; Strong, A.L.; Jones, K.L.; Ungerer, M.C. Bar-Coded Pyrosequencing Reveals Shared Bacterial Community Properties along the Temperature Gradients of Two Alkaline Hot Springs in Yellowstone National Park. Appl Environ Microbiol 2009, 75, 4565–4572, doi:10.1128/AEM.02792-08.

35. Garneau, M.-È.; Vincent, W.F.; Terrado, R.; Lovejoy, C. Importance of Particle-Associated Bacterial Heterotrophy in a Coastal Arctic Ecosystem. Journal of Marine Systems 2009, 75, 185–197, doi:10.1016/j.jmarsys.2008.09.002.

36. Dang, H.; Lovell, C.R. Microbial Surface Colonization and Biofilm Development in Marine Environments. Microbiol Mol Biol Rev 2016, 80, 91–138, doi:10.1128/MMBR.00037-15.

37. Dai, T.; Zhang, Y.; Tang, Y.; Bai, Y.; Tao, Y.; Huang, B.; Wen, D. Identifying the Key Taxonomic Categories That Characterize Microbial Community Diversity Using Full-Scale Classification: A Case Study of Microbial Communities in the Sediments of Hangzhou Bay. FEMS Microbiol Ecol. 2017, 93, doi:10.1093/femsec/fiw150.

38. Logue, J.B.; Findlay, S.E.G.; Comte, J. Editorial: Microbial Responses to Environmental Changes. Frontiers in Microbiology 2015, 6.

39. Kümmerer, K. Antibiotics in the Aquatic Environment--a Review--Part I. Chemosphere 2009, 75, 417–434, doi:10.1016/j.chemosphere.2008.11.086.

40. D'Costa, V.M.; King, C.E.; Kalan, L.; Morar, M.; Sung, W.W.L.; Schwarz, C.; Froese, D.; Zazula, G.; Calmels, F.; Debruyne, R.; et al. Antibiotic Resistance Is Ancient. Nature 2011, 477, 457–461, doi:10.1038/nature10388.

41. Fleming, A. On the Antibacterial Action of Cultures of a Penicillium, with Special Reference to Their Use in the Isolation of B. Influenzæ. Br J Exp Pathol 1929, 10, 226–236.

42. Levy, S.B. The Antibiotic Paradox: How Miracle Drugs Are Destroying the Miracle; Plenum Press: New York, 1992; ISBN 978-0-306-44331-2.

43. Versporten, A.; Bolokhovets, G.; Ghazaryan, L.; Abilova, V.; Pyshnik, G.; Spasojevic, T.; Korinteli, I.; Raka, L.; Kambaralieva, B.; Cizmovic, L.; et al. Antibiotic Use in Eastern Europe: A Cross-National Database Study in Coordination with the WHO Regional Office for Europe. Lancet Infect Dis 2014, 14, 381–387, doi:10.1016/S1473-3099(14)70071-4.

44. World Health Organization Antimicrobial Resistance: Global Report on Surveillance; World Health Organization: Geneva, 2014; ISBN 978-92-4-156474-8.

45. O'Neill, J. Review on Antimicrobial Resistance; Antimicrobial Resistance: Tackling a Crisis for the Health and Wealth of Nations.; 2014;

46. Murray, C.J.L.; Ikuta, K.S.; Sharara, F.; Swetschinski, L.; Robles Aguilar, G.; Gray, A.; Han, C.; Bisignano, C.; Rao, P.; Wool, E.; et al. Global Burden of Bacterial Antimicrobial Resistance in 2019: A Systematic Analysis. The Lancet 2022, 399, 629–655, doi:10.1016/S0140-6736(21)02724-0.

47. Freire-Moran, L.; Aronsson, B.; Manz, C.; Gyssens, I.C.; So, A.D.; Monnet, D.L.; Cars, O. Critical Shortage of New Antibiotics in Development against Multidrug-Resistant Bacteria—Time to React Is Now. Drug Resistance Updates 2011, 14, 118–124, doi:10.1016/j.drup.2011.02.003.

48. Ekwanzala, M.D.; Dewar, J.B.; Kamika, I.; Momba, M.N.B. Tracking the Environmental Dissemination of Carbapenem-Resistant Klebsiella Pneumoniae Using Whole Genome Sequencing. Science of The Total Environment 2019, 691, 80–92, doi:10.1016/j.scitotenv.2019.06.533.

49. Ekwanzala, M.D.; Dewar, J.B.; Kamika, I.; Momba, M.N.B. Comparative Genomics of Vancomycin-Resistant Enterococcus Spp. Revealed Common Resistome Determinants from Hospital Wastewater to Aquatic Environments. Science of The Total Environment 2020, 719, 137275, doi:10.1016/j.scitotenv.2020.137275.

50. Griffin, D.; Banks, K.; Gregg, K.; Shedler, S.; Walker, B. Antibiotic Resistance in Marine Microbial Communities Proximal to a Florida Sewage Outfall System. Antibiotics 2020, 9, 118, doi:10.3390/antibiotics9030118.

51. Zheng, D.; Yin, G.; Liu, M.; Chen, C.; Jiang, Y.; Hou, L.; Zheng, Y. A Systematic Review of Antibiotics and Antibiotic Resistance Genes in Estuarine and Coastal Environments. Sci Total Environ 2021, 777, 146009, doi:10.1016/j.scitotenv.2021.146009.

52. Yin, X.; Deng, Y.; Ma, L.; Wang, Y.; Chan, L.Y.L.; Zhang, T. Exploration of the Antibiotic Resistome in a Wastewater Treatment Plant by a Nine-Year Longitudinal Metagenomic Study. Environment International 2019, 133, 105270, doi:10.1016/j.envint.2019.105270.

53. Pazda, M.; Kumirska, J.; Stepnowski, P.; Mulkiewicz, E. Antibiotic Resistance Genes Identified in Wastewater Treatment Plant Systems – A Review. Science of The Total Environment 2019, 697, 134023, doi:10.1016/j.scitotenv.2019.134023.

54. Soler, N.; Forterre, P. Vesiduction: The Fourth Way of HGT. Environmental Microbiology 2020, 22, 2457–2460, doi:10.1111/1462-2920.15056.

55. Hocquet, D.; Muller, A.; Bertrand, X. What Happens in Hospitals Does Not Stay in Hospitals: Antibiotic-Resistant Bacteria in Hospital Wastewater Systems. Journal of Hospital Infection 2016, 93, 395–402, doi:10.1016/j.jhin.2016.01.010.

56. Harris, S.; Morris, C.; Morris, D.; Cormican, M.; Cummins, E. Antimicrobial Resistant Escherichia Coli in the Municipal Wastewater System: Effect of Hospital Effluent and Environmental Fate. Science of The Total Environment 2014, 468–469, 1078–1085, doi:10.1016/j.scitotenv.2013.09.017.

57. Manaia, C.M.; Rocha, J.; Scaccia, N.; Marano, R.; Radu, E.; Biancullo, F.; Cerqueira, F.; Fortunato, G.; Iakovides, I.C.; Zammit, I.; et al. Antibiotic Resistance in Wastewater Treatment Plants: Tackling the Black Box. Environ Int 2018, 115, 312–324, doi:10.1016/j.envint.2018.03.044.

58. Ju, F.; Beck, K.; Yin, X.; Maccagnan, A.; McArdell, C.S.; Singer, H.P.; Johnson, D.R.; Zhang, T.; Bürgmann, H. Wastewater Treatment Plant Resistomes Are Shaped by Bacterial Composition, Genetic Exchange, and Upregulated Expression in the Effluent Microbiomes. ISME J 2019, 13, 346–360, doi:10.1038/s41396-018-0277-8.

59. Marano, R.B.M.; Fernandes, T.; Manaia, C.M.; Nunes, O.; Morrison, D.; Berendonk, T.U.; Kreuzinger, N.; Tenson, T.; Corno, G.; Fatta-Kassinos, D.; et al. A Global Multinational Survey of Cefotaxime-Resistant Coliforms in Urban Wastewater Treatment Plants. Environ Int 2020, 144, 106035, doi:10.1016/j.envint.2020.106035.

60. Lee, J.; Ju, F.; Maile-Moskowitz, A.; Beck, K.; Maccagnan, A.; McArdell, C.S.; Dal Molin, M.; Fenicia, F.; Vikesland, P.J.; Pruden, A.; et al. Unraveling the Riverine Antibiotic Resistome: The Downstream Fate of Anthropogenic Inputs. Water Research 2021, 197, 117050, doi:10.1016/j.watres.2021.117050.

61. Rodriguez-Mozaz, S.; Chamorro, S.; Marti, E.; Huerta, B.; Gros, M.; Sànchez-Melsió, A.; Borrego, C.M.; Barceló, D.; Balcázar, J.L. Occurrence of Antibiotics and Antibiotic Resistance Genes in Hospital and Urban Wastewaters and Their Impact on the Receiving River. Water Res 2015, 69, 234–242, doi:10.1016/j.watres.2014.11.021.

62. Pei, M.; Zhang, B.; He, Y.; Su, J.; Gin, K.; Lev, O.; Shen, G.; Hu, S. State of the Art of Tertiary Treatment Technologies for Controlling Antibiotic Resistance in Wastewater Treatment Plants. Environment International 2019, 131, 105026, doi:10.1016/j.envint.2019.105026.

63. EU Directive 2006/7/EC of the European Parliament and of the Council of 15 February 2006 Concerning the Management of Bathing Water Quality and Repealing Directive 76/160/EEC 2006.

64. Vlada Republike Hrvatske Uredba o Kakvoći Mora Za Kupanje (73/08); 2008;

65. Nocker, A.; Burr, M.; Camper, A.K. Genotypic Microbial Community Profiling: A Critical Technical Review. Microb Ecol 2007, 54, 276–289, doi:10.1007/s00248-006-9199-5.

66. Dinsdale, E.A.; Edwards, R.A.; Hall, D.; Angly, F.; Breitbart, M.; Brulc, J.M.; Furlan, M.; Desnues, C.; Haynes, M.; Li, L.; et al. Functional Metagenomic Profiling of Nine Biomes. Nature 2008, 452, 629–632, doi:10.1038/nature06810.

67. Fresia, P.; Antelo, V.; Salazar, C.; Giménez, M.; D'Alessandro, B.; Afshinnekoo, E.; Mason, C.; Gonnet, G.H.; Iraola, G. City-Wide Metagenomics Uncover Antibiotic Resistance Reservoirs in Urban Beach and Sewage Waters; Genomics, 2018;

68. Nowrotek, M.; Jałowiecki, Ł.; Harnisz, M.; Płaza, G.A. Culturomics and Metagenomics: In Understanding of Environmental Resistome. Front. Environ. Sci. Eng. 2019, 13, 40, doi:10.1007/s11783-019-1121-8.

69. Lagier, J.-C.; Armougom, F.; Million, M.; Hugon, P.; Pagnier, I.; Robert, C.; Bittar, F.; Fournous, G.; Gimenez, G.; Maraninchi, M.; et al. Microbial Culturomics: Paradigm Shift in the Human Gut Microbiome Study. Clinical Microbiology and Infection 2012, 18, 1185–1193, doi:10.1111/1469-0691.12023.

70. Cui, Q.; Huang, Y.; Wang, H.; Fang, T. Diversity and Abundance of Bacterial Pathogens in Urban Rivers Impacted by Domestic Sewage. Environmental Pollution 2019, 249, 24–35, doi:10.1016/j.envpol.2019.02.094.

71. Ranjan, R.; Rani, A.; Metwally, A.; McGee, H.S.; Perkins, D.L. Analysis of the Microbiome: Advantages of Whole Genome Shotgun versus 16S Amplicon Sequencing. Biochemical and Biophysical Research Communications 2016, 469, 967–977, doi:10.1016/j.bbrc.2015.12.083.

72. Suenaga, H. Targeted Metagenomics: A High-Resolution Metagenomics Approach for Specific Gene Clusters in Complex Microbial Communities. Environmental Microbiology 2012, 14, 13–22, doi:10.1111/j.1462-2920.2011.02438.x.

73. Gahlot, P.; Alley, K.D.; Arora, S.; Das, S.; Nag, A.; Tyagi, V.K. Wastewater Surveillance Could Serve as a Pandemic Early Warning System for COVID-19 and Beyond. WIREs Water 2023, 10, e1650, doi:10.1002/wat2.1650.

74. Costello, E.K.; Lauber, C.L.; Hamady, M.; Fierer, N.; Gordon, J.I.; Knight, R. Bacterial Community Variation in Human Body Habitats across Space and Time. Science 2009, 326, 1694–1697, doi:10.1126/science.1177486.

75. Arumugam, M.; Raes, J.; Pelletier, E.; Le Paslier, D.; Yamada, T.; Mende, D.R.; Fernandes, G.R.; Tap, J.; Bruls, T.; Batto, J.-M.; et al. Enterotypes of the Human Gut Microbiome. Nature 2011, 473, 174–180, doi:10.1038/nature09944.

76. Lozupone, C.; Knight, R. UniFrac: A New Phylogenetic Method for Comparing Microbial Communities. Appl Environ Microbiol 2005, 71, 8228–8235, doi:10.1128/AEM.71.12.8228-8235.2005.

77. Schloss, P.D.; Westcott, S.L.; Ryabin, T.; Hall, J.R.; Hartmann, M.; Hollister, E.B.; Lesniewski, R.A.; Oakley, B.B.; Parks, D.H.; Robinson, C.J.; et al. Introducing Mothur: Open-Source, Platform-Independent, Community-Supported Software for Describing and Comparing Microbial Communities. Appl Environ Microbiol 2009, 75, 7537–7541, doi:10.1128/AEM.01541-09.

78. Caporaso, J.G.; Kuczynski, J.; Stombaugh, J.; Bittinger, K.; Bushman, F.D.; Costello, E.K.; Fierer, N.; Peña, A.G.; Goodrich, J.K.; Gordon, J.I.; et al. QIIME Allows Analysis of High-Throughput Community Sequencing Data. Nat Methods 2010, 7, 335–336, doi:10.1038/nmeth.f.303.

79. Human Microbiome Jumpstart Reference Strains Consortium; Nelson, K.E.; Weinstock, G.M.; Highlander, S.K.; Worley, K.C.; Creasy, H.H.; Wortman, J.R.; Rusch, D.B.; Mitreva, M.; Sodergren, E.; et al. A Catalog of Reference Genomes from the Human Microbiome. Science 2010, 328, 994–999, doi:10.1126/science.1183605.

80. Janecko, N.; Martz, S.-L.; Avery, B.P.; Daignault, D.; Desruisseau, A.; Boyd, D.; Irwin, R.J.; Mulvey, M.R.; Reid-Smith, R.J. Carbapenem-Resistant Enterobacter Spp. in Retail Seafood Imported from Southeast Asia to Canada. Emerg. Infect. Dis. 2016, 22, 1675–1677, doi:10.3201/eid2209.160305.

81. Logan, L.K.; Weinstein, R.A. The Epidemiology of Carbapenem-Resistant Enterobacteriaceae: The Impact and Evolution of a Global Menace. The Journal of Infectious Diseases 2017, 215, S28–S36, doi:10.1093/infdis/jiw282.

82. Potter, R.F.; D'Souza, A.W.; Dantas, G. The Rapid Spread of Carbapenem-Resistant Enterobacteriaceae. Drug Resistance Updates 2016, 29, 30–46, doi:10.1016/j.drup.2016.09.002.

83. Peleg, A.Y.; Hooper, D.C. Hospital-Acquired Infections Due to Gram-Negative Bacteria. N Engl J Med 2010, 362, 1804–1813, doi:10.1056/NEJMra0904124.

84. Xu, Z.-Q.; Flavin, M.T.; Flavin, J. Combating Multidrug-Resistant Gram-Negative Bacterial Infections. Expert Opin Investig Drugs 2014, 23, 163–182, doi:10.1517/13543784.2014.848853.

85. Meletis, G. Carbapenem Resistance: Overview of the Problem and Future Perspectives. Ther Adv Infect Dis 2016, 3, 15–21, doi:10.1177/2049936115621709.

86. Bonomo, R.A.; Burd, E.M.; Conly, J.; Limbago, B.M.; Poirel, L.; Segre, J.A.; Westblade, L.F. Carbapenemase-Producing Organisms: A Global Scourge. Clin Infect Dis 2018, 66, 1290–1297, doi:10.1093/cid/cix893.

87. Brolund, A.; Lagerqvist, N.; Byfors, S.; Struelens, M.J.; Monnet, D.L.; Albiger, B.; Kohlenberg, A.; European Antimicrobial Resistance Genes Surveillance Network (EURGen-Net) capacity survey group Worsening Epidemiological Situation of Carbapenemase-Producing Enterobacteriaceae in Europe, Assessment by National Experts from 37 Countries, July 2018. Euro Surveill 2019, 24, 1900123, doi:10.2807/1560-7917.ES.2019.24.9.1900123.

88. Bush, K.; Jacoby, G.A.; Medeiros, A.A. A Functional Classification Scheme for β-Lactamases and Its Correlation with Molecular Structure. 1995, 39.

89. Walsh, T.R. Clinically Significant Carbapenemases: An Update: Current Opinion in Infectious Diseases 2008, 21, 367–371, doi:10.1097/QCO.0b013e328303670b.

90. Schwaber, M.J.; Carmeli, Y. Carbapenem-Resistant Enterobacteriaceae: A Potential Threat. JAMA 2008, 300, 2911–2913, doi:10.1001/jama.2008.896.

91. Chang-Seop, L.; Yohei, D. Therapy of Infections Due to Carbapenem-Resistant Gram-Negative Pathogens. Infec t Chemother 2014, 46, 149–164, doi:http://dx.doi.org/10.3947/ic.2014.46.3.149.

92. Naas, T.; Nordmann, P. Analysis of a Carbapenem-Hydrolyzing Class A Beta-Lactamase from Enterobacter Cloacae and of Its LysR-Type Regulatory Protein. Proc Natl Acad Sci U S A 1994, 91, 7693–7697, doi:10.1073/pnas.91.16.7693.

93. van Duin, D.; Doi, Y. The Global Epidemiology of Carbapenemase-Producing Enterobacteriaceae. Virulence 2017, 8, 460–469, doi:10.1080/21505594.2016.1222343.

94. Galvin, S.; Boyle, F.; Hickey, P.; Vellinga, A.; Morris, D.; Cormican, M. Enumeration and Characterization of Antimicrobial-Resistant Escherichia Coli Bacteria in Effluent from Municipal, Hospital, and Secondary Treatment Facility Sources. Appl Environ Microbiol 2010, 76, 4772–4779, doi:10.1128/AEM.02898-09.

95. Ferreira da Silva, M.; Vaz-Moreira, I.; Gonzalez-Pajuelo, M.; Nunes, O.C.; Manaia, C.M. Antimicrobial Resistance Patterns in Enterobacteriaceae Isolated from an Urban Wastewater Treatment Plant. FEMS Microbiol Ecol 2007, 60, 166–176, doi:10.1111/j.1574-6941.2006.00268.x.

96. Martins da Costa, P.; Vaz-Pires, P.; Bernardo, F. Antimicrobial Resistance in Enterococcus Spp. Isolated in Inflow, Effluent and Sludge from Municipal Sewage Water Treatment Plants. Water Res 2006, 40, 1735–1740, doi:10.1016/j.watres.2006.02.025.

97. Mahon, B.M.; Brehony, C.; McGrath, E.; Killeen, J.; Cormican, M.; Hickey, P.; Keane, S.; Hanahoe, B.; Dolan, A.; Morris, D. Indistinguishable NDM-Producing Escherichia Coli Isolated from Recreational Waters, Sewage, and a Clinical Specimen in Ireland, 2016 to 2017. Euro Surveill 2017, 22, 30513, doi:10.2807/1560-7917.ES.2017.22.15.30513.

98. Mahon, B.M.; Brehony, C.; Cahill, N.; McGrath, E.; O'Connor, L.; Varley, A.; Cormican, M.; Ryan, S.; Hickey, P.; Keane, S.; et al. Detection of OXA-48-like-Producing Enterobacterales in Irish Recreational Water. Sci Total Environ 2019, 690, 1–6, doi:10.1016/j.scitotenv.2019.06.480.

99. Bleichenbacher, S.; Stevens, M.J.A.; Zurfluh, K.; Perreten, V.; Endimiani, A.; Stephan, R.; Nüesch-Inderbinen, M. Environmental Dissemination of Carbapenemase-Producing Enterobacteriaceae in Rivers in Switzerland. Environ Pollut 2020, 265, 115081, doi:10.1016/j.envpol.2020.115081.

100. Nordmann, P.; Naas, T.; Poirel, L. Global Spread of Carbapenemase-Producing Enterobacteriaceae. Emerg. Infect. Dis. 2011, 17, 1791–1798, doi:10.3201/eid1710.110655.

101. Jelic, M.; Butic, I.; Plecko, V.; Cipris, I.; Jajic, I.; Bejuk, D.; Koscak, I.; Marinkovic, S.; Pal, M.P.; Andrasevic, A.T. KPC-Producing Klebsiella Pneumoniae Isolates in Croatia: A Nationwide Survey. Microbial Drug Resistance 2016, 22, 662–667, doi:10.1089/mdr.2015.0150.

102. Bedenić, B.; Sardelić, S.; Bogdanić, M.; Zarfel, G.; Beader, N.; Šuto, S.; Krilanović, M.; Vraneš, J. Klebsiella Pneumoniae Carbapenemase (KPC) in Urinary Infection Isolates. Arch Microbiol 2021, 203, 1825–1831, doi:10.1007/s00203-020-02161-x.

103. Zujić Atalić, V.; Bedenić, B.; Kocsis, E.; Mazzariol, A.; Sardelić, S.; Barišić, M.; Plečko, V.; Bošnjak, Z.; Mijač, M.; Jajić, I.; et al. Diversity of Carbapenemases in Clinical Isolates of Enterobacteriaceae in Croatia—the Results of a Multicentre Study. Clinical Microbiology and Infection 2014, 20, O894–O903, doi:10.1111/1469-0691.12635.

104. Novak, A.; Goic-Barisic, I.; Andrasevic, A.T.; Butic, I.; Radic, M.; Jelic, M.; Rubic, Z.; Tonkic, M. Monoclonal Outbreak of VIM-1-Carbapenemase-Producing Enterobacter Cloacae in Intensive Care Unit, University Hospital Centre Split, Croatia. Microbial Drug Resistance 2014, 20, 399–403, doi:10.1089/mdr.2013.0203.

105. Jelić, M.; Hrenović, J.; Dekić, S.; Goić-Barišić, I.; Tambić Andrašević, A. First Evidence of KPC-Producing ST258 Klebsiella Pneumoniae in River Water. J Hosp Infect 2019, 103, 147–150, doi:10.1016/j.jhin.2019.04.001.

106. Dželalija, M.; Kvesić Ivanković, M.; Jozić, S.; Ordulj, M.; Kalinić, H.; Pavlinović, A.; Šamanić, I.; Maravic, A. Marine Resistome of a Temperate Zone: Distribution, Diversity, and Driving Factors across the Trophic Gradient. Water Research 2023.

107. Hrvatske vode Plan Upravljanja Vodnim Područjima Do 2027.; 2023;

108. Šantić, D.; Stojan, I.; Matić, F.; Trumbić, Ž.; Vrdoljak Tomaš, A.; Fredotović, Ž.; Piwosz, K.; Lepen Pleić, I.; Šestanović, S.; Šolić, M. Picoplankton Diversity in an Oligotrophic and High Salinity Environment in the Central Adriatic Sea | Scientific Reports. Sci Rep 2023, 13, doi:https://doi.org/10.1038/s41598-023-34704-9.

109. Do, T.T.; Delaney, S.; Walsh, F. 16S rRNA Gene Based Bacterial Community Structure of Wastewater Treatment Plant Effluents. FEMS Microbiol Lett 2019, 366, fnz017, doi:10.1093/femsle/fnz017.

110. Tiwari, A.; Hokajärvi, A.-M.; Domingo, J.S.; Elk, M.; Jayaprakash, B.; Ryu, H.; Siponen, S.; Vepsäläinen, A.; Kauppinen, A.; Puurunen, O.; et al. Bacterial Diversity and Predicted Enzymatic Function in a Multipurpose Surface Water System – from Wastewater Effluent Discharges to Drinking Water Production. Environmental Microbiome 2021, 16, 11, doi:10.1186/s40793-021-00379-w.

111. McLellan, S.L.; Huse, S.M.; Mueller-Spitz, S.R.; Andreishcheva, E.N.; Sogin, M.L. Diversity and Population Structure of Sewage-Derived Microorganisms in Wastewater Treatment Plant Influent. Environmental Microbiology 2010, 12, 378–392, doi:10.1111/j.1462-2920.2009.02075.x.

112. Freitas, S.; Hatosy, S.; Fuhrman, J.A.; Huse, S.M.; Mark Welch, D.B.; Sogin, M.L.; Martiny, A.C. Global Distribution and Diversity of Marine Verrucomicrobia. ISME J 2012, 6, 1499–1505, doi:10.1038/ismej.2012.3.

113. Korlević, M.; Markovski, M.; Herndl, G.J.; Najdek, M. Temporal Variation in the Prokaryotic Community of a Nearshore Marine Environment. Sci Rep 2022, 12, 16859, doi:10.1038/s41598-022-20954-6.

114. Li, D.; Liu, C.-M.; Luo, R.; Sadakane, K.; Lam, T.-W. MEGAHIT: An Ultra-Fast Single-Node Solution for Large and Complex Metagenomics Assembly via Succinct de Bruijn Graph. Bioinformatics 2015, 31, 1674–1676, doi:10.1093/bioinformatics/btv033.

115. Li, H.; Durbin, R. Fast and Accurate Short Read Alignment with Burrows-Wheeler Transform. Bioinformatics 2009, 25, 1754–1760, doi:10.1093/bioinformatics/btp324.

116. Hyatt, D.; Chen, G.-L.; LoCascio, P.F.; Land, M.L.; Larimer, F.W.; Hauser, L.J. Prodigal: Prokaryotic Gene Recognition and Translation Initiation Site Identification. BMC Bioinformatics 2010, 11, 119, doi:10.1186/1471-2105-11-119.

117. Buchfink, B.; Xie, C.; Huson, D.H. Fast and Sensitive Protein Alignment Using DIAMOND. Nat Methods 2015, 12, 59–60, doi:10.1038/nmeth.3176.

118. Espinoza, J.L.; Dupont, C.L. VEBA: A Modular End-to-End Suite for in Silico Recovery, Clustering, and Analysis of Prokaryotic, Microeukaryotic, and Viral Genomes from Metagenomes. BMC Bioinformatics 2022, 23, 419, doi:10.1186/s12859-022-04973-8.

119. Feldgarden, M.; Brover, V.; Gonzalez-Escalona, N.; Frye, J.G.; Haendiges, J.; Haft, D.H.; Hoffmann, M.; Pettengill, J.B.; Prasad, A.B.; Tillman, G.E.; et al. AMRFinderPlus and the Reference Gene Catalog Facilitate Examination of the Genomic Links among Antimicrobial Resistance, Stress Response, and Virulence. Sci Rep 2021, 11, 12728, doi:10.1038/s41598-021-91456-0.

120. McMurdie, P.J.; Holmes, S. Phyloseq: An R Package for Reproducible Interactive Analysis and Graphics of Microbiome Census Data. PLOS ONE 2013, 8, e61217, doi:10.1371/journal.pone.0061217.

121. Osunmakinde, C.O.; Selvarajan, R.; Mamba, B.; Msagati, T.A.M. Viral Communities Distribution and Diversity in a Wastewater Treatment Plants Using High-Throughput Sequencing Analysis. Pol. J. Environ. Stud. 2021, 30, 3189–3201, doi:10.15244/pjoes/127888.

122. Kvesić, M.; Kalinić, H.; Dželalija, M.; Šamanić, I.; Andričević, R.; Maravić, A. Microbiome and Antibiotic Resistance Profiling in Submarine Effluent-Receiving Coastal Waters in Croatia. Environ Pollut 2022, 292, 118282, doi:10.1016/j.envpol.2021.118282.

123. Jantharadej, K.; Kongprajug, A.; Mhuantong, W.; Limpiyakorn, T.; Suwannasilp, B.B.; Mongkolsuk, S.; Sirikanchana, K. Comparative Genomic Analyses of Pathogenic Bacteria and Viruses and Antimicrobial Resistance Genes in an Urban Transportation Canal. Science of The Total Environment 2022, 848, 157652, doi:10.1016/j.scitotenv.2022.157652.

124. Manoharan, R.K.; Srinivasan, S.; Shanmugam, G.; Ahn, Y.-H. Shotgun Metagenomic Analysis Reveals the Prevalence of Antibiotic Resistance Genes and Mobile Genetic Elements in Full Scale Hospital Wastewater Treatment Plants. Journal of Environmental Management 2021, 296, 113270, doi:10.1016/j.jenvman.2021.113270.

125. Leroy-Freitas, D.; Machado, E.C.; Torres-Franco, A.F.; Dias, M.F.; Leal, C.D.; Araújo, J.C. Exploring the Microbiome, Antibiotic Resistance Genes, Mobile Genetic Element, and Potential Resistant Pathogens in Municipal Wastewater Treatment Plants in Brazil. Science of The Total Environment 2022, 842, 156773, doi:10.1016/j.scitotenv.2022.156773.

126. Numberger, D.; Ganzert, L.; Zoccarato, L.; Mühldorfer, K.; Sauer, S.; Grossart, H.-P.; Greenwood, A.D. Characterization of Bacterial Communities in Wastewater with Enhanced Taxonomic Resolution by Full-Length 16S rRNA Sequencing. Sci Rep 2019, 9, 9673, doi:10.1038/s41598-019-46015-z.

127. An, X.-L.; Su, J.-Q.; Li, B.; Ouyang, W.-Y.; Zhao, Y.; Chen, Q.-L.; Cui, L.; Chen, H.; Gillings, M.R.; Zhang, T.; et al. Tracking Antibiotic Resistome during Wastewater Treatment Using High Throughput Quantitative PCR. Environ Int 2018, 117, 146–153, doi:10.1016/j.envint.2018.05.011.

128. Calderón-Franco, D.; Corbera-Rubio, F.; Cuesta-Sanz, M.; Pieterse, B.; De Ridder, D.; Van Loosdrecht, M.C.M.; Van Halem, D.; Laureni, M.; Weissbrodt, D.G. Microbiome, Resistome and Mobilome of Chlorine-Free Drinking Water Treatment Systems. Water Research 2023, 235, 119905, doi:10.1016/j.watres.2023.119905.

129. Rose, J.B.; Huffman, D.E.; Riley, K.; Farrah, S.R.; Lukasik, J.O.; Hamann, C.L. Reduction of Enteric Microorganisms at the Upper Occoquan Sewage Authority Water Reclamation Plant. Water Environment Research 2001, 73, 711–720, doi:10.2175/106143001X143457.

130. García-Aljaro, C.; Blanch, A.R.; Campos, C.; Jofre, J.; Lucena, F. Pathogens, Faecal Indicators and Human-specific Microbial Source-tracking Markers in Sewage. Journal of Applied Microbiology 2019, 126, 701–717, doi:10.1111/jam.14112.

131. Cook, K.L.; Rothrock, M.J.; Lovanh, N.; Sorrell, J.K.; Loughrin, J.H. Spatial and Temporal Changes in the Microbial Community in an Anaerobic Swine Waste Treatment Lagoon. Anaerobe 2010, 16, 74–82, doi:10.1016/j.anaerobe.2009.06.003.

132. Su, J.-Q.; An, X.-L.; Li, B.; Chen, Q.-L.; Gillings, M.R.; Chen, H.; Zhang, T.; Zhu, Y.-G. Metagenomics of Urban Sewage Identifies an Extensively Shared Antibiotic Resistome in China. Microbiome 2017, 5, 84, doi:10.1186/s40168-017-0298-y.

133. Sivalingam, P.; Sabatino, R.; Sbaffi, T.; Fontaneto, D.; Corno, G.; Di Cesare, A. Extracellular DNA Includes an Important Fraction of High-Risk Antibiotic Resistance Genes in Treated Wastewaters. Environmental Pollution 2023, 323, 121325, doi:10.1016/j.envpol.2023.121325.

134. Rodríguez, E.A.; Ramirez, D.; Balcázar, J.L.; Jiménez, J.N. Metagenomic Analysis of Urban Wastewater Resistome and Mobilome: A Support for Antimicrobial Resistance Surveillance in an Endemic Country. Environmental Pollution 2021, 276, 116736, doi:10.1016/j.envpol.2021.116736.

135. Ng, C.; Tan, B.; Jiang, X.-T.; Gu, X.; Chen, H.; Schmitz, B.W.; Haller, L.; Charles, F.R.; Zhang, T.; Gin, K. Metagenomic and Resistome Analysis of a Full-Scale Municipal Wastewater Treatment Plant in Singapore Containing Membrane Bioreactors. Front. Microbiol. 2019, 10, 172, doi:10.3389/fmicb.2019.00172.

136. Newton, R.J.; McLellan, S.L.; Dila, D.K.; Vineis, J.H.; Morrison, H.G.; Eren, A.M.; Sogin, M.L. Sewage Reflects the Microbiomes of Human Populations. mBio 2015, 6, e02574, doi:10.1128/mBio.02574-14.

137. European Centre for Disease Prevention and Control Antimicrobial Consumption in the EU/EEA (ESAC-Net)) - Annual Epidemiological Report for 2021; Stockholm: ECDC, 2022;

138. Antimicrobial Resistance: Global Report on Surveillance; World Health Organization, Ed.; World Health Organization: Geneva, Switzerland, 2014; ISBN 978-92-4-156474-8.

139. Dželalija, M.; Kvesić, M.; Novak, A.; Fredotović, Ž.; Kalinić, H.; Šamanić, I.; Ordulj, M.; Jozić, S.; Goić Barišić, I.; Tonkić, M.; et al. Microbiome Profiling and Characterization of Virulent and Vancomycin-Resistant Enterococcus Faecium from Treated and Untreated Wastewater, Beach Water and Clinical Sources. Science of The Total Environment 2023, 858, 159720, doi:10.1016/j.scitotenv.2022.159720.

140. Elabed, H.; González-Tortuero, E.; Ibacache-Quiroga, C.; Bakhrouf, A.; Johnston, P.; Gaddour, K.; Blázquez, J.; Rodríguez-Rojas, A. Seawater Salt-Trapped Pseudomonas Aeruginosa Survives for Years and Gets Primed for Salinity Tolerance. BMC Microbiology 2019, 19, 142, doi:10.1186/s12866-019-1499-2.

141. Lewenza, S.; Abboud, J.; Poon, K.; Kobryn, M.; Humplik, I.; Bell, J.R.; Mardan, L.; Reckseidler-Zenteno, S. Pseudomonas Aeruginosa Displays a Dormancy Phenotype during Long-Term Survival in Water. PLoS One 2018, 13, e0198384, doi:10.1371/journal.pone.0198384.

142. Bebrone, C. Metallo-Beta-Lactamases (Classification, Activity, Genetic Organization, Structure, Zinc Coordination) and Their Superfamily. Biochem Pharmacol 2007, 74, 1686–1701, doi:10.1016/j.bcp.2007.05.021.

143. Sekizuka, T.; Itokawa, K.; Tanaka, R.; Hashino, M.; Yatsu, K.; Kuroda, M. Metagenomic Analysis of Urban Wastewater Treatment Plant Effluents in Tokyo. Infect Drug Resist 2022, 15, 4763–4777, doi:10.2147/IDR.S370669.

144. Milaković, M.; Križanović, S.; Petrić, I.; Šimatović, A.; González-Plaza, J.J.; Gužvinec, M.; Andrašević, A.T.; Pole, L.; Fuka, M.M.; Udiković-Kolić, N. Characterization of Macrolide Resistance in Bacteria Isolated from Macrolide-Polluted and Unpolluted River Sediments and Clinical Sources in Croatia. Sci Total Environ 2020, 749, 142357, doi:10.1016/j.scitotenv.2020.142357.

145. Hou, L.; Zhang, L.; Li, F.; Huang, S.; Yang, J.; Ma, C.; Zhang, D.; Yu, C.-P.; Hu, A. Urban Ponds as Hotspots of Antibiotic Resistome in the Urban Environment. Journal of Hazardous Materials 2021, 403, 124008, doi:10.1016/j.jhazmat.2020.124008.

146. Rajasekar, A.; Vadde, K.K.; Murava, R.T.; Qiu, M.; Guo, S.; Yu, T.; Wang, R.; Zhao, C. Occurrence of Antibiotic Resistance Genes and Potentially Pathogenic Bacteria in the Yangtze River Tributary (Nanjing Section) and Their Correlation with Environmental Factors. Environ. Res. Commun. 2023, 5, 035001, doi:10.1088/2515-7620/acbd8c.

147. Chi, T.; Zhang, A.; Zhang, X.; Li, A.-D.; Zhang, H.; Zhao, Z. Characteristics of the Antibiotic Resistance Genes in the Soil of Medical Waste Disposal Sites. Science of The Total Environment 2020, 730, 139042, doi:10.1016/j.scitotenv.2020.139042.

148. Zong, G.; Zhong, C.; Fu, J.; Zhang, Y.; Zhang, P.; Zhang, W.; Xu, Y.; Cao, G.; Zhang, R. The Carbapenem Resistance Gene blaOXA-23 Is Disseminated by a Conjugative Plasmid Containing the Novel Transposon Tn6681 in Acinetobacter Johnsonii M19. Antimicrobial Resistance & Infection Control 2020, 9, 182, doi:10.1186/s13756-020-00832-4.

149. Šamanić, I.; Kalinić, H.; Fredotović, Ž.; Dželalija, M.; Bungur, A.-M.; Maravić, A. Bacteria Tolerant to Colistin in Coastal Marine Environment: Detection, Microbiome Diversity and Antibiotic Resistance Genes' Repertoire. Chemosphere 2021, 281, 130945, doi:10.1016/j.chemosphere.2021.130945.

150. Anyanwu, M.U.; Okpala, C.O.R.; Chah, K.F.; Shoyinka, V.S. Prevalence and Traits of Mobile Colistin Resistance Gene Harbouring Isolates from Different Ecosystems in Africa. BioMed Research International 2021, 2021, e6630379, doi:10.1155/2021/6630379.

151. Mmatli, M.; Mbelle, N.M.; Osei Sekyere, J. Global Epidemiology, Genetic Environment, Risk Factors and Therapeutic Prospects of Mcr Genes: A Current and Emerging Update. Front Cell Infect Microbiol 2022, 12, 941358, doi:10.3389/fcimb.2022.941358.

7. SUPPLEMENTAL MATERIAL

7.1. Supplemental material to Paper II

Fig. S1. The locations of sampling sites (WWTPs effluents of Stobreč and Katalinića Brig) in the coastal area of Split, central Adriatic Sea

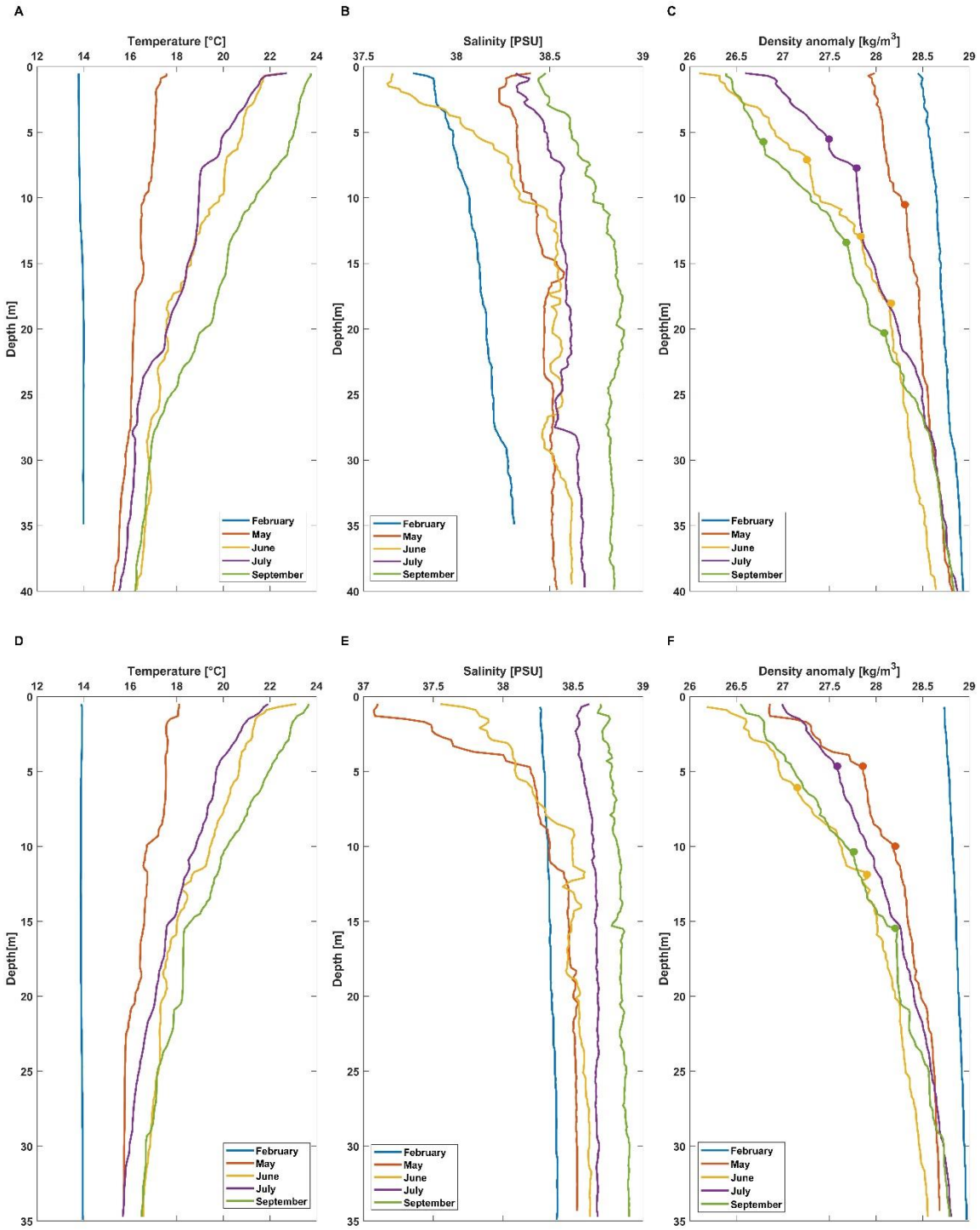

Fig. S2. Vertical profiles of temperature (A), salinity (B) and density anomaly (C) sampled at the Katalinića Brig location and at the Stobreč outfall (temperature (D), salinity (E) and density anomaly (F)) during the sampling period. Pycnocline depth is marked with a colored dot corresponding to the line for each month.

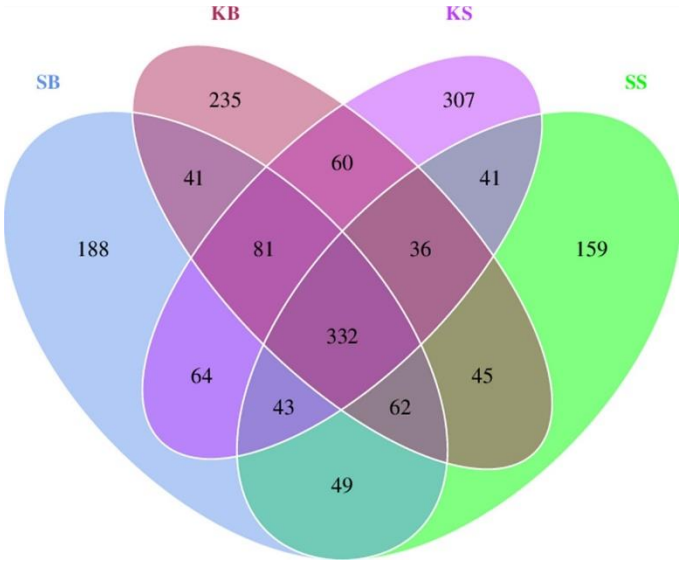

Fig. S3. Venn diagram based on OTUs diversity with values in overlapping parts representing OTUs common to more than one microbiome.

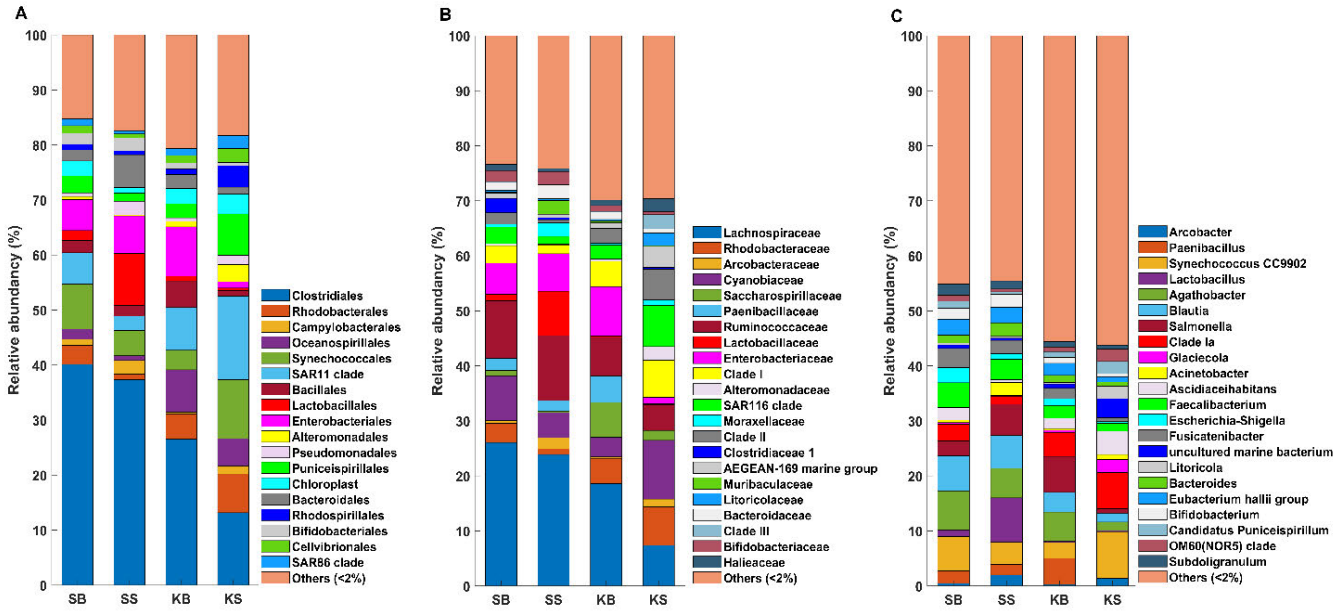

Fig. S4. Relative abundance (%) of bacterial taxa at order (A), family (B) and genus (C) levels in the studied samples. The abundance is expressed as the percentage of the individual taxa in the total number of reads.

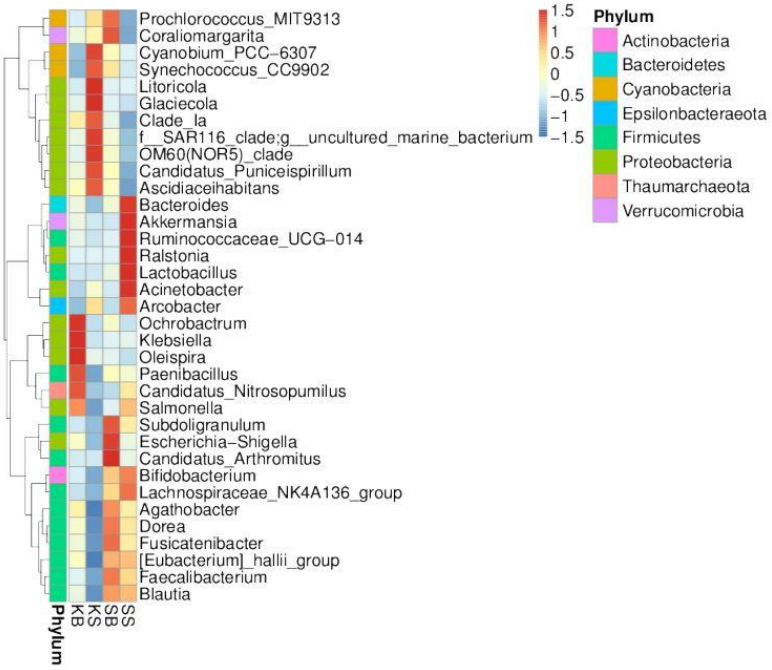

Fig. S5. Taxonomic abundance cluster heatmap plotted by sample name and the 35 most common genera. The absolute 'z' value represents the distance between the raw score and the mean of the standard deviation. 'Z' is negative when the raw score is below the mean, and *vice versa*.

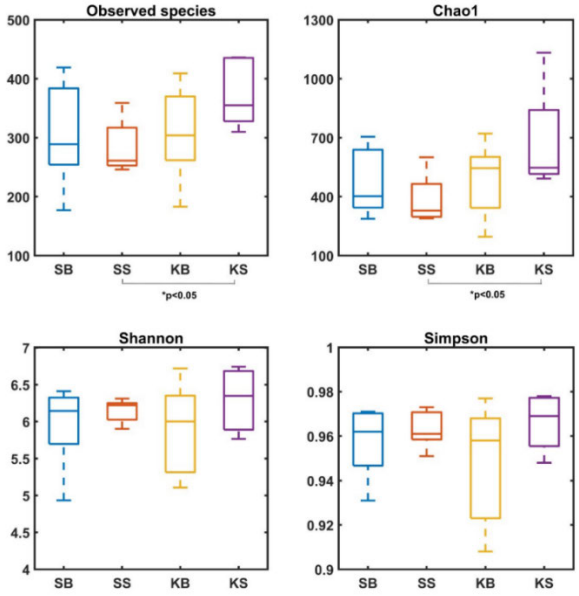

Fig. S6. Boxplots representing alpha diversity by community richness (observed species and Chao1 indices) and diversity (Shannon and Simpson indices) between bacterial communities at two effluent-receiving sites. SB (orange), SS (green), KB (blue), KS (purple). Alpha indices that were significantly different between groups ($p < 0.05$) are marked with an asterisk.

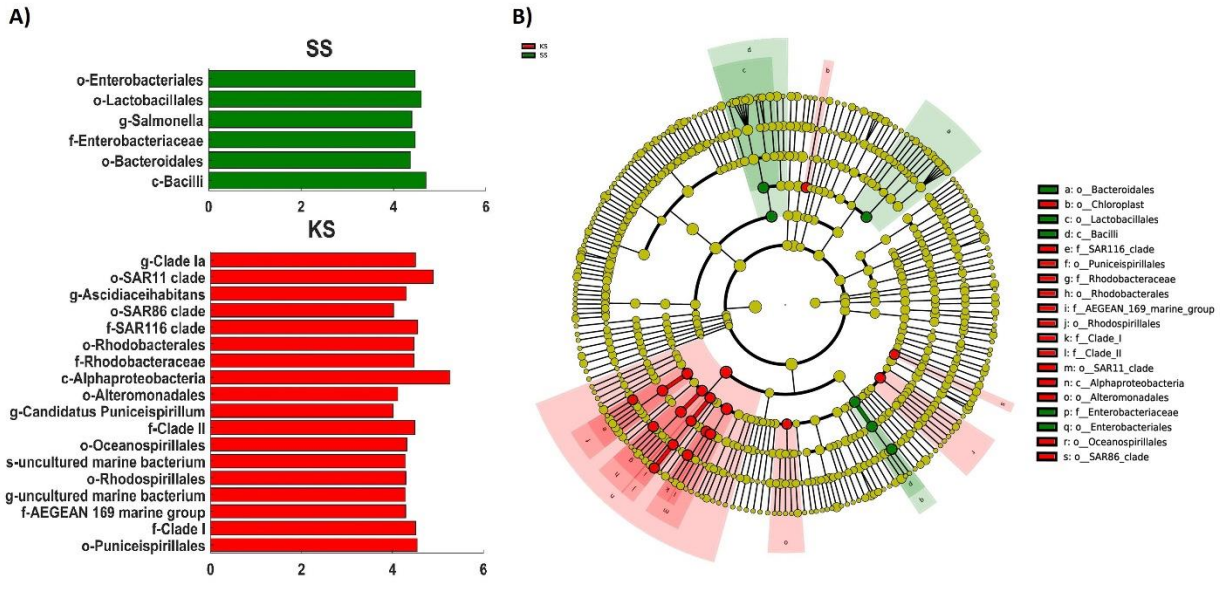

Fig. S7. Histogram of the LDA scores (A) and cladogram (B) showing the phylogenetic distribution of the microbial communities associated with SS and KS with LDA values of 2.0 or higher as determined by LEfSe. Red indicates KS and green indicates SS; yellow represents insignificant difference. The diameter of each circle is proportional to a taxon's abundance. Circles from inner region to outer region represent the phylogenetic levels from class to genus.

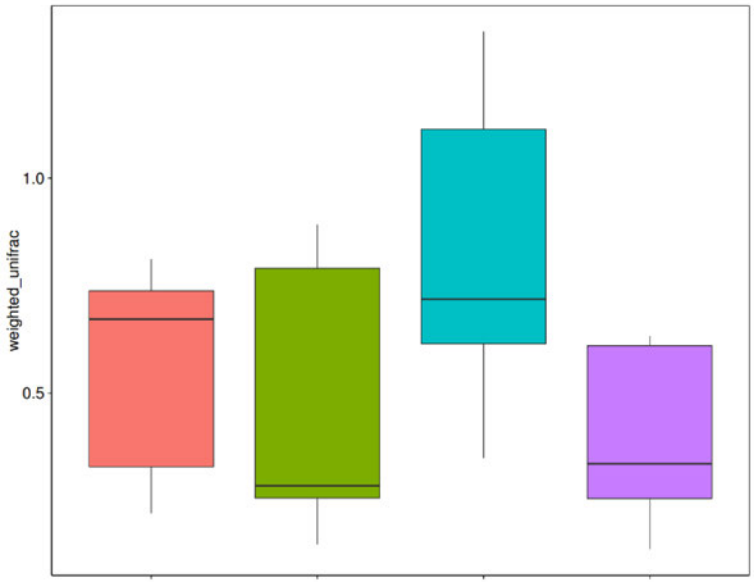

Fig. S8. Weighted UniFrac beta-diversity indices were statistically significant (p<0.05, Wilcox test) in case of KS and KB. SB (orange), SS (green), KB (blue), KS (purple)

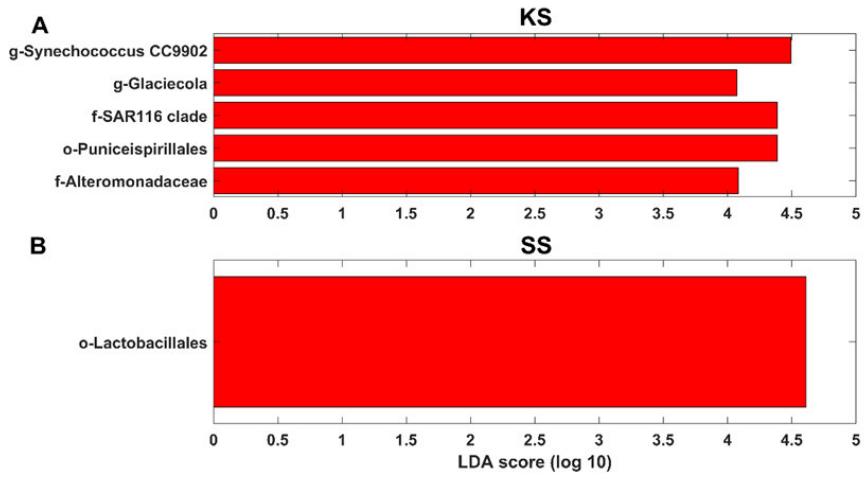

Fig. S9. Indicators of microbial taxa enriched in KS and SS, in comparison to KB and SB, with LDA values higher than 2.0.

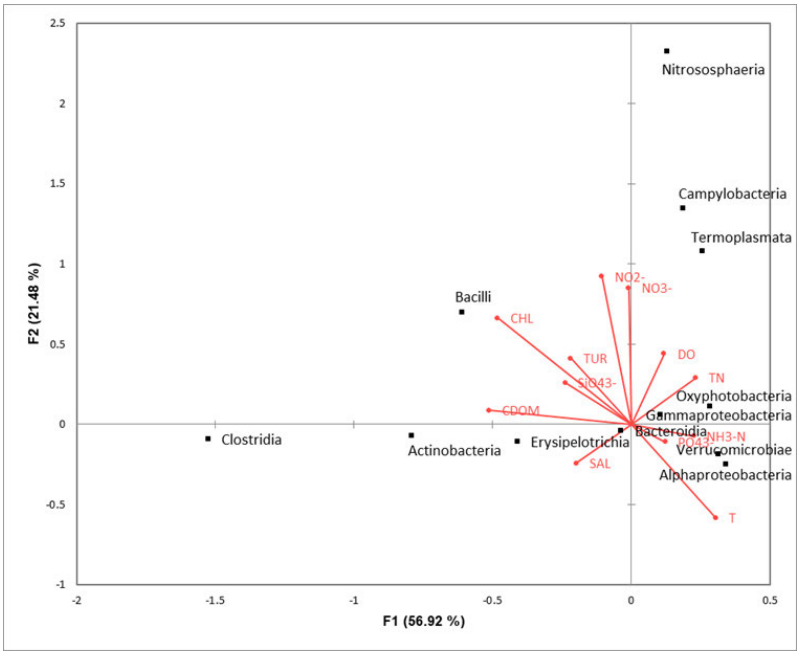

Fig. S10. Canonical correspondence analysis (CCA) plot relates the abundance of bacterial classes to environmental variables. T: temperature; SAL: salinity; CHL: chlorophyll a; TUR: turbidity; CDOM: colored dissolved organic matter; PO_4^{3-}: phosphate anions; NH_4^+: ammonium cation; NO_3^-: nitrate anions; NO_2^-: nitrite anions; SiO_4^{3-}: silicate anions.

Table S1. Physico-chemical parameters of seawater samples at submarine outfalls: Stobreč(bottom and surface, SB and SS) and Katalinića Brig (bottom and surface, KB and KS)

DATE	SITE	T [°C]	SAL [PSU]	SIGMA [kg/m^3]	DO [mg/l]	CHL a [ug/l]	CDOM [ppb]	TUR [NTU]	NO_3^- [umol/L]	NO_2^- [umol/L]	NH_4^+ [umol/L]	TN [umol/L]	PO_4^{3-} [umol/L]
02/2020	SB	13.96	38.39	28.97	8.46	0.49	0.00	0.60	1.12	0.29	0.04	5.88	0.08
02/2020	SS	13.90	38.01	28.73	8.28	0.45	0.10	0.60	1.08	0.28	0.09	8.40	0.19
02/2020	KB	13.99	38.32	28.93	8.52	0.52	0.00	0.50	0.91	0.24	0.03	6.93	0.11
02/2020	KS	13.79	37.84	28.45	8.70	0.34	0.01	0.50	1.01	0.17	0.04	6.77	0.13
05/2020	SB	15.72	38.53	28.68	8.59	0.22	0.01	0.50	0.17	0.02	0.05	5.58	0.13
05/2020	SS	18.10	37.10	26.86	8.28	0.17	0.00	0.40	0.34	0.01	0.15	5.11	0.08
05/2020	KB	15.27	38.54	28.82	8.00	0.37	0.14	0.70	0.63	0.08	0.53	6.00	0.12
05/2020	KS	17.57	38.30	27.99	8.51	0.14	0.00	0.40	0.48	0.01	0.16	10.65	0.13
06/2020	SB	16.57	38.62	28.56	7.67	0.34	0.04	0.60	0.04	0.01	0.05	6.15	0.17
06/2020	SS	23.12	37.72	26.18	7.53	0.10	0.00	0.30	0.04	0.02	0.04	7.83	0.09
06/2020	KB	16.28	38.62	28.64	7.38	0.46	0.14	0.90	0.15	0.07	0.06	5.11	0.12
06/2020	KS	22.50	37.65	26.10	7.43	0.13	0.00	0.40	0.03	0.02	0.04	5.20	0.38
07/2020	SB	15.69	38.68	28.81	7.85	0.37	0.34	0.50	0.13	0.05	0.05	5.78	0.19
07/2020	SS	21.92	38.62	26.99	8.25	0.11	0.00	0.20	0.29	0.02	0.01	5.62	0.11
07/2020	KB	15.57	38.69	28.87	8.07	0.28	0.19	0.50	0.12	0.02	0.02	5.24	0.12
07/2020	KS	22.72	38.34	26.84	7.79	0.06	0.00	0.40	0.09	0.01	0.17	7.82	0.22
09/2020	SB	16.50	38.90	28.79	7.95	0.17	0.30	0.48	0.03	0.04	0.03	6.95	0.08
09/2020	SS	23.67	38.70	26.54	7.98	0.16	0.00	0.27	0.10	0.04	0.01	10.72	0.07
09/2020	KB	16.23	38.84	28.84	7.88	0.28	0.27	0.46	0.08	0.06	0.01	7.38	0.10
09/2020	KS	23.76	38.46	26.39	7.85	0.09	0.00	0.29	0.09	0.03	0.09	9.63	0.10

Abbreviations: T: temperature; SAL: salinity; Sigma: density anomaly; CHL: chlorophyll a; CDOM: color dissolved organic matter; TUR: turbidity; PO43-: phosphate anions; NH4+: ammonium cation; NO3-: nitrate anions; NO2-: nitrite anions; SiO43-: silicate anions

Table S2. Results of analysis of similarities (ANOSIM) and multi-response permutation procedure (MRPP) analysis evaluating the variation among and within bacterial communities from WWTP effluents Stupe (bottom and surface, SB and SS) and Katalinića Brig (bottom and surface, KB and KS)

ANOSIM			MRPP			
Group	R-value	P-value	A	observed-delta	expected-delta	Significance
SB-SS	-0.052	0.566	-0.01314	0.6933	0.6843	0.422
KB-SS	-0.034	0.455	-0.004446	0.7154	0.7123	0.378
KB-SB	-0.148	0.897	-0.04571	0.7583	0.7251	0.91
KS-SS	0.428[a]	0.03[b]	0.1342[c]	0.617	0.7127	0.013[d]
KS-SB	0.136[a]	0.124	0.03692[c]	0.6599	0.6852	0.139
KS-KB	0.172[a]	0.087	0.03587[c]	0.6821	0.7074	0.149

[a] Inter-group variation is considered significant.

[b, d] Statistically significant (p -value <0.05)

[c] Variations among groups are larger than variation within groups.

Table S3. PICRUSt

	h4	h5	h6	SB.6	SS.6	KB.6	KS.6	SB.5	SS.5	KB.5	KS.5	SB.9	SS.9	KB.9	KS.9	SB.7	SS.7	KB.7	KS.7	SB.2	SS.2	KB.2	KS.2	stat_SBvsSS	p_SBvsSS	stat_KBvsKS	p_KBvsKS	stat_SBvsKB	p_SBvsKB	stat_SSvsKS	p_SSvsKS	stat_SBvsKS	p_SBvsKS	stat_KBvsSS	p_KBvsSS
0	Gene variants	Aminoglycoside resistance genes	16S rRNA methyltransferases	0.00	0.00	0.00	0.00	0.00	0.00	0.00	0.00	0.00	0.00	0.00	0.00	0.00	0.00	0.00	0.00	0.00	0.00	0.00	0.00	0.77	0.48	-1.01	0.35	1.01	0.37	0.92	0.39	0.91	0.41	-1.74	0.14
1	Gene variants	Phenicol resistance genes	23S rRNA methyltransferase	0.00	0.00	0.00	0.00	0.00	0.00	0.00	0.00	0.00	0.00	0.00	0.00	0.00	0.00	0.00	0.00	0.00	0.00	0.00	0.00	-0.54	0.60	0.60	0.57	0.27	0.80	1.64	0.14	0.93	0.38	-0.81	0.44
2	Gene variants	Macrolide resistance genes	23S rRNA methyltransferases	0.00	0.00	0.00	0.00	0.00	0.00	0.00	0.00	0.00	0.00	0.00	0.00	0.00	0.00	0.00	0.00	0.00	0.00	0.00	0.00	-0.63	0.55	-0.19	0.85	0.55	0.60	0.60	0.57	0.18	0.86	-1.24	0.25
3	Gene variants	Quinolone resistance genes	ADP-ribosyl transferases	0.00	0.00	0.00	0.00	0.00	0.00	0.00	0.00	0.00	0.00	0.00	0.00	0.00	0.00	0.00	0.00	0.00	0.00	0.00	0.00	-0.57	0.60	-0.09	0.93	-0.29	0.79	0.25	0.81	-0.58	0.59	-0.29	0.78
4	Gene variants	Phenicol resistance genes	Acetyltransferases	0.05	0.06	0.05	0.02	0.02	0.04	0.03	0.02	0.02	0.04	0.04	0.01	0.06	0.04	0.01	0.01	0.04	0.01	0.03	0.05	-0.07	0.95	1.02	0.34	0.58	0.58	1.67	0.14	1.58	0.15	-0.65	0.53
5	Gene sets	CAMP resistance modules	Cationic antimicrobial peptide (CAMP) resistance, VraFG transporter [MD:M00730]	0.00	0.00	0.00	0.00	0.00	0.00	0.00	0.00	0.00	0.00	0.00	0.00	0.00	0.00	0.00	0.00	0.00	0.00	0.00	0.01	-0.49	0.64	-1.04	0.36	0.70	0.51	-0.99	0.38	-1.01	0.37	-0.98	0.36
6	Gene sets	CAMP resistance modules	Cationic antimicrobial peptide (CAMP) resistance, dltABCD operon [MD:M00725]	0.04	0.04	0.03	0.01	0.00	0.08	0.01	0.04	0.03	0.07	0.02	0.01	0.04	0.03	0.01	0.01	0.02	0.06	0.01	0.05	-2.46	0.04	-0.77	0.47	1.27	0.25	2.45	0.04	0.26	0.81	-3.86	0.01
7	Gene sets	CAMP resistance modules	Cationic antimicrobial peptide (CAMP) resistance, lysyl-phosphatidylglycerol (L-PG) synthase MprF [MD:M00726]	0.01	0.00	0.00	0.01	0.00	0.02	0.01	0.01	0.01	0.02	0.01	0.01	0.00	0.01	0.01	0.01	0.00	0.00	0.00	0.02	-1.51	0.19	-2.14	0.08	0.01	0.99	0.52	0.62	-1.67	0.13	-1.62	0.17
8	Gene sets	CAMP resistance modules	Cationic antimicrobial peptide (CAMP) resistance, protease PgtE [MD:M00744]	0.02	0.02	0.02	0.04	0.03	0.03	0.03	0.03	0.02	0.03	0.03	0.02	0.01	0.02	0.03	0.02	0.04	0.01	0.04	0.02	0.52	0.62	1.14	0.29	-1.29	0.24	-0.94	0.37	-0.28	0.79	2.27	0.05
9	Gene variants	beta-Lactamase genes	Class A [MT]	0.00	0.00	0.00	0.00	0.00	0.01	0.00	0.00	0.00	0.01	0.00	0.00	0.01	0.01	0.00	0.00	0.01	0.00	0.00	0.01	-1.86	0.12	2.67	0.05	-2.44	0.07	2.34	0.07	0.73	0.49	1.29	0.24
10	Gene variants	beta-Lactamase genes	Class B [MT]	0.00	0.00	0.00	0.00	0.00	0.00	0.00	0.00	0.00	0.00	0.00	0.00	0.00	0.00	0.00	0.00	0.00	0.00	0.00	0.00	0.99	0.38	-0.07	0.95	0.31	0.77	-2.27	0.08	0.30	0.78	1.36	0.25
11	Gene variants	beta-Lactamase genes	Class C [MT]	0.00	0.00	0.00	0.00	0.00	0.00	0.00	0.00	0.00	0.00	0.00	0.00	0.00	0.00	0.00	0.00	0.00	0.00	0.00	0.00	-0.90	0.40	1.15	0.31	-1.13	0.31	0.92	0.40	-0.08	0.94	0.31	0.77
12	Gene variants	beta-Lactamase genes	Class D [MT]	0.00	0.00	0.00	0.00	0.00	0.00	0.00	0.00	0.00	0.00	0.00	0.00	0.00	0.00	0.00	0.00	0.00	0.00	0.00	0.00	-2.45	0.04	1.79	0.14	-1.32	0.25	4.03	0.01	1.18	0.28	0.21	0.84
13	Gene variants	Trimethoprim resistance genes	Dihydrofolate reductases	0.00	0.00	0.00	0.00	0.00	0.00	0.00	0.00	0.00	0.00	0.00	0.00	0.00	0.00	0.00	0.00	0.00	0.00	0.01	0.00	-1.55	0.17	1.47	0.19	-1.57	0.18	1.34	0.22	0.12	0.91	0.42	0.69
14	Gene variants	Sulfonamide resistance genes	Dihydropteroate synthase	0.01	0.01	0.01	0.00	0.00	0.01	0.00	0.00	0.00	0.02	0.02	0.00	0.01	0.01	0.00	0.01	0.01	0.00	0.02	0.01	-1.56	0.17	1.62	0.18	-1.30	0.25	2.14	0.09	0.84	0.44	0.27	0.80
15	Gene sets	beta-Lactam resistance modules	Imipenem resistance, repression of porin OprD [MD:M00745]	0.02	0.01	0.02	0.04	0.05	0.02	0.05	0.04	0.04	0.02	0.03	0.04	0.01	0.04	0.06	0.04	0.03	0.04	0.03	0.03	0.36	0.73	0.33	0.75	-0.84	0.43	-1.15	0.28	-0.66	0.53	1.22	0.26
16	Gene sets	beta-Lactam resistance modules	Methicillin resistance [MD:M00625]	0.00	0.00	0.00	0.00	0.00	0.00	0.00	0.00	0.00	0.00	0.00	0.00	0.00	0.00	0.00	0.00	0.00	0.00	0.00	0.01	-0.10	0.92	-1.06	0.35	1.14	0.29	-0.99	0.38	-1.00	0.38	-0.91	0.40
17	Gene sets	Multidrug resistance modules	Multidrug resistance, efflux pump AbcA [MD:M00700]	0.01	0.00	0.00	0.00	0.00	0.00	0.00	0.00	0.00	0.00	0.00	0.00	0.00	0.00	0.00	0.00	0.00	0.00	0.01	0.01	-0.03	0.97	0.23	0.83	-0.35	0.74	-0.06	0.96	-0.08	0.94	0.32	0.76
18	Gene sets	Multidrug resistance modules	Multidrug resistance, efflux pump AcrEF-TolC [MD:M00696]	0.04	0.04	0.05	0.12	0.11	0.06	0.11	0.09	0.08	0.06	0.07	0.12	0.03	0.05	0.13	0.14	0.08	0.06	0.09	0.04	0.88	0.42	-0.57	0.58	-1.07	0.32	-2.67	0.05	-1.49	0.18	2.46	0.06
19	Gene sets	Multidrug resistance modules	Multidrug resistance, efflux pump AdeABC [PATH:map01501] [MD:M00649]	0.00	0.00	0.00	0.00	0.00	0.00	0.00	0.01	0.01	0.00	0.01	0.00	0.00	0.00	0.00	0.00	0.02	0.00	0.00	0.00	-0.51	0.64	0.05	0.96	-0.53	0.61	0.28	0.79	-0.54	0.61	-0.26	0.81
20	Gene sets	Multidrug resistance modules	Multidrug resistance, efflux pump BpeEF-OprC [MD:M00698]	0.00	0.00	0.00	0.02	0.02	0.00	0.01	0.01	0.01	0.00	0.01	0.01	0.00	0.01	0.01	0.02	0.00	0.02	0.00	0.00	-0.04	0.97	-1.14	0.29	-0.18	0.86	-1.03	0.33	-1.11	0.30	0.12	0.90
21	Gene sets	Multidrug resistance modules	Multidrug resistance, efflux pump MdtEF-TolC [MD:M00697]	0.03	0.02	0.03	0.13	0.12	0.04	0.12	0.10	0.09	0.03	0.04	0.13	0.02	0.03	0.13	0.14	0.06	0.06	0.04	0.03	1.30	0.25	-1.07	0.32	-0.37	0.72	-3.14	0.03	-1.52	0.17	1.61	0.17
22	Gene sets	Multidrug resistance modules	Multidrug resistance, efflux pump MepA [MD:M00705]	0.00	0.00	0.00	0.00	0.00	0.00	0.00	0.00	0.00	0.00	0.00	0.00	0.00	0.00	0.00	0.00	0.00	0.00	0.00	0.00	0.09	0.93	0.69	0.52	-0.46	0.66	0.31	0.77	0.49	0.64	0.49	0.64
23	Gene sets	Multidrug resistance modules	Multidrug resistance, efflux pump MexAB-OprM [MD:M00718]	0.06	0.05	0.06	0.23	0.25	0.08	0.22	0.28	0.21	0.08	0.09	0.23	0.04	0.08	0.29	0.26	0.08	0.32	0.10	0.05	0.10	0.93	-0.94	0.37	-0.43	0.68	-1.39	0.20	-1.41	0.19	0.49	0.64
24	Gene sets	Multidrug resistance modules	Multidrug resistance, efflux pump MexCD-OprJ [MD:M00639]	0.00	0.00	0.00	0.00	0.00	0.00	0.00	0.00	0.00	0.00	0.00	0.00	0.00	0.00	0.00	0.00	0.00	0.00	0.00	0.00	0.44	0.68	-1.39	0.20	-0.13	0.90	-2.09	0.08	-1.66	0.14	0.51	0.63
25	Gene sets	Multidrug resistance modules	Multidrug resistance, efflux pump MexEF-OprN [MD:M00641]	0.00	0.00	0.00	0.01	0.01	0.00	0.01	0.01	0.01	0.00	0.00	0.01	0.00	0.00	0.00	0.01	0.01	0.00	0.00	0.00	1.33	0.25	-0.99	0.35	-0.59	0.57	-3.62	0.02	-1.86	0.10	1.67	0.17
26	Gene sets	Multidrug resistance modules	Multidrug resistance, efflux pump MexJK-OprM [MD:M00642]	0.01	0.01	0.01	0.04	0.04	0.02	0.04	0.06	0.05	0.02	0.02	0.03	0.01	0.02	0.03	0.04	0.01	0.09	0.02	0.01	-0.60	0.57	-1.43	0.20	-0.19	0.85	-0.28	0.79	-1.33	0.22	-0.54	0.62
27	Gene sets	Multidrug resistance modules	Multidrug resistance, efflux pump MexPQ-OprE [MD:M00769]	0.01	0.01	0.01	0.01	0.00	0.02	0.01	0.01	0.00	0.02	0.02	0.01	0.01	0.02	0.01	0.01	0.01	0.03	0.03	0.01	-1.64	0.15	1.93	0.12	-1.65	0.16	2.18	0.09	0.51	0.63	0.52	0.62
28	Gene sets	Multidrug resistance modules	Multidrug resistance, efflux pump MexXY-OprM [MD:M00643]	0.01	0.01	0.01	0.02	0.02	0.02	0.02	0.05	0.03	0.02	0.02	0.02	0.01	0.02	0.02	0.02	0.01	0.07	0.02	0.01	-1.08	0.32	-1.07	0.34	-0.25	0.81	0.35	0.74	-1.04	0.33	-1.05	0.35
29	Gene sets	Multidrug resistance modules	Multidrug resistance, efflux pump NorB [MD:M00702]	0.00	0.00	0.00	0.00	0.00	0.00	0.00	0.00	0.00	0.00	0.00	0.00	0.00	0.00	0.00	0.00	0.00	0.00	0.01	0.00	-0.07	0.95	-0.29	0.78	-1.02	0.35	-0.80	0.46	-0.83	0.45	0.95	0.38
30	Gene sets	Multidrug resistance modules	Multidrug resistance, efflux pump QacA [MD:M00714]	0.01	0.01	0.01	0.01	0.01	0.01	0.01	0.01	0.01	0.01	0.02	0.01	0.01	0.01	0.01	0.01	0.01	0.03	0.01	-1.88	0.10	1.79	0.14	-1.72	0.15	2.24	0.07	0.09	0.93	0.84	0.44
31	Gene sets	Multidrug resistance modules	Multidrug resistance, repression of porin OmpF [MD:M00746]	0.01	0.01	0.02	0.01	0.01	0.02	0.00	0.00	0.00	0.02	0.02	0.00	0.01	0.01	0.01	0.00	0.01	0.00	0.04	0.01	-1.40	0.21	2.09	0.10	-1.40	0.22	2.63	0.04	1.64	0.15	0.49	0.64
32	Gene variants	Aminoglycoside resistance genes	N-Acetyltransferases	0.03	0.02	0.02	0.03	0.02	0.02	0.02	0.02	0.02	0.02	0.02	0.02	0.03	0.02	0.02	0.02	0.01	0.04	0.02	0.32	0.76	1.17	0.29	-1.03	0.35	-0.04	0.97	0.29	0.78	1.18	0.28
33	Gene variants	Aminoglycoside resistance genes	O-Nucleotidyltransferases	0.04	0.04	0.04	0.01	0.01	0.04	0.02	0.01	0.01	0.04	0.04	0.01	0.04	0.04	0.01	0.01	0.04	0.01	0.04	0.04	-0.36	0.73	1.51	0.17	0.15	0.89	2.09	0.07	1.75	0.12	-0.49	0.64
34	Gene variants	Aminoglycoside resistance genes	O-Phosphotransferases	0.03	0.02	0.04	0.02	0.02	0.02	0.02	0.01	0.01	0.03	0.03	0.02	0.04	0.03	0.01	0.01	0.02	0.01	0.03	0.02	0.51	0.62	2.13	0.08	-0.41	0.69	1.19	0.28	1.82	0.12	0.89	0.40
35	Gene variants	Quinolone resistance genes	Other	0.00	0.00	0.00	0.01	0.01	0.00	0.01	0.00	0.00	0.00	0.00	0.00	0.00	0.00	0.00	0.01	0.00	0.00	0.00	0.00	0.94	0.39	-0.40	0.70	-0.08	0.94	-2.18	0.07	-0.37	0.72	1.57	0.17
36	Gene variants	Aminoglycoside resistance genes	Other acetyltransferases	0.00	0.00	0.00	0.00	0.00	0.00	0.00	0.00	0.00	0.00	0.00	0.00	0.00	0.00	0.00	0.00	0.00	0.00	0.00	0.00	0.62	0.56	0.71	0.51	-0.17	0.87	0.11	0.92	0.65	0.54	0.68	0.53
37	Gene variants	Phenicol resistance genes	Others	0.06	0.07	0.06	0.02	0.02	0.05	0.03	0.03	0.03	0.05	0.05	0.02	0.08	0.05	0.01	0.01	0.05	0.02	0.04	0.07	-0.08	0.94	0.68	0.52	0.78	0.46	1.45	0.19	1.29	0.23	-0.93	0.38
38	Gene variants	Phenicol resistance genes	Phosphotransferase	0.00	0.00	0.00	0.00	0.00	0.00	0.00	0.00	0.00	0.00	0.00	0.00	0.00	0.00	0.00	0.01	0.00	0.00	0.00	0.01	-0.26	0.81	0.83	0.45	-0.55	0.61	0.74	0.50	0.93	0.39	0.35	0.74
39	Gene sets	Vancomycin resistance modules	Tetracycline resistance, efflux pump Tet38 [MD:M00704]	0.01	0.00	0.00	0.00	0.00	0.00	0.00	0.00	0.00	0.00	0.00	0.00	0.00	0.00	0.01	0.00	0.00	0.00	0.01	0.01	0.05	0.96	0.38	0.72	-0.12	0.91	0.31	0.76	0.35	0.74	0.16	0.88
40	Gene variants	Quinolone resistance genes	Transporter	0.01	0.01	0.01	0.01	0.01	0.01	0.01	0.01	0.01	0.01	0.02	0.01	0.01	0.01	0.01	0.01	0.01	0.01	0.03	0.01	-1.88	0.10	1.79	0.14	-1.72	0.15	2.24	0.06	0.09	0.93	0.85	0.44
41	Gene variants	Quinolone resistance genes	Transporters	0.10	0.09	0.09	0.05	0.05	0.09	0.06	0.04	0.04	0.08	0.09	0.05	0.09	0.09	0.03	0.04	0.08	0.03	0.09	0.09	-0.26	0.80	1.18	0.28	0.06	0.96	1.50	0.18	1.30	0.23	-0.31	0.77
42	Gene sets	Vancomycin resistance modules	Vancomycin resistance, D-Ala-D-Lac type [MD:M00651]	0.18	0.19	0.17	0.07	0.09	0.13	0.09	0.06	0.16	0.14	0.12	0.13	0.19	0.14	0.08	0.08	0.18	0.08	0.08	0.18	1.03	0.33	0.20	0.84	2.11	0.07	1.09	0.31	2.00	0.08	-1.04	0.33
43	Gene sets	Vancomycin resistance modules	Vancomycin resistance, D-Ala-D-Ser type [MD:M00652]	0.12	0.14	0.12	0.01	0.00	0.09	0.02	0.02	0.03	0.08	0.08	0.01	0.16	0.10	0.00	0.01	0.10	0.00	0.03	0.12	0.11	0.91	0.61	0.56	0.84	0.43	1.50	0.17	1.38	0.21	-0.87	0.41
44	Gene sets	beta-Lactam resistance modules	beta-Lactam resistance, Bla system [MD:M00627]	0.08	0.08	0.07	0.04	0.04	0.06	0.03	0.03	0.06	0.06	0.06	0.06	0.11	0.08	0.04	0.05	0.05	0.04	0.03	0.08	0.35	0.74	-0.37	0.72	1.52	0.17	1.18	0.27	1.24	0.26	-1.55	0.16

h6	SB	SS	KB	KS	avg	avg*100 (%)
ADP-ribosyl transferases	0.001342229	0.001623039	0.001446958	0.001486454	0.00147467	0.147467001
Acetyltransferases	0.036832739	0.037536826	0.030911291	0.021517864	0.03169968	3.169967984
VraFG transporter	0.000251372	0.000306535	0.000171207	0.002939252	0.000917092	0.091709152
dltABCD operon	0.027018209	0.055880038	0.016331228	0.024057014	0.030821622	3.082162228
lysyl-phosphatidylglycerol (L-PG) synthase MprF	0.00541115	0.01158994	0.005387239	0.009437595	0.007956481	0.795648092
protease PgtE	0.022481244	0.019387717	0.030375753	0.024247784	0.024123125	2.412312455
Class A	0.002252081	0.004136278	0.006730991	0.001891764	0.003752779	0.375277867
Class B	0.000788467	0.000123782	0.000556001	0.000581753	0.000512501	0.051250083
Class C	0.0001799	0.000297554	0.000353645	0.000185848	0.000254237	0.025423662
Class D	0.001319883	0.002479593	0.002705788	0.000889434	0.001848675	0.184867463
Dihydrofolate reductases	0.001457877	0.002452775	0.002893114	0.001382149	0.002046479	0.204647883
Dihydropteroate synthase	0.006125511	0.010195775	0.011424358	0.005064495	0.008202535	0.820253488
Imipenem resistance, repression of porin OprD	0.027474768	0.024135991	0.036509284	0.03329835	0.030354598	3.035459827
Methicillin resistance	0.000206904	0.000220837	0.000107258	0.001832217	0.000591804	0.059180384
AbcA	0.002988691	0.00304596	0.003894927	0.003184482	0.003278515	0.327851523
AcrEF-TolC	0.068704083	0.054457257	0.091101018	0.104207054	0.079617353	7.961735296
AdeABC	0.00244	0.004666247	0.003514679	0.003423486	0.003511103	0.351110299
BpeEF-OprC	0.006874798	0.007087075	0.007636009	0.01226429	0.008465543	0.8465543
MdtEF-TolC	0.061207689	0.03476614	0.071874535	0.104273032	0.068030349	6.803034888
MepA	0.000334035	0.00030423	0.000605177	0.000205293	0.000362184	0.036218397
MexAB-OprM	0.127009013	0.120835282	0.153058435	0.208901989	0.15245118	15.24511799
MexCD-OprJ	0.000408128	0.00025167	0.000463581	0.001150779	0.00056854	0.056853965
MexEF-OprN	0.002903268	0.000780739	0.00449564	0.007271262	0.003862727	0.38627273
MexJK-OprM	0.022033512	0.032431813	0.023760085	0.037393704	0.028904779	2.89047786
MexPQ-OpmE	0.008220534	0.014245997	0.017434764	0.007202127	0.011775855	1.177585534
MexXY-OprM	0.016546445	0.029761695	0.017942367	0.025252785	0.022375823	2.237582305
NorB	0.001547211	0.001576409	0.002263197	0.002697599	0.002021104	0.202110424
QacA	0.008078168	0.011180356	0.014270761	0.007970031	0.010374829	1.037482904
repression of porin OmpF	0.008811087	0.0140996	0.017326298	0.004966068	0.011300763	1.13007632
N-Acetyltransferases	0.020964709	0.020004378	0.025756344	0.020135602	0.021715258	2.171525827
O-Nucleotidyltransferases	0.0299335	0.033340925	0.02847499	0.014508119	0.026564384	2.656438355
O-Phosphotransferases	0.024552221	0.021909598	0.026836898	0.016975348	0.022568516	2.256851643
Other	0.002533946	0.000825704	0.002688746	0.003282774	0.002332792	0.233279241
Other acetyltransferases	0.000274431	0.000201947	0.000306526	0.000194228	0.000244283	0.024428318
Others	0.047271576	0.048307619	0.037541667	0.02922992	0.040587696	4.058769572
Phosphotransferase	0.001859922	0.002195908	0.003030235	0.001305046	0.002097778	0.209777771
Tetracycline resistance, efflux pump Tet38	0.003489989	0.003393747	0.003813737	0.002683234	0.003345177	0.334517684
Transporter	0.008078073	0.011164182	0.014270393	0.007967346	0.010369998	1.036999818
Transporters	0.072000073	0.07647995	0.071094601	0.053980284	0.068388727	6.838872704
Vancomycin resistance, D-Ala-D-Lac type	0.160461379	0.133907208	0.108643111	0.103063231	0.126518732	12.65187322
Vancomycin resistance, D-Ala-D-Ser type	0.08343058	0.07933171	0.052300592	0.03327916	0.06208551	6.208551032
beta-Lactam resistance, Bla system	0.070650547	0.065374999	0.047391736	0.051761329	0.058794653	5.879465269

Table S4_KEGG BRITE ARGs

	Aminoglycoside resistance genes	CAMP resistance modules	Macrolide resistance genes	Multipdrug resistance modules	Phenicol resistance genes	Quinolone resistance genes	Sulfonamide resistance genes	Tetracycline resistance genes	Vancomycin resistance modules	beta-Lactam resistance modules	beta-Lactamase genes
g__Acinetobacter-SS	0.09	0.00	0.09	1.54	0.09	0.09	0.00	0.00	0.00	0.18	0.00
g__Acinetobacter-KS	0.72	0.00	0.90	15.81	0.90	0.72	0.00	0.00	0.00	1.80	0.00
g__Acinetobacter-SB	1.92	0.00	2.17	40.15	2.25	1.94	0.00	0.00	0.00	4.54	0.15
g__Acinetobacter-KB	0.09	0.00	0.09	1.80	0.09	0.09	0.00	0.00	0.00	0.19	0.00
g__Arcobacter-SS	0.00	0.00	0.00	0.00	0.00	0.00	0.00	0.00	0.00	0.00	0.00
g__Arcobacter-KS	0.00	2.73	0.00	16.50	0.00	0.00	0.00	0.00	0.00	0.00	0.00
g__Arcobacter-SB	0.00	9.50	0.00	57.22	0.00	0.00	0.00	0.00	0.00	0.00	0.00
g__Arcobacter-KB	0.00	0.19	0.00	1.14	0.00	0.00	0.00	0.00	0.00	0.00	0.00
g__Bacteroides-SS	0.00	0.00	1.84	25.41	1.90	0.00	0.00	0.55	1.49	1.67	0.03
g__Bacteroides-KS	0.00	0.00	0.33	2.68	0.37	0.00	0.00	0.20	0.24	0.25	0.01
g__Bacteroides-SB	0.00	0.00	0.63	6.29	0.70	0.00	0.00	0.41	0.57	0.68	0.01
g__Bacteroides-KB	0.00	0.00	0.98	13.84	1.17	0.00	0.00	0.55	0.95	1.00	0.01
g__Bifidobacterium-SS	0.37	0.00	1.13	1.36	0.00	0.00	0.00	2.19	1.43	0.00	0.37
g__Bifidobacterium-KS	0.00	0.00	0.02	0.05	0.00	0.00	0.00	0.05	0.04	0.00	0.00
g__Bifidobacterium-SB	0.00	0.00	0.08	0.25	0.00	0.00	0.00	0.20	0.16	0.00	0.00
g__Bifidobacterium-KB	0.05	0.00	0.62	1.42	0.00	0.00	0.00	1.38	1.04	0.00	0.05
g__Clostridium_sensu_stricto_1-SS	0.18	0.05	0.02	0.00	0.00	0.00	0.00	0.03	0.76	0.20	0.00
g__Clostridium_sensu_stricto_1-KS	0.04	0.00	0.00	0.00	0.00	0.00	0.00	0.00	0.14	0.04	0.00
g__Clostridium_sensu_stricto_1-SB	0.00	0.00	0.00	0.00	0.00	0.00	0.00	0.00	0.00	0.00	0.00
g__Clostridium_sensu_stricto_1-KB	0.00	0.01	0.00	0.00	0.00	0.00	0.00	0.01	0.01	0.00	0.00
g__Escherichia-Shigella-SS	0.00	0.97	0.48	10.18	0.00	0.00	0.00	0.00	0.00	0.00	0.00
g__Escherichia-Shigella-KS	0.00	0.00	0.00	0.00	0.00	0.00	0.00	0.00	0.00	0.00	0.00
g__Escherichia-Shigella-SB	0.00	0.05	0.03	0.53	0.00	0.00	0.00	0.00	0.00	0.00	0.00
g__Escherichia-Shigella-KB	0.00	3.26	1.63	34.22	0.00	0.00	0.00	0.00	0.00	0.00	0.00
g__Helicobacter-SS	0.09	0.00	0.00	0.73	0.00	0.00	0.00	0.00	0.00	0.00	0.00
g__Helicobacter-KS	0.00	0.00	0.00	0.00	0.00	0.00	0.00	0.00	0.00	0.00	0.00
g__Helicobacter-SB	0.00	0.00	0.00	0.00	0.00	0.00	0.00	0.00	0.00	0.00	0.00
g__Helicobacter-KB	0.09	0.00	0.00	0.76	0.00	0.00	0.00	0.00	0.00	0.00	0.00
g__Klebsiella-SS	0.14	0.09	0.09	1.00	0.05	0.09	0.05	0.00	0.00	0.18	0.14
g__Klebsiella-KS	0.00	0.00	0.00	0.00	0.00	0.00	0.00	0.00	0.00	0.00	0.00
g__Klebsiella-SB	0.00	0.00	0.00	0.00	0.00	0.00	0.00	0.00	0.00	0.00	0.00
g__Klebsiella-KB	3.37	2.25	2.25	24.72	1.12	2.25	1.12	0.00	0.00	4.49	3.37
g__Lactobacillus-SS	0.77	111.46	19.31	0.73	0.00	0.00	0.00	0.00	21.44	3.86	0.00
g__Lactobacillus-KS	0.07	0.47	0.14	0.00	0.00	0.00	0.00	0.00	0.04	0.18	0.00
g__Lactobacillus-SB	0.23	0.91	0.00	0.45	0.00	0.00	0.00	0.00	0.00	0.23	0.00
g__Lactobacillus-KB	0.05	1.32	0.09	0.09	0.00	0.00	0.00	0.00	0.19	0.14	0.00
g__Ochrobactrum-SS	0.00	0.00	0.00	0.00	0.00	0.00	0.00	0.00	0.00	0.00	0.00
g__Ochrobactrum-KS	0.00	0.00	0.00	0.00	0.00	0.00	0.00	0.00	0.00	0.00	0.00
g__Ochrobactrum-SB	0.00	0.00	0.00	0.00	0.00	0.00	0.00	0.00	0.00	0.00	0.00
g__Ochrobactrum-KB	0.00	4.30	0.00	30.13	0.00	0.00	0.00	0.00	0.00	0.00	0.00
g__Pseudomonas-SS	0.00	0.00	0.00	0.00	0.00	0.00	0.00	0.00	0.00	0.00	0.00
g__Pseudomonas-KS	2.39	2.53	0.70	34.89	0.70	0.70	0.00	0.70	1.40	12.11	0.00
g__Pseudomonas-SB	0.57	0.91	0.15	9.50	0.15	0.15	0.00	0.15	0.30	3.13	0.00
g__Pseudomonas-KB	0.19	0.28	0.05	2.75	0.05	0.05	0.00	0.05	0.09	0.95	0.00
g__Salmonella-SS	3.41	5.12	1.71	22.19	0.00	1.71	0.00	0.00	1.71	0.00	0.00
g__Salmonella-KS	0.01	0.02	0.01	0.07	0.00	0.01	0.00	0.00	0.01	0.00	0.00
g__Salmonella-SB	0.04	0.06	0.02	0.28	0.00	0.02	0.00	0.00	0.02	0.00	0.00
g__Salmonella-KB	4.23	6.35	2.12	27.51	0.00	2.12	0.00	0.00	2.12	0.00	0.00
g__Staphylococcus-SS	0.00	0.00	0.00	0.00	0.00	0.00	0.00	0.00	0.00	0.00	0.00
g__Staphylococcus-KS	0.00	0.47	0.00	0.18	0.00	0.00	0.00	0.00	0.04	0.11	0.00
g__Staphylococcus-SB	0.00	0.49	0.00	0.19	0.00	0.00	0.00	0.00	0.04	0.11	0.00
g__Staphylococcus-KB	0.00	0.00	0.00	0.00	0.00	0.00	0.00	0.00	0.00	0.00	0.00
g__Streptococcus-SS	0.15	0.83	0.00	0.00	0.00	0.00	0.00	0.05	0.45	0.00	0.00
g__Streptococcus-KS	0.01	0.11	0.00	0.00	0.00	0.00	0.00	0.04	0.04	0.00	0.00
g__Streptococcus-SB	0.11	1.13	0.00	0.00	0.00	0.00	0.00	0.30	0.47	0.00	0.00
g__Streptococcus-KB	0.04	0.28	0.00	0.00	0.00	0.00	0.00	0.05	0.14	0.00	0.00

7.1. Supplemental material to Paper III

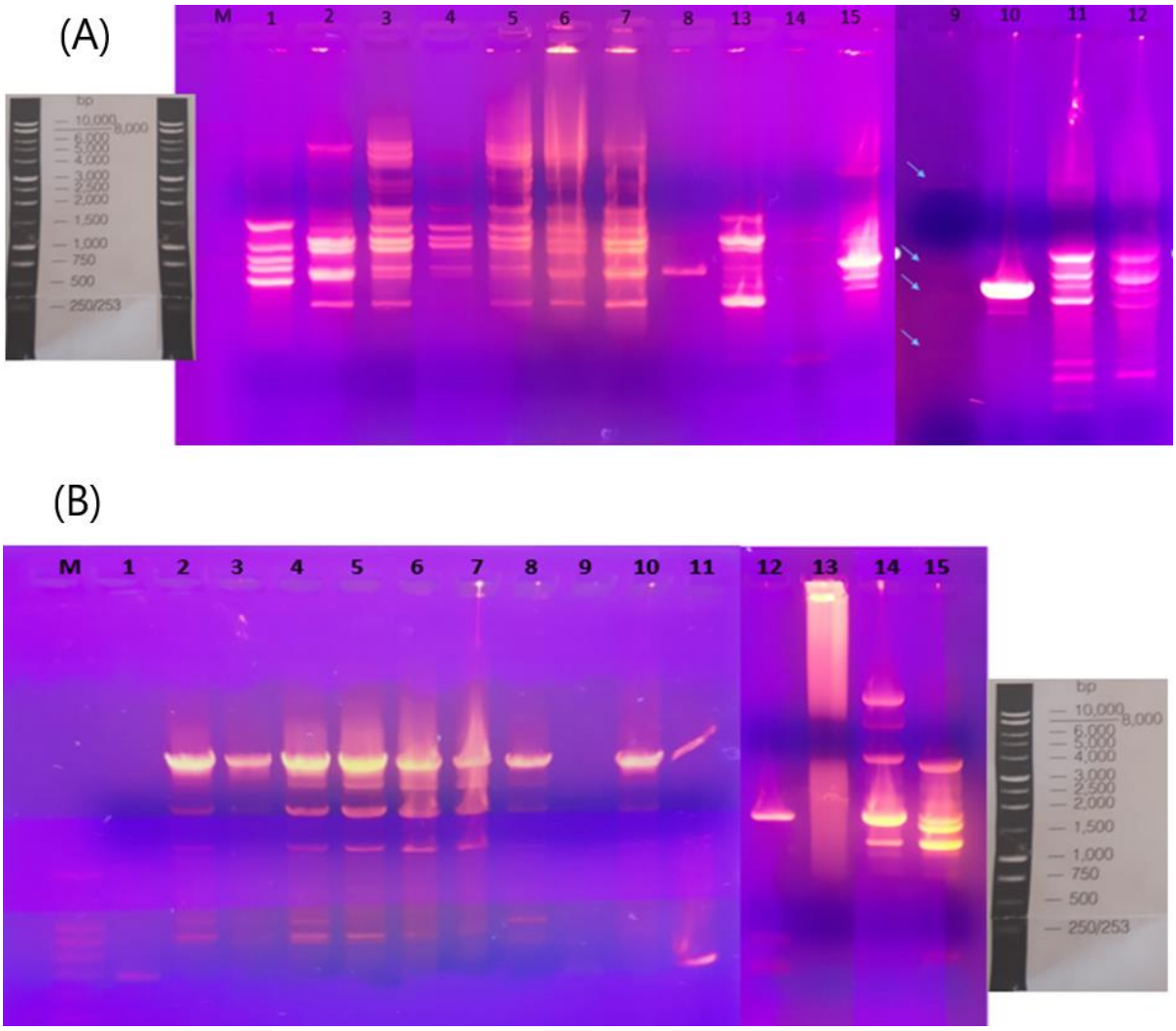

Figure S1. (A) BOX-PCR and (B) ERIC-PCR profiles of KPC-producing *Enterobacteriaceae*: *E. coli* isolates M20 (line 2), M19 (line 3), M16 (line 4), M13 (line 5), M14 (line 6), M15 (line 7), M17 (line 8), M12 (line 10), M18 (line 13); *K. pneumoniae* isolates 5a (line 1), M11 (line 9), C2 (line 11) and C1 (line 12); *C. freundii* isolates CF1 (line 14) and CF2 (line 15). 1 kb DNA ladder (Promega, USA) was used.

M12 E. coli **(Table S1)**

ResFinder 4.1

Resistance gene	Identity (%)	Alignment Length/Gene Length	Coverage (%)	Position in reference	Phenotype	Accession no.
dfrA14	100	474/474	100	1..475	Trimethoprim resistance	KF921535
qnrVC4	100	657/657	100	1..658	Quinolone resistance	GQ891757
cmlA1	99.68	1260/1260	100	1..1261	Phenicol resistance	M64556
mdf(A)	99.92	1233/1233	100	1..1234	Macrolide resistance	Y08743
blaKPC-2	100	882/882	100	1..883	Beta-lactam resistance	AY034847
blaGES-2	100	864/864	100	1..865	Beta-lactam resistance	AF326355
blaOXA-2	100	828/828	100	1..829	Beta-lactam resistance	DQ112222
blaOXA-48	100	798/798	100	1..799	Beta-lactam resistance	AY236073
blaOXA-10	100	801/801	100	1..802	Beta-lactam resistance Alternate name; PSE-2	J03427
ant(3'')-Ii-aac(6')-IId	98.71	1393/1392	99.78	1..1394	Aminoglycoside resistance	AF453998
ant(3'')-Ia	98.97	972/972	99.28	1..973	Aminoglycoside resistance	X02340

PlasmidFinder 2.1

Database	Plasmid	Identity	Query / Template length	Accession number
enterobacteriaceae	Col440I	96.49	114 / 114	CP023920
enterobacteriaceae	IncC	100	417 / 417	JN157804
enterobacteriaceae	IncFIB(K)	99.82	560 / 560	JN233704
enterobacteriaceae	IncL	100	661 / 661	JN626286
enterobacteriaceae	IncP6	99.88	806 / 806	JF785550

MLST 2.0 (Multi-Locus Sequence Typing)

Locus	Identity	Coverage	Alignment Length	Allele Length	Gaps	Allele	ST
adk	100	100	536	536	0	adk_64	2795
fumC	100	100	469	469	0	fumC_4	
gyrB	100	100	460	460	0	gyrB_5	
icd	100	100	518	518	0	icd_1	
mdh	100	100	452	452	0	mdh_8	
purA	100	100	478	478	0	purA_8	
recA	100	100	510	510	0	recA_6	

SerotypeFinder 2.0

Database	Gene	Serotype	Identity	Template / HSP length	Accession number
O_type	wzy	O21	100	1083 / 1083	EU694098
O_type	wzx	O21	100	1236 / 1236	EU694098
H_type	fliC	H27	91.17	1338 / 1461	AM231154

VirulenceFinder 2.0

Database	Virulence factor	Identity	Query / Template length	Protein function	Accession number
virulence_ecoli	*gad*	100	1401 / 1401	Glutamate decarboxylase	AP009240
virulence_ecoli	*gad*	99.93	1401 / 1401	Glutamate decarboxylase	AP010953
virulence_ecoli	*lpfA*	99.83	573 / 573	Long polar fimbriae	AP010953
virulence_ecoli	*lpfA*	91.45	524 / 573	Long polar fimbriae	CP002185
virulence_ecoli	*lpfA*	91.62	559 / 573	Long polar fimbriae	HE616528
virulence_ecoli	*terC*	99.02	714 / 714	Tellurium ion resistance protein	CP007491
virulence_ecoli	*terC*	98.96	966 / 966	Tellurium ion resistance protein	MG591698
virulence_ecoli	*terC*	100	1041 / 1041	Tellurium ion resistance protein	UGAE01000003

Plasmids detected by ARESdb cloud platform

Plasmid	Identity	Query / Template length	Accession number
Col(pHAD28)	91.60%	131 / 131	KU674895
Col(pHAD28)	92.50%	120 / 131	KU674895
Col440I	96.49%	114 / 114	CP023920
IncC	100.00%	417 / 417	JN157804
IncFIB(K)	99.82%	560 / 560	JN233704
IncL	100.00%	661 / 661	JN626286
IncP6	99.88%	806 / 806	JF785550

Virulence Factors detected by ARESdb cloud platform

Marker Class	Marker	Variant(s)	Alignment Length	Sequence Identity	Sequence Coverage
virulence factors	*ydeH*	-	442 aa	98.6%	100%
virulence factors	*ydaM*	-	410 aa	98%	100%
virulence factors	*yafQ*	-	82 aa	98.8%	100%
virulence factors	*soj*	-	261 aa	99.6%	100%
virulence factors	*sfaH*	-	304 aa	97.4%	100%
virulence factors	*potD*	-	348 aa	91.1%	100%
virulence factors	*pemK*	-	110 aa	96.4%	100%
virulence factors	*pemI*	-	85 aa	96.5%	100%
virulence factors	*nagA*	-	139 aa	98.6%	94.6%
virulence factors	*mqsA*	-	131 aa	100%	100%
virulence factors	*mqo*	-	548 aa	99.3%	100%
virulence factors	*manZ*	-	269 aa	98.5%	100%
virulence factors	*manX*	-	144 aa	97.9%	100%
fimbria	*LpfA*	-	190 aa	100%	100%
virulence factors	*ldrD*	-	91 aa	94.5%	100%
virulence factors	*fliZ*	-	108 aa	98.1%	99.1%
virulence factors	*fliZ*	-	62 aa	96.8%	100%
virulence factors	*fliY*	-	266 aa	92.1%	100%
virulence factors	*fliQ*	-	89 aa	93.3%	100%
virulence factors	*fliI*	-	456 aa	95.6%	100%
virulence factors	*fliG*	-	332 aa	96.7%	100%
virulence factors	*fliA*	-	239 aa	99.6%	100%
virulence factors	*flhA*	-	692 aa	94.4%	100%
virulence factors	*fimD*	-	517 aa	98.6%	100%
virulence factors	*fdeC*	-	1416 aa	93.6%	100%
virulence factors	*EspX1*	-	473 aa	91.5%	100%
virulence factors	*epsJ*	-	300 aa	98%	100%
virulence factors	*elfG*	-	357 aa	100%	100%
virulence factors	*cstA*	-	701 aa	92.4%	100%

Antibiotic resistance genes detected by ARESdb cloud platform

Marker Class	Marker	Variant(s)	Alignment Length	Sequence Identity	Sequence Coverage
ABC efflux pump	*YojI*	-	547 aa	100%	100%
putative efflux transport	*yheI*	-	590 aa	98.1%	100%
Vga	*Vga(C)*	-	74 aa	94.6%	97.4%
efflux	*TolC*	-	495 aa	100%	100%
beta-lactamase TEM	*TEM-160*	-	190 aa	98.9%	66.4%
efflux regulation	*SoxR*	R4K	152 aa	93.4%	100%
RND efflux transporter	*SilC*	-	461 aa	99.3%	100%
RND efflux transporter	*SilB*	-	430 aa	99.3%	100%
RND efflux transporter	*SilA*	-	1048 aa	98.8%	100%
target protection	*Rpsl*	-	124 aa	93.5%	100%
regulation of resistance	*rpoS*	-	172 aa	100%	100%
MFS efflux transporter	*RosB*	-	558 aa	91.9%	100%
Qnr	*QnrVC4*	-	218 aa	100%	100%
multidrug efflux SMR transporter	*QacF*	-	110 aa	99.1%	100%
Pmr	*PmrL*	-	660 aa	100%	100%
Pmr	*PmrF*	-	322 aa	100%	100%
Pmr	*PmrE*	-	388 aa	99%	100%
Pmr	*PmrC*	-	480 aa	99.2%	87.8%
efflux regulation	*PhoQ*	-	486 aa	99.4%	100%
ABC efflux pump	*PatA*	-	459 aa	99.8%	100%
DNA topoisomerase subunit	*parC*	T57S	752 aa	94.9%	100%
beta-lactamase OXA	*OXA-48*	-	265 aa	100%	100%
beta-lactamase OXA	*OXA-2*	-	275 aa	100%	100%
beta-lactamase OXA	*OXA-10*	-	266 aa	100%	100%
regulation of resistance	*ompR*	-	239 aa	100%	100%
porin	*OmpC*	-	368 aa	96.5%	100%
ABC efflux pump	*MsrB*	-	137 aa	100%	100%
ABC efflux pump	*MsbA*	-	582 aa	100%	100%
macrolide phosphotransferase	*Mph(B)*	-	157 aa	98.1%	99.4%
compensation mechanism	*MgrB*	-	46 aa	100%	97.9%
regulation of resistance	*MerR*	-	144 aa	100%	100%
MFS efflux transporter	*MdtP*	-	488 aa	97.7%	100%

MFS efflux transporter	*MdtO*	-	683 aa	99.6%	100%
MFS efflux transporter	*MdtN*	-	343 aa	100%	100%
MFS efflux transporter	*MdtM*	-	410 aa	98%	100%
MFS efflux transporter	*MdtH*	-	402 aa	100%	100%
MFS efflux transporter	*MdtG*	-	408 aa	99.8%	100%
RND efflux transporter	*MdtF*	-	1037 aa	99.7%	100%
RND efflux transporter	*MdtE*	-	385 aa	99.7%	100%
RND efflux transporter	*MdtC*	-	1024 aa	99.7%	99.9%
RND efflux transporter	*MdtB*	-	1040 aa	99.6%	100%
RND efflux transporter	*MdtA*	-	415 aa	99.3%	100%
ABC efflux pump	*mdlB*	-	593 aa	99.5%	100%
MFS efflux transporter	*MdfA*	-	410 aa	99.8%	100%
efflux regulation	*MarR*	G103S, Y137H	144 aa	97.9%	100%
efflux regulation	*MarA*	-	129 aa	99.2%	100%
ABC efflux pump	*MacA*	-	371 aa	99.7%	100%
fimbria	*LpfA*	-	190 aa	100%	100%
beta-lactamase KPC	*KPC-2*	-	293 aa	100%	100%
efflux regulation	*KdpE*	-	225 aa	99.1%	100%
efflux regulation	*H-NS*	-	137 aa	100%	100%
DNA topoisomerase subunit	*gyrA*	S83L	875 aa	99.9%	100%
putative efflux transport	*gspA*	-	270 aa	98.1%	100%
influx	*GlpT*	G206A	423 aa	93.1%	93.8%
influx	*GlpT*	E448K	452 aa	98.2%	100%
beta-lactamase GES	*GES-2*	-	287 aa	100%	100%
efflux regulation	*GadX*	-	274 aa	98.5%	100%
efflux regulation	*GadW*	-	242 aa	93.4%	100%
efflux regulation	*EvgS*	-	1065 aa	99.2%	89%
efflux regulation	*EvgA*	-	204 aa	100%	100%
beta-lactamase ESC	*ESC-148*	-	420 aa	98.3%	100%
MFS efflux transporter	*EmrY*	-	512 aa	99.6%	100%
MFS efflux transporter	*EmrK*	-	372 aa	98.1%	96.1%
multidrug efflux SMR transporter	*EmrE*	-	110 aa	98.2%	100%
MFS efflux transporter	*EmrD*	-	394 aa	99.7%	100%
MFS efflux transporter	*EmrB*	-	512 aa	100%	100%
MFS efflux transporter	*EmrA*	-	390 aa	99.7%	100%
Dfr	*DfrA14*	-	160 aa	99.4%	100%

influx	*cycA*	S263A	467 aa	98.3%	100%
putative efflux transport	*cusR*	-	227 aa	95.2%	100%
putative efflux transport	*cusF*	-	110 aa	97.3%	100%
efflux regulation	*CRP*	-	210 aa	99.5%	100%
efflux regulation	*CpxA*	-	457 aa	99.1%	100%
MFS efflux transporter	*CmlA5*	-	437 aa	99.8%	100%
BaeSR	*BaeS*	-	467 aa	100%	100%
BaeSR	*BaeR*	-	240 aa	100%	100%
undecaprenyl-diphosphatase	*BacA*	-	273 aa	100%	100%
beta-lactamase regulation	*argR*	-	156 aa	94.2%	100%
beta-lactamase regulation	*ampR*	-	105 aa	94.3%	85.4%
beta-lactamase ampC	*ampH*	-	385 aa	99.5%	100%
beta-lactamase ampC	*ampC1*	-	434 aa	99.8%	100%
efflux regulation	*AcrS*	-	220 aa	99.5%	100%
RND efflux transporter	*AcrF*	-	1034 aa	99.3%	100%
RND efflux transporter	*AcrE*	-	385 aa	100%	100%
RND efflux transporter	*AcrD*	-	1037 aa	99.9%	100%
RND efflux transporter	*AcrB*	-	1049 aa	100%	100%
RND efflux transporter	*AcrA*	-	397 aa	100%	100%
ANT(3'')-Ia	*aadA11*	-	269 aa	100%	95.7%
ANT(3'')-Ia	*aadA*	-	275 aa	100%	99.6%
AAC(6')-I	*AAC(6')-Ib*	-	192 aa	99%	94.6%

M14 E. coli **(Table S2)**

ResFinder 4.1

Resistance gene	Identity (%)	Alignment Length/Gene Length	Coverage (%)	Position in reference	Phenotype	Accession no.
dfrA14	100	474/474	100	1..475	Trimethoprim resistance	KF921535
qnrS1	100	657/657	100	1..658	Quinolone resistance	AB187515
aac(6')-Ib-cr	97.67	599/600	99.83	5..604	Fluoroquinolone and aminoglycoside resistance	DQ303918
aph(3'')-Ib	99.88	804/804	100	1..805	Aminoglycoside resistance	AF321551
mdf(A)	99.92	1233/1233	100	1..1234	Macrolide resistance	Y08743
blaKPC-2	100	882/882	100	1..883	Beta-lactam resistance	AY034847
blaOXA-48	100	798/798	100	1..799	Beta-lactam resistance	AY236073
blaGES-1	100	864/864	100	1..865	Beta-lactam resistance	HQ170511
blaOXA-10	100	801/801	100	1..802	Beta-lactam resistance Alternate name; PSE-2	J03427
sul2	100	816/816	100	1..817	Sulphonamide resistance	AY034138

PlasmidFinder 2.1

Database	Plasmid	Identity (%)	Query / Template length	Accession number
enterobacteriaceae	IncFIB(K)	99.82	560 / 560	JN233704
enterobacteriaceae	IncFII	99.62	261 / 261	AY458016
enterobacteriaceae	IncL	100	661 / 661	JN626286
enterobacteriaceae	IncN	99.81	514 / 514	AY046276
enterobacteriaceae	IncP6	99.88	806 / 806	JF785550
enterobacteriaceae	IncX5	100	576 / 576	MF062700
enterobacteriaceae	IncY	98.95	765 / 765	K02380

VirulenceFinder 2.0

Database	Virulence factor	Identity	Query / Template length	Protein function	Accession number
virulence_ecoli	*gad*	100	1401 / 1401	Glutamate decarboxylase	AP009239
virulence_ecoli	*gad*	99.93	1401 / 1401	Glutamate decarboxylase	AP009240
virulence_ecoli	*lpfA*	99.83	573 / 573	Long polar fimbriae	AP010953
virulence_ecoli	*lpfA*	91.45	524 / 573	Long polar fimbriae	AP010953
virulence_ecoli	*lpfA*	91.62	559 / 573	Long polar fimbriae	CP002185
virulence_ecoli	*terC*	99.02	714 / 714	Tellurium ion resistance protein	HE616528
virulence_ecoli	*terC*	98.96	966 / 966	Tellurium ion resistance protein	CP007491
virulence_ecoli	*terC*	100	1041 / 1041	Tellurium ion resistance protein	MG591698

MLST 2.0 (Multi-Locus Sequence Typing)

Locus	Identity	Coverage	Alignment Length	Allele Length	Gaps	Allele	ST
adk	100	100	536	536	0	adk_64	2795
fumC	100	100	469	469	0	fumC_4	
gyrB	100	100	460	460	0	gyrB_5	
icd	100	100	518	518	0	icd_1	
mdh	100	100	452	452	0	mdh_8	
purA	100	100	478	478	0	purA_8	
recA	100	100	510	510	0	recA_6	

SerotypeFinder 2.0

Database	Gene	Serotype	Identity	Template / HSP length	Accession number
O_type	wzy	O21	100	1083 / 1083	EU694098
O_type	wzx	O21	100	1236 / 1236	EU694098
H_type	fliC	H27	91.17	1338 / 1461	AM231154

Plasmids detected by ARESdb cloud platform

Plasmid	Identity	Query / Template length	Accession number
Col440I	95.61%	114 / 114	CP023920
Col440I	94.74%	114 / 114	CP023920
Col440II	91.10%	281 / 282	CP023921
IncFIB(K)	99.82%	560 / 560	JN233704
IncFII	99.62%	261 / 261	AY458016
IncFII(Yp)	92.64%	231 / 230	CP000670
IncL	100.00%	661 / 661	JN626286
IncN	99.81%	514 / 514	AY046276
IncP6	99.88%	806 / 806	JF785550
IncX5	100.00%	576 / 576	MF062700
IncY	98.95%	765 / 765	K02380

Virulence Factors detected by ARESdb cloud platform

Marker Class	Marker	Variant(s)	Alignment Length	Sequence Identity	Sequence Coverage
virulence factors	*ydeH*	-	442 aa	98.6%	100%
virulence factors	*ydaM*	-	410 aa	98%	100%
virulence factors	*sfaH*	-	304 aa	97.4%	100%
virulence factors	*potD*	-	348 aa	91.1%	100%
virulence factors	*pemK*	-	110 aa	100%	100%
virulence factors	*pemI*	-	85 aa	100%	100%
virulence factors	*nagA*	-	139 aa	98.6%	94.6%
virulence factors	*mqsA*	-	131 aa	100%	100%
virulence factors	*mqo*	-	548 aa	99.3%	100%
virulence factors	*manZ*	-	269 aa	98.5%	100%
virulence factors	*manX*	-	144 aa	97.9%	100%
virulence factors	*ldrD*	-	91 aa	94.5%	100%
virulence factors	*fliZ*	-	108 aa	98.1%	99.1%
virulence factors	*fliZ*	-	62 aa	96.8%	100%
virulence factors	*fliY*	-	266 aa	92.1%	100%
virulence factors	*fliQ*	-	89 aa	93.3%	100%
virulence factors	*fliI*	-	456 aa	95.6%	100%
virulence factors	*fliG*	-	332 aa	96.7%	100%
virulence factors	*fliA*	-	239 aa	99.6%	100%
virulence factors	*flhA*	-	692 aa	94.4%	100%
virulence factors	*fimD*	-	517 aa	98.6%	100%
virulence factors	*EspX1*	-	473 aa	91.5%	100%
virulence factors	*epsJ*	-	300 aa	98%	100%
virulence factors	*elfG*	-	357 aa	100%	100%
virulence factors	*cstA*	-	701 aa	92.4%	100%
fimbria	*LpfA*	-	190 aa	100%	100%

Antibiotic resistance genes detected by ARESdb cloud platform

Marker Class	Marker	Variant(s)	Alignment Length	Sequence Identity	Sequence Coverage
Vga	*Vga(C)*	-	74 aa	94.6%	97.4%
undecaprenyl-diphosphatase	*BacA*	-	273 aa	100%	100%
target protection	*Rpsl*	-	124 aa	93.5%	100%
Sul	*Sul2*	-	282 aa	98.9%	98.3%
RND efflux transporter	*MdtF*	-	1037 aa	99.7%	100%
RND efflux transporter	*MdtE*	-	385 aa	99.7%	100%
RND efflux transporter	*MdtC*	-	1024 aa	99.7%	99.9%
RND efflux transporter	*MdtB*	-	1040 aa	99.6%	100%
RND efflux transporter	*MdtA*	-	415 aa	99.3%	100%
RND efflux transporter	*AcrF*	-	1034 aa	99.3%	100%
RND efflux transporter	*AcrE*	-	385 aa	100%	100%
RND efflux transporter	*AcrD*	-	1037 aa	99.9%	100%
RND efflux transporter	*AcrB*	-	1049 aa	100%	100%
RND efflux transporter	*AcrA*	-	397 aa	100%	100%
regulation of resistance	*rpoS*	-	172 aa	100%	100%
regulation of resistance	*ompR*	-	239 aa	100%	100%
Qnr	*QnrS7*	-	218 aa	100%	100%
putative efflux transport	*yheI*	-	590 aa	98.1%	100%
putative efflux transport	*gspA*	-	270 aa	98.1%	100%
putative efflux transport	*cusR*	-	227 aa	95.2%	100%
putative efflux transport	*cusF*	-	110 aa	97.3%	100%
porin	*OmpC*	-	368 aa	96.5%	100%
Pmr	*PmrL*	-	660 aa	99.8%	100%
Pmr	*PmrF*	-	322 aa	100%	100%
Pmr	*PmrE*	-	388 aa	99%	100%
multidrug efflux SMR transporter	*EmrE*	-	110 aa	98.2%	100%
MFS efflux transporter	*RosB*	-	558 aa	91.9%	100%
MFS efflux transporter	*MdtM*	-	410 aa	98%	100%
MFS efflux transporter	*MdtH*	-	402 aa	100%	100%
MFS efflux transporter	*MdtG*	-	408 aa	99.8%	100%
MFS efflux transporter	*MdfA*	-	410 aa	99.8%	100%
MFS efflux transporter	*EmrY*	-	512 aa	99.6%	100%
MFS efflux transporter	*EmrK*	-	372 aa	98.1%	96.1%

MFS efflux transporter	*EmrD*	-	394 aa	99.7%	100%
MFS efflux transporter	*EmrB*	-	512 aa	100%	100%
MFS efflux transporter	*EmrA*	-	390 aa	99.7%	100%
macrolide phosphotransferase	*Mph(B)*	-	157 aa	98.1%	99.4%
influx	*GlpT*	G206A	423 aa	93.1%	93.8%
influx	*GlpT*	E448K	452 aa	98.2%	100%
influx	*cycA*	S263A	467 aa	98.3%	100%
fimbria	*LpfA*	-	190 aa	100%	100%
efflux regulation	*SoxR*	R4K	152 aa	93.4%	100%
efflux regulation	*PhoQ*	-	486 aa	99.4%	100%
efflux regulation	*MarR*	G103S, Y137H	144 aa	97.9%	100%
efflux regulation	*MarA*	-	129 aa	99.2%	100%
efflux regulation	*KdpE*	-	225 aa	99.1%	100%
efflux regulation	*H-NS*	-	137 aa	100%	100%
efflux regulation	*GadX*	-	274 aa	98.5%	100%
efflux regulation	*GadW*	-	242 aa	93.4%	100%
efflux regulation	*EvgS*	-	1197 aa	99.3%	100%
efflux regulation	*EvgA*	-	204 aa	100%	100%
efflux regulation	*CRP*	-	210 aa	99.5%	100%
efflux regulation	*CpxA*	-	457 aa	99.1%	100%
efflux regulation	*AcrS*	-	220 aa	99.5%	100%
efflux	*TolC*	-	495 aa	100%	100%
DNA topoisomerase subunit	*parC*	T57S	752 aa	95.1%	100%
DNA topoisomerase subunit	*gyrA*	S83L	875 aa	99.9%	100%
Dfr	*DfrA14*	-	160 aa	99.4%	100%
compensation mechanism	*MgrB*	-	46 aa	100%	97.9%
beta-lactamase TEM	*TEM-160*	-	190 aa	98.9%	66.4%
beta-lactamase regulation	*argR*	-	156 aa	94.2%	100%
beta-lactamase regulation	*ampR*	-	105 aa	94.3%	85.4%
beta-lactamase OXA	*OXA-48*	-	265 aa	100%	100%
beta-lactamase OXA	*OXA-10*	-	266 aa	100%	100%
beta-lactamase KPC	*KPC-2*	-	293 aa	100%	100%
beta-lactamase GES	*GES-1*	-	287 aa	100%	100%
beta-lactamase ESC	*ESC-148*	-	420 aa	98.3%	100%
beta-lactamase ampC	*ampH*	-	385 aa	99.7%	100%
beta-lactamase ampC	*ampC1*	-	434 aa	99.8%	100%
BaeSR	*BaeS*	-	467 aa	100%	100%

BaeSR	*BaeR*	-	240 aa	100%	100%
APH(3'')	*APH(3'')-Ib*	-	277 aa	99.6%	91.7%
ABC efflux pump	*YojI*	-	547 aa	100%	100%
ABC efflux pump	*PatA*	-	459 aa	99.8%	100%
ABC efflux pump	*MsrB*	-	137 aa	100%	100%
ABC efflux pump	*MsbA*	-	582 aa	100%	100%
ABC efflux pump	*mdlB*	-	593 aa	99.5%	100%
ABC efflux pump	*MacA*	-	371 aa	99.7%	100%
AAC(6')-I	*AAC(6')-Ib*	-	192 aa	100%	94.6%

M17 E. coli **(Table S3)**

ResFinder 4.1

Resistance gene	Identity (%)	Alignment Length/Gene Length	Coverage (%)	Position in reference	Phenotype	Accession no.
aac(6')-Ib-cr	100	600/600	100	1..601	Fluoroquinolone and aminoglycoside resistance	DQ303918
aadA16	99.65	846/846	100	1..847	Aminoglycoside resistance	EU675686
blaKPC-2	100	882/882	100	1..883	Beta-lactam resistance	AY034847
aac(6')-Ib-cr	100	600/600	100	1..601	Fluoroquinolone and aminoglycoside resistance	DQ303918
qnrB6	100	645/645	100	1..646	Quinolone resistance	EF523819
mdf(A)	99.92	1233/1233	100	1..1234	Macrolide resistance	Y08743
sul1	100	840/840	100	1..841	Sulphonamide resistance	U12338
ARR-3	99.45	543/543	100	1..544	Rifampicin resistance	FM207631
ARR-3	100	453/453	100	1..454	Rifampicin resistance	JF806499
dfrA27	100	474/474	100	1..475	Trimethoprim resistance	FJ459817

PlasmidFinder 2.1

Database	Plasmid	Identity (%)	Query / Template length	Accession number
enterobacteriaceae	IncFIB(K)	99.82	560 / 560	JN233704
enterobacteriaceae	IncFII	99.62	261 / 261	AY458016
enterobacteriaceae	IncP6	99.88	806 / 806	JF785550
enterobacteriaceae	IncR	99.2	251 / 251	DQ449578

VirulenceFinder 2.0

Database	Virulence factor	Identity	Query / Template length	Protein function	Accession number
virulence_ecoli	*gad*	100	1401 / 1401	Glutamate decarboxylase	AP009240
virulence_ecoli	*gad*	99.93	1401 / 1401	Glutamate decarboxylase	AP010953
virulence_ecoli	*lpfA*	99.83	573 / 573	Long polar fimbriae	AP010953
virulence_ecoli	*lpfA*	96.68	573 / 573	Long polar fimbriae	CP002185
virulence_ecoli	*terC*	95.24	686 / 714	Tellurium ion resistance protein	CP007491
virulence_ecoli	*terC*	98.96	966 / 966	Tellurium ion resistance protein	MG591698
virulence_ecoli	*terC*	100	1041 / 1041	Tellurium ion resistance protein	UGAE01000003

MLST 2.0 (Multi-Locus Sequence Typing)

Locus	Identity	Coverage	Alignment Length	Allele Length	Gaps	Allele	ST
adk	100	100	536	536	0	adk_64	2795
fumC	100	100	469	469	0	fumC_4	
gyrB	100	100	460	460	0	gyrB_5	
icd	100	100	518	518	0	icd_1	
mdh	100	100	452	452	0	mdh_8	
purA	100	100	478	478	0	purA_8	
recA	100	100	510	510	0	recA_6	

SerotypeFinder 2.0

Database	Gene	Serotype	Identity	Template / HSP length	Accession number
H_type	fliC	H27	91.17	1337 / 1461	AM231154
O_type	wzy	O21	98.8	1083 / 1083	EU694098
O_type	wzx	O21	100	1236 / 1236	EU694098

Plasmids detected by ARESdb cloud platform

Plasmid	Identity	Query / Template length	Accession number
Col(pHAD28)	92.37%	131 / 131	KU674895
Col440I	90.99%	111 / 114	CP023920
IncFIB(K)	99.82%	560 / 560	JN233704
IncFII	99.62%	261 / 261	AY458016
IncFII(Yp)	92.64%	231 / 230	CP000670
IncP6	99.88%	806 / 806	JF785550
IncR	99.20%	251 / 251	DQ449578

Virulence Factors detected by ARESdb cloud platform

Marker Class	Marker	Variant(s)	Alignment Length	Sequence Identity	Sequence Coverage
virulence factors	*ydeH*	-	442 aa	98.6%	100%
virulence factors	*ydaM*	-	410 aa	98%	100%
virulence factors	*sfaH*	-	304 aa	97.4%	100%
virulence factors	*potD*	-	348 aa	91.1%	100%
virulence factors	*pemK*	-	110 aa	100%	100%
virulence factors	*pemI*	-	85 aa	100%	100%
virulence factors	*nagA*	-	139 aa	98.6%	94.6%
virulence factors	*mqsA*	-	131 aa	100%	100%
virulence factors	*mqo*	-	548 aa	99.3%	100%
virulence factors	*manZ*	-	269 aa	98.5%	100%
virulence factors	*manX*	-	144 aa	97.9%	100%
virulence factors	*ldrD*	-	91 aa	94.5%	100%
virulence factors	*fliZ*	-	108 aa	98.1%	99.1%
virulence factors	*fliZ*	-	62 aa	96.8%	100%
virulence factors	*fliY*	-	266 aa	92.1%	100%
virulence factors	*fliQ*	-	89 aa	93.3%	100%
virulence factors	*fliI*	-	456 aa	95.6%	100%
virulence factors	*fliG*	-	332 aa	96.7%	100%
virulence factors	*fliA*	-	239 aa	99.6%	100%
virulence factors	*flhA*	-	692 aa	94.4%	100%
virulence factors	*fimD*	-	517 aa	98.6%	100%
virulence factors	*EspX1*	-	473 aa	91.5%	100%
virulence factors	*epsJ*	-	300 aa	98%	100%
virulence factors	*elfG*	-	357 aa	100%	100%
virulence factors	*cstA*	-	701 aa	92.4%	100%
fimbria	*LpfA*	-	190 aa	100%	100%

Antibiotic resistance genes detected by ARESdb cloud platform

Marker Class1	Marker2	Variant(s)	Alignment Length	Sequence Identity	Sequence Coverage
Vga	*Vga(C)*	-	74 aa	94.6%	97.4%
undecaprenyl-diphosphatase	*BacA*	-	273 aa	100%	100%
target protection	*Rpsl*	-	124 aa	93.5%	100%
Sul	*Sul1*	-	308 aa	99.4%	100%
RND efflux transporter	*MdtF*	-	1037 aa	99.7%	100%
RND efflux transporter	*MdtE*	-	385 aa	99.7%	100%
RND efflux transporter	*MdtC*	-	1024 aa	99.7%	99.9%
RND efflux transporter	*MdtB*	-	1040 aa	99.6%	100%
RND efflux transporter	*MdtA*	-	415 aa	99.3%	100%
RND efflux transporter	*AcrF*	-	1034 aa	99.3%	100%
RND efflux transporter	*AcrE*	-	385 aa	100%	100%
RND efflux transporter	*AcrD*	-	1037 aa	99.9%	100%
RND efflux transporter	*AcrB*	-	1049 aa	100%	100%
RND efflux transporter	*AcrA*	-	397 aa	100%	100%
regulation of resistance	*virB*	-	324 aa	91%	100%
regulation of resistance	*rpoS*	-	172 aa	100%	100%
regulation of resistance	*ompR*	-	239 aa	100%	100%
Qnr	*QnrB6*	-	226 aa	98.2%	100%
putative efflux transport	*yheI*	-	590 aa	98.1%	100%
putative efflux transport	*gspA*	-	270 aa	98.1%	100%
putative efflux transport	*cusR*	-	227 aa	95.2%	100%
putative efflux transport	*cusF*	-	110 aa	97.3%	100%
porin	*OmpC*	-	368 aa	96.7%	100%
Pmr	*PmrL*	-	660 aa	99.8%	100%

Pmr	*PmrF*	-	322 aa	100%	100%
Pmr	*PmrE*	-	388 aa	98.7%	100%
Pmr	*PmrC*	-	547 aa	99.6%	100%
multidrug efflux SMR transporter	*EmrE*	-	110 aa	98.2%	100%
MFS efflux transporter	*RosB*	-	558 aa	91.9%	100%
MFS efflux transporter	*MdtP*	-	488 aa	97.7%	100%
MFS efflux transporter	*MdtO*	-	683 aa	99.6%	100%
MFS efflux transporter	*MdtN*	-	343 aa	100%	100%
MFS efflux transporter	*MdtM*	-	410 aa	98%	100%
MFS efflux transporter	*MdtH*	-	402 aa	100%	100%
MFS efflux transporter	*MdtG*	-	408 aa	99.8%	100%
MFS efflux transporter	*MdfA*	-	410 aa	99.8%	100%
MFS efflux transporter	*EmrY*	-	512 aa	99.6%	100%
MFS efflux transporter	*EmrK*	-	372 aa	98.1%	96.1%
MFS efflux transporter	*EmrD*	-	394 aa	99.7%	100%
MFS efflux transporter	*EmrB*	-	512 aa	100%	100%
MFS efflux transporter	*EmrA*	-	390 aa	99.7%	100%
macrolide phosphotransferase	*Mph(B)*	-	157 aa	98.1%	99.4%
influx	*GlpT*	G206A	423 aa	93.1%	93.8%
influx	*GlpT*	E448K	452 aa	98.2%	100%
influx	*cycA*	S263A	467 aa	98.3%	100%
fimbria	*LpfA*	-	190 aa	100%	100%
efflux regulation	*SoxR*	R4K	152 aa	93.4%	100%
efflux regulation	*PhoQ*	-	486 aa	99.4%	100%
efflux regulation	*MarR*	G103S, Y137H	144 aa	97.9%	100%
efflux regulation	*MarA*	-	129 aa	99.2%	100%
efflux regulation	*KdpE*	-	225 aa	99.1%	100%
efflux regulation	*H-NS*	-	137 aa	100%	100%

efflux regulation	*GadX*	-	274 aa	98.5%	100%
efflux regulation	*GadW*	-	242 aa	93.4%	100%
efflux regulation	*EvgS*	-	1197 aa	99.3%	100%
efflux regulation	*EvgA*	-	204 aa	100%	100%
efflux regulation	*CRP*	-	210 aa	99.5%	100%
efflux regulation	*CpxA*	-	457 aa	99.1%	100%
efflux regulation	*AcrS*	-	220 aa	99.5%	100%
efflux	*TolC*	-	495 aa	100%	100%
DNA topoisomerase subunit	*parC*	T57S	752 aa	95.1%	100%
DNA topoisomerase subunit	*gyrA*	S83L	875 aa	99.9%	100%
Dfr	*DfrA27*	-	157 aa	99.4%	100%
compensation mechanism	*MgrB*	-	46 aa	100%	97.9%
beta-lactamase TEM	*TEM-160*	-	190 aa	98.9%	66.4%
beta-lactamase regulation	*argR*	-	156 aa	94.2%	100%
beta-lactamase regulation	*ampR*	-	105 aa	94.3%	85.4%
beta-lactamase KPC	*KPC-2*	-	293 aa	100%	100%
beta-lactamase ESC	*ESC-148*	-	420 aa	98.3%	100%
beta-lactamase ampC	*ampH*	-	385 aa	99.7%	100%
beta-lactamase ampC	*ampC1*	-	434 aa	99.8%	100%
BaeSR	*BaeS*	-	467 aa	100%	100%
BaeSR	*BaeR*	-	240 aa	100%	100%
Arr	*Arr-3*	-	162 aa	99.4%	82.2%
ANT(3")-Ia	*aadA16*	-	281 aa	100%	100%
ABC efflux pump	*YojI*	-	547 aa	100%	100%
ABC efflux pump	*PatA*	-	459 aa	99.8%	100%
ABC efflux pump	*MsrB*	-	137 aa	100%	100%
ABC efflux pump	*MsbA*	-	582 aa	100%	100%
ABC efflux pump	*mdlB*	-	593 aa	99.5%	100%
ABC efflux pump	*MacA*	-	371 aa	99.7%	100%
AAC(6')-I	*AAC(6')-Ib-cr*	-	199 aa	100%	100%

M20 E. coli **(Table S4)**

ResFinder 4.1

Resistance gene	Identity (%)	Alignment Length/Gene Length	Coverage (%)	Position in reference	Phenotype	Accession no.
dfrA14	100	474/474	100	1..475	Trimethoprim resistance	KF921535
sul2	100	816/816	100	1..817	Sulphonamide resistance	AY034138
blaOXA-10	100	801/801	100	1..802	Beta-lactam resistance Alternate name; PSE-2	J03427
blaGES-1	100	864/864	100	1..865	Beta-lactam resistance	HQ170511
blaKPC-2	100	882/882	100	1..883	Beta-lactam resistance	AY034847
blaOXA-48	100	798/798	100	1..799	Beta-lactam resistance	AY236073
aph(3'')-Ib	99.88	804/804	100	1..805	Aminoglycoside resistance	AF321551
mdf(A)	99.92	1233/1233	100	1..1234	Macrolide resistance	Y08743
qnrS1	100	657/657	100	1..658	Quinolone resistance	AB187515

PlasmidFinder 2.1

Database	Plasmid	Identity	Query / Template length	Accession number
enterobacteriaceae	Col(IRGK)	98.37	185 / 184	AY543071
enterobacteriaceae	IncFIB(K)	99.82	560 / 560	JN233704
enterobacteriaceae	IncFII	99.62	261 / 261	AY458016
enterobacteriaceae	IncL	100	661 / 661	JN626286
enterobacteriaceae	IncN	99.81	514 / 514	AY046276
enterobacteriaceae	IncP6	99.88	806 / 806	JF785550
enterobacteriaceae	IncY	98.95	765 / 765	K02380

VirulenceFinder 2.0

Database	Virulence factor	Identity	Query / Template length	Protein function	Accession number
virulence_ecoli	*gad*	100	1401 / 1401	Glutamate decarboxylase	AP009240
virulence_ecoli	*gad*	99.93	1401 / 1401	Glutamate decarboxylase	AP010953
virulence_ecoli	*lpfA*	100	573 / 573	Long polar fimbriae	AP010953
virulence_ecoli	*lpfA*	98.78	573 / 573	Long polar fimbriae	CP002185
virulence_ecoli	*terC*	99.02	714 / 714	Tellurium ion resistance protein	CP007491
virulence_ecoli	*terC*	98.96	966 / 966	Tellurium ion resistance protein	MG591698
virulence_ecoli	*terC*	100	1041 / 1041	Tellurium ion resistance protein	UGAE01000003

MLST 2.0 (Multi-Locus Sequence Typing)

Locus	Identity	Coverage	Alignment Length	Allele Length	Gaps	Allele	ST
adk	100	100	536	536	0	adk_64	2795
fumC	100	100	469	469	0	fumC_4	
gyrB	100	100	460	460	0	gyrB_5	
icd	100	100	518	518	0	icd_1	
mdh	100	100	452	452	0	mdh_8	
purA	100	100	478	478	0	purA_8	
recA	100	100	510	510	0	recA_6	

Plasmids detected by ARESdb cloud platform

Plasmid	Identity	Query / Template length	Accession number
Col(IRGK)	98.37%	184 / 184	AY543071
Col440I	95.61%	114 / 114	CP023920
Col440II	91.10%	281 / 282	CP023921
IncFIB(K)	99.82%	560 / 560	JN233704
IncFII	99.62%	261 / 261	AY458016
IncFII(Yp)	92.64%	231 / 230	CP000670
IncL	100.00%	661 / 661	JN626286
IncN	99.81%	514 / 514	AY046276
IncP6	99.88%	806 / 806	JF785550
IncY	98.95%	765 / 765	K02380

Virulence Factors detected by ARESdb cloud platform

Marker Class	Marker	Variant(s)	Alignment Length	Sequence Identity	Sequence Coverage
virulence factors	*ydeH*	-	442 aa	98.6%	100%
virulence factors	*ydaM*	-	410 aa	98%	100%
virulence factors	*sfaH*	-	304 aa	97.4%	100%
virulence factors	*potD*	-	348 aa	91.1%	100%
virulence factors	*pemK*	-	110 aa	100%	100%
virulence factors	*pemI*	-	85 aa	100%	100%
virulence factors	*nagA*	-	139 aa	98.6%	94.6%
virulence factors	*mqsA*	-	131 aa	100%	100%
virulence factors	*mqo*	-	548 aa	99.3%	100%
virulence factors	*manZ*	-	269 aa	98.5%	100%
virulence factors	*manX*	-	144 aa	97.9%	100%
virulence factors	*ldrD*	-	91 aa	94.5%	100%
virulence factors	*fliZ*	-	108 aa	98.1%	99.1%
virulence factors	*fliZ*	-	62 aa	96.8%	100%
virulence factors	*fliY*	-	266 aa	92.1%	100%
virulence factors	*fliQ*	-	89 aa	93.3%	100%
virulence factors	*fliI*	-	456 aa	95.6%	100%
virulence factors	*fliG*	-	332 aa	96.7%	100%
virulence factors	*fliA*	-	239 aa	99.6%	100%
virulence factors	*flhA*	-	692 aa	94.4%	100%
virulence factors	*fimD*	-	517 aa	98.6%	100%
virulence factors	*EspX1*	-	473 aa	91.5%	100%
virulence factors	*epsJ*	-	300 aa	98%	100%
virulence factors	*elfG*	-	357 aa	100%	100%
virulence factors	*cstA*	-	701 aa	92.4%	100%
fimbria	*LpfA*	-	190 aa	100%	100%

Antibiotic resistance genes detected by ARESdb cloud platform

Marker Class	Marker	Variant(s)	Alignment Length	Sequence Identity	Sequence Coverage
Vga	*Vga(C)*	-	74 aa	94.6%	97.4%
undecaprenyl-diphosphatase	*BacA*	-	273 aa	100%	100%
target protection	*Rpsl*	-	124 aa	93.5%	100%
Sul	*Sul2*	-	282 aa	98.9%	98.3%
RND efflux transporter	*MdtF*	-	1037 aa	99.7%	100%
RND efflux transporter	*MdtE*	-	385 aa	99.7%	100%
RND efflux transporter	*MdtC*	-	1024 aa	99.7%	99.9%
RND efflux transporter	*MdtB*	-	1040 aa	99.6%	100%
RND efflux transporter	*MdtA*	-	415 aa	99.3%	100%
RND efflux transporter	*AcrF*	-	1034 aa	99.3%	100%
RND efflux transporter	*AcrE*	-	385 aa	100%	100%
RND efflux transporter	*AcrD*	-	1037 aa	99.9%	100%
RND efflux transporter	*AcrB*	-	1049 aa	100%	100%
RND efflux transporter	*AcrA*	-	397 aa	100%	100%
regulation of resistance	*rpoS*	-	172 aa	100%	100%
regulation of resistance	*ompR*	-	239 aa	100%	100%
Qnr	*QnrS1*	-	218 aa	100%	100%
putative efflux transport	*yheI*	-	590 aa	98.1%	100%
putative efflux transport	*gspA*	-	270 aa	98.1%	100%
putative efflux transport	*cusR*	-	227 aa	95.2%	100%
putative efflux transport	*cusF*	-	110 aa	97.3%	100%
porin	*OmpC*	-	368 aa	96.5%	100%
Pmr	*PmrL*	-	660 aa	99.8%	100%
Pmr	*PmrF*	-	322 aa	100%	100%
Pmr	*PmrE*	-	388 aa	99%	100%

multidrug efflux SMR transporter	*EmrE*	-	110 aa	98.2%	100%
MFS efflux transporter	*RosB*	-	558 aa	91.9%	100%
MFS efflux transporter	*MdtM*	-	410 aa	98%	100%
MFS efflux transporter	*MdtH*	-	402 aa	100%	100%
MFS efflux transporter	*MdtG*	-	408 aa	99.8%	100%
MFS efflux transporter	*MdfA*	-	410 aa	99.8%	100%
MFS efflux transporter	*EmrY*	-	512 aa	99.6%	100%
MFS efflux transporter	*EmrK*	-	372 aa	98.1%	96.1%
MFS efflux transporter	*EmrD*	-	394 aa	99.7%	100%
MFS efflux transporter	*EmrB*	-	512 aa	100%	100%
MFS efflux transporter	*EmrA*	-	390 aa	99.7%	100%
macrolide phosphotransferase	*Mph(B)*	-	157 aa	98.1%	99.4%
influx	*GlpT*	G206A	423 aa	93.1%	93.8%
influx	*GlpT*	E448K	452 aa	98.2%	100%
influx	*cycA*	S263A	467 aa	98.3%	100%
fimbria	*LpfA*	-	190 aa	100%	100%
efflux regulation	*SoxR*	R4K	152 aa	93.4%	100%
efflux regulation	*PhoQ*	-	486 aa	99.4%	100%
efflux regulation	*MarR*	G103S, Y137H	144 aa	97.9%	100%
efflux regulation	*MarA*	-	129 aa	99.2%	100%
efflux regulation	*KdpE*	-	225 aa	99.1%	100%
efflux regulation	*H-NS*	-	137 aa	100%	100%
efflux regulation	*GadX*	-	274 aa	98.5%	100%
efflux regulation	*GadW*	-	242 aa	93.4%	100%
efflux regulation	*EvgS*	-	1197 aa	99.3%	100%
efflux regulation	*EvgA*	-	204 aa	100%	100%
efflux regulation	*CRP*	-	210 aa	99.5%	100%
efflux regulation	*CpxA*	-	457 aa	99.1%	100%
efflux regulation	*AcrS*	-	220 aa	99.5%	100%
efflux	*TolC*	-	495 aa	100%	100%

DNA topoisomerase subunit	*parC*	T57S	752 aa	95.1%	100%
DNA topoisomerase subunit	*gyrA*	S83L	875 aa	99.9%	100%
Dfr	*DfrA14*	-	160 aa	99.4%	100%
compensation mechanism	*MgrB*	-	46 aa	100%	97.9%
beta-lactamase TEM	*TEM-160*	-	190 aa	98.9%	66.4%
beta-lactamase regulation	*argR*	-	156 aa	94.2%	100%
beta-lactamase regulation	*ampR*	-	105 aa	94.3%	85.4%
beta-lactamase OXA	*OXA-48*	-	265 aa	100%	100%
beta-lactamase OXA	*OXA-10*	-	266 aa	100%	100%
beta-lactamase KPC	*KPC-2*	-	293 aa	100%	100%
beta-lactamase GES	*GES-1*	-	287 aa	100%	100%
beta-lactamase ESC	*ESC-148*	-	420 aa	98.3%	100%
beta-lactamase ampC	*ampH*	-	385 aa	99.7%	100%
beta-lactamase ampC	*ampC1*	-	434 aa	99.8%	100%
BaeSR	*BaeS*	-	467 aa	100%	100%
BaeSR	*BaeR*	-	240 aa	100%	100%
APH(3")	*APH(3")-Ib*	-	277 aa	99.6%	91.7%
ABC efflux pump	*YojI*	-	547 aa	100%	100%
ABC efflux pump	*PatA*	-	459 aa	99.8%	100%
ABC efflux pump	*MsrB*	-	137 aa	100%	100%
ABC efflux pump	*MsbA*	-	582 aa	100%	100%
ABC efflux pump	*mdlB*	-	593 aa	99.5%	100%
ABC efflux pump	*MacA*	-	371 aa	99.7%	100%
AAC(6')-I	*AAC(6')-Ib*	-	192 aa	100%	94.6%

5a K. pneumoniae **(Table S5)**

ResFinder 4.1

Resistance gene	Identity	Alignment Length/Gene Length	Coverage	Position in reference	Phenotype	Accession no.
sul1	100	840/840	100	1..841	Sulphonamide resistance	U12338
tet(A)	100	1200/1200	100	1..1201	Tetracycline resistance	AJ517790
OqxA	100	1176/1176	100	1..1177	Disinfectant resistance	EU370913
OqxB	99.97	3153/3153	100	1..3154	Disinfectant resistance	EU370913
oqxB	99.97	3153/3153	100	1..3154	Quinolone resistance	EU370913
aac(6')-Ib-cr	94.61	519/519	95.95	1..520	Fluoroquinolone and aminoglycoside resistance	EF636461
oqxA	100	1176/1176	100	1..1177	Quinolone resistance	EU370913
blaCTX-M-3	100	876/876	100	1..877	Beta-lactam resistance	Y10278
blaOXA-2	100	828/828	100	1..829	Beta-lactam resistance	DQ112222
blaGES-5	100	864/864	100	1..865	Beta-lactam resistance	DQ236171
aph(3'')-Ib	100	804/804	100	1..805	Aminoglycoside resistance	AF024602
aph(6)-Id	100	837/837	100	1..838	Aminoglycoside resistance	M28829
fosA	99.29	420/420	100	1..421	Fosfomycin resistance	ACWO01000079
blaKPC-2	100	882/882	100	1..883	Beta-lactam resistance	AY034847

PlasmidFinder 2.1

Database	Plasmid	Identity	Query / Template length	Accession number
enterobacteriaceae	Col(pHAD28)	95.42	131 / 131	KU674895
enterobacteriaceae	Col440II	97.16	282 / 282	CP023921
enterobacteriaceae	IncFIA(HI1)	96.91	388 / 388	AF250878
enterobacteriaceae	IncFII(K)	97.97	148 / 148	CP000648
enterobacteriaceae	IncX5	100	576 / 576	MF062700
enterobacteriaceae	IncY	99.48	765 / 765	K02380

MLST 2.0 (Multi-Locus Sequence Typing)

Locus	Identity	Coverage	Alignment Length	Allele Length	Gaps	Allele	ST
gapA	100	100	450	450	0	gapA_2	37
infB	100	100	318	318	0	infB_9	
mdh	100	100	477	477	0	mdh_2	
pgi	100	100	432	432	0	pgi_1	
phoE	100	100	420	420	0	phoE_13	
rpoB	100	100	501	501	0	rpoB_1	
tonB	100	100	414	414	0	tonB_16	

Antibiotic resistance genes detected by ARESdb cloud platform

Marker Class	Marker	Variant(s)	Alignment Length	Sequence Identity	Sequence Coverage
Vga	*Vga(C)*	-	74 aa	94.6%	97.4%
target protection	*Rpsl*	-	124 aa	94.4%	100%
Sul	*Sul1*	-	308 aa	99.4%	100%
RND efflux transporter	*SilC*	-	461 aa	100%	100%
RND efflux transporter	*SilB*	-	430 aa	97.9%	100%
RND efflux transporter	*SilA*	-	1048 aa	99%	100%
RND efflux transporter	*OqxB*	-	1050 aa	99.9%	100%
RND efflux transporter	*OqxA*	-	391 aa	100%	100%
RND efflux transporter	*MdtC*	-	1024 aa	91.6%	99.9%
RND efflux transporter	*MdtB*	-	1040 aa	90.1%	100%
RND efflux transporter	*AcrD*	-	1037 aa	91%	100%
RND efflux transporter	*AcrB*	-	1049 aa	91.5%	100%
RND efflux transporter	*AcrA*	-	397 aa	100%	100%
regulation of resistance	*virB*	-	324 aa	91.7%	100%
regulation of resistance	*rpoS*	-	172 aa	99.4%	100%
regulation of resistance	*rnfC*	-	562 aa	91.6%	75.9%
regulation of resistance	*ompR*	-	239 aa	100%	100%
regulation of resistance	*mtfA*	-	265 aa	100%	100%
regulation of resistance	*MerR*	-	121 aa	91.7%	100%
regulation of resistance	*MerR*	-	144 aa	100%	100%
regulation of resistance	*MerR*	-	116 aa	93.1%	80.6%
regulation of resistance	*leuO*	-	308 aa	99.4%	100%
Qnr	*QnrB12*	-	215 aa	92.1%	100%
putative efflux transport	*cusR*	-	227 aa	99.1%	100%
porin	*OmpK37*	D275T, E244D, I128M, I70M, M233Q, N230G, N274S, R239K, V277I	384 aa	94.3%	100%
porin	*OmpK36*	-	369 aa	99.2%	100%
porin	*OmpK36*	A217S, D223G, E232R, F198Y, F207Y, G189T, L229A, L59V, N304E, T222L	369 aa	93.5%	100%
porin	*OmpK35*	-	195 aa	100%	85.9%
Pmr	*PmrE*	-	388 aa	99.5%	100%

phospholipid biosynthesis pathway	*tesA*	-	184 aa	92.4%	100%
MFS efflux transporter	*Tet(A)*	-	424 aa	100%	100%
MFS efflux transporter	*RosB*	-	558 aa	100%	100%
MFS efflux transporter	*RosA*	-	406 aa	99.3%	100%
MFS efflux transporter	*KpnH*	-	512 aa	93.4%	100%
MFS efflux transporter	*KpnG*	-	390 aa	99.7%	100%
MFS efflux transporter	*KpnF*	-	109 aa	100%	100%
MFS efflux transporter	*KpnE*	-	120 aa	99.2%	100%
MFS efflux transporter	*KdeA*	-	410 aa	100%	100%
MFS efflux transporter	*EmrD*	-	394 aa	99.5%	100%
influx regulation	*bamB*	A176T	360 aa	94.4%	100%
influx	*UhpT*	E350Q	456 aa	96.1%	98.5%
influx	*GlpT*	G206A	423 aa	93.4%	93.8%
influx	*cycA*	S263A	467 aa	92.7%	100%
glutathione transferase	*FosA*	-	139 aa	99.3%	100%
efflux regulation	*MarA*	-	123 aa	93.5%	96.9%
efflux regulation	*H-NS*	-	135 aa	93.3%	98.5%
efflux regulation	*CRP*	-	210 aa	99%	100%
efflux regulation	*CpxA*	-	461 aa	98.7%	100%
DNA topoisomerase subunit	*parC*	T57S	752 aa	94.3%	100%
DNA topoisomerase subunit	*gyrA*	S83Y	877 aa	99.8%	100%
beta-lactamase regulation	*argR*	-	156 aa	100%	100%
beta-lactamase OXA	*OXA-2*	-	275 aa	100%	100%
beta-lactamase GES	*GES-5*	-	287 aa	100%	100%
beta-lactamase CTX-M	*CTX-M-3*	-	291 aa	100%	100%
BasRS	*BasS* synonym *PmrB*	R256G	365 aa	99.5%	100%
BaeSR	*BaeS*	-	492 aa	99.4%	100%
BaeSR	*BaeR*	-	240 aa	99.6%	100%
APH(6)	*APH(6)-Id*	-	278 aa	100%	100%
APH(3")	*APH(3")-Ib*	-	290 aa	99.7%	96%
ABC efflux pump	*PatA*	-	459 aa	94.6%	100%
ABC efflux pump	*MsbA*	-	582 aa	91.9%	100%
AAC(6')-I	*AAC(6')-Ib*	-	179 aa	100%	88.2%

Virulence Factors detected by ARESdb cloud platform

Marker Class	Marker	Variant(s)	Alignment Length	Sequence Identity	Sequence Coverage
virulence factors	*sinR*	-	180 aa	90%	99.4%
virulence factors	*sfaG*	-	182 aa	100%	100%
virulence factors	*potD*	-	348 aa	94.8%	100%
virulence factors	*gmr*	-	551 aa	100%	100%
virulence factors	*fliY*	-	310 aa	100%	100%
virulence factors	*fliY*	-	266 aa	92.1%	100%
virulence factors	*fimD*	-	859 aa	99.5%	100%
virulence factors	*feoB*	T755A	772 aa	94.2%	100%
virulence factors	*eutB*	-	453 aa	94.9%	100%
virulence factors	*cnrA*	-	1030 aa	99.8%	100%

Plasmids detected by ARESdb cloud platform

Plasmid	Identity	Query / Template length	Accession number
Col(pHAD28)	93.89%	131 / 131	KU674895
Col440I	95.61%	114 / 114	CP023920
Col440II	97.16%	282 / 282	CP023921
IncFIA(HI1)	96.91%	388 / 388	AF250878
IncFII(K)	97.97%	148 / 148	CP000648
IncFII(Yp)	92.21%	231 / 230	CP000670
IncX5	100.00%	576 / 576	MF062700
IncY	99.48%	765 / 765	K02380

M11 K. pneumoniae **(Table S6)**

ResFinder 4.1

Resistance gene	Identity (%)	Alignment Length/Gene Length	Coverage (%)	Position in reference	Phenotype	Accession no.
fosA	99.29	420/420	100	1..421	Fosfomycin resistance	ACWO01000079
OqxA	100	1176/1176	100	1..1177	Disinfectant resistance	EU370913
OqxB	99.97	3153/3153	100	1..3154	Disinfectant resistance	EU370913
blaGES-5	100	864/864	100	1..865	Beta-lactam resistance	DQ236171
blaKPC-2	100	882/882	100	1..883	Beta-lactam resistance	AY034847
blaOXA-2	100	828/828	100	1..829	Beta-lactam resistance	DQ112222
blaCTX-M-3	100	876/876	100	1..877	Beta-lactam resistance	Y10278
aph(3'')-Ib	99.88	803/804	99.88	2..805	Aminoglycoside resistance	AF024602
aph(6)-Id	100	837/837	100	1..838	Aminoglycoside resistance	M28829
oqxA	100	1176/1176	100	1..1177	Quinolone resistance	EU370913
oqxB	99.97	3153/3153	100	1..3154	Quinolone resistance	EU370913
tet(A)	97.57	1244/1275	97.57	1..1245	Tetracycline resistance	AF534183
sul1	100	840/840	100	1..841	Sulphonamide resistance	U12338

PlasmidFinder 2.1

Database	Plasmid	Identity (%)	Query / Template length	Accession number
enterobacteriaceae	Col(pHAD28)	95.42	131 / 131	KU674895
enterobacteriaceae	Col440II	97.16	282 / 282	CP023921
enterobacteriaceae	IncFIA(HI1)	96.91	388 / 388	AF250878
enterobacteriaceae	IncFII(K)	97.97	148 / 148	CP000648
enterobacteriaceae	IncX5	100	576 / 576	MF062700
enterobacteriaceae	IncY	99.48	765 / 765	K02380

MLST 2.0 (Multi-Locus Sequence Typing)

Locus	Identity	Coverage	Alignment Length	Allele Length	Gaps	Allele	ST
gapA	100	100	450	450	0	gapA_2	37
infB	100	100	318	318	0	infB_9	
mdh	100	100	477	477	0	mdh_2	
pgi	100	100	432	432	0	pgi_1	
phoE	100	100	420	420	0	phoE_13	
rpoB	100	100	501	501	0	rpoB_1	
tonB	100	100	414	414	0	tonB_16	

Virulence Factors detected by ARESdb cloud platform

Marker Class1	Marker2	Variant(s)	Alignment Length	Sequence Identity	Sequence Coverage
virulence factors	*sinR*	-	180 aa	90%	99.4%
virulence factors	*sfaG*	-	182 aa	100%	100%
virulence factors	*potD*	-	348 aa	94.8%	100%
virulence factors	*gmr*	-	551 aa	100%	100%
virulence factors	*fliY*	-	310 aa	100%	100%
virulence factors	*fliY*	-	266 aa	92.1%	100%
virulence factors	*fimD*	-	859 aa	99.5%	100%
virulence factors	*feoB*	T755A	772 aa	94.2%	100%
virulence factors	*eutB*	-	453 aa	94.9%	100%
virulence factors	*cnrA*	-	1030 aa	99.8%	100%

Plasmids detected by ARESdb cloud platform

Plasmid	Identity	Query / Template length	Accession number
Col(pHAD28)	94.66%	131 / 131	KU674895
Col440I	95.61%	114 / 114	CP023920
Col440II	97.16%	282 / 282	CP023921
IncFIA(HI1)	96.91%	388 / 388	AF250878
IncFII(K)	97.97%	148 / 148	CP000648
IncFII(Yp)	92.21%	231 / 230	CP000670
IncX5	100.00%	576 / 576	MF062700
IncY	99.48%	765 / 765	K02380

Antibiotic resistance genes detected by ARESdb cloud platform

Marker Class	Marker	Variant(s)	Alignment Length	Sequence Identity	Sequence Coverage
Vga	*Vga(C)*	-	74 aa	94.6%	97.4%
target protection	*Rpsl*	-	124 aa	94.4%	100%
Sul	*Sul1*	-	308 aa	99.4%	100%
RND efflux transporter	*SilC*	-	461 aa	100%	100%
RND efflux transporter	*SilB*	-	430 aa	97.9%	100%
RND efflux transporter	*SilA*	-	1048 aa	99%	100%
RND efflux transporter	*OqxB*	-	1050 aa	99.9%	100%
RND efflux transporter	*OqxA*	-	391 aa	100%	100%
RND efflux transporter	*MdtC*	-	1024 aa	91.6%	99.9%
RND efflux transporter	*MdtB*	-	1040 aa	90.1%	100%
RND efflux transporter	*AcrD*	-	1037 aa	91%	100%
RND efflux transporter	*AcrB*	-	1049 aa	91.5%	100%
RND efflux transporter	*AcrA*	-	397 aa	100%	100%
regulation of resistance	*virB*	-	324 aa	91.7%	100%

regulation of resistance	*rpoS*	-	172 aa	99.4%	100%
regulation of resistance	*rnfC*	-	562 aa	91.6%	75.9%
regulation of resistance	*ompR*	-	239 aa	100%	100%
regulation of resistance	*mtfA*	-	265 aa	100%	100%
regulation of resistance	*MerR*	-	121 aa	91.7%	100%
regulation of resistance	*MerR*	-	144 aa	100%	100%
regulation of resistance	*MerR*	-	116 aa	93.1%	80.6%
regulation of resistance	*leuO*	-	308 aa	99.4%	100%
Qnr	*QnrB12*	-	215 aa	92.1%	100%
putative efflux transport	*cusR*	-	227 aa	99.1%	100%
porin	*OmpK37*	D275T, E244D, I128M, I70M, M233Q, N230G, N274S, R239K, V277I	384 aa	94.3%	100%
porin	*OmpK36*	-	368 aa	99.2%	100%
porin	*OmpK36*	A217S, D223G, E232R, F198Y, F207Y, G189T, L229A, L59V, N304E, T222L	368 aa	93.5%	100%
porin	*OmpK35*	-	195 aa	100%	85.9%
Pmr	*PmrE*	-	388 aa	99.5%	100%
phospholipid biosynthesis pathway	*tesA*	-	184 aa	92.4%	100%
MFS efflux transporter	*Tet(A)*	-	424 aa	100%	100%
MFS efflux transporter	*RosB*	-	558 aa	100%	100%
MFS efflux transporter	*RosA*	-	406 aa	99.3%	100%
MFS efflux transporter	*KpnH*	-	512 aa	93.4%	100%
MFS efflux transporter	*KpnG*	-	390 aa	99.7%	100%
MFS efflux transporter	*KpnF*	-	109 aa	100%	100%

MFS efflux transporter	*KpnE*	-	120 aa	99.2%	100%
MFS efflux transporter	*KdeA*	-	410 aa	100%	100%
MFS efflux transporter	*EmrD*	-	394 aa	99.5%	100%
influx regulation	*bamB*	A176T	360 aa	94.4%	100%
influx	*UhpT*	E350Q	456 aa	96.1%	98.5%
influx	*GlpT*	G206A	423 aa	93.4%	93.8%
influx	*cycA*	S263A	467 aa	92.7%	100%
glutathione transferase	*FosA*	-	139 aa	99.3%	100%
efflux regulation	*MarA*	-	123 aa	93.5%	96.9%
efflux regulation	*H-NS*	-	135 aa	93.3%	98.5%
efflux regulation	*CRP*	-	210 aa	99%	100%
efflux regulation	*CpxA*	-	461 aa	98.7%	100%
DNA topoisomerase subunit	*parC*	T57S	752 aa	94.3%	100%
DNA topoisomerase subunit	*gyrA*	S83Y	877 aa	99.8%	100%
beta-lactamase regulation	*argR*	-	156 aa	100%	100%
beta-lactamase OXA	*OXA-2*	-	275 aa	100%	100%
beta-lactamase GES	*GES-5*	-	287 aa	100%	100%
beta-lactamase CTX-M	*CTX-M-3*	-	291 aa	100%	100%
BasRS	*BasS* synonym *PmrB*	R256G	365 aa	99.5%	100%
BaeSR	*BaeS*	-	492 aa	99.4%	100%
BaeSR	*BaeR*	-	240 aa	99.6%	100%
APH(6)	*APH(6)-Id*	-	278 aa	100%	100%
APH(3")	*APH(3")-Ib*	-	290 aa	99.7%	96%
ABC efflux pump	*PatA*	-	459 aa	94.6%	100%
ABC efflux pump	*MsbA*	-	582 aa	91.9%	100%
AAC(6')-I	*AAC(6')-Ib*	-	179 aa	100%	88.2%

C2 K. pneumoniae **(Table S7)**

ResFinder 4.1

Resistance gene	Identity (%)	Alignment Length/Gene Length	Coverage	Position in reference	Phenotype	Accession no.
oqxB	98.92	3153/3153	100	1..3154	Quinolone resistance	EU370913
oqxA	99.32	1176/1176	100	1..1177	Quinolone resistance	EU370913
aac(6')-Ib-cr	98	600/600	100	1..601	Fluoroquinolone and aminoglycoside resistance	DQ303918
sul1	100	840/840	100	1..841	Sulphonamide resistance	U12338
blaKPC-2	100	882/882	100	1..883	Beta-lactam resistance	AY034847
blaGES-5	100	864/864	100	1..865	Beta-lactam resistance	DQ236171
blaSHV-11	92.8	861/861	92.8	1..862	Beta-lactam resistance	AF535128
blaOXA-48	100	798/798	100	1..799	Beta-lactam resistance	AY236073
fosA	99.05	420/420	100	1..421	Fosfomycin resistance	ACWO01000079
OqxB	98.92	3153/3153	100	1..3154	Disinfectant resistance	EU370913
OqxA	99.32	1176/1176	100	1..1177	Disinfectant resistance	EU370913

PlasmidFinder 2.1

Database	Plasmid	Identity (%)	Query / Template length	Accession number
enterobacteriaceae	Col(pHAD28)	100	131 / 131	KU674895
enterobacteriaceae	IncFIB(K)	98.93	560 / 560	JN233704
enterobacteriaceae	IncFII(pKP91)	95.22	230 / 230	CP000966
enterobacteriaceae	IncL	100	661 / 661	JN626286
enterobacteriaceae	IncR	99.6	251 / 251	DQ449578

MLST 2.0 (Multi-Locus Sequence Typing)

Locus	Identity	Coverage	Alignment Length	Allele Length	Gaps	Allele	ST
gapA	100	100	450	450	0	gapA_2	534
infB	100	100	318	318	0	infB_1	
mdh	100	100	477	477	0	mdh_1	
pgi	100	100	432	432	0	pgi_2	
phoE	100	100	420	420	0	phoE_61	
rpoB	100	100	501	501	0	rpoB_4	
tonB	100	100	408	408	0	tonB_132	

Virulence Factors detected by ARESdb cloud platform

Marker Class	Marker	Variant(s)	Alignment Length	Sequence Identity	Sequence Coverage
virulence factors	*sinR*	-	180 aa	90%	99.4%
virulence factors	*sfaG*	-	183 aa	97.8%	100%
virulence factors	*potD*	-	348 aa	95.1%	100%
virulence factors	*pemK*	-	110 aa	96.4%	100%
virulence factors	*pemI*	-	85 aa	96.5%	100%
virulence factors	*gmr*	-	551 aa	100%	100%
virulence factors	*fliY*	-	310 aa	99.7%	100%
virulence factors	*fimD*	-	859 aa	98.7%	100%
virulence factors	*feoB*	T755A	772 aa	94.2%	100%
virulence factors	*eutB*	-	453 aa	94.9%	100%
virulence factors	*cstA*	-	701 aa	92.6%	100%
virulence factors	*cnrA*	-	1030 aa	99.2%	100%

Antibiotic resistance genes detected by ARESdb cloud platform

Marker Class	Marker	Variant(s)	Alignment Length	Sequence Identity	Sequence Coverage
Vga	*Vga(C)*	-	76 aa	100%	100%
target protection	*Rpsl*	-	124 aa	94.4%	100%
Sul	*Sul1*	-	308 aa	99.4%	100%
RND efflux transporter	*SilC*	-	461 aa	100%	100%
RND efflux transporter	*SilB*	-	430 aa	97.9%	100%
RND efflux transporter	*SilA*	-	1048 aa	98.9%	100%
RND efflux transporter	*MdtC*	-	1024 aa	91.2%	99.9%
RND efflux transporter	*MdtB*	-	1040 aa	90.7%	100%
RND efflux transporter	*AcrD*	-	1037 aa	91%	100%
RND efflux transporter	*AcrB*	-	1049 aa	91.4%	100%
RND efflux transporter	*AcrA*	-	397 aa	99.7%	100%
regulation of resistance	*virB*	-	324 aa	92.3%	100%
regulation of resistance	*rpoS*	-	172 aa	99.4%	100%
regulation of resistance	*rnfC*	-	562 aa	91.8%	75.9%
regulation of resistance	*ompR*	-	239 aa	100%	100%
regulation of resistance	*mtfA*	-	265 aa	100%	100%
regulation of resistance	*leuO*	-	308 aa	99.4%	100%
Qnr	*QnrB12*	-	215 aa	92.1%	100%
putative efflux transport	*setB*	A200E	393 aa	99.5%	100%
putative efflux transport	*cusR*	-	227 aa	98.7%	100%
porin	*OmpK37*	I128M, I70M	374 aa	99.5%	100%
porin	*OmpK36*	-	375 aa	95.5%	100%
porin	*OmpK36*	A217S, D223G, E232R, F198Y, F207Y, G189T, L229A, L59V, T222L	375 aa	90.9%	100%
porin	*OmpK35*	-	226 aa	100%	99.6%
Pmr	*PmrE*	-	388 aa	99%	100%

phospholipid biosynthesis pathway	*tesA*	-	184 aa	92.4%	100%
OqxB	*OqxB19*	-	1050 aa	100%	100%
OqxA	*OqxA10*	-	391 aa	100%	100%
MFS efflux transporter	*RosB*	-	558 aa	100%	100%
MFS efflux transporter	*RosA*	-	406 aa	100%	100%
MFS efflux transporter	*KpnH*	-	512 aa	93.4%	100%
MFS efflux transporter	*KpnG*	-	390 aa	99.5%	100%
MFS efflux transporter	*KpnF*	-	109 aa	100%	100%
MFS efflux transporter	*KpnE*	-	120 aa	100%	100%
MFS efflux transporter	*KdeA*	-	410 aa	99.8%	100%
MFS efflux transporter	*EmrD*	-	394 aa	99.5%	100%
influx regulation	*bamB*	A176T	360 aa	94.4%	100%
influx	*UhpT*	E350Q	456 aa	96.1%	98.5%
influx	*GlpT*	G206A	423 aa	93.4%	93.8%
influx	*cycA*	S263A	467 aa	92.5%	100%
glutathione transferase	*FosA*	-	139 aa	99.3%	100%
efflux regulation	*RamA*	-	113 aa	92%	91.1%
efflux regulation	*MarA*	-	123 aa	93.5%	96.9%
efflux regulation	*H-NS*	-	135 aa	93.3%	98.5%
efflux regulation	*CRP*	-	210 aa	99%	100%
efflux regulation	*CpxA*	-	461 aa	98.5%	100%
efflux regulation	*AcrR*	F172S, F197I, G164A, K201M, L195V, P161R, R173G	216 aa	96.8%	100%
DNA topoisomerase subunit	*parC*	T57S	752 aa	94.1%	100%
DNA topoisomerase subunit	*gyrA*	S83Y	877 aa	99.8%	100%
beta-lactamase SHV	*SHV-11*	-	286 aa	100%	100%
beta-lactamase regulation	*argR*	-	156 aa	100%	100%
beta-lactamase OXA	*OXA-48*	-	265 aa	100%	100%
beta-lactamase GES	*GES-5*	-	287 aa	100%	100%
BaeSR	*BaeS*	-	492 aa	99.4%	100%

BaeSR	*BaeR*	-	240 aa	99.2%	100%
ABC efflux pump	*PatA*	-	459 aa	94.6%	100%
ABC efflux pump	*MsbA*	-	582 aa	91.9%	100%
AAC(6')-I	*AAC(6')-Ib7*	-	210 aa	99%	100%

Plasmids detected by ARESdb cloud platform

Plasmid	**Identity**	**Query / Template length**	**Accession number**
Col(pHAD28)	100.00%	131 / 131	KU674895
Col440I	95.61%	114 / 114	CP023920
IncFIB(K)	98.93%	560 / 560	JN233704
IncFII(pKP91)	96.07%	229 / 230	CP000966
IncFII(pMET)	90.92%	584 / 577	EU383016
IncL	100.00%	661 / 661	JN626286
IncQ1	93.58%	779 / 796	M28829
IncR	99.60%	251 / 251	DQ449578

CF1 C. freundii **(Table S8)**

ResFinder 4.1

Resistance gene	Identity (%)	Alignment Length/Gene Length	Coverage	Position in reference	Phenotype	Accession no.
blaKPC-2	100	882/882	100	1..883	Beta-lactam resistance	AY034847

PlasmidFinder 2.1

Database	Plasmid	Identity	Query / Template length	Accession number
enterobacteriaceae	IncFIB(pHCM2)	96.69	875 / 875	AL513384

MLST 2.0 (Multi-Locus Sequence Typing)

Locus	Identity	Coverage	Alignment Length	Allele Length	Gaps	Allele	ST
arcA	100	100	435	435	0	arcA_14	128
aspC	100	100	513	513	0	aspC_23	
clpX	100	100	567	567	0	clpX_20	
dnaG	100	100	444	444	0	dnaG_58	
fadD	100	100	483	483	0	fadD_36	
lysP	100	100	477	477	0	lysP_62	
mdh	100	100	549	549	0	mdh_60	

Antibiotic resistance genes detected by ARESdb cloud platform

Marker Class	Marker	Variant(s)	Alignment Length	Sequence Identity	Sequence Coverage
undecaprenyl-diphosphatase	*BacA*	-	273 aa	92.7%	100%
target protection	*Rpsl*	-	124 aa	93.5%	100%
RND efflux transporter	*SilC*	-	461 aa	97.6%	100%
RND efflux transporter	*SilB*	-	430 aa	96.5%	100%
RND efflux transporter	*SilA*	-	1048 aa	98.9%	100%
RND efflux transporter	*MdtC*	-	1025 aa	92.7%	100%
RND efflux transporter	*MdtB*	-	1040 aa	92.8%	100%
RND efflux transporter	*AcrD*	-	1037 aa	94.7%	100%
RND efflux transporter	*AcrB*	-	1049 aa	94.5%	100%
RND efflux transporter	*AcrA*	-	397 aa	91.7%	100%
regulation of resistance	*rpoS*	-	172 aa	100%	100%
regulation of resistance	*rnfC*	-	560 aa	91.1%	83.2%
regulation of resistance	*ompR*	-	239 aa	100%	100%
putative efflux transport	*sugE*	-	105 aa	99%	100%
putative efflux transport	*cusR*	-	226 aa	97.3%	99.6%
phospholipid biosynthesis pathway	*tesA*	-	183 aa	90.2%	99.5%
MFS efflux transporter	*RosB*	-	557 aa	92.5%	99.8%
MFS efflux transporter	*MdtH*	-	402 aa	91.3%	100%
MFS efflux transporter	*MdtG*	-	406 aa	91.4%	99.5%
MFS efflux transporter	*MdfA*	-	410 aa	91%	100%
MFS efflux transporter	*EmrB*	-	512 aa	95.3%	100%
influx	*UhpT*	E350Q	463 aa	95.7%	100%
influx	*GlpT*	G206A	423 aa	92.9%	93.8%

influx	*cycA*	S263A	466 aa	96.1%	99.8%
efflux regulation	*SoxR*	R4K	152 aa	93.4%	100%
efflux regulation	*SoxR*	T38S	152 aa	94.1%	98.7%
efflux regulation	*MarR*	Y137H	144 aa	90.3%	100%
efflux regulation	*MarA*	-	128 aa	93%	99.2%
efflux regulation	*KdpE*	-	224 aa	90.6%	99.6%
efflux regulation	*H-NS*	-	137 aa	94.2%	100%
efflux regulation	*CRP*	-	210 aa	99%	100%
efflux regulation	*CpxA*	-	457 aa	98%	100%
DNA topoisomerase subunit	*parC*	T57S	752 aa	96%	100%
DNA topoisomerase subunit	*gyrA*	S83T	875 aa	92.5%	99.8%
beta-lactamase regulation	*argR*	-	156 aa	94.2%	100%
beta-lactamase CMY	*cmy-157*	-	381 aa	97.4%	100%
beta-lactamase ampC	*ampH*	-	385 aa	91.7%	100%
BaeSR	*BaeR*	-	239 aa	96.2%	99.6%
ABC efflux pump	*YojI*	-	547 aa	91.2%	100%
ABC efflux pump	*PatA*	-	458 aa	95%	99.8%
ABC efflux pump	*MsbA*	-	582 aa	94.7%	100%
ABC efflux pump	*mdlB*	-	592 aa	91%	99.8%
ABC efflux pump	*MacB*	-	376 aa	94.9%	100%

Virulence Factors detected by ARESdb cloud platform

Marker Class	Marker	Variant(s)	Alignment Length	Sequence Identity	Sequence Coverage
virulence factors	*potD*	-	348 aa	93.4%	100%
virulence factors	*fliY*	-	266 aa	94%	100%
virulence factors	*fliQ*	-	89 aa	91%	100%
virulence factors	*fliP*	-	245 aa	91.4%	100%
virulence factors	*fliI*	-	456 aa	95.8%	100%
virulence factors	*fliG*	-	332 aa	96.4%	100%
virulence factors	*fliA*	-	239 aa	96.2%	100%
virulence factors	*flhA*	-	692 aa	94.5%	100%
virulence factors	*eutB*	-	453 aa	97.6%	100%
virulence factors	*cstA*	-	701 aa	91.4%	100%

8. CURRICULUM VITAE

MARIJA KVESIĆ IVANKOVIĆ

Date of birth: 8th September 1994

e-mail: mkvesic@unist.hr

EDUCATION

- 09/2020.-today
  Postgraduate university study in Biophysics, Faculty of Science, University of Split
- 09/2016.-10/2018.
  Graduate university study in Chemistry, Faculty of Chemistry and Technology, University of Split
- 09/2013.-09/2016.
  Undergraduate university study in Biology and Chemistry, Faculty of Science, University of Split

EMPLOYMENT

- 03/2019.-today
  Research Asistent at Center of Excellence for Science and Technology - Integration of Mediterranean region (STIM), University of Split, Croatia

PROJECTS

- 2022./2023.: Project Leader 'Impact of Submarine Discharges on Antibiotic Resistance in Marine Environment', Croatian Academy of Sciences and Arts
- 2021./2022.: Project Leader 'Impact of Submarine Discharges on the Development and Spread of Antibiotic-Resistant Human Pathogens', Croatian Academy of Sciences and Arts

AWARDS

- Poster award, 1st place, at 'The 9th International Conference on Water Resource and Environment (WRE 2023)', 2023.
- Dean award, Faculty of Science, University of Split, 2016

TEACHING

- Faculty of Science, University of Split, Part-time adjunct assistant for the course *Molecular biology*
- Faculty of Science, University of Split, Part-time adjunct assistant for the course *Algae and fungi*

9. LIST OF PUBLICATIONS

Dželalija, M.; **Kvesić Ivanković, M.**; Jozić, S.; Ordulj, M.; Kalinić, H.; Pavlinović, A.; Šamanić, I.; Maravic, A. Marine Resistome of a Temperate Zone: Distribution, Diversity, and Driving Factors across the Trophic Gradient. Water Research 2023 Nov 1;246:120688. doi: 10.1016/j.watres.2023.120688. Epub 2023 Oct 3. PMID: 37806125.

Galešić Divić, M., **Kvesić Ivanković, M**., Kišević, M., Panić, M., Lugonja, P., Crnojević, V., and Andričević, R. Prediction of water quality parameters in oligotrophic coastal waters using UAV-obtained hyperspectral data. Journal of Marine Science and Engineering. 2023; 11(10):2026. https://doi.org/10.3390/jmse11102026

Dželalija, M., **Kvesić, M**., Novak, A., Fredotović, Ž., Kalinić, H., Šamanić, I., Ordulj, M., Jozić, S., Barišić, I.G., Tonkić, M. and Maravić, A., 2022. Microbiome profiling and characterization of virulent and vancomycin-resistant Enterococcus faecium from treated and untreated wastewater, beach water and clinical sources. Science of The Total Environment, 159720.

Kvesić, M., Šamanić, I., Novak, A., Fredotović, Ž., Dželalija, M., Kamenjarin, J., Goić Barišić, I., Tonkić, M. and Maravić, A., 2022. Submarine Outfalls of Treated Wastewater Effluents are Sources of Extensively-and Multidrug-Resistant KPC-and OXA-48-Producing Enterobacteriaceae in Coastal Marine Environment. Frontiers in Microbiology, 1486.

Kvesić, M., Kalinić, H., Dželalija, M., Šamanić, I., Andričević, R. and Maravić, A., 2022. Microbiome and antibiotic resistance profiling in submarine effluent-receiving coastal waters in Croatia. Environmental Pollution, 292, 118282.

Kvesić, M., Vojković, M., Kekez, T., Maravić, A. and Andričević, R., 2021. Spatial and Temporal Vertical Distribution of Chlorophyll in Relation to Submarine Wastewater Effluent Discharges. Water, 13(15), p.2016.